

# **Crosstalk of cells in bone metastasis: Molecular and cellular analysis of the mutual effects of prostate cancer cells and osteoblasts**

vom Fachbereich Biologie der Technischen Universität Kaiserslautern  
zur Verleihung des akademischen Grades „Doktor der Naturwissenschaften“  
genehmigte Dissertation

vorgelegt von

**Agnieszka Halas**

Referent: Prof. Dr. Walter G. Pyerin  
Abteilung Biochemische Zellphysiologie, DKFZ Heidelberg

Koreferent: Prof. Dr. John A. Cullum  
Abteilung Genetik, Technische Universität Kaiserslautern

**Die wissenschaftliche Aussprache fand am 15.01.2010 in Kaiserslautern statt.**

**Heidelberg 2010  
D 386**

## Acknowledgements

The following dissertation was prepared in the Division of Biochemical Cell Physiology (A135/PROMET) of the German Cancer Research Center (DKFZ) in Heidelberg, under the scientific supervision of Prof. Walter Pyerin.

I would like to take the opportunity to thank all the persons who have helped me in various ways:

**Prof. Walter Pyerin** for welcoming me into his group, for constructive discussions, friendly encouragement and for presenting the dissertation as main reviewer to the Faculty of Biology of the Technical University of Kaiserslautern,

**Prof. John Cullum** for reviewing the dissertation as second reviewer, **Prof. Johannes Herrmann** for leading the doctoral examination and **Dr. Karin Ackermann** for her friendliness and valuable advice as second scientific supervisor,

**Andrea Waxmann** and **Michael Emmenlauer** for expert technical assistance, **Dr. Sabine Eisenberger** for her patience and advice, and all other group members for helpful discussions,

**Dr. Bernhard Korn** for technical advice and **Sabine Henze** (Microarray Unit, DKFZ Heidelberg) for expert technical assistance with the microarrays,

**Prof. Wolfgang Hagmann** (Division of Molecular Gastroenterology, DKFZ Heidelberg) for helpful advice,

the **Ernst Schering Foundation, Berlin** for financial support,

and last but not least, **my parents** and my fiance **Dr. Jerzy Żuchowski** for encouragement throughout.

This work was supported by a doctoral stipend from the Ernst Schering Foundation in the years 2006-2007.

## Publications

**Halas A, Ackermann K, Pyerin W.** (2009) Crosstalk with prostate cancer cells induces transcriptome alterations in osteoblasts causing perturbed differentiation and function accompanied by repressed TGF $\beta$  signaling.  
*Clinical and Experimental Metastasis, submitted.*

## Posters

**Halas A, Ackermann K, Pyerin W.** (2007) Osteoblast-released protein factors that contribute to osteomimicry in prostate cancer metastases to bone.  
*XII Graduate Seminar of the DKFZ International Ph.D. Program, Landesakademie für Jugendbildung, Weil der Stadt, 19-24.07.2007*

**Halas A, Ackermann K, Pyerin W.** (2007) Gene expression alterations in prostate cancer cells due to crosstalk with osteoblasts in the process of bone metastasis.  
*SENECA: European Conference on Cancer and Ageing. Warsaw, Poland, 4-6.10.2007*  
*Abstract in: Acta Biochimica Polonica, Vol. 54 Suppl. 5/2007*

**Halas A, Ackermann K, Pyerin W.** (2007) Gene expression alterations in prostate cancer cells and osteoblasts due to their crosstalk in the process of bone metastasis.  
*DKFZ Poster Presentation, DKFZ Communication Center, Heidelberg, 12.2007*

**Halas A, Ackermann K, Pyerin W.** (2008) Gene expression alterations in prostate cancer cells and osteoblasts due to their crosstalk in the process of bone metastasis.  
*XIII Graduate Seminar of the DKFZ International Ph.D. Program, Landesakademie für Jugendbildung, Weil der Stadt, 25-27.07.2008*

**Halas A, Ackermann K, Pyerin W.** (2009) Changes in the osteoblast transcriptome induced by crosstalk with prostate cancer cells indicate perturbed differentiation and function, coupled with repression of TGF $\beta$  signaling.  
*Heidelberg Forum for Young Life Scientists, DKFZ Communication Center, Heidelberg, 10-11.09.2009*

## Presentations

**Halas A.** (2007) Gene expression alterations in prostate cancer cells due to crosstalk with osteoblasts in the process of bone metastasis.  
*“Pizza and talk” seminar of the DKFZ International Ph.D. Program, Heidelberg, 11.09.2007*

*Other scientific publications, not involving parts of this dissertation:*

**Johnson JL, Halas A, Flom G.** (2007) Nucleotide-dependent interaction of *Saccharomyces cerevisiae* Hsp90 with the cochaperone proteins Sti1, Cpr6, and Sba1. *Mol Cell Biol.* 27: 768-776.

## Abstract

Prostate cancer preferentially metastasizes to the skeleton and abundant evidence exists that osteoblasts specifically support the metastatic process, including cancer stem cell niche formation. At early stages of bone metastasis, crosstalk of prostate cancer cells and osteoblasts through soluble molecules results in a decrease of cancer cell proliferation, accompanied by altered adhesive properties and increased expression of bone-specific genes, or osteomimicry.

Osteoblasts synthesize a plethora of biologically active factors, which comprise the unique bone microenvironment. By means of quantitative real-time RT-PCR it was determined that exposure to the osteoblast secretome induced gene expression changes in prostate cancer cells, including the upregulation of osteomimetic genes such as *BMP2*, *AP*, *COL1A1*, *OPG* and *RANKL*. IL6 and TGF $\beta$ 1 signaling pathway components also became upregulated at early time points. Moreover, osteoblast-released IL6 and TGF $\beta$ 1 contributed to the upregulation of *OPG* mRNA in LNCaP. Thus, the earliest response of prostate cancer cells to osteoblast-released factors, which ultimately cause metastatic cells to assume an osteomimetic phenotype, involved activation of paracrine and autocrine IL6 and TGF $\beta$  signaling. On the other hand, a microarray analysis showed that osteoblasts exposed to the secretome of prostate cancer cells exhibited gene expression alterations suggestive of repressed proliferation, decreased matrix synthesis and inhibited immune response, which together indicate enhanced preosteocytic differentiation. TGF $\beta$  signaling, known to inhibit osteoblast maturation, was strongly suppressed, as shown by elevated expression of negative regulators, downregulation of pathway components and of numerous target genes. Transcriptional downregulation of osteoblast inhibitory molecules such as *DKK1* and *FST* also occurred, with concomitant upregulation of the osteoinductive molecules *ADM*, *STC1* and *BMP2*, and of the transcription factors *CBFA1* and *HES1*, which promote osteoblast differentiation. Finally, the mRNA encoding *NPPB*, the precursor of a molecule implicated in the inhibition of TGF $\beta$  effects, in bone formation and in stem cell maintenance, became upregulated after coculture both in osteoblasts and in prostate cancer cells. These results provide an insight into potential mechanisms of dysregulated bone formation in metastatic prostate cancer, as well as mechanisms by which osteoblasts might enhance the invasive, osteomimetic and stem cell-like properties of the tumor cells. In particular, the differential modulation of TGF $\beta$  signaling in prostate cancer cells and osteoblasts appears to merit further research.

**Abbreviations:**

A - absorbance  
 Ab - antibody  
 ADM<sup>1</sup> - adrenomedullin  
 AMP - adenosine monophosphate  
 AP - alkaline phosphatase  
 APS - ammonium persulphate  
 AR - androgen receptor  
 ATP - adenosine triphosphate  
 bp - base pairs  
 BMP - bone morphogenetic protein  
 BMU - basic multicellular unit  
 BNP - brain natriuretic peptide  
 BSA - bovine serum albumin  
 CBFA1 - core binding factor 1  
 Cdk - cyclin-dependent kinase  
 cDNA - complementary DNA  
 C/EBP - CCAAT/enhancer-binding protein  
 COL1A1 - collagen type 1 alpha 1  
 CK - casein kinase  
 CM - conditioned medium  
 CSC - cancer stem cell  
 Ct - threshold cycle  
 CXCL12 - chemokine (C-X-C motif) ligand 12  
 Da - Dalton  
 DAB2 - disabled 2  
 DEPC - diethyl pyrocarbonate  
 DKFZ - Deutsches Krebsforschungszentrum  
 DKK1 - dickkopf 1  
 DMEM - Dulbecco's Minimal Essential Medium  
 DMSO - dimethyl sulfoxide  
 DNA - deoxyribonucleic acid  
 dNTP - 2'-deoxynucleotide-5'-triphosphate  
 DTT - dithiothreitol  
 ECM - extracellular matrix  
 EDTA - ethylenediamine-N, N, N', N'-tetraacetic acid  
 ER - endoplasmic reticulum  
 ERK - extracellular signal-regulated kinase  
 ET1 - endothelin 1  
 FCS - fetal calf serum  
 FGF - fibroblast growth factor  
 FGFR - fibroblast growth factor receptor  
 Fig. - Figure  
 g - gram  
 ·g - units of gravity (relative centrifugal force)  
 GC - guanylyl cyclase  
 GTP - guanosine triphosphate  
 h - hour  
 HES - Hairy/Enhancer of split  
 HRP - horseradish peroxidase  
 HSC - hematopoietic stem cell  
 HT - High Tris  
 Ig - immunoglobulin  
 IGF - insulin-like growth factor  
 IL - interleukin  
 IL6R - interleukin 6 receptor  
 IL6 RE-BP - IL6 response element binding protein  
 IRF 1/2 - interleukin-6 response factor 1/2

IVT - *in vitro* transcription  
 JAK/STAT - Janus kinase/signal transducer and activator of transcription  
 JNK - c-Jun N-terminal kinase  
 k - kilo (10<sup>3</sup>)  
 l - liter  
 LT - Low Tris  
 m - meter  
 m - milli (1/10<sup>3</sup>)  
 M - molar  
 MAPK - mitogen-activated protein kinase  
 MEM - Minimal Essential Medium  
 MES - 2-(N-morpholino)ethanesulfonic acid  
 min. - minute  
 mRNA - messenger RNA  
 MTT - thiazolyl blue tetrazolium bromide  
 n - nano (1/ 10<sup>9</sup>)  
 NEAA - non-essential amino acids  
 NF-κB - nuclear factor kappa B  
 NOG - noggin  
 °C - degrees Celsius  
 OC - osteocalcin  
 OPG - osteoprotegerin  
 OPN - osteopontin  
 p - pico (1/10<sup>12</sup>)  
 PAGE - polyacrylamide gel electrophoresis  
 PBS - phosphate-buffered saline  
 PCR - polymerase chain reaction  
 pH - power of hydrogen  
 PKC - protein kinase C  
 PMSF - phenylmethylsulfonyl fluoride  
 PPM1A - protein phosphatase 1A  
 PSA - prostate-specific antigen  
 PTHrP - parathyroid hormone-related protein  
 PVDF - polyvinylidene difluoride  
 qRT-PCR - quantitative RT-PCR  
 RANK(L) - receptor activator of nuclear factor kappa B (ligand)  
 RNA - ribonucleic acid  
 RNase - ribonuclease  
 RPMI - Roswell Park Memorial Institute  
 RT - reverse transcription  
 s - second  
 SCID - severe combined immunodeficient  
 SD - standard deviation  
 SDS - sodium dodecyl sulfate  
 SNF1LK - sucrose nonfermented 1-like kinase  
 Sp - specific protein  
 STC1 - stanniocalcin 1  
 Tab. - Table  
 Taq - *Thermus aquaticus*  
 TBS - Tris-buffered saline  
 TEMED - N, N, N', N'-tetramethylethylenediamine  
 TESS - Transcription Element Search System  
 TGFβ - transforming growth factor beta  
 TGFBR - TGFβ receptor  
 TRAIL - tumor necrosis factor-related apoptosis inducing ligand  
 Tris - tris(hydroxymethyl)aminomethane  
 U - units  
 UDG - uracil-DNA glycosylase  
 uPA - urokinase-type plasminogen activator  
 V - volt  
 v/v - volume/volume  
 w/v - weight/volume  
 x - times  
 μ - micro (1/10<sup>6</sup>)

<sup>1</sup> In accordance with guidelines for gene nomenclature advocated by the HUGO Gene Nomenclature Committee (HGNC) [Wain *et al.* 2002], human gene symbols have been designated by upper-case letters and italicized, while protein symbols are represented in upper-case standard font.

## Table of contents

<b>Acknowledgements.....</b>	<b>1</b>
<b>Publications.....</b>	<b>2</b>
<b>Abstract.....</b>	<b>3</b>
<b>Abbreviations.....</b>	<b>4</b>
<b>Table of contents.....</b>	<b>5</b>
<b>1. Introduction.....</b>	<b>9</b>
<b>1.1. Bone and bone remodeling.....</b>	<b>9</b>
1.1.1. Bone structure and functions.....	9
1.1.2. Bone cells.....	10
1.1.3. Osteoblast differentiation and function.....	10
1.1.3.1. Stages of osteoblast differentiation and the central role of <i>CBFA1/RUNX2</i> .....	10
1.1.3.2. Main pathways regulating osteoblast biology.....	12
1.1.3.3. Bone remodeling by the basic multicellular unit.....	14
1.1.3.4. The <i>RANKL/RANK/OPG</i> axis.....	15
1.1.4. Osteoblasts as the hematopoietic stem cell niche in bone.....	17
<b>1.2. Bone metastasis of prostate cancer.....</b>	<b>18</b>
1.2.1. The origins of prostate cancer.....	18
1.2.2. Androgen independence.....	19
1.2.3. The metastatic cascade.....	20
1.2.4. Bone metastasis - phenotypes and mechanisms.....	22
1.2.5. Current perspectives for bone metastasis therapy.....	25
1.2.6. Osteomimicry.....	26
<b>1.3. Aims.....</b>	<b>28</b>
<b>2. Materials and methods.....</b>	<b>29</b>
<b>2.1. Cell culture.....</b>	<b>29</b>
2.1.1. Cell cultivation, passaging and harvest.....	31
2.1.2. Freezing and thawing cells.....	32
2.1.3. <i>In vitro</i> metastasis model.....	32
2.1.4. Preparation of conditioned medium.....	33

2.1.5. Cell treatment with conditioned medium, antibody neutralization assays and recombinant protein stimulation.....	34
2.1.6. MTT cell proliferation assay.....	34
<b>2.2. RNA and DNA.....</b>	<b>35</b>
2.2.1. RNA isolation.....	36
2.2.2. RNA quantification and quality control.....	37
2.2.3. Reverse transcription.....	38
2.2.4. Quantitative real-time RT-PCR.....	38
2.2.5. Primer design and optimization of annealing temperatures.....	39
<b>2.3. OligoDNA chip technology.....</b>	<b>40</b>
2.3.1. GeneChip array target preparation (one-cycle target labeling).....	42
2.3.1.1. RNA purification.....	42
2.3.1.2. Synthesis and purification of double-stranded cDNA.....	43
2.3.1.3. In vitro transcription (IVT) and purification of biotin-labeled cRNA.....	44
2.3.1.4. Target fragmentation.....	44
2.3.2. Target hybridization.....	45
2.3.3. Washing, staining and scanning the array.....	45
2.3.4. Data analysis.....	46
<b>2.4. Protein analysis.....</b>	<b>47</b>
2.4.1. Protein sample preparation: whole-cell lysates and conditioned medium.....	48
2.4.2. Lowry protein assay.....	48
2.4.3. SDS-polyacrylamide gel electrophoresis (SDS-PAGE) and Western blot.....	49
2.4.4. Silver staining of proteins.....	52
2.4.5. Estimating the molecular weight of protein bands.....	52
<b>3. Results.....</b>	<b>55</b>
<b>3.1. The response of prostate cancer cells to osteoblasts.....</b>	<b>55</b>
3.1.1. Osteotropic prostate cancer cell lines express elevated levels of bone-associated genes .....	55
3.1.2. Osteoblast-released factors induce osteomimicry in prostate cancer cells.....	57
3.1.3. Osteoblast-released IL6 and TGF $\beta$ 1 participate in the induction of osteomimicry in prostate cancer cells.....	61

3.1.4. Osteoblast-released factors increase the expression of IL6 and TGFβ signaling pathway components in prostate cancer cells.....	64
<b>3.2. The response of osteoblasts to prostate cancer cells.....</b>	<b>70</b>
3.2.1. Exposure of osteoblasts to the secretome of prostate cancer cells significantly alters their pattern of gene expression.....	70
3.2.2. Universal osteoblast responses - genes similarly affected in osteoblasts by both osteolytic and osteoinductive prostate cancer cells.....	72
3.2.3. Universal osteoblast responses – both osteolytic and osteoinductive prostate cancer cells suppress proliferation, but to different extents.....	90
3.2.4. Cell type-specific osteoblast responses - osteolytic and osteoinductive prostate cancer cell lines may have differing effects on the osteoblast transcriptome. ....	91
3.2.5. The effect of prostate cancer cells on IL6 production by osteoblasts can depend on the experimental model.....	93
3.2.6. BNP may be potentially relevant in prostate cancer bone metastasis.....	95
<b>4. Discussion</b>	
<b>4.1. Bone metastasis - the significance of “seed-soil” interactions and validity of the <i>in vitro</i> model.....</b>	<b>99</b>
<b>4.2. Modulation of the prostate cancer cell phenotype by the osteoblast secretome - an early step on the path to skeletal metastases.....</b>	<b>99</b>
4.2.1. Osteomimicry is induced in prostate cancer cells by crosstalk with osteoblasts and may facilitate cancer cell survival in bone.....	101
4.2.2. The first response of prostate cancer cells to the osteoblast secretome involves intensified IL6 and TGFβ signaling, which may participate in the induction of osteomimicry.....	104
<b>4.3. The osteoblast response to prostate cancer cells - potential consequences for the microenvironment and for the whole organism.....</b>	<b>109</b>
4.3.1. Alterations of the osteoblast phenotype induced by crosstalk with prostate cancer cells.....	109
4.3.1.1. <i>Gene expression pattern suggestive of preosteocytic differentiation.....</i>	<i>109</i>
4.3.1.2. <i>Potential osteoinductive mechanisms with significance for metastasis.....</i>	<i>113</i>
4.3.1.3. <i>DKK1 in prostate cancer bone metastasis.....</i>	<i>115</i>
4.3.1.4. <i>The potential significance of BNP in prostate cancer bone metastasis.....</i>	<i>117</i>



4.3.3. Prostate cancer cells may suppress the host's immune response..... 118

4.3.4. Modulation of TGF $\beta$  signaling in osteoblasts as one of the switches  
differentiating between osteolytic and osteoblastic metastasis?..... 119

**4.4. Crosstalk between prostate cancer cells and osteoblasts in light of the  
cancer stem cell hypothesis: does the bone furnish a niche for cancer stem cells?..... 123**

**5. Conclusions..... 127**

**References..... 128**

**Supplementary data..... 137**

*Curriculum vitae*..... 148

Erklärung (Declaration)..... 149

# **1. Introduction**

## **1.1. Bone and bone remodeling**

### **1.1.1. Bone structure and functions**

Bone and cartilage constitute the skeletal system, which provides support and protection of vital internal organs, serves as the muscle attachment for locomotion and contains a reserve of calcium and phosphate necessary for the maintenance of serum homeostasis [Hadjidakis & Androulakis 2006, Datta *et al.* 2008]. Bone is a dynamic tissue which undergoes constant formation and resorption in response to changes in mechanical loading or altered serum calcium levels. Bone remodeling is also regulated by a wide range of secreted factors, both systemic and local [Sims & Gooi 2008].

There are two main histological types of mature bone: cortical bone, which has a dense, ordered structure, and trabecular bone, which is lighter, less compact and has an irregular structure. Although macroscopically and microscopically different, the two forms are identical in their chemical composition. Cortical bone, which comprises 80% of the skeleton, has a slow turnover rate and a high mechanical resistance, and constitutes the outer part of all skeletal structures. It is composed of bone matrix laid down concentrically in rings, so-called lamellae, around central spaces known as Haversian canals, which contain blood vessels, lymphatics, nerves and connective tissue. Trabecular bone, which forms the ends of long bones and the inner parts of flat bones, represents 20% of the skeletal mass and has a higher turnover rate than cortical bone. It is composed of interconnecting bars called trabeculae, aligned along lines of stress; the spaces contain bone marrow. Trabecular bone is ideally suited to withstanding compressive stress and hence is the predominant bone in vertebrae [Hadjidakis & Androulakis 2006, Datta *et al.* 2008].

Bone is a type of connective tissue, consisting of an extracellular matrix (largely mineralized) and cells. The mineralized bone matrix is made up of organic and inorganic components. Type I collagen constitutes 95% of the organic part, and the remaining 5% is composed of proteoglycans and noncollagenous proteins such as osteopontin (OPN), osteonectin (ON) and osteocalcin (OC). The inorganic component of bone consists of calcium hydroxyapatite crystals [Hadjidakis & Androulakis 2006].

### 1.1.2. Bone cells

Osteoblasts are located on inner bone surfaces and are cells of mesenchymal origin, responsible for bone formation. They secrete a characteristic mixture of extracellular matrix proteins called osteoid. Cells of the osteoblastic lineage also provide factors essential for the differentiation of osteoclasts, thus playing a central role in the regulation of skeletal architecture [Mackie 2003]. Furthermore, osteoblasts are a crucial element in hematopoiesis, constituting a niche for hematopoietic stem cells that home to the bone marrow [Wilson & Trumpp 2006, Zhu & Emerson 2004, Neiva *et al.* 2005].

Some osteoblasts ultimately become encased in mineralized bone matrix and turn into osteocytes. These cells reside in spaces called lacunae and form a network throughout bone tissue, communicating with each other and with surface osteoblasts through long cellular extensions located within so-called canaliculi in the mineralized bone matrix. Osteocytes are the most common cell type found in bone, comprising 90% of adult bone cells, and their half-life has been estimated at 25 years, whereas the average lifespan of active osteoblasts is only about three months. Osteocytes are believed to act as mechanosensory cells and participate in the control of bone turnover [Franz-Odenaal *et al.* 2005, Datta *et al.* 2008, Noble 2008].

Osteoclasts are multinucleated cells of monocyte/macrophage lineage which carry out the unique function of resorbing mineralized bone matrix. They are formed by the attraction of hemopoietic myelomonocytic precursors to the resorption site, followed by their fusion and attachment of the resultant multinucleated cell to the bone surface. Osteoclasts break down bone by acidification and proteolysis of the bone matrix and undergo apoptosis when resorption has been completed [Hadjidakis & Androulakis 2006, Sims & Gooi 2008].

Bone development can occur through two distinct pathways: intramembranous and endochondral ossification. In intramembranous ossification, mesenchymal cells condense and directly differentiate into osteoblasts. In contrast, in endochondral ossification, mesenchymal cells condense and then become chondrocytes. This cartilage mold then directs the formation of osteoblasts, which form mature bone [Kobayashi & Kronenberg 2005].

### 1.1.3. Osteoblast differentiation and function

#### 1.1.3.1. Stages of osteoblast differentiation and the central role of *CBFA1/RUNX2*

Osteogenic differentiation is controlled by a range of hormonal and local factors converging onto a finite number of transcriptional regulators that ultimately determine the fate of cells committing to the osteogenic lineage [Karsenty & Wagner 2002]. In the course of

osteoblast differentiation, peak levels of expressed genes reflect a sequence characterized by three principal periods: proliferation, extracellular matrix maturation and mineralization [Lian & Stein 1995] (Fig. 1).

Osteoprogenitors develop from bone marrow-derived multipotent mesenchymal stem cells that also give rise to fibroblasts, myoblasts, adipocytes and chondrocytes. They undergo further differentiation to preosteoblasts that still proliferate, and these cells then develop into osteoblasts that no longer divide, but instead lay down bone matrix. Osteoblasts can ultimately undergo one of three fates: they can become osteocytes upon entrapment within the mineralized matrix; they can evolve into inactive lining cells that protect the bone matrix from osteoclasts; or they can undergo apoptosis, which appears to be the fate of up to 80% of the cells. Some of the key proteins expressed by osteoblasts are type I collagen, alkaline phosphatase (AP), bone sialoprotein (BSP) and OC [Lian & Stein 1995].

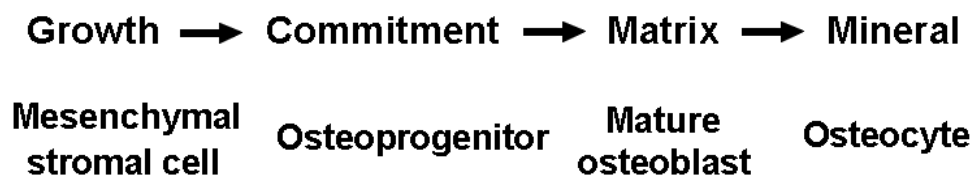


**Fig. 1 Stages of osteoblast differentiation.** [Lian *et al.* 2006]

Osteoblastic differentiation is orchestrated by multiple signaling pathways converging on the transcription factor core binding factor 1/ runt-related transcription factor 2 (CBFA1/RUNX2), which controls the expression of all major genes responsible for the osteoblast phenotype [Ducy 2000]. CBFA1 overexpression in nonosteogenic cells such as skin fibroblasts induced them to express genes characteristic for osteoblasts [Ducy *et al.* 1997] and introduction of CBFA1 into mesenchymal stem cells stimulated differentiation along the osteoblast lineage [Byers & Garcia 2004], whereas its targeted disruption resulted in a complete arrest of osteoblast maturation and lack of bone formation [Ducy *et al.* 1997].

The role of CBFA1 extends beyond development and differentiation, as this transcription factor also regulates the rate of bone matrix deposition by osteoblasts. Thus, CBFA1 is a critical gene not only for osteoblast differentiation but also for osteoblast function [Ducy 2000, Schroeder *et al.* 2005]. Significantly, CBFA1 overexpression inhibits osteoblast

maturation, matrix deposition and mineralization [Liu *et al.* 2001], indicating that CBFA1 levels in lineage-restricted osseous cells must be tightly regulated.

CBFA1 cooperates with numerous proteins, is posttranslationally modified, and associates with the nuclear matrix to integrate a variety of signals. The pathways regulating its activity are just beginning to be understood. CBFA1 can be phosphorylated and activated by the mitogen-activated protein kinase (MAPK) pathway, which is stimulated by multiple signals, including those initiated by mechanical loading, contact with the extracellular matrix and by osteogenic growth factors. Furthermore, CBFA1 activity is enhanced by interaction with other transcription factors, resulting in the assembly of higher-order transactivation complexes. In sum, CBFA1 appears to play a central role in coordinating myriad signals involved in osteoblast differentiation [Franceschi & Xiao 2003, Schroeder *et al.* 2005].

Two other transcription factors crucial for osteoblast differentiation are osterix, which acts downstream of CBFA1, and  $\beta$ -catenin [Kobayashi & Kronenberg 2005].

### ***1.1.3.2. Main pathways regulating osteoblast biology***

Factors that directly regulate osteoblast differentiation and function include, among others, the bone morphogenetic proteins (BMPs), transforming growth factor  $\beta$  1 (TGF $\beta$ 1), fibroblast growth factors (FGFs) and WNTs. The four main signal transduction pathways involved in bone formation are depicted in Fig. 2.

BMPs, which belong to the TGF $\beta$  superfamily, induce the differentiation of mesenchymal cells towards the osteoblastic lineage and also enhance osteoblast function. These molecules initiate signaling from the cell surface by interacting with two distinct serine/threonine kinase receptors. The binding of BMP ligands to preformed heteromeric receptor complexes leads to phosphorylation of the SMAD1 and SMAD5 proteins, which translocate to the nucleus and regulate transcription, whereas BMP-induced formation of heteromeric receptor complexes results in activation of the MAPK pathway. CBFA1 and osterix are both downstream targets of BMP signaling. The effects of BMPs can be blocked by extracellular antagonists such as noggin (NOG), which inhibits bone formation [Canalis *et al.* 2003, Logothetis & Lin 2005, Wan & Cao 2005].

TGF $\beta$ 1, the prototypic member of the TGF $\beta$  superfamily, is one of the most important factors in the bone microenvironment, helping to maintain the balance between the dynamic processes of bone resorption and bone formation [Janssens *et al.* 2005, Kanaan & Kanaan 2006]. TGF $\beta$  signals through type I and type II transmembrane serine/threonine receptor

kinases. Ligand binding to the TGF $\beta$  receptor type II initiates phosphorylation of the TGF $\beta$  receptor type I, which then propagates the signal downstream *via* phosphorylation of receptor-activated SMAD2/3 - the so-called canonical pathway, and *via* noncanonical routes such as the MAPK pathway [Shi & Massague 2003, Derynck & Zhang 2003].

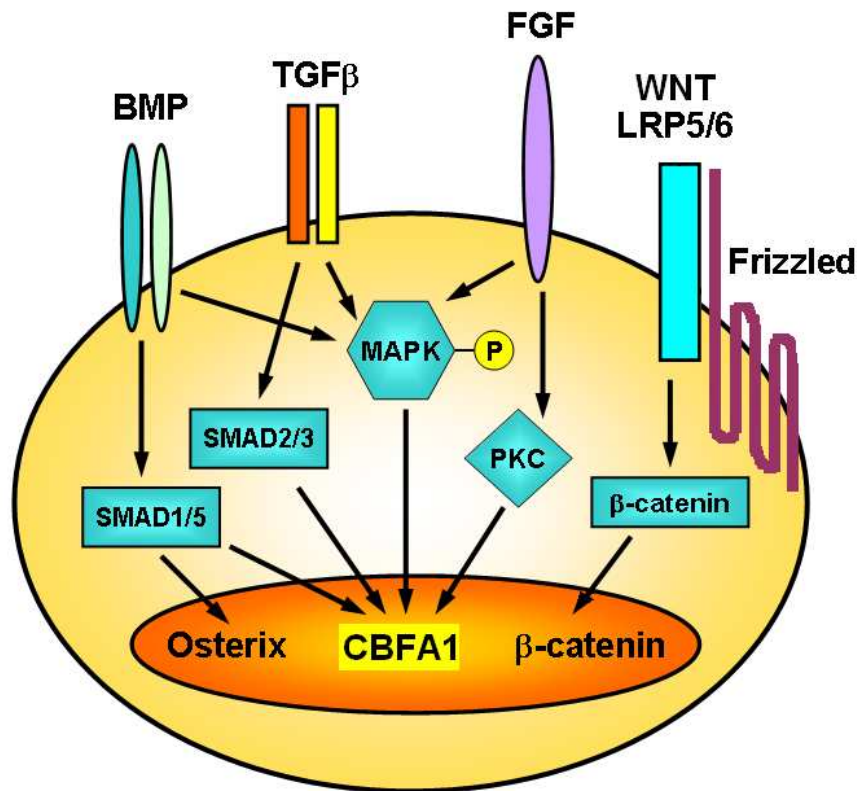


**Fig. 2 Major signal transduction pathways that regulate osteoblast function.** For details see text.  
[based on: Logothetis & Lin 2005]

FGFs signal through a group of high-affinity transmembrane receptors (FGFRs) which have intrinsic tyrosine kinase activities. In osteoblasts, the interaction of FGFs like FGF2 with their FGFRs induces receptor dimerization and autophosphorylation, which in turn activates downstream kinase cascades. FGF signaling promotes bone formation by regulating osteoprogenitor proliferation, as well as osteoblast differentiation and survival. E.g. FGF2 acting *via* protein kinase C (PKC) and *via* p42/44 MAPK enhances the expression and activity of CBFA1, stimulating the expression of osteoblast-specific genes [Marie 2003, Franceschi & Xiao 2003, Logothetis & Lin 2005].

The WNT ligands interact with WNT receptor Frizzled and a coreceptor, the low density lipoprotein receptor-related protein 5 or 6 (LRP5/6) to activate a signaling pathway that stabilizes cytoplasmic  $\beta$ -catenin. Stabilized  $\beta$ -catenin is then translocated to the nucleus to regulate genes that promote bone formation. WNT/ $\beta$ -catenin signaling represses alternative mesenchymal differentiation pathways and promotes osteoblast proliferation, differentiation, and mineralization activity [Krishnan *et al.* 2006, Yavropoulou & Yovos 2007, Milat & Ng 2009]. Canonical WNT signaling promotes bone formation directly, e.g. by elevating CBFA1 expression in osteoblasts, which contributes to their maturation [Gaur *et al.* 2005] and by preventing osteoblast apoptosis [Almeida *et al.* 2005], as well as indirectly by decreasing bone resorption, since OPG, which inhibits osteoclast formation, is a WNT target gene [Glass *et al.* 2005].

The soluble antagonist dickkopf 1 (DKK1), which blocks WNT signaling by binding to LRP5/6 receptors and promoting their internalization and degradation, is an inhibitor of osteoblast differentiation and bone formation [Pinzone *et al.* 2008].

Osteoblast differentiation can also be promoted by other factors, e.g. by interleukin 6 (IL6), which stimulates maturation of committed osteoprogenitors and the expression of osteoblast-specific genes [Bellido *et al.* 1997, Erices *et al.* 2002, Li *et al.* 2008].

### ***1.1.3.3. Bone remodeling by the basic multicellular unit***

Bone remodeling, a complex process wherein old bone is constantly replaced, occurs continuously at discrete sites within the skeleton. It requires interaction between different cell types and is regulated by a plethora of biochemical and mechanical cues. The remodeling cycle consists of three consecutive phases: resorption, during which osteoclasts digest old bone; reversal, when mononuclear cells appear on the bone surface; and formation, when osteoblasts lay down new bone until the resorbed bone is completely replaced. Bone remodeling serves to adjust bone architecture to meet changing mechanical needs. It also helps to repair microdamages in bone matrix, and plays an important role in maintaining plasma calcium homeostasis [Hadjidakis & Androulakis 2006, Sims & Gooi 2008].

The basic multicellular unit (BMU) responsible for coordinated bone remodeling consists of osteocytes, osteoclasts and osteoblasts (Fig. 3). Its activation is at least partly regulated by the osteocytes, which detect mechanical stress and respond to biochemical stimuli. The lining cells of the endosteal surface then become retracted and release matrix metalloproteinases, which digest the endosteal collagenous membrane. Osteoclasts become recruited and, after activation, resorb the underlying bone. Subsequently, osteoblasts are

recruited to the resorption cavity and lay down new osteoid, which eventually becomes calcified; this process is completed in approximately 3-6 months. The rate of bone turnover varies according to the type of bone, being highest in sites where trabecular bone predominates [Hadjidakis & Androulakis 2006, Datta *et al.* 2008, Sims & Gooi 2008].

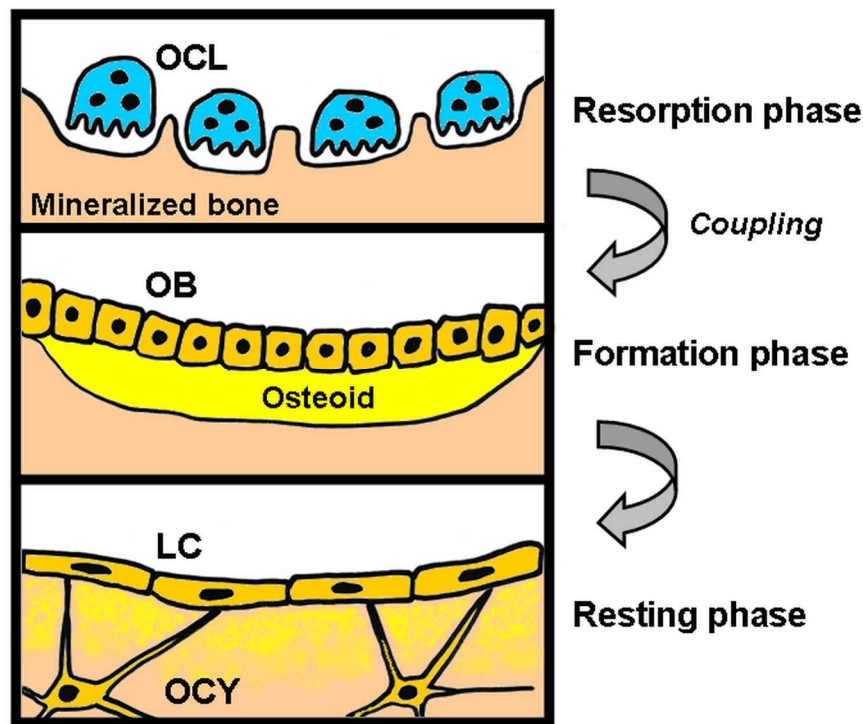


**Fig. 3 The basic multicellular unit (BMU).** These temporary anatomic structures resorb bone and subsequently induce bone formation. In the resorption phase, multinucleated osteoclasts (OCL) resorb the calcified matrix. Preosteoblasts then migrate to the region and differentiate into osteoblasts (OB). In the formation phase, these lay down new, uncalcified bone matrix, referred to as osteoid. Subsequently, the osteoid becomes mineralized. In the end or resting phase of bone remodeling, osteoblasts trapped in the matrix become osteocytes (OCY); others die or transform into lining cells (LC) found on the bone surface and characterized by low/absent bone-forming activity. The number of BMUs can be modulated by mechanical loading, hormones and cytokines, marrow hematopoiesis and drugs, e.g. bisphosphonates. [Buijs & van der Pluijm 2009]

### 1.1.3.4. The RANKL/RANK/OPG axis

Under normal conditions, a dynamic balance is maintained within the skeleton between the activities of osteoblasts and osteoclasts. The processes of bone formation and resorption are tightly regulated, and any shift in their balance leads either to osteoporosis (loss of bone density) or osteosclerosis (abnormal bone thickening) [Sims & Gooi 2008].

Recently, a novel cytokine system responsible for the regulation of bone resorption has been identified and extensively characterized. This cytokine system is comprised of a ligand,



receptor activator of nuclear factor- $\kappa$ B ligand (RANKL), its specific receptor - receptor activator of nuclear factor- $\kappa$ B (RANK), and its decoy receptor osteoprotegerin (OPG). RANKL, RANK, and OPG constitute an axis that is capable of regulating all aspects of osteoclast function, including proliferation, differentiation, fusion, activation and apoptosis [Hofbauer & Heufelder 2001, Hofbauer *et al.* 2001, Boyce & Xing 2007].

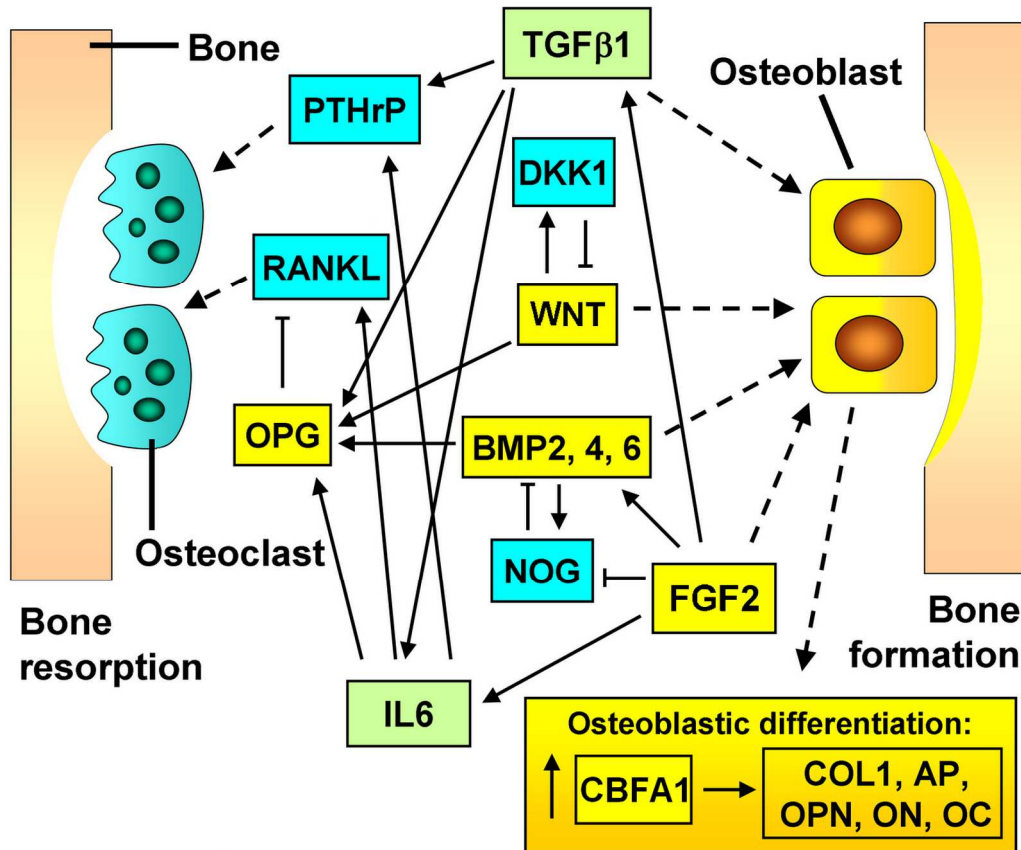


**Fig. 4 The network of factors that regulate bone remodeling.** Blue - factors promoting bone resorption; yellow - factors promoting bone formation; green - factors that influence both processes. Arrows - induction; T signs - repression.

[Kozawa *et al.* 1997; Hofbauer *et al.* 1998; Franchimont *et al.* 2000; Lindemann *et al.* 2001; Thirunavukkarasu *et al.* 2001; Palmqvist *et al.* 2002; Canalis *et al.* 2003; Marie 2003; Fakhry *et al.* 2004; Guillen *et al.* 2004; Farhadi *et al.* 2005; Glass *et al.* 2005; Janssens *et al.* 2005; Logothetis & Lin 2005; Krishnan *et al.* 2006; Pinzone *et al.* 2008]

RANKL is expressed by activated T cells, bone marrow stromal cells and osteoblasts. Alternative splicing of RANKL mRNA allows its expression as a transmembrane glycoprotein or a soluble ligand; soluble RANKL can also be released from its membrane-

bound state by metalloproteinases. It binds to its receptor, RANK, which is expressed by osteoclast precursors and mature osteoclasts. The binding of RANKL to RANK promotes osteoclast maturation and activation. OPG, mainly secreted by bone marrow stromal cells and osteoblasts, is a soluble decoy receptor for RANKL which blocks the RANKL-RANK interaction and thus inhibits osteoclast differentiation and function [Hofbauer & Heufelder 2001, Hofbauer *et al.* 2001].

OPG and RANKL mediate the stimulatory or inhibitory effects of a variety of systemic hormones, growth factors, and cytokines on osteoclastogenesis. The so-called “convergence hypothesis” proposes that the activity of many resorptive and antiresorptive agents “converges” at the level of these two mediators, whose final ratio controls the degree of osteoclast differentiation, activation, and apoptosis [Hofbauer *et al.* 2001]. The RANKL/OPG ratio becomes deregulated in many conditions characterized by pathological rates of bone resorption, including osteoporosis and cancer metastasis to bone [Wittrant *et al.* 2004, Blair *et al.* 2005].

Osteoblasts, which not only lay down new bone matrix, but also indirectly regulate bone resorption by expressing both RANKL and OPG, act as the “central switch” in the skeleton that regulates bone turnover in response to local or systemic cues [Mackie 2003]. Some of the local factors involved in the regulation of bone remodeling are presented in Fig. 4.

### 1.1.4. Osteoblasts as the hematopoietic stem cell niche in bone

All blood cell production comes from hematopoietic stem cells (HSCs), the great majority of which are contained in the bone marrow. To maintain their pluripotency, stem cells require a niche, or spatial structure where they are housed and can undergo self-renewal in the absence of differentiation. In the bone marrow, HSCs stay in close proximity to endosteal bone surfaces, and recent publications suggest that osteoblasts are a major, defining component of the HSC niche, responsible for regulating HSC proliferation and survival. The functions of the HSC niche depend on the expression of a broad array of adhesion molecules and cytokines [Wilson & Trumpp 2006, Zhu & Emerson 2004, Neiva *et al.* 2005, Suda *et al.* 2005]. Osteoblasts and HSCs stay in direct contact through homotypic N-cadherin interactions, and specialized spindle-shaped N-cadherin-expressing osteoblasts located in the endosteum have been postulated to function as essential niche cells, helping to maintain HSC quiescence [Zhang *et al.* 2003]. Suppression of N-cadherin expression by oxidative stress causes HSCs to detach from the osteoblastic niche [Hosokawa *et al.* 2007]. OPN expressed by

osteoblasts also mediate HSC attachment to the niche and negatively regulate their proliferation, limiting the size of the stem cell pool [Nilsson *et al.* 2005, Stier *et al.* 2005]. Finally, osteoblasts secrete chemokine (C-X-C motif) ligand 12 (CXCL12), also known as stromal derived factor 1 (SDF1), a chemokine which acts as a potent chemoattractant for immature and mature hematopoietic cells. CXCL12 plays an important role in the homing of HSCs, which express its receptor CXCR4, to the bone marrow [Juarez & Bendall 2004].

### 1.2. Bone metastasis of prostate cancer

Prostate cancer is the most commonly diagnosed cancer in males and the second leading cause of cancer-related death among men [Jemal *et al.* 2008]. It frequently metastasizes to the skeleton, and bone metastasis is usually associated with the development of hormone-refractory disease with poor prognosis. The skeletal lesions typically cause severe pain, as well as complications such as anemia, pathological fractures and spinal cord compression, and thus pose a significant clinical problem. Bone metastases of prostate cancer are characterized by increased osteoblastic activity, and accumulating evidence suggests that the crosstalk of prostate cancer cells and osteoblasts is an important step in the metastatic process [Keller *et al.* 2001, Mundy 2002, Edlund *et al.* 2004, Logothetis & Lin 2005, Yin *et al.* 2005, Choueiri *et al.* 2006 and others].

#### 1.2.1. The origins of prostate cancer

The prostate is a complex tubulo-alveolar gland composed of an epithelial parenchyma embedded within a connective tissue matrix. The epithelial cells are organized in glands that branch out from the urethra and terminate in secretory acini. The main cell types present within normal prostatic epithelium are luminal, basal and neuroendocrine cells [Lang *et al.* 2009].

The luminal cells, which constitute the exocrine compartment of the prostate, are terminally differentiated and represent the major cell type in normal epithelium. They express high levels of the androgen receptor (AR) and are dependent on androgens for their survival. In contrast, basal cells are relatively undifferentiated and lack secretory activity. They rest on the basement membrane, express low/undetectable levels of AR and are independent of androgens for their survival. Significant populations of neuroendocrine cells, which are

terminally differentiated, post-mitotic and androgen insensitive, also reside amongst the basal cell compartment [Lang *et al.* 2009].

Prostate stem cells are thought to reside in the basal cell compartment. Studies have shown that basal cells preferentially survive androgen ablation, whereas most of the luminal epithelial cells are lost through apoptosis. Androgen treatment restores the secretory glandular structure, suggesting that the basal compartment contains stem cells which undergo amplification to repopulate the luminal epithelium [Kasper 2008, Lang *et al.* 2009].

Several lines of evidence suggest that prostate cancer arises as a result of mutations in normal prostate stem cells. Tumor-initiating cells are present within prostate tumors, in line with the cancer stem cell theory [Kasper 2008, Lang *et al.* 2009]. According to this theory, solid tumors originate as a result of the transformation of stem or progenitor cells. Normal stem cells give rise to all tissues during embryonic development and control tissue homeostasis in the adult. They have the ability to perpetuate themselves through self-renewal and to generate other, differentiated cell types [Reya *et al.* 2001]. Undifferentiated cells capable of self-renewal remain present within a heterogeneous tumor mass, and these “cancer stem cells” (CSCs) fuel tumor growth and initiate metastases. The CSC is defined as a cell within a tumor that possesses the capacity to self-renew and differentiate into the heterogeneous lineages of malignant cells that comprise a tumor. Current treatments target the bulk of differentiated cells which are not tumor-initiating, while the CSCs survive, so that tumors recur after therapy. In order to achieve long-term success, anti-cancer treatment needs to be aimed at the CSCs, which enter the cell cycle infrequently and thus are refractory to standard therapies [Reya *et al.* 2001, Clarke *et al.* 2006, Lobo *et al.* 2007].

A CSC population possessing a significant capability for self-renewal and differentiation into phenotypically mixed populations has been isolated from human prostate tumors. These cells share surface antigens with normal prostate stem cells [Collins 2005]. The prostate cancer cell line PC3 also contains a subpopulation of self-renewing, tumor-initiating cells [Li 2008]. Cocciadiferro *et al.* (2009) have recently reported that both androgen-responsive and androgen-independent prostate tumor cell lines contain a presumptive CSC population that can be identified using a panel of selected gene markers, while Klarmann *et al.* (2008) found that prostate cancer cell subpopulations with strongly invasive properties are also tumor-initiating and possess a stem cell-like genomic signature.

### 1.2.2. Androgen independence

The AR is pivotal not only to the initiation and growth of prostate cancers, but also in their responses to therapy. Localized prostate cancer can be effectively treated by surgery or radiation. Like normal prostate tissue, most prostate cancers initially require the presence of androgens for growth and survival, and the majority of patients with advanced disease respond at first to androgen ablation therapy, aimed at blocking signaling through the AR. Unfortunately, aggressive androgen-independent cancers refractory to conventional hormonal therapies eventually develop, and subsequently widespread metastasis occurs [Devlin & Mudryj 2009, Lang *et al.* 2009].

Androgen independence is a state where prostate cancer cells can survive and proliferate even in the presence of very low androgen levels. The molecular events that drive the transition from an androgen-dependent to androgen-independent state remain unclear, but several mechanisms have been proposed, including overexpression of the AR, AR mutations or AR activation by non-steroid ligands such as growth factors and cytokines. It has been suggested that androgen ablation therapy might actually promote disease progression by activating normally quiescent CSCs to repopulate the tumour with androgen-independent cells [Devlin & Mudryj 2009, Lang *et al.* 2009].

### 1.2.3. The metastatic cascade

Metastasis requires that cancer cells escape from the primary tumor, become dispersed through the circulation, seed at distant sites and grow. This extremely inefficient process involves several distinct steps: cell detachment from the tumor mass, intravasation, survival within the blood or lymphatic systems, extravasation and homing to a new location, where the microenvironment must permit the cancer cell to adhere, survive and propagate to establish a secondary lesion (Fig. 5) [Chambers *et al.* 2002].

Certain cancers preferentially metastasize to some organs, but rarely to others. The organ specificity of metastasis is determined by blood flow patterns, but also by intrinsic properties of the cancer cells and the target organ. In 1889, Stephen Paget proposed that certain tumors, compared to “seeds”, have a special affinity for particular organs, the “soil”, and the seed-soil interaction determines whether tumors survive and grow at a distant site. Paget’s premise still holds true today, and the modern seed-and-soil hypothesis has been defined by Fidler (2003) as consisting of three principles. First, cancerous tissues contain heterogeneous subpopulations of cells with different angiogenic, invasive, and metastatic

properties. Second, the metastatic process is selective for the small subpopulation of cells that have survived the journey to a distant site. Third, the survival and growth of those metastatic cells depends on their ability to interact with their new milieu [Arya *et al.* 2006, Chambers *et al.* 2002, Fidler 2003].

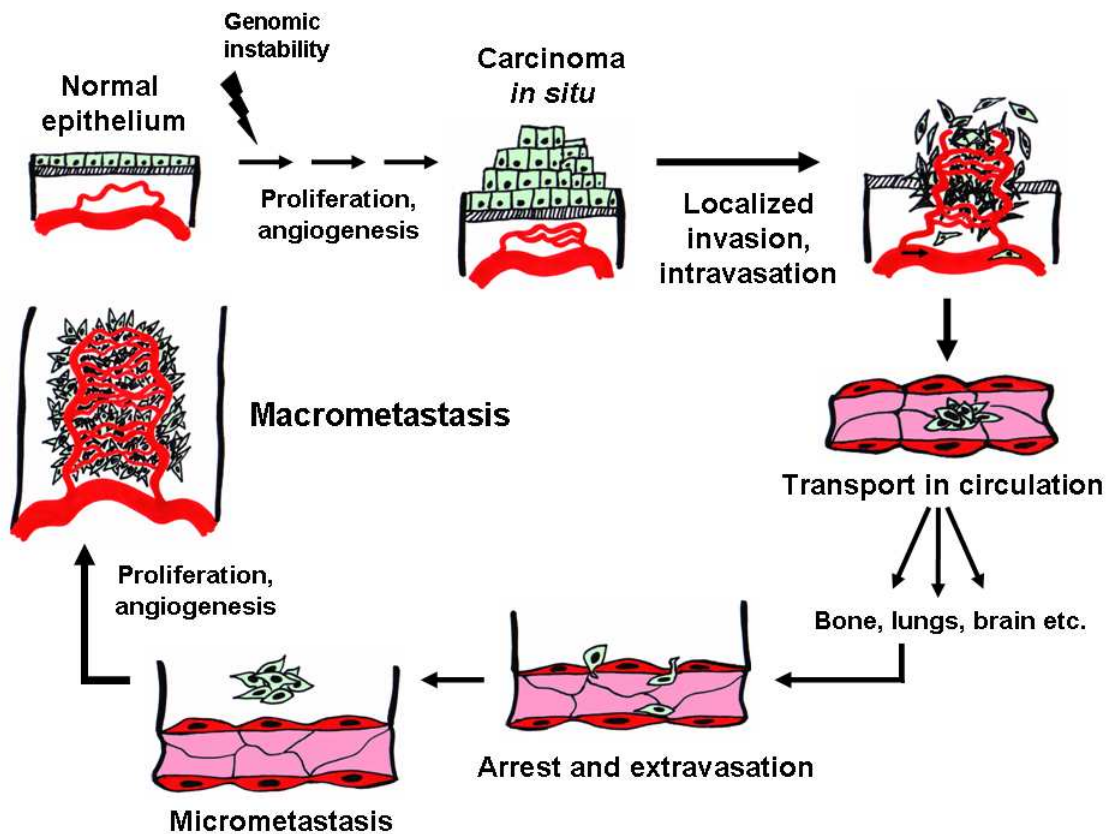


**Fig. 5 Main steps in tumor progression and metastasis.** The small probability of successfully completing all steps of this cascade explains the low likelihood that any single cancer cell leaving a primary tumor will succeed in becoming the founder of a distant, macroscopic metastasis. [Buijs & van der Pluijm 2009]

Metastases can occur many years after primary cancer treatment. Tumor dormancy might be due to pre-angiogenic micrometastases that subsequently acquire the ability to become vascularized, or to solitary cells that persist for an extended period of time without division in a secondary site. These cells would be resistant to current cancer therapies that target actively dividing cells. Treatments aimed at the specific “seed-soil” compatibility that results in organ-specific metastatic growth could prove especially useful [Chambers *et al.* 2002].

### 1.2.4. Bone metastasis - phenotypes and mechanisms

Bone, particularly trabecular bone, is one of the most preferential metastatic target sites for malignancies such as breast, prostate and lung cancers. Skeletal metastasis frequently leads to pain, fractures and other complications. Crosstalk between tumor cells and bone cells, both through direct cell-cell contact and through soluble factors, is considered critical for the development and progression of bone metastases [Keller *et al.* 2001, Mundy 2002, Edlund *et al.* 2004, Logothetis & Lin 2005, Yin *et al.* 2005 and others].

Depending on their radiographic appearance, bone metastases can be predominantly osteolytic, involving bone destruction, or osteoblastic (osteoinductive, osteosclerotic), characterized by increased deposition of new bone. The lesion phenotype reflects the local interaction between tumor cells and the bone remodeling system [Virk & Lieberman 2007]. Prostate cancer metastases are typically osteoblastic [Logothetis & Lin 2005], whereas breast cancer metastases are usually osteolytic [Kozlow & Guise 2005]. More precisely, recent observations suggest that bone metastases represent a spectrum. At one end, osteolytic lesions are associated with increased bone resorption and reduced osteoblast activity, but an attempt at bone repair is often also present, whereas bone metastases that are predominantly osteoblastic also show enhanced bone resorption. Dysregulated bone resorption by osteoclasts is necessary for the establishment of metastases, since it releases growth factors from the bone matrix, fueling tumor growth [Keller *et al.* 2001, Chirgwin *et al.* 2004, Keller & Brown 2004, Kozlow & Guise 2005, Guise *et al.* 2006].

Tumor cells produce chemokine receptors, cell adhesion molecules and cell surface receptors which enable them to home to bone and attach to the endosteal surfaces [Yin *et al.* 2005]. Although tumor cells secrete proteolytic enzymes and can directly destroy bone matrix *in vitro*, the main mediators of bone destruction within a metastatic lesion are the osteoclasts [Kozlow & Guise 2005]. The bone matrix is a rich deposit of growth factors which become released into the tumor microenvironment as a result of osteolysis. These factors stimulate the growth of tumor cells and alter their phenotype, thus promoting a vicious cycle of metastasis and bone pathology. Physical factors within the bone microenvironment, including low oxygen levels, acidic pH, and high extracellular calcium concentrations, may also enhance tumor growth [Kingsley *et al.* 2007, Virk & Lieberman 2007].

A simplified model of the molecular mechanisms involved in osteolytic and osteoblastic metastasis is presented in Figs. 6 and 7.

Tumor-produced parathyroid hormone-related protein (PTHrP) is one of the important mediators of the osteolytic process occurring in metastatic breast carcinoma. TGF $\beta$ , which is

abundant in bone matrix and becomes released as a result of osteoclastic bone resorption, promotes osteolysis by stimulating PTHrP production by tumor cells. PTHrP then stimulates osteoclastic bone resorption by increasing osteoblast production of RANKL and decreasing their production of OPG (Fig. 6) [Guise 2000, Kozlow & Guise 2005]. Cancer cells can also secrete multiple other cytokines that stimulate osteoclastogenesis [Virk & Lieberman 2007]. Furthermore, there is evidence that osteolytic lesions are linked with impaired osteoblast differentiation and activity [Mercer *et al.* 2004, Hall *et al.* 2005, Hall *et al.* 2006, Bu *et al.* 2008] and elevated osteoblast apoptosis [Mastro *et al.* 2004].

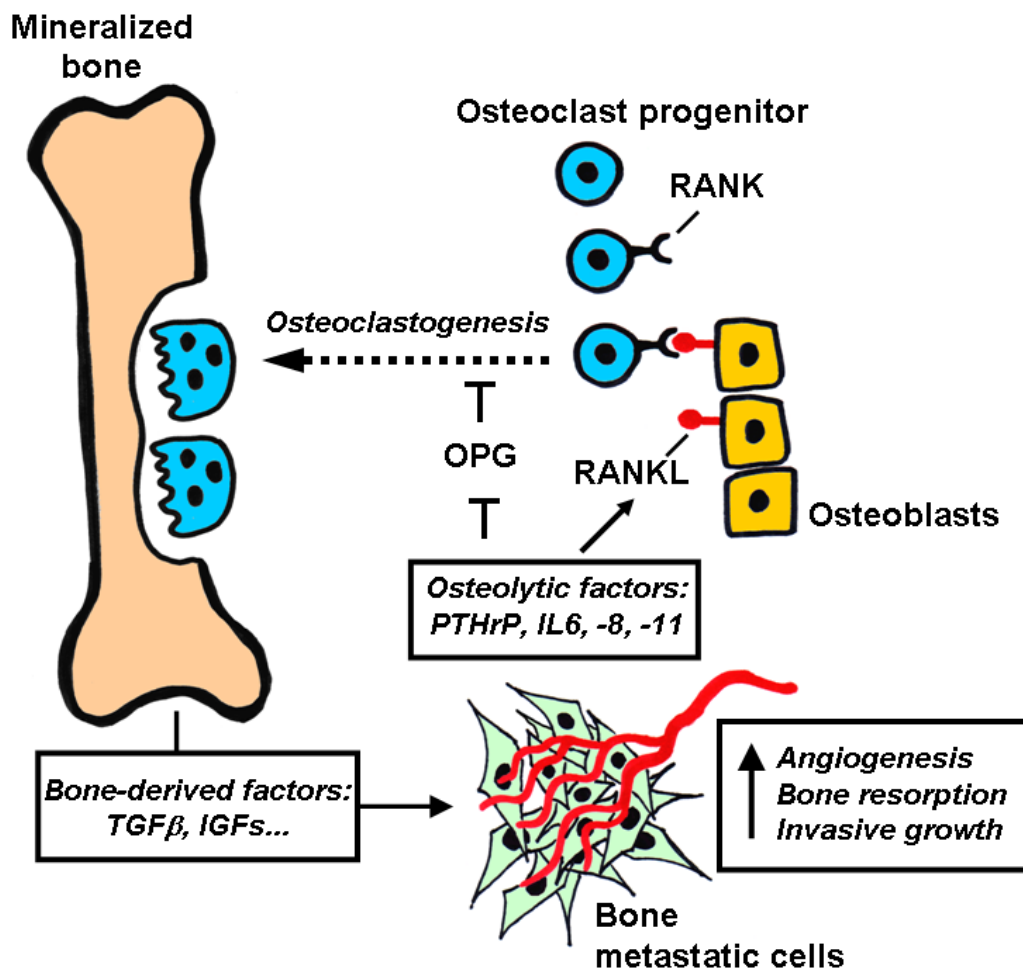


**Fig. 6 Pathophysiology of osteolytic bone metastasis.** Release of osteolytic factors by metastatic breast cancer cells causes nearby osteoblasts to increase RANKL synthesis. RANKL induces osteoclast precursors to mature into functional osteoclasts. The latter undertake osteolysis, which causes bone demineralization and liberation of growth factors such as TGFβ and insulin-like growth factors (IGFs) which stimulate cancer cell proliferation and survival. Additionally, TGFβ released from the bone matrix stimulates production of PTHrP by the cancer cell, resulting in a self-sustaining positive feedback loop that has been termed the “vicious cycle” of osteolytic metastasis. [Buijs & van der Pluijm 2009]



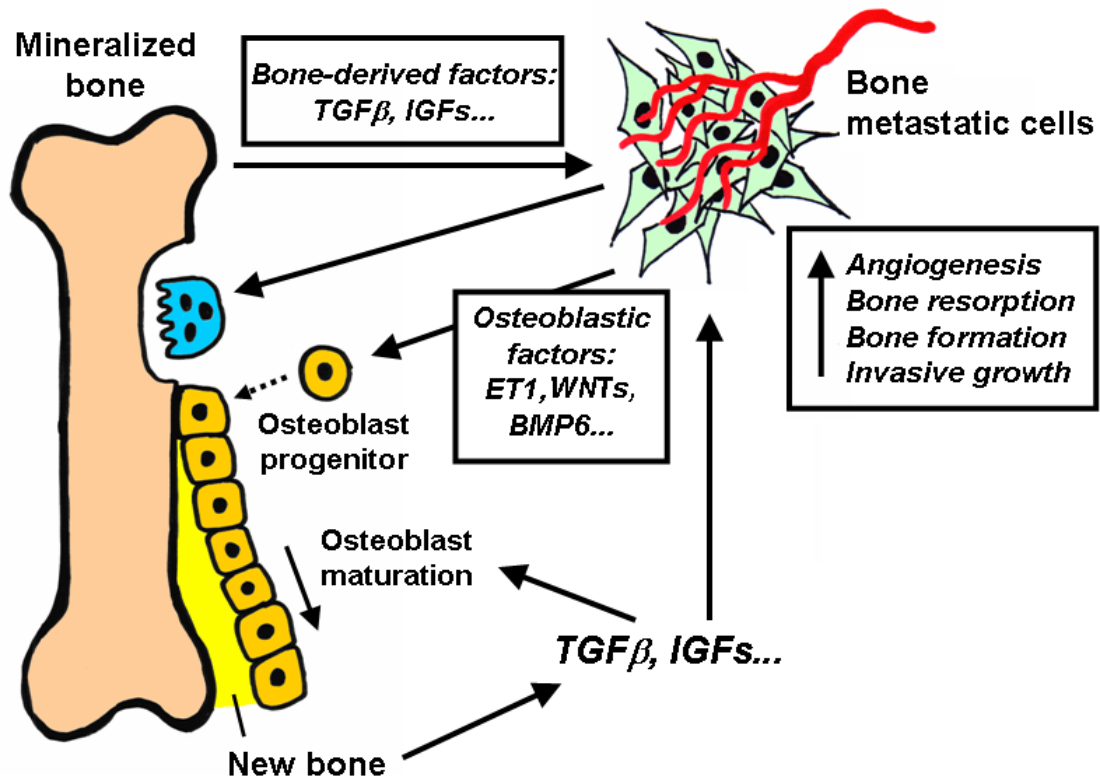


**Fig. 7 Pathophysiology of osteoblastic bone metastasis.** Release of ET1 and of different BMPs and WNTs by metastatic prostate cancer cells causes nearby osteoblast progenitors to differentiate into osteoblasts. These secrete growth factors which can stimulate cancer cell growth. Therefore, a 'vicious cycle' is also considered to occur in osteoblastic metastasis. [Buijs & van der Pluijm 2009]

On the other hand, in the case of osteoblastic metastasis, osteoblast proliferation and matrix deposition become increased [Yang *et al.* 2001, Logothetis & Lin 2005, Hall *et al.* 2005, Hall *et al.* 2006]. Prostate cancer cells alter bone homeostasis by secreting factors such as BMPs, WNTs and endothelin 1 (ET1) that directly affect osteoblast function, as well as PSA and other proteases which influence bone formation indirectly, e.g. by releasing and activating growth factors present in the bone microenvironment (Tab. 1) [Logothetis & Lin 2005, Yin *et al.* 2005, Rentsch *et al.* 2009]. The net result is increased osteoblast proliferation and differentiation, leading to increased deposition of abnormal, woven bone. Osteoblast-secreted factors in turn promote tumor cell survival and growth, enforcing the cycle (Fig. 7) [Mundy 2002, Logothetis & Lin 2005, Yin *et al.* 2005, Choueiri *et al.* 2006]. Prostate cancer cells also produce factors that stimulate osteoclast activity [Keller & Brown 2004].

**Tab. 1 Factors produced by prostate cancer cells that induce bone formation** [Logothetis & Lin 2005]

Factor	Target	Effect on osteoblasts
BMP2, 6	Osteoblasts	Induced differentiation
TGF $\beta$	Osteoblasts	Increased proliferation
PDGF	Osteoblasts	Increased proliferation
FGF	Osteoblasts	Increased proliferation and differentiation
VEGF	Osteoblasts	Increased proliferation
WNT	Osteoblasts	Increased proliferation and differentiation
ET1	Osteoblasts	Increased proliferation and differentiation
PSA	PTHrP (cleaves)	Increased proliferation
uPA	IGFBP3 (cleaves)	Increased proliferation

IGFBP3, IGF-binding protein 3; PDGF, platelet-derived growth factor; VEGF, vascular endothelial growth factor.  
For other abbreviations, see Abbreviations.

Different prostate cancer cell lines are capable of causing either osteolytic or osteoblastic bone metastases in immunocompromised mouse models [Nemeth *et al.* 1999, Thalmann *et al.* 2000, Fisher *et al.* 2002]. The degree of osteolytic or osteoblastic capability can be linked to differences in the cancer cell secretome, more specifically - to the secreted factors that affect the bone microenvironment. In particular, recent studies show that cancer cell-secreted DKK1 and NOG, which suppress bone formation by inhibiting - respectively - WNT and BMP signaling in osteoblasts, are crucial determinants of osteolytic metastasis [Hall *et al.* 2005, Hall *et al.* 2006, Schwaninger *et al.* 2007, Dai *et al.* 2008, Rentsch *et al.* 2009].

### 1.2.5. Current perspectives for bone metastasis therapy.

The number of skeletal metastatic foci is the most powerful independent prognostic factor of poor survival in advanced prostate cancer. Disease progression frequently occurs in the metastases, even though androgen ablation therapy still provides adequate control of disease at the primary site. The *in vivo* response of malignant cells to anticancer therapies is directly influenced by the local milieu. For example, in the case of prostate cancer cells, cytokines such as IL6 can transactivate the AR even in the absence of androgen, thereby inhibiting apoptosis. This can explain the long-term failure of androgen ablation therapy in prostate cancer [Bogdanos *et al.* 2003, Culig *et al.* 2002, Culig *et al.* 2005].

At present, despite advances in the diagnosis and management of prostate carcinoma, advanced disease with skeletal metastasis remains incurable. Current therapeutic options - mostly palliative - include hormonal therapy, pharmacological management of bone pain, radiotherapy for pain and spinal cord compression, various chemotherapy regimens, and the

use of bisphosphonates to inhibit osteoclast activity. Various targeted therapies, e.g. aimed at ET1 signaling or at normalizing the RANKL/OPG axis, are being developed. The complex nature of tumor-bone microenvironment interactions and the presence of multiple pathways that lead to bone metastasis suggests that simultaneous targeting of these pathways in the metastatic cascade is required for effective treatment [Mundy 2002, Logothetis & Lin 2005, Virk & Lieberman 2007].

Importantly, bone cells such as osteoblasts are thought to be involved in the establishment, maintenance and regulation of CSC niches. A novel concept suggests that prostate CSCs are required to initiate bone metastases and that bone provides a niche which enables their long-term survival. The presence of disseminated cancer cells in the bone marrow of prostate cancer patients is an early event; it has been suggested that the bone microenvironment enables them to remain viable and quiescent (i.e. non-dividing) for long periods, a situation known as minimal residual disease [Pantel & Brakenhoff 2004, Buijs & van der Pluijm 2009]. Changes in osteoblast physiology and function may, therefore, alter niche characteristics which mediate the dormancy and survival of CSCs in bone. Therapies targeted at the dormant CSCs and/or at the niche that supports them are an important future possibility.

Disseminated cancer cells within the bone marrow can remain quiescent, and thus invulnerable to chemotherapy, for years before a clinically evident lesion develops [Pinski *et al.* 2001, Buijs & van der Pluijm 2009]. There is evidence from *in vitro* models that crosstalk with osteoblasts induces gene expression changes in prostate cancer cells involving suppressed proliferation and enhanced adhesion, which favor the bone colonization process. Large-scale transcript profiling and quantitative RT-PCR have shown that osteoblast-released soluble factors cause the repression of various G<sub>1</sub> and S phase promoting genes, accompanied by an elevation of cell cycle inhibitory genes. This enhanced G<sub>0</sub>-G<sub>1</sub> checkpoint control diminishes tumor cell chemosensitivity. Genes encoding anchoring junction components are also elevated, presumably facilitating tumor cell adherence to inner bone surfaces [Pinski *et al.* 2001, Knerr *et al.* 2004]. Interactions such as these, if studied *in vivo*, might provide further options for therapy aimed at the prevention of skeletal metastasis.

### 1.2.6. Osteomimicry

Koenenman *et al.* (1999) have formulated the hypothesis that prostate cancer cells metastasizing to bone must become osteomimetic, i.e. express genes characteristic for the

osteoblast phenotype, in order to survive and grow within the skeleton. This hypothesis is substantiated by autopsy findings. The ability of prostate cancer cells to mimic bone could aid prostate cancer bone colonization. Osteomimicry appears to be facilitated by common growth factor tropisms between bone stromal cells, osteoblasts and prostate cancer cells, wherein a number of growth factors and their receptors are involved.

A model of prostate cancer progression and osteomimicry exists and has been extensively characterized. The sublines C4, C4-2, and C4-2B, which demonstrate increasing proliferative capability, invasiveness and capability to metastasize, were derived from the LNCaP prostate cancer cell line by co-culturing with human bone fibroblasts and growing in castrated athymic male mice [Thalmann *et al.* 2000]. C4-2B, derived from a bone metastasis of the androgen-independent and highly invasive C4-2, exhibited osteomimetic properties and showed the most potent ability to metastasize to bone *in vivo*. Unlike LNCaP cells, which are androgen-dependent, capable of growth in immunocompromised mice only when co-inoculated with supporting stromal cells and do not spontaneously generate metastases, the C4-2B subline has a high growth potential, is androgen-independent and osteotropic, i.e. capable of spontaneous metastasis to bone. It has an osteoblast-like phenotype, characterized by the expression of specific markers such as AP, BSP, OC, OPG and RANKL. Most importantly, C4-2B cells produce mineralized nodules in culture. These data demonstrate a novel mechanism through which prostate cancer cells may directly contribute to the formation of osteoblastic lesions [Thalmann *et al.* 2000, Lin *et al.* 2001]. In another study, C4-2B also induced approximately 80% more osteoclastogenesis than the parental LNCaP line, with strong evidence that this effect is linked to RANKL expression by the cancer cells [Zhang *et al.* 2001]. Thus, metastatic prostate cancer cells within bone appear to usurp some of the functions of osteoblasts. The LNCaP progression model is thought to accurately reflect the stages of prostate cancer progression *in vivo* [Thalmann *et al.* 2000].

The mechanisms of osteomimicry remain unclear. The expression of bone-specific proteins by prostate cancer cells might be mediated by the same transcription factors which are active in osteoblasts [Koeneman *et al.* 1999, Lin *et al.* 2001]. C4-2B cells acquire osteoblastic properties in part through the activation of Notch and ERK signaling pathways, which are essential for CBFA1 DNA binding activity and *OC* gene expression [Zayzafoon *et al.* 2004]. Curcumin, a non-toxic tyrosine kinase inhibitor, reverses osteomimicry in C4-2B cells by interfering with growth factor receptor pathways [Dorai *et al.* 2004]. Finally, it has been reported that  $\beta$ 2-microglobulin, secreted by osteoblasts and by prostate cancer cell lines, enhances BSP and OC expression in human prostate cancer cells by activating a cyclic AMP-

dependent protein kinase A signaling pathway [Huang *et al.* 2005, Huang *et al.* 2006]. The mechanisms regulating the expression of other osteomimetic genes have yet to be elucidated.

To summarize, the establishment of skeletal metastatic lesions in prostate cancer is fueled by a synergistic paracrine loop existing between the cancer cells and osteoblasts. Investigating the molecular mechanisms of their crosstalk may prove the key to effective therapy or prevention of prostate cancer bone metastases.

### 1.3. Aims

The aims of the here presented dissertation were as follows:

- Investigating the mechanisms of the crosstalk between prostate cancer cells and osteoblasts, known to affect the transcriptomes of both cell types. Identifying the secreted proteins that contribute to this crosstalk, with a focus on osteomimicry and bone remodeling.
- Identifying genes and pathways affected in osteoblasts by crosstalk with prostate cancer cells, creating a picture of the early-stage events ultimately leading to bone colonization by prostate cancer cells and dysregulated bone formation within metastatic lesions.

## 2. Materials and methods

Frequently-used chemicals were obtained from Carl Roth GmbH, Fluka, Merck or Sigma-Aldrich and are not listed separately. In the case of reagents, materials and equipment used for multiple applications, the source is listed only once.

### 2.1. Cell culture

Cells that are cultured directly from a subject are known as primary cells and usually have a limited lifespan, whereas an established or immortalized cell line has acquired the ability to proliferate indefinitely. Numerous cell lines have been established by researchers. They can be used as an *in vitro* model for the living organism, since they retain the characteristic qualities of their ontogenetic origin.

Cells are grown and maintained in sterile, controlled conditions. Culture conditions may vary widely depending on the cell type, and their variation for a particular cell type can result in different phenotypes being expressed.

Cells can be grown in suspension or as adherent cultures, attached to a surface such as the bottom of a plastic culture flask. Most cells derived from solid tissues are adherent.

#### Media and supplements

RPMI 1640 + GlutaMAX (Gibco BRL)

Dulbecco's Minimal Essential Medium (DMEM) + 4500 mg/ml glucose + GlutaMAX (Gibco BRL)

DMEM/F12 + GlutaMAX (Gibco BRL)

Fetal calf serum (FCS) (Biochrom AG)

Geneticin (50 mg/ml) (Gibco BRL)

MEM Non-essential amino acids (NEAA), 100x (Gibco BRL)

#### Reagents

Dimethyl sulfoxide (DMSO) (Sigma-Aldrich)

Hydrochloric acid (HCl) 37% w/v (Prolabo)

Sodium dodecylsulfate (SDS) (GERBU Biotechnik GmbH)

Thiazolyl blue tetrazolium bromide (MTT) (Sigma-Aldrich)

Trypsin 2,5% w/v (Gibco BRL)

#### Materials

Cell culture flasks, plastic (75 cm<sup>2</sup>) (Greiner Bio-One)

Cell culture plates, 6-well, Falcon™ (Becton Dickinson Labware)

Cell culture plates, 6-well (Greiner Bio-One)

## 2. Materials and methods

Cell culture plates, 12-well, Falcon™ (Becton Dickinson Labware)  
 Cell scrapers (“rubber policeman”) (Corning Incorporated)  
 Cryo-tubes (Nalgene)  
 ELISA strips (Greiner Bio-One)  
 15 ml plastic tubes (Greiner Bio-One)  
 50 ml plastic tubes (Greiner Bio-One)  
 Inserts for 6-well cell culture plates, 1 µm pore size (Becton Dickinson Labware)

### **Equipment**

Automatic pipetting help, neoAccupette 3-9905 (NeoLab Migge Laborbedarf-Vertriebs GmbH)  
 Centrifuge with cooling, Megafuge 1.0 R (Heraeus); rotors #3041, #3360  
 Centrifuge with cooling, Sorvall RC 5C Plus (GMI); rotor #SS-34  
 Freezer (-20°C) (Liebherr)  
 Freezer (-80°C) (Sanyo)  
 Incubator, Steri-Cult 200 (Labotect)  
 Incubator, B5060 EK/CO<sub>2</sub> (Heraeus)  
 Light microscope, Telaval 3 (Zeiss)  
 Microplate reader, Multiskan MS (Labsystems)  
 Neubauer chamber for counting cells (Brand)  
 Laminar flow cabinet, Bio Gard Hood (Baker Company)  
 Water bath, SW-20 (Julabo)

**Tab. 2 Prostate cancer cell lines used.**

<b>Cell line</b>	<b>LNCaP</b>	<b>C4-2B4</b>	<b>PC3</b>
<b>Description</b>	Human prostate adenocarcinoma	Human prostate adenocarcinoma - subline of LNCaP	Human prostate adenocarcinoma
<b>Morphology</b>	Epithelial	Epithelial	Epithelial
<b>Derived from</b>	Supraclavicular lymph node metastasis in 50-year-old Caucasian male [Horoszewicz <i>et al.</i> 1983]	Bone metastasis of androgen-independent LNCaP subline C4-2	Bone metastasis of a grade IV prostatic adenocarcinoma from a 62-year-old male Caucasian [Kaighn <i>et al.</i> 1979]
<b>Lesions produced in nude mice</b>	Mixed osteoblastic-osteolytic [Nemeth <i>et al.</i> 1999]	Osteoblastic [Thalmann <i>et al.</i> 2000]	Osteolytic [Nemeth <i>et al.</i> 1999]
<b>Androgen independency</b>	No	Yes	Yes
<b>Metastatic potential</b>	Low	High	High
<b>Source</b>	Dr. G. Thalmann, University of Bern, Bern, Switzerland	Dr. G. Thalmann, University of Bern, Bern, Switzerland	Dr. H. Corban-Wilhelm, DKFZ, Clinical Cooperation Unit, Radiation Therapy

**Tab. 3 Non-prostate cell lines used.**

Cell line	HeLa	IMR-90	hfOB 1.19
<b>Description</b>	Human cervical adenocarcinoma	Lung fibroblasts	Human fetal osteoblasts, conditionally immortalized by stable transfection with SV40 large T antigen
<b>Derived from</b>	Cervical lesion in 31-year-old black female	Lungs of a 16-week female fetus	Bone biopsies from a spontaneous miscarriage
<b>Morphology</b>	Epithelial	Fibroblast	Osteoblast
<b>Properties</b>	Malignant cells with high proliferative capacity [Gey <i>et al.</i> 1952]	Standard diploid fibroblast strain; undergo senescence after a certain number of population doublings. [Nichols <i>et al.</i> 1977]	Able to differentiate into mature osteoblasts expressing typical bone formation markers. [Harris <i>et al.</i> 1995]
<b>Source</b>	J. Richards; Division of Pathochemistry (B0100), DKFZ Heidelberg, Germany	American Type Culture Collection (ATCC), CCL186	Dr N. Schuetze and Dr T. Spelsberg, Endocrine Research, Mayo Clinic, Rochester, Minnesota, USA

The cells were tested and found free of *Mycoplasma spp.* contamination.

### 2.1.1. Cell cultivation, passaging and harvest

As they divide, adherent cells fill the available surface and undergo growth inhibition upon reaching confluence. It is necessary to dislodge them, dilute the cell suspension and seed a smaller number out. This is known as passaging or splitting cells. During passaging, cells are commonly detached from the flask by the action of the endopeptidase trypsin, which hydrolyzes the peptide bonds between lysine and arginine in protein chains.

LNCaP, C4-2B4, PC3 and HeLa were cultured at 37°C in RPMI-1640 containing 10% FCS and 1% nonessential amino acids. IMR-90 were cultured at 37°C in DMEM containing 4500 mg/ml glucose and 10% FCS, and cells between passages 10 and 20 were used. hfOB were cultured at 33.5°C in DMEM-F12 containing 10% FCS and 30 µg/ml geneticin, and cells between passages 16 and 24 were used. All cell lines were cultured in an atmosphere containing 95% air and 5% CO<sub>2</sub>, with 4% humidity.

When passaging was necessary, the medium was aspirated. Cells were washed with 5 ml PBS (128 mM NaCl; 2 mM KCl; 8 mM Na<sub>2</sub>HPO<sub>4</sub>; 2 mM KH<sub>2</sub>PO<sub>4</sub>; pH 7.2-7.4), then treated with 2 ml trypsin-EDTA solution (0.25% w/v trypsin; 0.5 mM EDTA; pH 7.2) and incubated briefly at 37°C. The trypsinized cells were resuspended in medium and a small number was seeded out again.



### 2.1.2. Freezing and thawing cells

The phenotype of a cell line may change as a result of prolonged culturing *in vitro*. To maintain the original characteristics of a cell line over many years, it is necessary to permanently store aliquots with a low passage number frozen in liquid nitrogen. These aliquots can then periodically be used to replace the cells in culture. To protect the cells from ice crystal damage during freezing, the cryoprotectant DMSO must be added to medium.

Before freezing, cells were trypsinized, resuspended in medium and counted.  $1 \cdot 10^6$  cells were transferred to a cryo-tube and DMSO was added in drops to a final concentration of 10%. Cells were initially frozen at  $-80^{\circ}\text{C}$  and transferred to liquid nitrogen ( $-196^{\circ}\text{C}$ ) after several hours.

Cells taken out from liquid nitrogen were thawed in a water bath at  $37^{\circ}\text{C}$  and seeded out in 15 ml fresh medium. The medium was changed after 24 h to remove traces of DMSO.

### 2.1.3. *In vitro* metastasis model

Cell crosstalk can be mediated either by direct physical contact *via* adhesion molecules or by released factors. An *in vitro* bicompartiment coculture system has been characterized in literature as a model for paracrine interactions in the early stages of bone metastasis [Knerr *et al.* 2004, Pinski *et al.* 2001, Yang *et al.* 2001]. Prostate cancer cells and bone cells are seeded, respectively, in culture plates and transwell inserts with a porous membrane bottom. Inserts are subsequently placed into wells and the cells are cocultured in shared media (Fig. 8). This model limits cell crosstalk to soluble factors. Cells from inserts and wells can then be harvested separately and assayed for changes in transcript and protein levels. Paracrine interactions without direct cell-cell contact have been proved to induce significant changes in gene expression in both prostate cancer cells and osteoblasts [Yang *et al.* 2001, Pinski *et al.* 2001, Knerr *et al.* 2004, Zayzafoon *et al.* 2004].

For coculture experiments described in section 3.1,  $6 \cdot 10^5$  LNCaP, C4-2B4 or PC3 cells were seeded in 6-well Falcon<sup>TM</sup> culture plates and  $6 \cdot 10^5$  hfOB cells were seeded into inserts possessing 1  $\mu\text{m}$  porous membrane bottoms. After allowing cells to grow overnight, hfOB-containing inserts were placed into wells lined with either LNCaP, C4-2B4 or PC3 and cocultured in a 1:1 mixture of respective media (6 ml/well) at  $37^{\circ}\text{C}$  for the designated times. Cells were harvested by scraping in PBS and pelleted by centrifugation for 4 min. at  $1431 \cdot g$ ,  $4^{\circ}\text{C}$ . After removing the supernatant, pellets were stored frozen at  $-80^{\circ}\text{C}$  until analysis.

## 2. Materials and methods

For coculture experiments described in section 3.2, hfOB ( $6 \cdot 10^5$ ) were seeded in 6-well Falcon™ culture plates.  $4 \cdot 10^5$  cells from either LNCaP, C4-2B4, PC3, HeLa or IMR-90 were seeded into inserts possessing 1  $\mu\text{m}$  porous membrane bottoms. After allowing cells to grow overnight, the inserts were placed into wells lined with hfOB. Cells were cocultured in a 1:1 mixture of respective media at 37°C for 48 h.

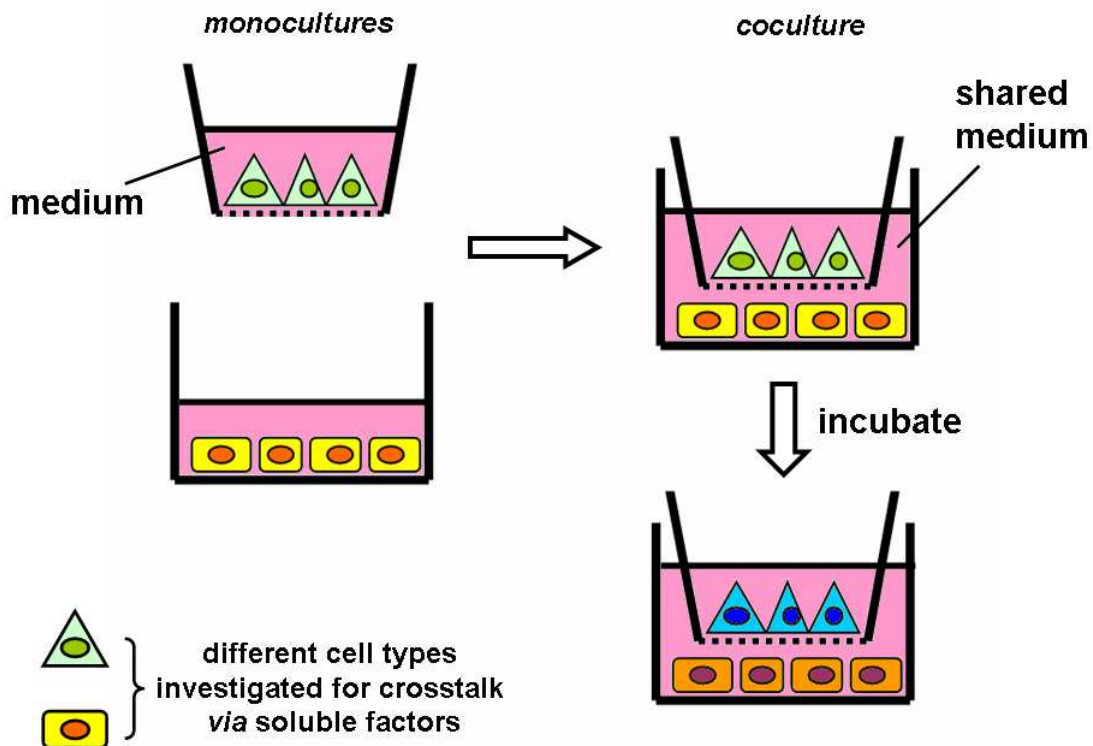


Fig. 8 *In vitro* metastasis model.

### 2.1.4. Preparation of conditioned medium

Conditioned medium (CM) was prepared by culturing cells in the flask to 90% confluence, washing twice with 10 ml PBS, then incubating with 12 ml serum-free RPMI-1640 + 1% nonessential amino acids (LNCaP, C4-2B4, PC3) or DMEM-F12 + 30  $\mu\text{g}/\text{ml}$  geneticin (hfOB) at 37°C. Supernatants containing secreted proteins were collected after 24 h and centrifuged (5000-g, 30 min, 4°C) to pellet debris. Conditioned medium was either used fresh in cell culture experiments or frozen at -20°C for later analysis.

### 2.1.5. Cell treatment with conditioned medium, antibody neutralization assays and recombinant protein stimulation

For experiments described in section 3.1.2, cells (LNCaP, C4-2B4 or PC3) were seeded in 6-well culture plates and grown to 80% confluence, then washed twice with PBS and switched to serum-free 1:1 RPMI 1640+DMEM-F12 (control) or 1:1 RPMI 1640 + hfOB CM (see above) for the designated times. For antibody neutralization experiments, 400 ng/ml of anti-IL6 (sc-7920), anti-TGF $\beta$ 1 (sc-146) or anti-FGF2 (sc-7911) antibodies (all rabbit, polyclonal) were added to the medium. All antibodies were from Santa Cruz Biotechnology.

For stimulation with recombinant proteins, 80% confluent LNCaP cells were washed twice with PBS and incubated in serum-free RPMI1640 for 24 h, then incubated with 10 ng/ml human IL6 (ImmunoTools) or 10 ng/ml human TGF $\beta$ 1 (Santa Cruz Biotechnology) for 24 h.

In the experiments described in sections 3.2.3 and 3.2.5, hfOB were seeded in 6-well culture plates and grown to 90% confluence, then washed twice with PBS and switched to serum-free 1:1 RPMI 1640+DMEM-F12 (control) or 1:1 DMEM-F12 + LNCaP CM or PC3 CM (see above) for the designated times.

Serum-free media, whenever mentioned, contained all other necessary supplements except FCS.

### 2.1.6. MTT cell proliferation assay

The reduction of tetrazolium salts is widely accepted as a reliable way to examine cell proliferation. The yellow tetrazolium compound MTT (3-(4,5-dimethylthiazolyl-2)-2,5-diphenyltetrazolium bromide) is reduced by metabolically active cells to crystals of insoluble purple formazan, which can be solubilized and quantified by spectrophotometric means. Absorbance at 570 nm is directly proportional to the number of viable cells.

To investigate the influence of prostate cancer cell-related factors on osteoblast proliferation, hfOB cells ( $2 \cdot 10^5$ /well) were seeded out on 12-well plates and allowed to grow overnight, reaching a confluence of ca. 10%. Cells were then switched to 1:1 RPMI 1640 + DMEM-F12 + 5% FCS (control) or 1:1 DMEM-F12 + CM + 5% FCS and left to grow at 33.5°C (the permissive temperature for hfOB proliferation). After 72 h, MTT solution (5 mg/ml MTT in PBS) was added to the wells to a final working concentration of 0.45 mg/ml. A cell-free well with control medium and MTT served as the blank. After 3 h of further

incubation at 33.5°C, the newly formed formazan crystals were dissolved by adding 1 ml/well acidified SDS solution (20% w/v SDS, 20 mM HCl). Plates were incubated overnight at room temperature in the dark. Then, the contents of each well were mixed and 100 µl were transferred in triplicate to wells on an ELISA microplate strip. Absorbance was read at 570 nm.

### 2.2. RNA and DNA

According to the central dogma of molecular biology, the main carrier of genetic information in the cell is double-stranded DNA, which is transcribed into complementary copies of RNA. Messenger RNA (mRNA) then in turn serves as the template for protein synthesis, known as translation. Gene expression is subject to many levels of regulation, both at the stages of transcription and translation. However, mRNA transcript levels, which can change dynamically in response to signaling input from many different pathways, can offer important clues as to the events occurring in the cell.

RNA is sensitive to degradation by ubiquitous RNase enzymes, present e.g. in dust and on the skin surface. Therefore all procedures involving RNA must be performed on ice, and RNase contamination of the sample must be avoided by clean working conditions and wearing gloves. All solutions must be prepared using water treated with diethyl pyrocarbonate (DEPC), which inactivates RNAses.

#### **Reagents**

Biozym LE Agarose (Biozym Scientific GmbH)

Chloroform (Sigma-Aldrich)

DEPC (Sigma-Aldrich)

DEPC-treated H<sub>2</sub>O (ultrapure H<sub>2</sub>O treated with 0,1% DEPC for several hours, then autoclaved)

EDTA (Acros Organics)

Ethidium bromide 1% w/v (Carl Roth GmbH)

50 kB DNA ladder (New England Biolabs)

Isopropanol (Fluka)

Platinum SYBR Green qPCR SuperMix-UDG (Invitrogen)

SuperScript III First-Strand Synthesis System (Invitrogen)

Taq DNA polymerase (Invitrogen)

TriFast (Peqlab)

Tris(hydroxymethyl)aminomethane (Tris) (Sigma-Aldrich)

### **Materials**

MicroAmp Optical 8-Cap Strips (Applied Biosystems)

MicroAmp Optical 96-Well Reaction Plates (Applied Biosystems)

### **Equipment**

Agarose gel running chambers (LMS GmbH Labortechnik)

Gradient PCR machine, Mastercycler gradient (Eppendorf)

Microcentrifuge, Biofuge Pico (Heraeus)

Electrophoresis power supply, model 200/2.0 (Bio-Rad)

Electrophoresis power supply, PowerPac 300 (Bio-Rad)

MultiImage™ Light Cabinet - camera and imaging system for gel visualisation (Alpha Innotech Corporation)

Mx3000P light cycler (Stratagene)

Spectrophotometer, LS 500 (Dr Lange)

Thermal blocks, Thermostat 5320 (Eppendorf)

Vacuum concentrator (Bachofer)

Vacuum pump (KNF-Neuberger)

Vortex mixer (NeoLab)

### **Software**

AlphaImager™ 4.1.0 (gel visualisation)

Primer Designer 2.0

MxPro 3.20 (quantitative real-time PCR)

### **2.2.1. RNA isolation**

Popular methods for isolating nucleic acids are based on a common principle. First, the cells are lysed with a reagent such as phenol, and extraction with a solvent is performed to separate the mixture into an aqueous phase and a phenol-solvent phase. Nucleic acids stay in the aqueous phase and can be precipitated with ethanol or isopropanol.

TriFast reagent is a variation of the single-step method reported by Chomczynski and Sacchi (1987) for total RNA isolation. Composed of guanidine isothiocyanate and phenol in a mono-phase solution, it effectively dissolves DNA, RNA, and protein. After adding chloroform and centrifuging, the mixture separates into 3 phases: an aqueous phase containing the RNA, the interphase containing DNA and an organic phase containing proteins. Each component can then be isolated after separating the phases.

Total RNA was extracted from frozen cell pellets using TriFast solution according to the manufacturer's instructions. Cells were lysed for 5 min. at room temperature with 1 ml of TriFast reagent per pellet. 0.2 ml chloroform was added to each tube, the mixture was agitated for 15 s, incubated for 3 min. at room temperature and centrifuged for 15 min. at 20 124-g at 4°C, resulting in separation into a lower (phenolic) and upper, colourless (water) phase. The water phase was removed to a fresh tube. 0.5 ml isopropanol/tube was added and the mixture was agitated, then incubated for 10 min. at room temperature. After centrifugation for 10 min. at 20 124-g, 4°C the supernatant was removed and each pellet was washed twice with 1 ml 70% ethanol, with 5 min. centrifugation at 20 124-g, 4°C between washes. After the second wash step, the supernatant was removed using a water pump. The pellets were then dried for 1-2 min in a vacuum concentrator and dissolved in an appropriate volume of DEPC-treated H<sub>2</sub>O (25-60 µl, depending on pellet size).

### 2.2.2. RNA quantification and quality control

RNA quantification was performed spectrophotometrically by measuring absorbance (A) at 260 nm (wavelength absorbed by DNA, RNA and proteins) and 280 nm (wavelength absorbed by proteins alone). For the measurements, 1 µl of RNA was diluted in 100 µl water and diluted further if necessary.

The RNA concentration was determined from the following formula:

$$(A_{260} \times 40 \times \text{dilution}) / 1000 = \text{RNA concentration } [\mu\text{g} / \mu\text{l}]$$

$A_{260} / A_{280}$  is an estimate of RNA purity (degree of protein contamination). It was ascertained that the purity quotient values for the RNA samples were always in the required range between 1.5 and 2.2.

RNA quality was verified by running 1 µg RNA/well on a 1% agarose gel. Before loading, samples were mixed with 5x RNA loading dye (50% v/v glycerol; 1 mM EDTA pH 8.0; 0.25% w/v bromophenol blue; 0.25% w/v xylene cyanol FF). Bands were visualised by staining the gel in ethidium bromide solution, then rinsing with H<sub>2</sub>O and photographing under UV light. Strong, distinct bands of ribosomal RNA indicate good RNA quality.

### 2.2.3. Reverse transcription

Reverse transcription is the process of making a DNA (deoxyribonucleic acid) molecule from a single-stranded RNA (ribonucleic acid) template. This reaction, catalyzed by the enzyme reverse transcriptase, is commonly used in research for mRNA profiling. The classical PCR technique can be applied only to DNA strands, but, with the help of reverse transcriptase, RNA can be transcribed into DNA, making PCR analysis of RNA molecules possible.

In a two-step RT-PCR approach, a cDNA template was synthesized using the SuperScript III First-Strand Synthesis System. 5 µg total RNA were combined with 1 µl oligo(dT)<sub>20</sub> primer (50 µM), 1 µl dNTPs (10 mM) and DEPC-treated H<sub>2</sub>O to 10 µl. After incubation for 5 min. at 65°C and 1 min. on ice, 2 µl 10x RT-buffer, 2 µl DTT (100 mM), 4 µl MgCl<sub>2</sub> (25 mM), 1 µl RNaseOUT (40 U/µl) and 1 µl SuperScript III reverse transcriptase (200 U/µl) were added, bringing the reaction volume up to 20 µl. Reverse transcription was carried out at 55°C for 50 min, followed by enzyme deactivation at 85°C for 5 min, after which the RNA strand was digested by 1 µl *E. coli* RNase H (2 U/µl) at 37°C for 20 min. At the end, reactions were diluted with sterile H<sub>2</sub>O to a final volume of 50 µl.

### 2.2.4. Quantitative real-time RT-PCR

The polymerase chain reaction (PCR) is one of the best-known techniques in molecular biology. It is used to amplify DNA *in vitro* with the use of two oligonucleotide primers, each of them complementary to one end of the target sequence. The primers are elongated by a thermostable DNA polymerase in repeated cycles of DNA denaturation, primer annealing and polymerisation, each of these steps occurring at a different temperature. A thermostable DNA polymerase such as Taq is used, since it can withstand repeated exposures to the high temperature required for DNA denaturation.

PCR technology is widely used for quantifying DNA because of its high sensitivity. In an optimized reaction, the target quantity will approximately double during each amplification cycle. In quantitative real-time PCR, a fluorescent reporter molecule such as the SYBR Green I dye, which binds to double-stranded DNA, is used to monitor the progress of the amplification reaction. The fluorescence intensity increases proportionally with each amplification cycle in response to the increased amplicon concentration. The first cycle in which the amplification-generated fluorescence rises above the ambient background signal is

called the threshold cycle, or Ct. This Ct value can be directly correlated to the initial target concentration in the sample.

cDNA was quantitatively PCR-amplified on 96-well microplates by combining 10  $\mu$ l 2x Platinum SYBR Green qPCR SuperMix-UDG, 1  $\mu$ l each of appropriate sense and antisense primers (20 pmol/ $\mu$ l) and 1  $\mu$ l RT sample (to minimize the pipetting error, 8  $\mu$ l were taken after diluting the samples 1:8 with H<sub>2</sub>O) in a 20  $\mu$ l reaction. Samples were assayed in duplicate. Thermal cycling was performed using the Mx3000P light cycler. The following program was used for all runs:

### **Segment 1**

95°C 10 min. (initial denaturation)

### **Segment 2** (30-45 cycles)

95°C 30 sec. (denaturation)

X°C 1 min. (annealing)

72°C 30 sec. (elongation)

### **Segment 3** (dissociation curve)

95°C 1 min. (denaturation)

X°C 30 sec. (annealing)

95°C 30 sec. (denaturation)

X = annealing temperature

Amplification rates were measured automatically using MxPro 3.20 software. Results were normalized to casein kinase II, beta subunit (*CK2B*), a housekeeping gene [Pyerin & Ackermann 2003]. A dissociation curve was included in every PCR program to verify that each reaction yields a single product. Additionally, the specificity of all PCR reactions was verified by electrophoresis on 2% agarose gels. Before separation, samples were mixed with 6x DNA loading dye (0.25% w/v bromophenol blue; 0.25% xylene cyanol FF; 30% glycerol) and a 50 kb DNA ladder was always separated in parallel.

For primer sequences and cycling conditions, see Tab. 4 (*pages 53-54*).

### **2.2.5. Primer design and optimization of annealing temperatures**

Primers were designed using Primer Designer 2.0 against mRNA sequences from the database Entrez Gene (for link see Materials and methods 2.3.4). Primer specificity was verified in each case by a Blast search against the complete human genome. With the



exception of *FOXO3*, all primers were exon-exon spanning to exclude the amplification of contaminating genomic DNA.

To determine optimal cycling conditions, 1  $\mu$ l cDNA was PCR-amplified in a 25  $\mu$ l reaction, comprising 2.5  $\mu$ l 10x PCR buffer (100 mM Tris-HCl pH 8.8; 50 mM KCl; 1% Triton X-100), 1  $\mu$ l dNTP mix (10 mM), 1  $\mu$ l MgCl<sub>2</sub> (50 mM), 1  $\mu$ l each sense and antisense primers (20 pmol/ $\mu$ l), 0.5  $\mu$ l Taq DNA polymerase (5 U/ $\mu$ l) and sterile H<sub>2</sub>O.

The following amplification program was used:

1. 94°C 3 min. (initial denaturation)
  2. 94°C 30 s (denaturation)
  3. X°C 1 min. (annealing)
  4. 72°C 30 s (elongation)
- (steps 2-4 repeated 39 x)
5. 72°C 3 min. (end polymerization).

A gradient PCR cycler was used, allowing different annealing temperatures to be tested in parallel. Reaction products were separated on a 2% agarose gel.

### 2.3. OligoDNA chip technology

A DNA microarray consists of thousands of microscopic spots of DNA oligonucleotides, called probes, chemically bonded to the surface of a glass or silicon chip. Each probe type is located in a specific area on the array called a probe cell, containing millions of copies of a given probe. A cDNA or cRNA sample, known as the target, is hybridized to the array under high-stringency conditions. Probe-target hybridization is usually detected and quantified by fluorescence-based detection of fluorophore-labeled targets to determine the relative abundance of nucleic acid sequences in the target. Gene expression profiling *via* microarrays makes it possible to simultaneously monitor the expression of thousands of genes.

In the Affymetrix oligoDNA array system (GeneChip), a biotin-labeled cRNA target is hybridized to chips containing 25 bp-long cDNA sequences complementary to different areas of mRNA transcripts. The chips are then stained with streptavidin-phycoerythrin and scanned (Fig. 9). The Human Genome U133A 2.0 array contains more than 22,000 probe sets corresponding to 14,500 well-characterized genes.

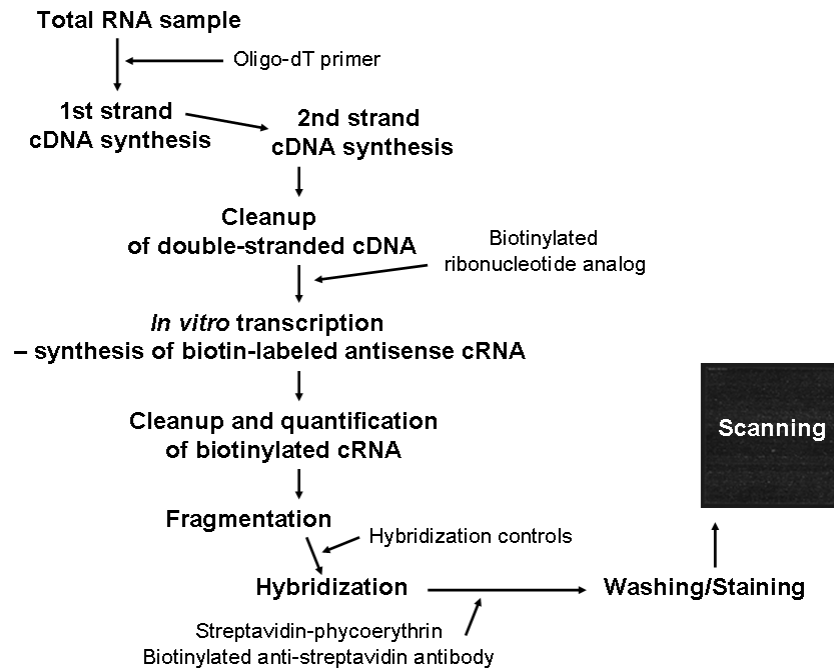


**Fig. 9 Flow chart of Affymetrix GeneChip array protocol.**

### Reagents

Control Oligo B2, 3 nM (Affymetrix)

DNA ligase (Invitrogen)

DNA polymerase I (Invitrogen)

Enzo BioArray HighYield RNA Transcript Labeling Kit (Affymetrix)

GeneChip Eukaryotic Hybridization Control Kit (Affymetrix)

GeneChip Hybridization, Wash and Stain Kit (Affymetrix)

Herring sperm DNA (Promega)

MES (Sigma-Aldrich)

Phenol:chloroform:isoamyl alcohol 25:24:1 (saturated with 10 mM Tris-HCl pH 8.0/1 mM EDTA) (Carl Roth GmbH)

RNeasy Mini Kit (Qiagen)

SuperScript II reverse transcriptase (Invitrogen)

T4 DNA polymerase (Invitrogen)

### Materials

Human Genome U133A Array (Affymetrix)

Tough-Spots™, Label Dots (USA Scientific)

### **Equipment**

GeneChip Scanner 3000 (Affymetrix)  
Fluidics Station 450 (Affymetrix)  
Hybridization Oven 640 (Affymetrix)  
Media bottles and pre-drilled bottle caps (Affymetrix)  
Tygon Tubing, 0,04'' inner diameter (Cole-Parmer)  
Refrigerated water bath (MGW Lauda)

### **Software**

GeneChip Operating Software (GCOS) 1.4

### **2.3.1. GeneChip array target preparation (one-cycle target labeling)**

In the Affymetrix one-cycle labeling protocol, double-stranded cDNA is synthesized from total RNA isolated from cells. An *in vitro* transcription (IVT) reaction is then performed to produce biotin-labeled cRNA from the cDNA. This step serves to amplify the target. The cRNA is fragmented before hybridization to the chip.

Two individual biological replicate samples were assayed per coculture set. Target labeling, hybridization, staining and scanning of the chips was performed according to the manufacturer's instructions.

#### ***2.3.1.1. RNA purification***

Total RNA isolated using TriFast was subjected to an additional column-based cleanup using silica-based columns from the RNeasy Mini Kit, according to the manufacturer's instructions. Nucleic acids precipitated by ethanol bind selectively to a silica membrane and can be eluted with H<sub>2</sub>O.

The sample was adjusted up to 100 µl with DEPC-treated H<sub>2</sub>O and mixed with 350 µl of buffer RLT. Then, 250 µl ethanol were added. After mixing, the sample was transferred to an RNeasy Mini Kit spin column placed in a 2 ml collection tube. After centrifuging for 15 s at 16 060·g in a microcentrifuge, the flow-through was discarded and the column was washed twice with 500 µl buffer RPE with 15 s, 16 060·g centrifugation after the first wash and 2 min, 16 060·g after the second. The flow-through was discarded. The spin column was placed in a fresh collection tube and centrifuged for another 1 min at 16 060·g to completely dry the silica membrane. The spin column was placed again in a fresh collection tube and 30µl DEPC-treated H<sub>2</sub>O were added directly to the membrane. After 1 min incubation at room

temperature, RNA was eluted by centrifuging for 1 min at 16 060·g. The elution was repeated with another 30 µl DEPC-treated H<sub>2</sub>O. Samples were dried completely in a vacuum concentrator, then the RNA was resuspended in a smaller volume of H<sub>2</sub>O depending on the expected yield. The RNA yield and purity were assessed spectrophotometrically and RNA quality was verified by agarose gel electrophoresis as described in section 2.2.2.

### *2.3.1.2. Synthesis and purification of double-stranded cDNA*

For first strand cDNA synthesis, 12 µg total RNA were combined with 1 µl T7-(dT)<sub>24</sub> primer (100 pmol/µl; described below) and DEPC-treated H<sub>2</sub>O to 11 µl. After incubation for 10 min at 70°C and 1 min on ice, 4 µl 5x first strand cDNA buffer (250 mM Tris-HCl pH 8.3; 375 mM KCl; 15 mM MgCl<sub>2</sub>), 2 µl DTT (100 mM), 1 µl dNTP mix (10 mM) and 2 µl SuperScript II reverse transcriptase (200 U/µl) were added to a final volume of 20 µl. After temperature adjustment (2 min, 42°C), the reaction mixture was incubated at 42°C for a further 1 h.

#### **T7-(dT)<sub>24</sub> oligomer:**

5'-GGCCAGTGAATTGTAATACGACTCACTATAGGGAGGCGG-(dT)<sub>24</sub>-3'

Second strand synthesis was performed in a reaction volume of 150 µl, containing 91 µl DEPC-treated H<sub>2</sub>O, 30 µl 5x second strand reaction buffer (94 mM Tris-HCl pH 7.0; 453 mM KCl; 23 mM MgCl<sub>2</sub>; 0.75 mM NAD<sup>+</sup>; 50 mM (NH<sub>4</sub>)<sub>2</sub>SO<sub>4</sub>), 3 µl dNTP mix (10 µM), 1 µl DNA ligase (10 U/µl), 4 µl DNA polymerase I (10 U/µl) and 1 µl RNase H (2 U/µl). Reactions were incubated at 16°C for 2 h in a cooling water bath. Afterwards, 2 µl T4 DNA polymerase (5U/µl) were added and, after incubation for 5 min at 16°C, 10 µl EDTA (0.5 M).

The cDNA was purified by phenol-chloroform extraction. 162 µl (an equal volume) of 25:24:1 phenol:chloroform:isoamyl alcohol was added to the final cDNA synthesis preparation, to a final volume of 324 µl. After vortexing, the mixture was centrifuged at 16 060·g for 2 minutes at room temperature. The aqueous upper phase was transferred to a fresh tube. The cDNA was precipitated by adding 0.5 volumes of 7.5 M ammonium acetate and 2.5 volumes of absolute ethanol (stored at -20°C). After vortexing and centrifugation at 16 060·g for 20 minutes at room temperature, the supernatant was removed and the pellet washed twice with 0.5 ml of 80% ethanol (stored at -20°C), with 5 min centrifugation

(16 060·g, room temperature) between washes. Pellets were allowed to air dry, then resuspended in 12 µl DEPC-treated H<sub>2</sub>O.

### **2.3.1.3. In vitro transcription (IVT) and purification of biotin-labeled cRNA**

Biotin-labeled cRNA was synthesized using the Enzo BioArray HighYield RNA Transcript Labeling Kit according to the manufacturer's instructions. 5 µl of cDNA solution were mixed with 4 µl 10x HY reaction buffer, 4 µl 10x biotin-labeled ribonucleotides, 4 µl 10x DTT, 4 µl RNase inhibitor mix, 2 µl 20x T7 RNA polymerase and 17 µl DEPC-treated H<sub>2</sub>O to a final volume of 40 µl. The reactions were incubated for 5 h at 37°C with gentle mixing every 30-45 minutes. Labeled cRNA was stored at -20°C until purification.

Cleanup of labeled cRNA was performed using RNeasy Mini Kit columns, as described in section 2.3.1.1. Ethanol precipitation was performed as described in section 2.3.1.2, but with overnight incubation of the cRNA-ethanol-ammonium acetate mixture at -20°C before centrifuging. cRNA quantity and purity were determined spectrophotometrically (see section 2.2.2).

The adjusted cRNA yield was calculated from the following formula:

$$\text{adjusted cRNA yield} = \text{RNA}_m - (\text{total RNA}_i)(y)$$

RNA<sub>m</sub> = amount of cRNA measured after IVT (µg)

total RNA<sub>i</sub> = starting amount of total RNA (µg)

y = fraction of cDNA reaction used in IVT

### **2.3.1.4. Target fragmentation**

The fragmentation mix, with a final unadjusted concentration of cRNA between 0.5 µg/ml and 2 µg/ml, was prepared by combining 2 µl of 5x fragmentation buffer (200 mM Tris acetate pH 8.1, set with glacial acetic acid; 500 mM potassium acetate; 150 mM magnesium acetate in DEPC-treated H<sub>2</sub>O) for every 8 ml cRNA plus H<sub>2</sub>O. The mixture was incubated at 94°C for 35 min., then put on ice. This procedure produces a distribution of RNA fragment sizes from ca. 35 to 200 bases. 1 µg aliquots of unfragmented and fragmented cRNA were run on a 1% agarose gel to verify that fragmentation was complete.

The undiluted, fragmented cRNA was stored at -20°C until hybridization.

### 2.3.2. Target hybridization

The following hybridization mix was prepared for each target: 15 µg cRNA (adjusted concentration); 50 pM control oligonucleotide B2; 100x control cRNA cocktail (1.5 pM *bioB*; 5 pM *bioC*; 25 pM *bioD*; 100 pM *cre*); 0.1 mg/ml herring sperm DNA; 0.5 mg/ml acetylated BSA; 2x MES hybridization buffer (final 1x concentration: 100 mM MES, 1M [Na<sup>+</sup>], 20 mM EDTA, 0.01% Tween-20). The final volume for the standard array format is 300 µl.

Immediately before use, the probe array was equilibrated to room temperature, then filled with 1x MES hybridization buffer and incubated at 45°C for 10 min. with rotation. The hybridization cocktail was heated at 99°C for 5 min. in a heat block, then transferred to 45°C for 5 min. and spun for 5 min. at 16 060·g to remove insoluble material. The probe array cartridge was emptied and refilled with 250 µl of the clarified hybridization cocktail. The hybridization was conducted at 45°C for 16 h in a rotisserie box with 60 rpm rotation.

### 2.3.3. Washing, staining and scanning the array

The washing and staining procedure was performed according to the manufacturer's instructions, using a fluidics station and reagents from the GeneChip Hybridization, Wash and Stain Kit. After hybridization was complete, the array was emptied, then refilled with Wash Buffer A. The fluidics protocol was as follows:

Post Hyb Wash #1: 10 cycles of 2 mixes/cycle with Wash Buffer A at 25°C

Post Hyb Wash #2: 4 cycles of 15 mixes/cycle with Wash Buffer B at 50°C

1<sup>st</sup> stain for 10 minutes with Stain Cocktail 1 at 25°C

Post Stain Wash: 10 cycles of 4 mixes/cycle with Wash Buffer A at 25°C

2<sup>nd</sup> stain for 10 minutes with Stain Cocktail 2 at 25°C

3<sup>rd</sup> stain for 10 minutes with Stain Cocktail 3 at 25°C

Final Wash: 15 cycles of 4 mixes/cycle with Wash Buffer A at 30°C.

After the procedure was completed, the array was filled with array holding buffer at 25°C, inspected for air bubbles, then scanned with the GeneChip Scanner 3000. Tough-Spots™ were applied to each of the two septa on the probe array cartridge to prevent leakage of fluids from the cartridge during scanning.

### 2.3.4. Data analysis

Initial analysis of the array data was performed using the GCOS 1.4 software package. Scanned images of the arrays were converted to numerical data by GCOS. To normalize for variations in signal intensity between arrays (caused by differences in staining, washing etc.), global scaling was carried out to a target intensity of 500. The signals for the eukaryotic hybridization controls (*bioB*, *bioC*, *bioD*, *cre*) were assessed and always found to be present with increasing signal values, reflecting their relative concentrations. *BioB*, *bioC* and *bioD* represent genes in the biotin synthesis pathway of *E. coli*, while *cre* is the recombinase gene from P1 bacteriophage. They are spiked into the hybridization cocktail independent of RNA sample preparation, and are used to evaluate sample hybridization efficiency. The good target quality of the samples (RNA integrity and quality of labeling) was confirmed by the signal value ratio of the 3' and 5' probe sets of internal control genes (*ACTB* and *GAPDH*).

After log transformation of the data, comparison analysis between the baseline (control) and experimental (coculture) arrays was performed in GCOS. Each transcript was assigned a Present or Absent call, and an Increase or Decrease call (with the corresponding Signal Log Ratio) in the experimental sample as compared to the baseline. The expression data was exported to Excel files and analyzed further in Microsoft Excel. Probe sets listed twice as Increase, with an average increase in signal of 2-fold or more (Signal Log Ratio  $\geq 1$ ), were listed as significant increases, and those with an average increase of at least 1.5-fold (Signal Log Ratio  $\geq 0.6$ ) as tendentious increases. Probe sets listed twice as Decrease, with an average decrease in signal of 2-fold or more (Signal Log Ratio  $\leq -1$ ) were listed as significant decreases, and those with an average decrease of at least 1.5 fold (Signal Log Ratio  $\leq -0.6$ ) as tendentious decreases. "Absent-Present" increases and "Present-Absent" decreases were considered significant, whereas "Absent-Absent" changes were excluded from the analysis.

The genes showing expression alterations were divided into functional groups using information from the databanks Entrez Gene and PubMed (NCBI, <http://www.ncbi.nlm.nih.gov/>). The expression changes of selected genes were subsequently verified using quantitative real-time RT-PCR with multiple biological replicates.

### 2.4. Protein analysis

An overwhelming part of the structural and enzymatic machinery of the cell is made up of proteins, polymers composed of amino acid building blocks joined by peptide bonds. Compared to the transcriptome, or mRNA levels, the proteome (intracellular proteins) and secretome (secreted proteins) are a more direct reflection of the events that are actually occurring in the cell at a given time.

Proteins are large, labile molecules. Biological material usually contains large amounts of protein-degrading enzymes, or proteases, which can be present within the cell or secreted. To prevent protease degradation of the sample, it is necessary to work on ice and use protease inhibitors, such as phenylmethylsulfonyl fluoride (PMSF).

#### **Reagents**

Amersham™ LMW Calibration Kit for SDS Electrophoresis (GE Healthcare)

Amersham™ ECL Western Blotting detection reagents, product code RPN2108 (GE Healthcare)

Ammonium persulfate (APS) (Sigma-Aldrich)

Bio-Rad D<sub>c</sub> Protein Assay (Bio-Rad)

Non-fat milk powder, blotting grade (Carl Roth GmbH)

PMSF (Roche Diagnostics)

Ponceau S (Sigma-Aldrich)

Rotiphorese<sup>R</sup> Gel 30 (37.5:1 acrylamide-bisacrylamide) (Carl Roth GmbH)

Secondary HRP-conjugated goat IgG (Dianova)

N, N, N', N'-tetramethylethylenediamine (TEMED) (Sigma-Aldrich)

#### **Materials**

Amersham™ Hyperfilm ECL - high performance chemiluminescence film (GE Healthcare)

Centriplus filter devices, membrane cutoff 10 kDa (Millipore Corporation)

Immobilon™ membrane, polyvinylidene difluoride (PVDF) (Millipore Corporation)

Whatman blotting paper

#### **Equipment**

Gel dryer (Drystar)

Metal film cassette 24x30 cm (Dr. Goos Suprema)

Mini Protean II SDS-PAGE apparatus - electrophoresis chambers, frames, glass plates, combs, spacers etc. (Bio-Rad)

Sonicator, Ultrasonic Processor XL (Heat Systems)

TransBlot SD Semi-Dry Transfer Cell (Bio-Rad)

USB Scanner (Plustek Technology GmbH)



### **Software**

Action Manager 32 (scanner software)

TINA 2.09

### **2.4.1. Protein sample preparation: whole-cell lysates and conditioned medium**

Cells were seeded on 6-well culture plates and grown to 80% confluence, washed twice with PBS, then lysed in lysis buffer (50 mM Tris pH 7.5; 1 M NaCl; 5 mM EDTA pH 8.0; 1% v/v Triton X-100) with 1 µl/ml protease inhibitor mix (1 mM pepstatin A, 1 mM leupeptin, 0.1 mM aprotinin in H<sub>2</sub>O) and 1 µl/ml PMSF (100 mM stock in methanol) added just prior to use. Lysates were sonicated on ice (4x 1 s) and cleared by centrifugation (20 124·g, 10 min, 4°C), after which the supernatant was removed to a fresh tube. Protein quantitation was performed using the Lowry method (see section 2.3.2). Samples were mixed with 5x SDS sample buffer (200 mM Tris pH 6.8; 20% v/v glycerol; 10% w/v SDS; 10 mM DTT; 0.05% w/v bromophenol blue) and denatured for 5 min at 95°C.

Conditioned medium was concentrated 60x at 4°C by ultrafiltration (rotating at 3000·g, 4°C) on Centriplus filter devices. The protein content was determined by the Lowry method and proteins were precipitated from the medium by 4 volumes of cold acetone at -20°C overnight. The precipitates were pelleted by centrifugation (20 124·g, 10 min, 4°C) and the supernatant removed. After drying, the pellets were resuspended in an appropriate volume of 1x SDS sample buffer and denatured for 5 min at 95°C.

### **2.4.2. Lowry protein assay**

The Lowry colorimetric assay is the most commonly referenced procedure for protein determination. It relies on two different reactions. The first is the formation of a copper ion complex with peptide bonds under alkaline conditions (a "biuret" chromophore). The second is the reduction of Folin-Ciocalteu reagent (phosphotungstate and phosphomolybdate) by the Cu<sup>2+</sup>-treated protein. Color development is mainly dependent on the number of tyrosine and tryptophan residues. The resulting blue color is quantifiable with a spectrophotometer at 650-750 nm [Lowry *et al.* 1951].

The Bio-Rad D<sub>C</sub> Protein Assay utilizes an improved version of the Lowry method, allowing reliable protein detection in the presence of interfering substances such as detergents (e.g. 1% Triton X-100 present in lysis buffer).

## 2. Materials and methods

To perform the assay, 5  $\mu$ l of the samples were pipetted into microplate wells, with either lysis buffer (cell lysates) or PBS (conditioned medium) serving as the blank. First 25  $\mu$ l of reagent A, then 200  $\mu$ l of reagent B were added to each well. After 15 min, the well contents were mixed and absorbances were read at 690 nm. If samples contained detergent, reagent S was added to reagent A before the assay (20  $\mu$ l reagent S per 1 ml required solution). Protein concentration in the samples was determined from a standard curve prepared with serial dilutions of bovine serum albumin in a buffer either containing 1% Triton X-100 or not.

### 2.4.3. SDS-polyacrylamide gel electrophoresis (SDS-PAGE) and Western blot

The underlying principle of electrophoresis is the migration property of charged species within an electric field. Polyacrylamide gels are neutral, hydrophilic, three-dimensional networks of long hydrocarbons crosslinked by methylene groups. Polymerisation is initiated by APS (source of free radicals) and catalysed by TEMED (a free radical donor and acceptor). The separation of molecules within the gel is determined by the relative size of the pores formed within the gel. The greater the acrylamide percentage, the slower the migration rate.

Tab. 5 Composition of SDS-PAGE gels.

	2 Bio-Rad Mini-Gels		
	Separating gel		Stacking gel
Acrylamide content	12%	15%	4.5%
Acrylamide/bisacrylamide (30%/0.8%)	8 ml	10 ml	1.5 ml
1 M Tris-HCl pH 6.8	---	---	1.25 ml
1 M Tris-HCl pH 8.9	8 ml	8 ml	---
H <sub>2</sub> O	4 ml	2 ml	7 ml
10% w/v SDS	216 $\mu$ l	216 $\mu$ l	100 $\mu$ l
10% w/v APS	160 $\mu$ l	160 $\mu$ l	100 $\mu$ l
TEMED	20 $\mu$ l	20 $\mu$ l	10 $\mu$ l

In denaturing SDS-PAGE, sample preparation involves heating the protein in the presence of SDS to fully unfold the protein and permit binding of negatively-charged SDS molecules throughout the length of the polypeptide. The SDS binds to proteins, *via* hydrophobic interactions, in a stoichiometry approximately proportional to the size of the

protein. Due to this, the charge to mass ratio of all the proteins in the mixture becomes constant and proteins migrate through the gel at a rate proportional to their molecular mass.

The resolution and focus of the protein bands is increased by using discontinuous gels (Laemmli system). The lower pH and acrylamide concentration of the stacking gel causes samples to enter the separating gel as a concentrated, narrow line [Laemmli 1970].

The popular Western blot technique allows the immunodetection of specific proteins. Proteins resolved on a polyacrylamide gel are transferred in an electric field to a membrane, to which they permanently bind. After blocking nonspecific binding sites on the membrane with an agent such as non-fat milk, proteins of interest can be detected using antibodies. A secondary antibody, directed against the first, is coupled with an enzyme such as horseradish peroxidase (HRP). After substrate addition, either the precipitation of a colored product or light emission (chemiluminescence detection) occurs in places where the antigen-antibody complex is present.

Samples of lysate and conditioned medium containing 30 µg total protein were re-denatured for 5 min at 95°C prior to loading and separated on 12% or 15% SDS-PAGE gels (100 V stacking, 200 V separation). The gel running buffer contained 25 mM Tris-HCl, 200 mM glycine, 0.1% w/v SDS. A protein standard with band molecular weights of 14.4, 20.1, 30, 43 and 67 kDa was always run in parallel to the samples.

When protein separation was complete, the separating gel was equilibrated for ca. 20 min. in 6-aminocaproic acid-containing buffer (25 mM Tris; 40 mM 6-aminocaproic acid; 20% v/v isopropanol; pH 9.4) to wash out SDS. A PVDF membrane was moistened with isopropanol and equilibrated for ca. 20 min. in Low Tris (LT) buffer (25 mM Tris; 20% v/v isopropanol; pH 10.4).

A semi-dry transfer apparatus was used. The transfer sandwich was assembled as follows (from the bottom):

- 4 rectangles of blotting paper soaked in High Tris (HT) buffer (300 mM Tris; 20% v/v isopropanol; pH 10.4)
- 5 rectangles of blotting paper soaked in LT buffer
- membrane
- gel
- 5 rectangles of blotting paper soaked in LT buffer
- 4 rectangles of blotting paper soaked in HT buffer.

Electrotransfer was carried out for 60 min. at 25 V. To verify that protein transfer was successful, membranes were briefly stained with Ponceau S (0.2% w/v Ponceau S; 3% w/v trichloroacetic acid), then destained in H<sub>2</sub>O and dried.

Prior to immunodetection, membranes were moistened with isopropanol and washed for 2x 5 min. in Tris-buffered saline + Tween-20 (TBST) (50 mM Tris-HCl pH 7.4; 150 mM NaCl; 0.1% v/v Tween-20), then blocked with 5% w/v milk in TBST. Detection of IL6, TGFβ1 and FGF2 was performed with the same primary antibodies, diluted 1:2000 in TBST, that were used for neutralization experiments (see section 2.1.5). CKIIβ, the loading control, was detected by a rabbit polyclonal antibody diluted 1:4000 in TBST. Secondary HRP-conjugated goat IgG was used at a 1:10 000 dilution in TBST.

The following basic protocol was followed for all blots:

1. Blocking - 1 h
2. Brief rinse in TBST
3. Primary antibody - 2 h
4. 3 x 10 min. washes in TBST
5. Secondary antibody - 1 h
6. 4 x 10 min. washes in TBST

The procedure was carried out at room temperature, on a shaker.

Bands were visualised using enhanced chemiluminescence (Amersham<sup>TM</sup> ECL Western Blotting detection reagents) according to the manufacturer's instructions. Equal amounts of reagent 1 and 2 (luminol and hydrogen peroxide solutions) were mixed and the membrane was incubated for 1 min. in the mixture, then packed in foil. The image was captured on photographic film in a cassette and developed. Exposure times ranged from 20 s to 30 min. depending on signal strength.

After immunodetection with antibodies against IL6, TGFβ1 or FGF2, blots were promptly stripped for 2 h at room temperature in stripping buffer (25 mM glycine; 1% w/v SDS, pH 2.0 set with HCl 37%), rinsed twice for 10 min. in TBST, reblocked and reblotted with the antibody against CKIIβ.

Blots were scanned and band density was quantified using TINA 2.09 software.

In the experiment shown in section 3.2.3, Fig. 26C, to revisualise all protein bands after immunodetection, the membrane was stained briefly with Coomassie blue solution (50% v/v isopropanol; 10% v/v acetic acid; 0.1% w/v Coomassie R250) and destained with ethanol.

### 2.4.4. Silver staining of proteins

Colloidal silver staining is a highly sensitive method for visualising proteins. To prepare an alkaline silver stain reagent, 21 ml 0.36% w/v NaOH and 1.6 ml 28% w/v  $\text{NH}_3 \cdot \text{H}_2\text{O}$  were mixed; then, 4 ml 20% w/v  $\text{AgNO}_3$  were added dropwise with intensive stirring. The solution was diluted to 100 ml with  $\text{H}_2\text{O}$  (final working concentration: 0.8%  $\text{AgNO}_3$ ; 0.076% NaOH; 0.45%  $\text{NH}_3 \cdot \text{H}_2\text{O}$ ) and used within 5 min.

After SDS-PAGE, the separating gel was fixed in 50% v/v methanol (3x 1 h), washed in  $\text{H}_2\text{O}$  for 10 min, then stained for 15 min in 100 ml freshly prepared alkaline silver stain solution, washed 3x 10 min in  $\text{H}_2\text{O}$  and developed in 100 ml developing solution (0.01% w/v citric acid; 0.038 % w/v formaldehyde in  $\text{H}_2\text{O}$ ) until bands appeared. The reaction was stopped by immersing the gel in 50% v/v methanol.

### 2.4.5. Estimating the molecular weight of protein bands

In SDS-PAGE, the migration distance of a protein depends on its molecular mass. The relationship between the relative mobility of a protein and the log of its molecular mass should be a linear function. A standard curve of log molecular mass versus relative mobility was plotted in Microsoft Excel on the basis of migration distances for the standard, and used to estimate the molecular masses of unknown proteins. Relative mobility for each band was determined by measuring the distance from the top of the gel to the middle of the dye front, measuring the distance from the top of the gel to the middle of the band, and dividing the second measurement by the first.

**Tab. 4 List of primers used for quantitative RT-PCR.**

Gene symbol	Accession number(s) of transcript(s) recognized*	Gene product	Annealing temperature	Sequence	Product size
<i>ACTB</i>	NM_001101.2	actin, beta	60°C	sense: 5'-GTCATAGTCCGCCTAGAA-3' antisense: 5'-CCAGCACAAATGAAGATCA-3'	175 bp
<i>AP</i>	NM_031313.2	alkaline phosphatase	59°C	sense: 5'-AGGTAATGAGTCTTCCTTGC-3' antisense: 5'-GATAGCAGTCCAGAGTCCAT-3'	179 bp
<i>BMP2</i>	NM_001200.2	bone morphogenetic protein 2	59°C	sense: 5'-ATGTTAGGATAAGCAGGTCT-3' antisense: 5'-TACAAAGGGTGTCTCTTACA-3'	178 bp
<i>CBFA1</i>	NM_001024630.2 NM_001015051.2 NM_004348.3	core binding factor 1	58°C	sense: 5'-CTCACTACCACACCTACCTG-3' antisense: 5'-ACGAAGTGCCATAGTAGAGA-3'	104 bp
<i>CDH1</i>	NM_004360.2	cadherin 1, type 1, E-cadherin (epithelial)	55°C	sense: 5'-CTTCACAGCAGAACTAACAC-3' antisense: 5'-GTCACTGGTCTTTATTCTG-3'	173 bp
<i>CDH2</i>	NM_001792.2	cadherin 2, type 1, N-cadherin (neuronal)	55°C	sense: 5'-CTCAAGTGTACCTCAAGAG-3' antisense: 5'-TAGTCACTGGAGATAAAGGA-3'	134 bp
<i>CDH11</i>	NM_001797.2	cadherin 11, type 2, OB-cadherin (osteoblast)	55°C	sense: 5'-ATGGCTTAGTCACATACAT-3' antisense: 5'-CTCATCAGCATCTTCTACTG-3'	238 bp
<i>CK2B</i>	NM_001320.5	casein kinase II, beta subunit	61°C	sense: 5'-CAAGAGACCTGCCAACCA-3' antisense: 5'-GTCAAAGACTGCAGGACAGG-3'	153 bp
<i>CLCA2</i>	NM_006536.4	chloride channel, calcium activated, family member 2	59°C	sense: 5'-CCCTATCTTGGACAGCA-3' antisense: 5'-TATCTCCCTGATGCCAG-3'	164 bp
<i>COL1A1</i>	NM_000088.3	collagen type 1, alpha strand 1	59°C	sense: 5'-GAACATCACCTACCACTGC-3' antisense: 5'-AGTGACGCTGTAGGTGAAG-3'	146 bp
<i>COL1A2</i>	NM_000089.3	collagen type 1, alpha strand 2	60°C	sense: 5'-GTTATAATACAAAGGTGCT-3' antisense: 5'-ACGATACAACCTCAATACAGG-3'	99 bp
<i>DKK1</i>	NM_012242.2	dickkopf homolog 1	64°C	sense: 5'-CACTTCTGGTCCAAGATCTG-3' antisense: 5'-CCTTCTCCACAGTAACAACG-3'	116 bp
<i>EGFR</i>	NM_005228.3	epidermal growth factor receptor	60°C	sense: 5'-GAGGACAGCATAGACGAC-3' antisense: 5'-GCTGGACAGTGTGAGAT-3'	196 bp
<i>FOXO3</i>	NM_201559.2 NM_001455.3	forkhead box O3	61°C	sense: 5'-CTCTTGCCACACTCCAGA-3' antisense: 5'-GGTCTCCTTCACATTTG-3'	165 bp
<i>GDF15</i>	NM_004864.2	growth differentiation factor 15	58°C	sense: 5'-CAGAGCTGGGAAGATTTCG-3' antisense: 5'-AACAGAGCCCCGGTGAAG-3'	164 bp
<i>IL6</i>	NM_000600.2	interleukin 6	61°C	sense: 5'-TAGTGAGGAACAAGCCAGAG-3' antisense: 5'-GATGAGTTGTCATGTCCTGC-3'	173 bp
<i>IL6R</i>	NM_000565.2	interleukin 6 receptor	66°C	sense: 5'-TACCACTGCCACATTCCTG-3' antisense: 5'-GCTTGTCTTGCTTCTTCA-3'	125 bp

\* In the case of alternatively spliced mRNAs, primers were designed to recognize as many isoforms as possible, without distinguishing between them.

Gene symbol	Accession number(s) of transcript(s) recognized	Gene product	Annealing temperature	Sequence	Product size
<i>NOG</i>	NM_005450.2	noggin	66°C	sense: 5'-TGTGCAAGCCGTCCAAGT-3' antisense: 5'-GAGCACTTGCCTCGGAAAT-3'	121 bp
<i>NPPB</i>	NM_002521.2	natriuretic peptide precursor B	61°C	sense: 5'-TTTGGGAGGAAGATGGAC-3' antisense: 5'-TGTGGAATCAGAAGCAGG-3'	109 bp
<i>OC</i>	NM_199173.2	osteocalcin	63°C	sense: 5'-GACTGTGACGAGTTGGCTGA-3' antisense: 5'-CTGGAGAGGAGCAGAACTGG-3'	118 bp
<i>OPG</i>	NM_002546.3	osteoprotegerin	57°C	sense: 5'-GCTGTTCTTACAAAGTTTAC-3' antisense: 5'-TCTACACTCTCTGCGTTTAC-3'	85 bp
<i>OPN</i>	NM_001040060.1 NM_001040058.1 NM_000582.2	osteopontin	58°C	sense: 5'-GATGTGATTGATAGTCAGGA-3' antisense: 5'-AGGTGTTTATCTTCTCCTT-3'	119 bp
<i>PLAUR</i>	NM_001005377.1 NM_001005376.1 NM_002659.2	plasminogen activator, urokinase receptor	61°C	sense: 5'-TTACCGAGGTTGTGTGTG-3' antisense: 5'-ATCCAGGCACTGTTCTTC-3'	176 bp
<i>RANKL</i>	NM_033012.2 NM_003701.2	receptor activator of NF-κB ligand	58°C	sense: 5'-AGGAGGAAGCACCAAGTATT-3' antisense: 5'-TCCTCTCCAGACCGTAACTT-3'	93 bp
<i>SMAD2</i>	NM_001003652.2 NM_005901.4	SMAD family member 2	59°C	sense: 5'-TCTTCTGGCTCAGTCTGTTA-3' antisense: 5'-TGTAGAGGTCCATTCAGATG-3'	165 bp
<i>SMAD3</i>	NM_005902.3	SMAD family member 3	63°C	sense: 5'-CGGAGTACAGGAGACAGACT-3' antisense: 5'-CTAAGACACACTGGAACAGC-3'	134 bp
<i>SMAD7</i>	NM_005904.2	SMAD family member 7	60°C	sense: 5'-CCAATGACCACGAGTTTAT-3' antisense: 5'-GCTGTTGAAGATGACCTCTA-3'	137 bp
<i>SQSTM1</i>	NM_003900.3	sequestosome 1	59°C	sense: 5'-AAGAAGTGGACCCGTCTA-3' antisense: 5'-GAGAGGGACTCAATCAGC-3'	166 bp
<i>SP3</i>	NM_003111.3 NM_001017371.3	Sp3 transcription factor	63°C	sense: 5'-CTCATCTGCGTTGGCATT-3' antisense: 5'-ATGTTTGGCAAGGTGGTC-3'	179 bp
<i>STC1</i>	NM_003155.2	stanniocalcin 1	64°C	sense: 5'-CTGAAGCCATCACTGAGG-3' antisense: 5'-TCATCACATTCCAGCAGG-3'	91 bp
<i>STMN1</i>	NM_005563.3 NM_203401.1 NM_203399.1	stathmin 1	63°C	sense: 5'-AGAGAACCAGAGGCACA-3' antisense: 5'-CAGCAGGGTCTTTGGATT-3'	104 bp
<i>TGFB1</i>	NM_000660.3	transforming growth factor beta 1	62°C	sense: 5'-CAGAAATACAGCAACAATTCTGG-3' antisense: 5'-TTGCAGTGTGTTATCCCTGCTGTC-3'	185 bp
<i>TGFBR1</i>	NM_004612.2	transforming growth factor beta receptor 1	63°C	sense: 5'-GATGCCTTCTGTTGACTGA-3' antisense: 5'-GATGCCTTCTGTTGACTGA-3'	128 bp
<i>TGFBR2</i>	NM_003242.5 NM_001024847.2	transforming growth factor beta receptor 2	63°C	sense: 5'-AACGTGTTGAGAGATCGAGG-3' antisense: 5'-AGATGCTCCAGCTCACTGAA-3'	164 bp

## 3. Results

### 3.1. The response of prostate cancer cells to osteoblasts

#### 3.1.1. Osteotropic prostate cancer cell lines express elevated levels of bone-associated genes.

To verify and extend already available data [Knerr *et al.* 2004] and gain a better understanding of the osteomimicry phenomenon in the wider context of the bone microenvironment, the expression of 7 genes associated with bone formation (*BMP2*<sup>2</sup>, *CBFA1*, *AP*, *COL1A1*, *OPN*, *OC*, *OPG*) and 3 associated with bone loss (*RANKL*, *DKK1*, *NOG*) (Tab. 6) was analyzed using quantitative real-time RT-PCR (qRT-PCR) in osteoblasts and in three prostate cancer cell lines characterized by different degrees of bone tropism.

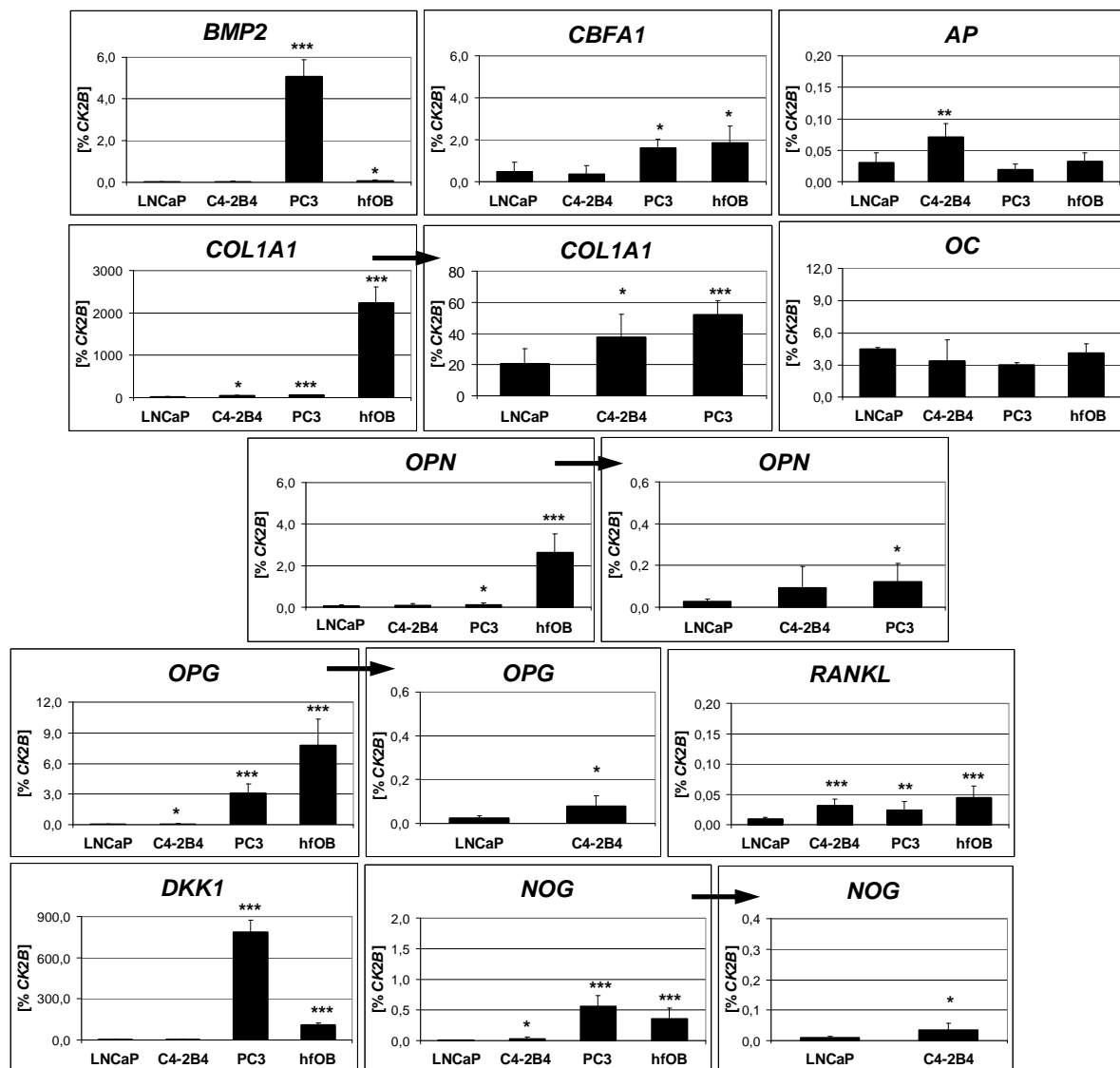
**Tab. 6 Brief descriptions of genes selected for assays** (based on information from Entrez Gene and PubMed databases; for link see Materials and methods 2.3.4).

	<b>Gene symbol</b>	<b>Gene product</b>	<b>Description</b>
Bone formation	<i>BMP2</i>	bone morphogenetic protein 2	Induces osteoblastic differentiation and bone formation.
	<i>CBFA1</i>	core binding factor 1	Transcription factor crucial for osteoblastic differentiation.
	<i>AP</i>	alkaline phosphatase	Enzyme responsible for bone matrix mineralization. Expressed at early stages of osteoblast differentiation.
	<i>COL1A1</i>	collagen, type I, alpha 1	Pro-alpha chains of a fibril collagen that is abundant in the bone matrix. Expressed at early stages of osteoblast differentiation.
	<i>OPN</i>	osteopontin	Noncollagenous bone matrix protein; overexpressed in many malignancies; important for adhesion, motility, invasion and survival of cancer cells.
	<i>OC</i>	osteocalcin	Noncollagenous bone matrix protein; marker of the terminal stage of osteoblast differentiation.
	<i>OPG</i>	osteoprotegerin	Soluble decoy receptor for RANKL. Inhibits bone resorption.
Bone loss	<i>RANKL</i>	receptor activator of nuclear factor kappa B ligand	Induces osteoclastic differentiation and bone resorption.
	<i>NOG</i>	noggin	Antagonist of BMP signaling; inhibits osteoblastic differentiation and bone formation.
	<i>DKK1</i>	dickkopf homolog 1	Antagonist of WNT signaling; inhibits osteoblastic differentiation and bone formation.

<sup>2</sup> In accordance with guidelines for gene nomenclature advocated by the HUGO Gene Nomenclature Committee (HGNC) [Wain *et al.* 2002], human gene symbols have been designated by upper-case letters and italicized, while protein symbols are represented in upper-case standard font.



A.



B.

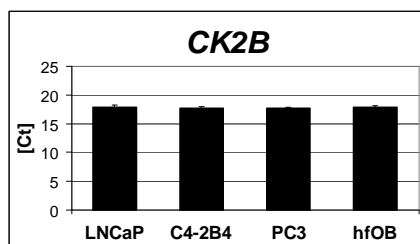


**Fig. 10** Steady-state mRNA expression of bone-associated genes (A) and of *CK2B*, a housekeeping gene (B) by prostate cancer cells and osteoblasts. Values in (A) are expressed as the ratio to *CK2B*. Error bars represent the mean  $\pm$  SD of at least three independent determinations. \*  $p < 0,05$ ; \*\*  $p < 0,01$ ; \*\*\*  $p < 0,001$  (vs. LNCaP)

Confluent human fetal osteoblasts (hfOB) cultured at 37°C, a temperature that enables this cell line to differentiate, but not mineralize [Harris *et al.* 1995], express high levels of *CBFA1*, *COL1A1*, *OPN*, *OC*, *OPG*, *DKK1* and *NOG*, and low levels of *BMP2*, *AP* and *RANKL* (Fig. 10A).

The osteolytic PC3 cells have a high expression of *DKK1* and *NOG*, which inhibit bone formation, whereas baseline expression of *DKK1* and *NOG* in LNCaP and C4-2B4 is very low. However, PC3 also express very high levels of *BMP2*, and elevated levels of *CBFA1*, *COL1A1*, *OPN* and *OPG*, all associated with increased bone formation. On the other hand, the bone metastasis-derived C4-2B4 subline has a higher baseline expression of *AP*, *COL1A1* and *OPG*, but also of *RANKL* and *NOG* than its parental line LNCaP. All three prostate cancer cell lines express *OC* (Fig. 10A).

In sum, the two bone metastasis-derived, osteotropic lines, C4-2B4 and PC3, both express significantly higher levels of *COL1A1*, *OPG*, *RANKL* and *NOG* than the lymph node-derived, less aggressive LNCaP. Additionally, C4-2B4 show a higher expression of *AP* than either LNCaP or PC3 (Fig. 10A).

It was confirmed that *CK2B*, the housekeeping gene [Pyerin & Ackermann 2003] that was used as a basis for comparing levels of all other mRNAs, is expressed at equal levels in all the investigated cell lines (Fig. 10B).

#### **3.1.2. Osteoblast-released factors induce osteomimicry in prostate cancer cells.**

The expression of bone-associated genes became modulated in prostate cancer cells after exposure to osteoblast-released factors. The cells were either cocultured with osteoblasts in a model that enables cell crosstalk *via* soluble molecules, or treated with conditioned medium, CM (thus with no dynamic cell crosstalk contributing to the results).

LNCaP, which had a low baseline expression of 9 out of 10 tested genes (Fig. 10A), showed the most dramatic gene expression changes in response to osteoblast-released factors. Coculture with osteoblasts for 24 or 48 h caused strong upregulation of *BMP2*, *AP*, *OPN*, *OPG*, *RANKL*, *DKK1* and *NOG*, and slight upregulation of *COL1A1*. Treatment with hfOB CM produced similar effects (Tab. 7). Time-course curves performed for *BMP2*, *OPG* and *RANKL* showed that significant gene expression changes were already established at early time points: after 16 h of coculture in the case of *OPG* and *RANKL*, and after 24 h in the case of *BMP2* (Fig. 11).

**Tab. 7 Changes in bone-associated gene expression induced in prostate cancer cells by osteoblast-released factors.** RNA was isolated, reverse transcribed and qRT-PCR was performed on cDNA from prostate cancer cell lines cocultured with hfOB or cultured in the presence of hfOB CM diluted 1:1 with fresh medium. Alterations with a t-test p value < 0,05 were considered significant. ▲▲, fold change ≥ 2; ▲, fold change ≥ 1,45; ▽, fold change ≤ 0,69 (-1,45); ▽▽, fold change ≤ 0,5 (-2); nc, no change). [X]<sup>hfOB</sup>, hfOB-cocultured prostate cancer cells; hfOB CM - osteoblast-conditioned medium.

Gene symbol	LNCaP <sup>hfOB</sup> 24 h	LNCaP <sup>hfOB</sup> 48 h	LNCaP + hfOB CM 48 h
<i>BMP2</i>	▲▲	▲▲	▲
<i>CBFA1</i>	nc	nc	▲
<i>AP</i>	▲▲	▲▲	▲▲
<i>COL1A1</i>	▲	▲	nc
<i>OPN</i>	nc	▲▲	▲▲
<i>OC</i>	nc	nc	nc
<i>OPG</i>	▲▲	▲▲	▲▲
<i>RANKL</i>	▲▲	▲▲	▲▲
<i>DKK1</i>	▲▲	▲▲	▲▲
<i>NOG</i>	▲▲	▲▲	▲▲

Gene symbol	C4-2B4 <sup>hfOB</sup> 24 h	C4-2B4 <sup>hfOB</sup> 48 h	C4-2B4 + hfOB CM 48 h
<i>BMP2</i>	▲	▲	▲
<i>CBFA1</i>	nc	nc	▲
<i>AP</i>	nc	▲	▲
<i>COL1A1</i>	nc	nc	nc
<i>OPN</i>	nc	▲▲	▲▲
<i>OC</i>	nc	▲	nc
<i>OPG</i>	▲▲	▲▲	▲
<i>RANKL</i>	nc	▲▲	▲▲
<i>DKK1</i>	▲▲	▲▲	nc
<i>NOG</i>	nc	▲▲	▲

Gene symbol	PC3 <sup>hfOB</sup> 24 h	PC3 <sup>hfOB</sup> 48 h	PC3 + hfOB CM 48 h
<i>BMP2</i>	▲▲	▲▲	nc
<i>CBFA1</i>	nc	▲	nc
<i>AP</i>	nc	▲	nc
<i>COL1A1</i>	▲	nc	nc
<i>OPN</i>	nc	nc	▲
<i>OC</i>	nc	nc	nc
<i>OPG</i>	▽	▽▽	nc
<i>RANKL</i>	nc	▲▲	▲
<i>DKK1</i>	nc	▽▽	nc
<i>NOG</i>	▲▲	▲▲	nc

In C4-2B4, coculture with osteoblasts consistently induced strong upregulation of *BMP2*, *OPN*, *OPG*, *RANKL*, *DKK* and *NOG*, and slight upregulation of *AP* and *OC*. *COL1A1* levels remained unaltered. After treatment with hfOB CM, only *OPN* and *RANKL* became strongly upregulated, while *BMP2*, *CBFA1*, *AP*, *OPG* and *NOG* showed tendential upregulation (Tab. 7).

In PC3, only *RANKL* consistently became upregulated both after coculture and after treatment with hfOB CM. Upregulation of *BMP2*, *CBFA1*, *AP* and *NOG* and downregulation of *OPG* and *DKK1* occurred after coculture, but not after treatment with hfOB CM (Tab. 7).

In sum, osteoblast-released factors induced the upregulation of a number of bone-associated genes in prostate cancer cells. Significantly, LNCaP and C4-2B4 began to express higher levels of *BMP2*, *OPG*, *DKK1* and *NOG*, which all show high baseline expression in PC3. *BMP2* and *RANKL* became strongly upregulated in all three prostate cancer cell lines. Additionally, LNCaP began to overexpress *COL1A1*, constitutively highly expressed by C4-2B4 and PC3, and *AP*, constitutively highly expressed by C4-2B4. Thus, osteoblast-released factors apparently lead prostate cancer cells to assume an osteomimetic phenotype, which has become permanently enforced in cell lines derived from bone metastases. Significantly, expression of genes characteristic of osteomimicry is not restricted to osteoblastic prostate cancer cell lines.

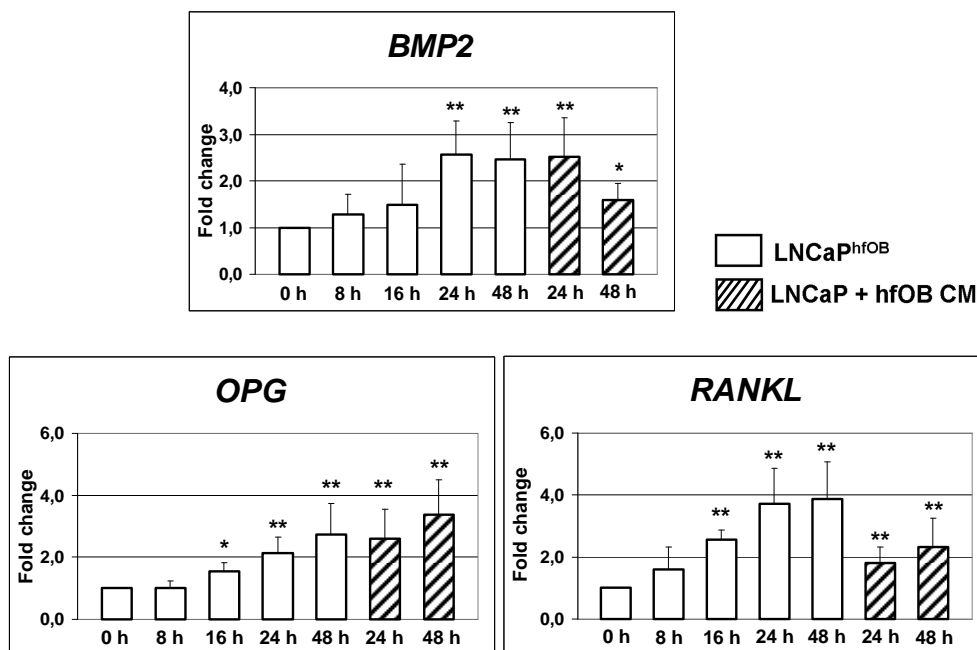
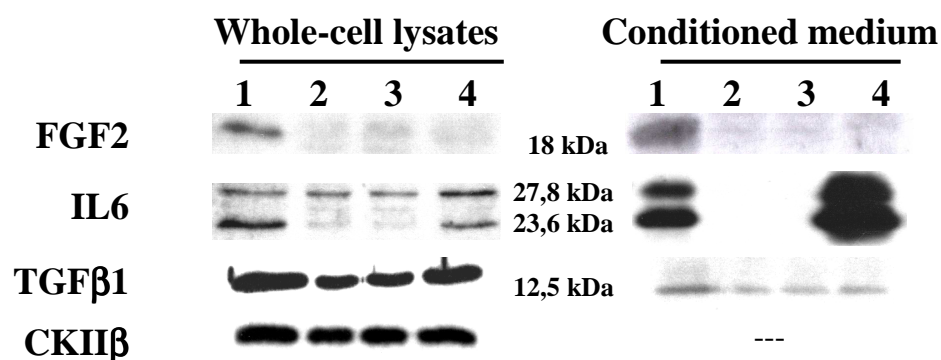


**Fig. 11 Time-course curves of *BMP2*, *OPG* and *RANKL* mRNA in LNCaP cocultured with osteoblasts or treated with osteoblast-conditioned medium.** For details see legend to Tab. 7. Error bars represent the mean  $\pm$  SD of at least three independent experiments. [X]<sup>hfOB</sup>, hfOB-cocultured prostate cancer cells; hfOB CM - osteoblast-conditioned medium. \*  $p < 0,05$ ; \*\*  $p < 0,01$

A.



B.

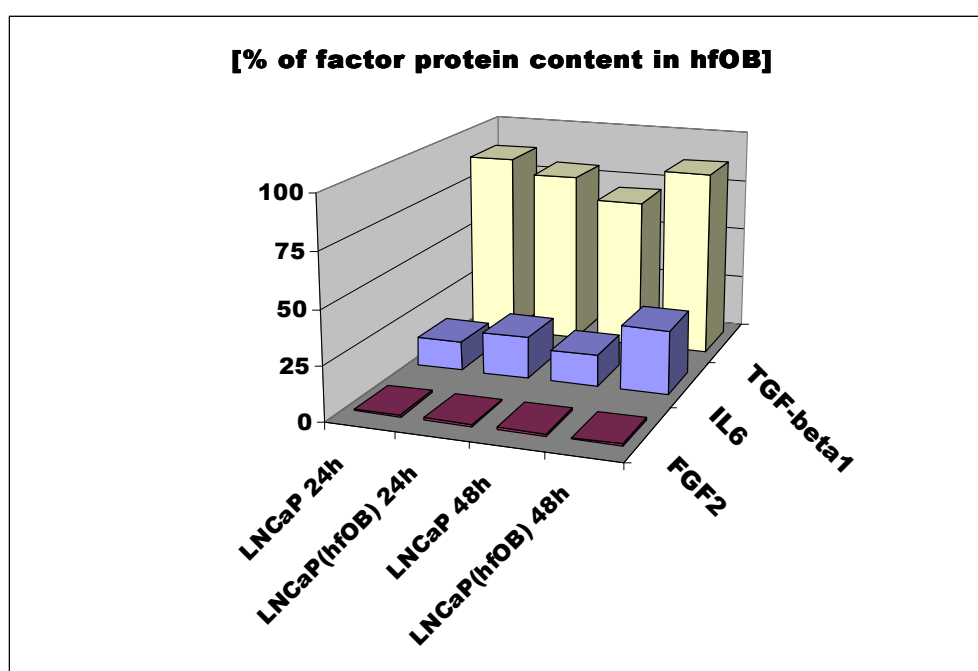


**Fig. 12 Production of putative osteomimetic factors by cancer cells and osteoblasts.**

**(A) Factor presence in whole-cell lysates and in conditioned medium.** The cells were grown to 80% confluence in medium containing 10% FCS, then switched to serum-free medium for 24 h, after which CM was collected and the cells lysed in lysis buffer. CM was concentrated 60x by ultrafiltration on centrifuge filter devices and subjected to protein precipitation by acetone at  $-20^{\circ}\text{C}$ . The precipitates and lysate samples containing 30  $\mu\text{g}$  total protein were mixed with SDS-PAGE sample buffer. SDS-PAGE was performed, followed by electrotransfer to a PVDF membrane and immunodetection using chemiluminescence. *Cells: 1, hfOB; 2, LNCaP; 3, C4-2B4; 4, PC3.*

**(B) Comparison of factor levels in *hfOB* and *LNCaP*.** Cell lysates were prepared from monocultured *hfOB*, *LNCaP* and *LNCaP* cocultured with *hfOB*. Protein separation, transfer and immunodetection were performed as described above. Blots were scanned and densitometric quantification of bands was carried out. Results were normalized to CKIIβ. *LNCaP(hfOB)*, *hfOB*-cocultured *LNCaP*.

#### 3.1.3. Osteoblast-released IL6 and TGFβ1 participate in the induction of osteomimicry in prostate cancer cells.

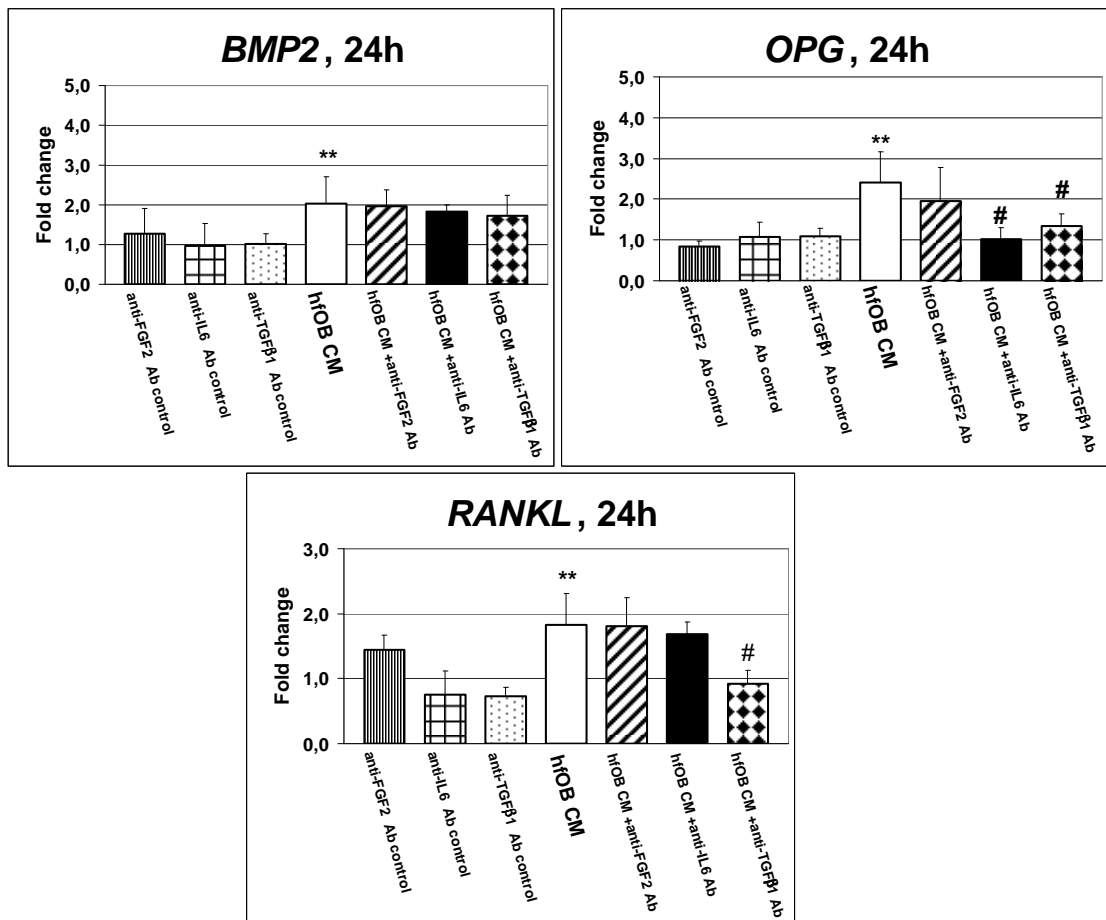
Some of the genes affected by the cell crosstalk are known targets of interleukin 6 (IL6) [Palmqvist *et al.* 2002, Li *et al.* 2008] and transforming growth factor beta 1 (TGFβ1) [Noda *et al.* 1988, Thirunavukkarasu *et al.* 2001, Wrana *et al.* 2001], which belong to the rich cocktail of bioactive molecules present in bone. IL6 [Bellido *et al.* 1997, Erices *et al.* 2002, Li *et al.* 2008] and TGFβ1 [Janssens *et al.* 2005, Kanaan & Kanaan 2006] are well established as regulators of osteoblast differentiation, and are also strongly implicated in prostate cancer progression [Chung *et al.* 1999, Shariat *et al.* 2001, Wikstrom *et al.* 1998, Wikstrom *et al.* 2001]. Another important regulator of osteoblast differentiation and function, fibroblast growth factor 2 (FGF2) [Franceschi & Xiao 2003, Marie 2003] is also presumed to play a significant role in prostate cancer [Kwabi-Addo *et al.* 2004]. It was confirmed that osteoblasts *in vitro* secrete high amounts of all three molecules (Fig. 12A). Although the levels of intracellular protein are only an indirect indicator of how much is actually secreted, it appears that in a coculture with LNCaP cells, osteoblasts are the main source of FGF2 and IL6, and also contribute large amounts of TGFβ1 to the coculture environment both at 24 h and at 48 h (Fig. 12B). Consequently, the role of all three factors in the induction of selected osteomimetic genes was investigated using neutralizing antibodies and recombinant proteins. A similar approach has been used by Lu *et al.* to investigate the contribution of osteoblast-released IL6 to the induction of prostate cell proliferation and prostate-specific antigen (PSA) expression [Lu *et al.* 2004].

Neutralizing antibodies against IL6 or TGFβ1 added to hfOB CM abolished the upregulation of *OPG* mRNA in LNCaP, whereas an antibody against FGF2 had no effect. RANKL upregulation was prevented by neutralizing TGFβ1, but not IL6 or FGF2. None of the three antibodies blocked the upregulation of *BMP2* mRNA (Fig. 13A).

Treating LNCaP cells with recombinant IL6 or TGFβ1 for 24 h resulted in significant upregulation of *OPG* mRNA (Fig. 13B); however, recombinant TGFβ1 did not induce upregulation of *RANKL* or of the known TGFβ target gene *OPN*. Recombinant FGF2 had no effect on *OPN*, *OPG* or *RANKL* mRNA expression after 24 h.

In sum, it could be shown that osteoblast-released IL6 and TGFβ1 increase *OPG* expression in LNCaP. Osteoblast-released TGFβ1 also appears to contribute to *RANKL* upregulation, but additional factors present in CM are apparently needed to cause this effect.

A.



B.

	24 h		
	FGF2 10 ng/ml	IL6 10 ng/ml	TGFβ1 10 ng/ml
<i>OPN</i>	nc	nc	nc
<i>OPG</i>	nc	▲▲	▲
<i>RANKL</i>	nc	nc	nc

**Fig. 13 Effect of candidate factors on osteomimetic gene expression by cancer cells.**

(A) Effect of neutralizing antibodies on the upregulation of osteomimetic genes in LNCaP by osteoblast-conditioned medium. Error bars represent the mean  $\pm$  SD of at least three independent experiments.

\*  $p < 0,05$ ; \*\*  $p < 0,01$  (vs. LNCaP); #  $p < 0,05$  (vs. LNCaP + hfOB CM).

(B) Effect of recombinant proteins on osteomimetic gene expression in LNCaP. Alterations with a t-test  $p$  value  $< 0,05$  were considered significant. ▲▲, fold change  $\geq 2$ ; ▲, fold change  $\geq 1,45$ ; nc, no change.

qRT-PCR was performed on cDNA from LNCaP cells cultured in FCS-free conditions (A) in plain medium (controls) or in hfOB CM diluted 1:1 with fresh medium, with or without the indicated antibodies (400 ng/ml), or (B) in plain medium in the presence of the indicated recombinant proteins. LNCaP cells cultured in plain medium served as the control.

The *OPG* promoter has been cloned and characterized [Morinaga *et al.* 1998]. It has been demonstrated that TGFβ treatment increases *OPG* mRNA and protein levels in osteoblasts, and

that a 183-bp proximal region (-372 to -190) of the *OPG* promoter is necessary and sufficient for mediating TGF $\beta$  effects [Thirunavukkarasu *et al.* 2001]. An *in silico* analysis (Transcription Element Search System - TESS, www.cbil.upenn.edu/tess) of the *OPG* promoter sequence reveals a number of potential binding sites for transcription factors inducible both by IL6 (IL6 RE-BP, IRF-1,2) and by TGF $\beta$  (Sp1) (Fig. 14). Significantly, a number of predicted Sp1 binding sites are located in the TGF $\beta$ -responsive region characterized by Thirunavukkarasu *et al.*

**Fig. 14** *In silico* analysis of the *OPG* promoter sequence - GenBank accession number AB008822. Potential transcription factor binding sites are listed along with the upstream signaling pathways known to activate those transcription factors.

**Green** - TESS analysis

**Blue** - Morinaga 1998

**Red** - Thirunavukkarasu 2001

**TIS** - transcription initiation sites [Morinaga *et al.* 1998]

AP-2 $\alpha$ 
LEF-1 <sup>Wnt/ $\beta$ -catenin</sup>

1 ctggagacat ataactgaa cacttgcccc tgatggggaa gcagctctgc agggactttt tcagccatct

c-Myb

71 gtaaacaatt tcagtggcaa cccgcgaaact gtaatccatg aatgggacca cactttacaa gtcacaaagt

TCF-4 <sup>Wnt/ $\beta$ -catenin</sup>

141 ctaacttcta gaccaggaa ttaatggggg agacagcgaa ccctagagca aagtgccaaa ctctgtcga

Sp1 <sup>TGF $\beta$</sup>  NF-AT

211 tagcttgagg ctagtggaaa gacctcgagg aggctactcc agaagttcag cgcgtaggaa gctccgatac

TCF-1,3,4/LEF-1 <sup>Wnt/ $\beta$ -catenin</sup> Sp1 <sup>TGF $\beta$</sup>  Sp1 <sup>TGF $\beta$</sup>  /AP-2

281 caatagccct ttgatgatgg tggggttggg gaagggaaca gtgctccgca aggttatccc tgccccaggc

GATA-1

351 agtccaattt tcaactctgca gattctctct ggctctaact accccagata acaaggagtg aatgcagaat

AP-1

421 agcacgggct ttagggccaa tcagacatta gtagaaaaa ttctactac atggttatg taaacttgaa

Sp1 <sup>TGF $\beta$</sup>

491 gatgaatgat tgcaactcc ccgaaaaggg ctcagacaat gccatgcata aagagggggcc ctgtaatttg

▲ TIS 3
▲ TIS 2



IRF1/2<sup>IL6</sup> AP-1 AP-2

561 aggtttcaga acccgaagtg aagggtcag gcagccgggt acggcggaaa ctcacagctt tcgccccagcg

IL-6 RE-BP<sup>IL6</sup> Msx-1 Sp1<sup>TGFβ</sup>

631 agaggacaaa ggtctgggac aactccaac tgcgtccgga tcttgctgg atcggactct ca<sup>gggtggag</sup>

Sp1<sup>TGFβ</sup> AP-2/Sp1<sup>TGFβ</sup> AP-2/Sp1<sup>TGFβ</sup>

701 gagacacaag cacagcaget gcccagcgtg tgcccagccc tcccaccgct ggtcccggct gccaggaggc

▲ -372 TGFβ-responsive region

AP-2 Sp1<sup>TGFβ</sup>/ERα Sp1<sup>TGFβ</sup> OSE<sub>2</sub> AP-2 Sp1<sup>TGFβ</sup>

771 tggccgctgg cgggaaaggg ccggga aacc tca gagcccc gcggagacag cagccgcctt gttcctcagc

IL-6 RE-BP<sup>IL6</sup> AP-2 SBE/Sp1<sup>TGFβ</sup> Sp1<sup>TGFβ</sup> AP-2/GATA-1 Sp1<sup>TGFβ</sup>

841 ccggtggctt tttttccc tgctctccca gggga cagac accaccgccc caccctca gccccacctc

TGFβ-responsive region [Thirunavukkarasu *et al.* 2001]

AP-2α Sp1<sup>TGFβ</sup> Sp1<sup>TGFβ</sup>

911 cctgggggat cctttcgccc ccagccctga aagcgttaat cctggagctt tctgcacacc ccccagaccg

▲ -190 (relative to TIS 1)

Sp1<sup>TGFβ</sup> TBP AREB6 c-Fos/TCF-1,3,4/LEF-1<sup>Wnt/β-catenin</sup>

981 tccgccc<sup>aa</sup> gcttct<sup>taaa</sup> aaagaaaggt gcaagtttg gtccaggata gaaaaatgac tgatcaaagg

c-Ets-1 TFIID

1051 caggcgatac ttcctgttgc cgggacgcta tatataacgt gatgagcgca cgggctgcgg agacgcaccg

▲ TIS 1

1121 gaggctcgc ccagccg<sup>ccg</sup> cctccaagcc cctgaggttt ccggggacca caatgaacaa

MetAsnLys

1181 gttgctgtgc tgccgctc

LeuLeuCysCysAlaLeu

### 3.1.4. Osteoblast-released factors increase the expression of IL6 and TGFβ signaling pathway components in prostate cancer cells.

Since the neutralization experiments indicated a possible role for IL6 and TGFβ1 in the induction of osteomimicry, it was investigated whether osteoblast-released factors affect the expression of these molecules and their receptors in prostate cancer cells.

### 3. Results

Different groups have reported either that LNCaP secrete no IL6 [Okamoto *et al.* 1997, Chung *et al.* 1999, Giri *et al.* 2001] or secrete it in low amounts [Siegall *et al.* 1990]. The highly sensitive qRT-PCR assay used here showed that LNCaP and C4-2B4 expressed small but detectable amounts of *IL6* mRNA. Furthermore, in the cell lysate of LNCaP and C4-2B4, an antibody against IL6 detected three bands between 23,6 and 27,8 kDa, corresponding to three glycosylation variants of IL6 (Fig. 12A), a cytokine which may range in size from 21 to 28 kDa. It has been reported that prostate cancer cells express IL6R, the ligand-binding receptor for IL6 [Siegall *et al.* 1990, Okamoto *et al.* 1997, Chung *et al.* 1999]. Here, *IL6R* mRNA expression could be confirmed in LNCaP, C4-2B4 and PC3 (Fig. 15). qRT-PCR data showed that *IL6* and *IL6R* both became significantly upregulated in LNCaP and C4-2B4 after crosstalk with osteoblasts or exposure to hfOB CM. In LNCaP, *IL6* upregulation became firmly established after only 16 h of coculture (Fig. 16). In PC3 cells, which constitutively expressed and secreted very high levels of IL6, crosstalk with osteoblasts did not cause changes in either *IL6* or *IL6R* expression (Tab. 8).

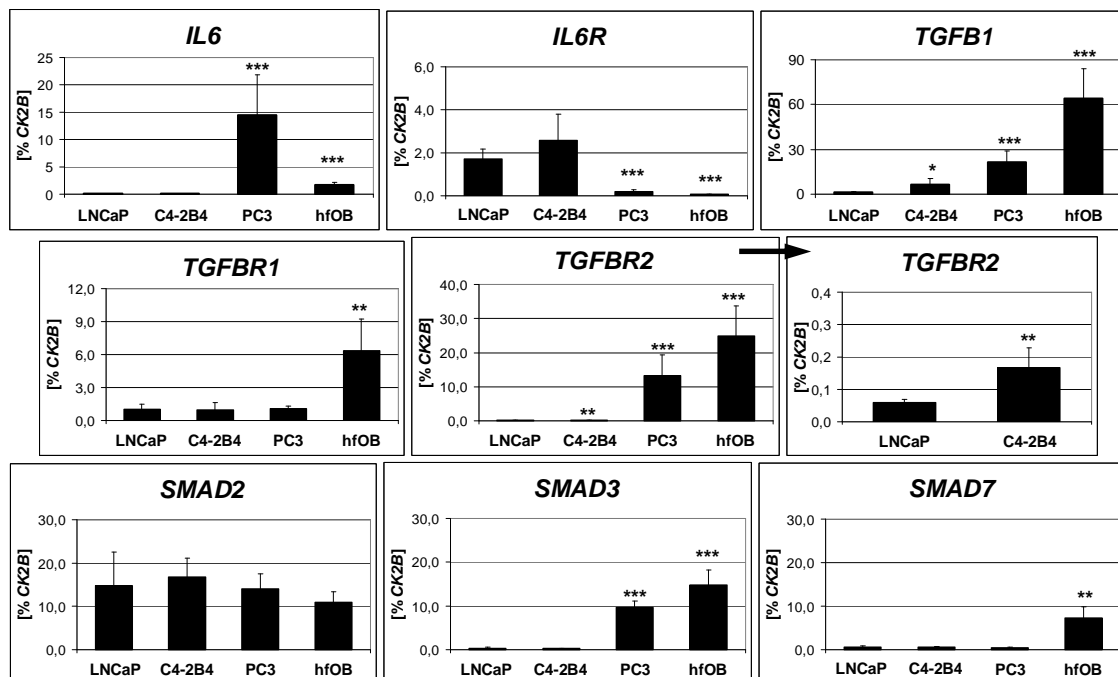


**Fig. 15 Steady-state mRNA levels of IL6 and TGFβ1 pathway components in prostate cancer cells and osteoblasts.** Error bars represent the mean ± SD of at least three independent values.

\* p < 0,05; \*\* p < 0,01; \*\*\* p < 0,001 (vs. LNCaP)

**Tab. 8 Changes in the expression of IL6 and TGF $\beta$ 1 pathway components, induced in prostate cancer cells by osteoblast-released factors.** For details see legend to Tab. 7. Alterations with a t-test p value < 0,05 were considered significant.  $\blacktriangle\blacktriangle$ , fold change  $\geq 2$ ;  $\blacktriangle$ , fold change  $\geq 1,45$ ;  $\nabla$ , fold change  $\leq 0,69$  (-1,45);  $\nabla\nabla$ , fold change  $\leq 0,5$  (-2); nc, no change; V, variable (clear tendency, but standard deviation too high;  $p > 0,05$ ). [X]<sup>hfOB</sup>, hfOB-cocultured prostate cancer cells; hfOB CM - osteoblast-conditioned medium diluted 1:1.

Gene symbol	LNCaP <sup>hfOB</sup> 24 h	LNCaP <sup>hfOB</sup> 48 h	LNCaP + hfOB CM 48 h
<i>IL6</i>	$\blacktriangle\blacktriangle$	$\blacktriangle\blacktriangle$	$\blacktriangle\blacktriangle$
<i>IL6R</i>	$\blacktriangle\blacktriangle$	$\blacktriangle$	nc
<i>TGFBI</i>	$\blacktriangle\blacktriangle$	$\nabla\nabla$	$\blacktriangle\blacktriangle$
<i>TGFBRI</i>	nc	$\blacktriangle\blacktriangle$	nc
<i>TGFBR2</i>	$\blacktriangle\blacktriangle$	nc	$\blacktriangle\blacktriangle$
<i>SMAD2</i>	nc	nc	nc
<i>SMAD3</i>	$\blacktriangle\blacktriangle$	$\blacktriangle\blacktriangle$	$\blacktriangle\blacktriangle$
<i>SMAD7</i>	nc	nc	nc

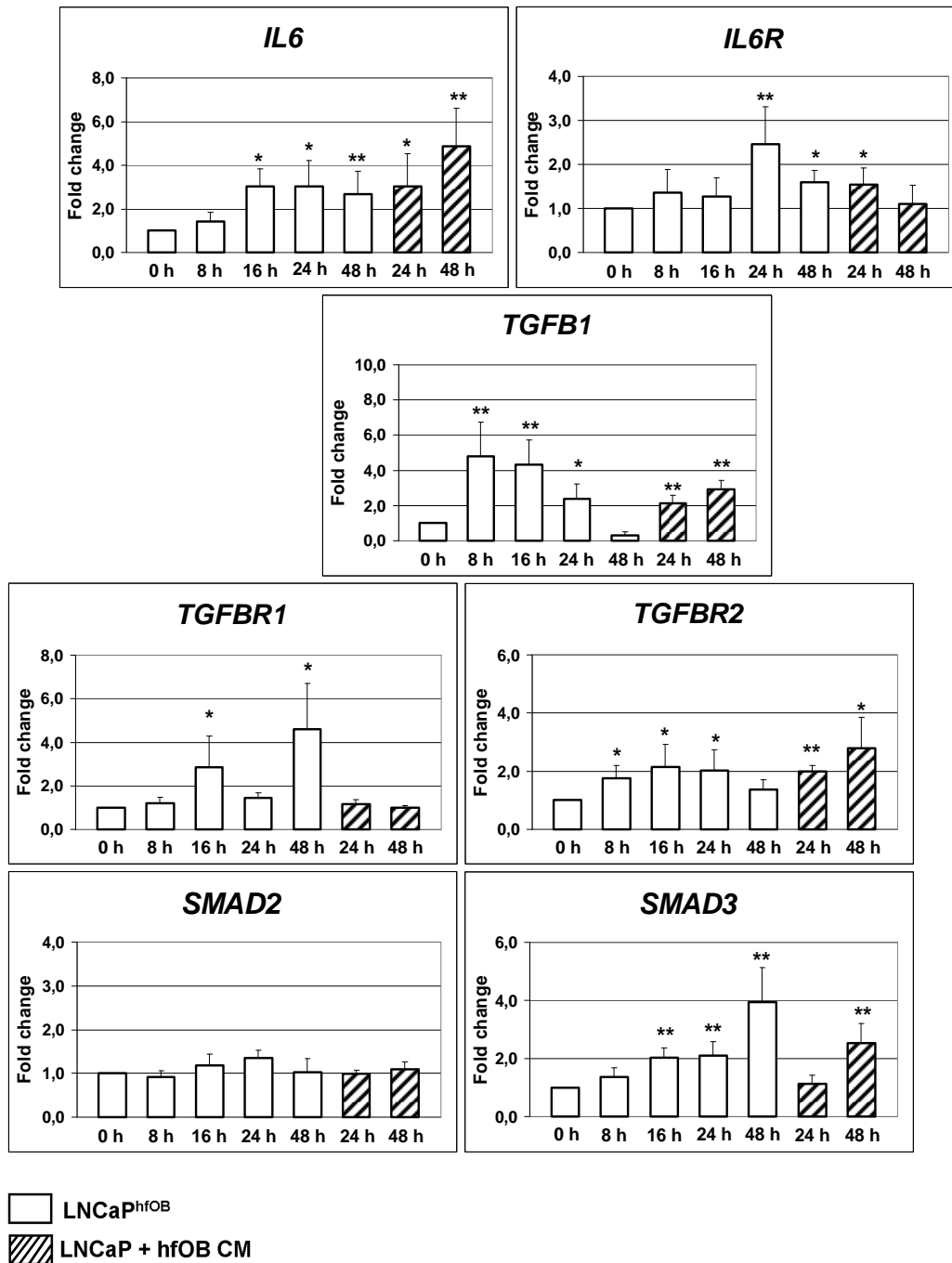
Gene symbol	C4-2B4 <sup>hfOB</sup> 24 h	C4-2B4 <sup>hfOB</sup> 48 h	C4-2B4 + hfOB CM 48 h
<i>IL6</i>	$\blacktriangle$	$\blacktriangle\blacktriangle$	$\blacktriangle\blacktriangle$
<i>IL6R</i>	$\blacktriangle$	$\blacktriangle\blacktriangle$	$\blacktriangle$
<i>TGFBI</i>	nc	$\nabla$	V
<i>TGFBRI</i>	$\blacktriangle$	$\blacktriangle$	nc
<i>TGFBR2</i>	$\blacktriangle$	nc	$\blacktriangle\blacktriangle$
<i>SMAD2</i>	$\blacktriangle$	$\blacktriangle$	nc
<i>SMAD3</i>	$\blacktriangle\blacktriangle$	$\blacktriangle\blacktriangle$	$\blacktriangle\blacktriangle$
<i>SMAD7</i>	nc	nc	nc

Gene symbol	PC3 <sup>hfOB</sup> 24 h	PC3 <sup>hfOB</sup> 48 h	PC3 + hfOB CM 48 h
<i>IL6</i>	nc	nc	nc
<i>IL6R</i>	nc	nc	nc
<i>TGFBI</i>	nc	nc	nc
<i>TGFBRI</i>	nc	$\blacktriangle$	nc
<i>TGFBR2</i>	nc	nc	nc
<i>SMAD2</i>	nc	nc	nc
<i>SMAD3</i>	nc	$\blacktriangle$	nc
<i>SMAD7</i>	nc	$\blacktriangle\blacktriangle$	V

All three prostate cancer cell lines expressed TGF $\beta$ 1 mRNA and protein (Fig. 15). There is controversy in literature regarding the expression of TGF $\beta$  receptors and sensitivity to TGF $\beta$  signaling in LNCaP, with some researchers reporting a lack of sensitivity due to a lack of expression of the type I (TGFBRI) [Kim *et al.* 1996a; for description of the TGF $\beta$  signaling pathway see Discussion 4.2.2] or type II (TGFBR2) TGF $\beta$  receptors, possibly due to silencing mediated by promoter methylation [Zhang *et al.* 2005b], while others observed sensitivity under certain conditions of growth factor or androgen stimulation [Schuurmans *et al.* 1991, Kim *et al.* 1996b]. The results presented here show that LNCaP and C4-2B4 both expressed high amounts of *TGFBRI* and low but detectable amounts of *TGFBR2* mRNA, and thus were potentially

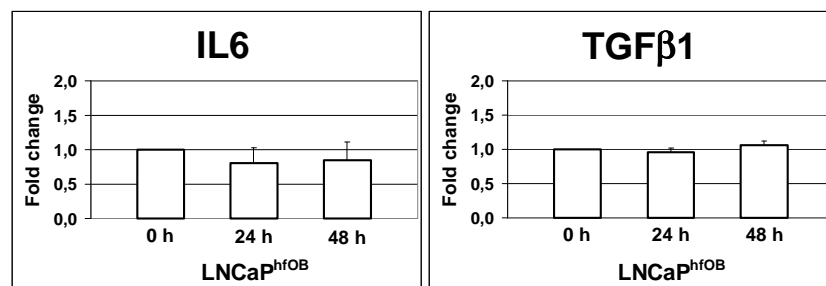
responsive to  $TGF\beta$ . Furthermore, expression of *TGFB1* and *TGFB2* mRNA was clearly higher in the osteotropic lines C4-2B4 and PC3 as compared to non-osteotropic LNCaP (Fig. 15).



**Fig. 16** Time-course curves of IL6 and  $TGF\beta$  pathway component mRNAs in LNCaP cocultured with osteoblasts or treated with osteoblast-conditioned medium. For details see legend to Tab. 7. Error bars represent the mean  $\pm$  SD of at least three independent experiments. \*  $p < 0,05$ ; \*\*  $p < 0,01$

Osteoblast-released factors caused an increase in the levels of TGF $\beta$  receptor mRNA in prostate cancer cells. *TGFBR1* became upregulated in all three prostate cancer cell lines after coculture with osteoblasts (Tab. 8). *TGFBR2* was also upregulated after 24 h of coculture and after 48 h of hfOB CM treatment in LNCaP and C4-2B4. *TGFBI* itself became upregulated only in LNCaP, the cell line which showed the lowest baseline expression of *TGFBI* mRNA. Time-course curves performed in LNCaP show that *TGFBI* became strongly upregulated after only 8 h of coculture with osteoblasts and the upregulation was still noticeable at 24 h, but disappeared after 48 h. When LNCaP cells were treated with hfOB CM, *TGFBI* was upregulated after 24 h and after 48 h (Fig. 16).

**A.**



**B.**

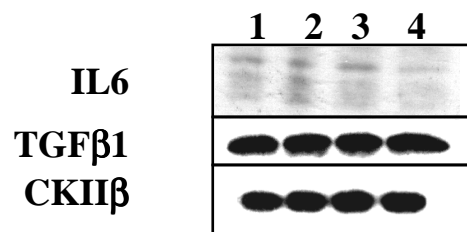


**Fig. 17 Levels of intracellular IL6 and TGF $\beta$ 1 protein in LNCaP after coculture with osteoblasts.** Shown are densitometric quantifications of respective bands (A) and representative blots (B). Results were normalized to CKII $\beta$ . For details see legend to Tab. 12. Error bars represent the mean  $\pm$  SD of three independent experiments. Cells: 1, LNCaP 24 h; 2, LNCaP 48 h; 3, LNCaP<sup>hfOB</sup> 24 h; 4, LNCaP<sup>hfOB</sup> 48 h.

In sum, expression of the mRNAs encoding TGF $\beta$ 1 and its receptors apparently increased when prostate cancer cells became exposed to the bone microenvironment. These results underscore a possible link between enhanced TGF $\beta$  signaling and the establishment of bone metastases. Differences in results obtained after coculture and after CM treatment suggest that dynamic cell crosstalk may modulate the final effect of osteoblast-released factors on TGF $\beta$  signaling in prostate cancer cells.

Intracellular protein levels of IL6 and TGF $\beta$ 1 remained unchanged in LNCaP after 24 h and 48 h of coculture with osteoblasts, indicating that the entire newly synthesized protein may be efficiently secreted (Fig. 17).

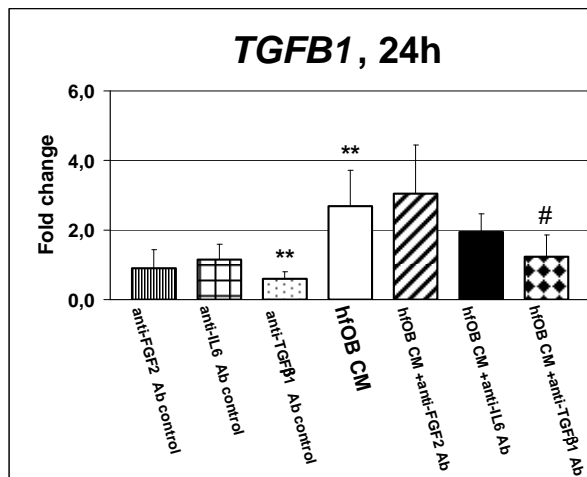
Expression of the TGF $\beta$  signaling mediators *SMAD2*, *SMAD3* and *SMAD7* was investigated as well. *SMAD2* and *SMAD3* belong to the class of receptor-activated SMADs; they become phosphorylated after ligand binding to the TGF $\beta$  receptor, associate with *SMAD4* and translocate into the nucleus, where they activate or repress the expression of target genes [Brown *et al.* 2007]. *SMAD7* inhibits TGF $\beta$  signaling both at the receptor level and in the nucleus and plays an essential role in the negative feedback regulation of this pathway [Afrakhte *et al.* 1998, Zhang *et al.* 2007]. Baseline *SMAD3* expression was significantly higher in C4-2B4 and PC3 than in LNCaP, whereas *SMAD2* and *SMAD7* levels did not differ significantly between the analyzed prostate cancer cell lines (Fig. 15). Furthermore, osteoblast-released factors caused strong upregulation of *SMAD3*, but not *SMAD2* mRNA in LNCaP and C4-2B4, both after coculture and after CM treatment (Fig. 16).

In the case of PC3 cells, coculture with osteoblasts for 48 h increased the mRNA levels of *TGFBR1* and *SMAD3*, but also of *SMAD7*, a negative regulator of TGF $\beta$  signaling. It could be hypothesized that in LNCaP and C4-2B4, the levels of autocrine TGF $\beta$  signaling are lower due to a lower constitutive expression of *TGFBI* and *TGFBR2* as compared with PC3, and thus, the negative feedback mechanism is not immediately activated after TGF $\beta$  stimulation. Significantly, all the investigated components of the TGF $\beta$  pathway except for *SMAD2* were much more abundantly expressed by osteoblasts than by prostate cancer cells (Fig. 15), underscoring the importance of TGF $\beta$  signaling in osteoblast biology.

*TGFBI* is a known target gene of FGF2 [Fenig *et al.* 2001] and of TGF $\beta$  signaling [Van Obberghen-Schilling *et al.* 1988]. It was investigated whether osteoblast-released FGF2, IL6 or TGF $\beta$ 1 contribute to *TGFBI* upregulation in LNCaP. Neutralizing antibodies against TGF $\beta$ 1, but not against FGF2 or IL6 abolished *TGFBI* mRNA upregulation in LNCaP in response to hfOB CM (Fig. 18A). The neutralizing antibody against TGF $\beta$ 1 also significantly reduced baseline expression of *TGFBI* mRNA, to ca. 60% of the control. However, treatment with recombinant TGF $\beta$ 1 alone did not induce *TGFBI* mRNA in LNCaP (Fig. 18B). Thus, baseline *TGFBI* expression in LNCaP cells appears to be maintained, at least in part, by autocrine TGF $\beta$  signaling and becomes elevated in response to TGF $\beta$ 1 (autocrine and paracrine) acting in synergism with other factors secreted by osteoblasts, whereas TGF $\beta$ 1 alone added to the medium is not enough to cause such an effect.

The baseline expression of *IL6* mRNA in LNCaP is so low that antibody neutralization experiments were not employed to investigate the mechanisms of its upregulation, since the error margin would have been very high. *IL6* is a known target gene of TGF $\beta$  signaling [Franchimont 2000], but treatment with recombinant TGF $\beta$  for 24 h did not increase *IL6* expression in LNCaP (Fig. 18B).

A.



B.

	8 h	24 h		
	TGF $\beta$ 1 10 ng/ml	IL6 10 ng/ml	TGF $\beta$ 1 10 ng/ml	IL6 10 ng/ml + TGF $\beta$ 1 10 ng/ml
<i>IL6</i>	nc	nc	nc	nc
<i>TGF<math>\beta</math>1</i>	nc	nc	nc	nc
<i>SMAD3</i>	nc	nc	nc	nc

**Fig. 18 Effect of candidate factors on the expression of signaling pathway components by cancer cells.**

(A) Effect of neutralizing antibodies on the upregulation of *TGF $\beta$ 1* in LNCaP by osteoblast-conditioned medium. \*  $p < 0,05$ ; \*\*  $p < 0,01$  (vs. LNCaP); #  $p < 0,05$  (vs. LNCaP + hfOB CM). Error bars represent the mean  $\pm$  SD of at least three independent experiments. (B) Effect of recombinant proteins on the expression of *IL6* and TGF $\beta$  pathway components in LNCaP. For details see legend to Fig 13. Alterations with a t-test  $p$  value  $< 0,05$  were considered significant. nc, no change.

### 3.2. The response of osteoblasts to prostate cancer cells

#### 3.2.1. Exposure of osteoblasts to the secretome of prostate cancer cells significantly alters their pattern of gene expression.

To investigate early effects of the prostate cancer cell secretome on osteoblasts, immortalized human fetal osteoblasts (hfOB 1.19) were cocultured with three different prostate

cancer cell lines: the osteolytic PC3 [Nemeth *et al.* 1999, Fisher *et al.* 2002], the mixed osteolytic/osteoblastic LNCaP [Nemeth *et al.* 1999] or the osteoblastic C4-2B4 [Thalman *et al.* 2000]. The cellular crosstalk was allowed to proceed for 48 h, followed by cell harvesting, RNA preparation and RNA quality check. Large-scale transcript profiling was then performed using Human Genome U133A 2.0 oligonucleotide array chips (Affymetrix) containing more than 22,000 probe sets corresponding to 14,500 well-characterized genes. Two individual biological replicate samples were assayed per coculture set. Transcript level differences between cocultured and monocultured osteoblasts were rated as significant when 2-fold or higher. Differences 1.5-fold or higher, but smaller than 2-fold were rated as tendentious.

The crosstalk between prostate cancer cells and osteoblasts for 48 h strongly affected the osteoblast transcriptome. Altogether, the expression of 309 genes became significantly altered, i.e., roughly 2% of all probed genes, and a tendency to expression alterations was noted for more than 1,100 genes (Fig. 19). The three employed prostate cancer cell lines contributed differently to these alterations. PC3 had the broadest effect; 242 genes showed significant expression changes, 117 of these were upregulated and 125 repressed. LNCaP was less effective, altering expression of 166 genes, of which 89 were upregulated and 77 repressed. C4-2B4 showed the weakest effect, changing expression of 138 genes, of which 61 were upregulated and 77 repressed.

Various genes in the osteoblast transcriptome responded selectively to either only one of the prostate cancer lines, to two, or to all three of them. Of these, the groups of genes responsive selectively to a certain type of prostate cancer cells only (cell type-specific osteoblast responses) and responsive unspecifically to all three prostate cancer lines (universal osteoblast responses) appeared to be of particular importance for the metastatic process (see below). Thus, 110 significantly altered genes were selectively responsive to PC3, 38 upregulated and 72 repressed; 33 genes were responsive only to LNCaP, 12 upregulated and 21 repressed; and 18 genes were only responsive to C4-2B4, 1 upregulated and 17 repressed. 89 genes were significantly affected by all three of the employed prostate cancer lines, i.e., regardless of their respective osteolytic or osteoblastic nature. Of these 89, 48 genes became upregulated and 41 repressed.



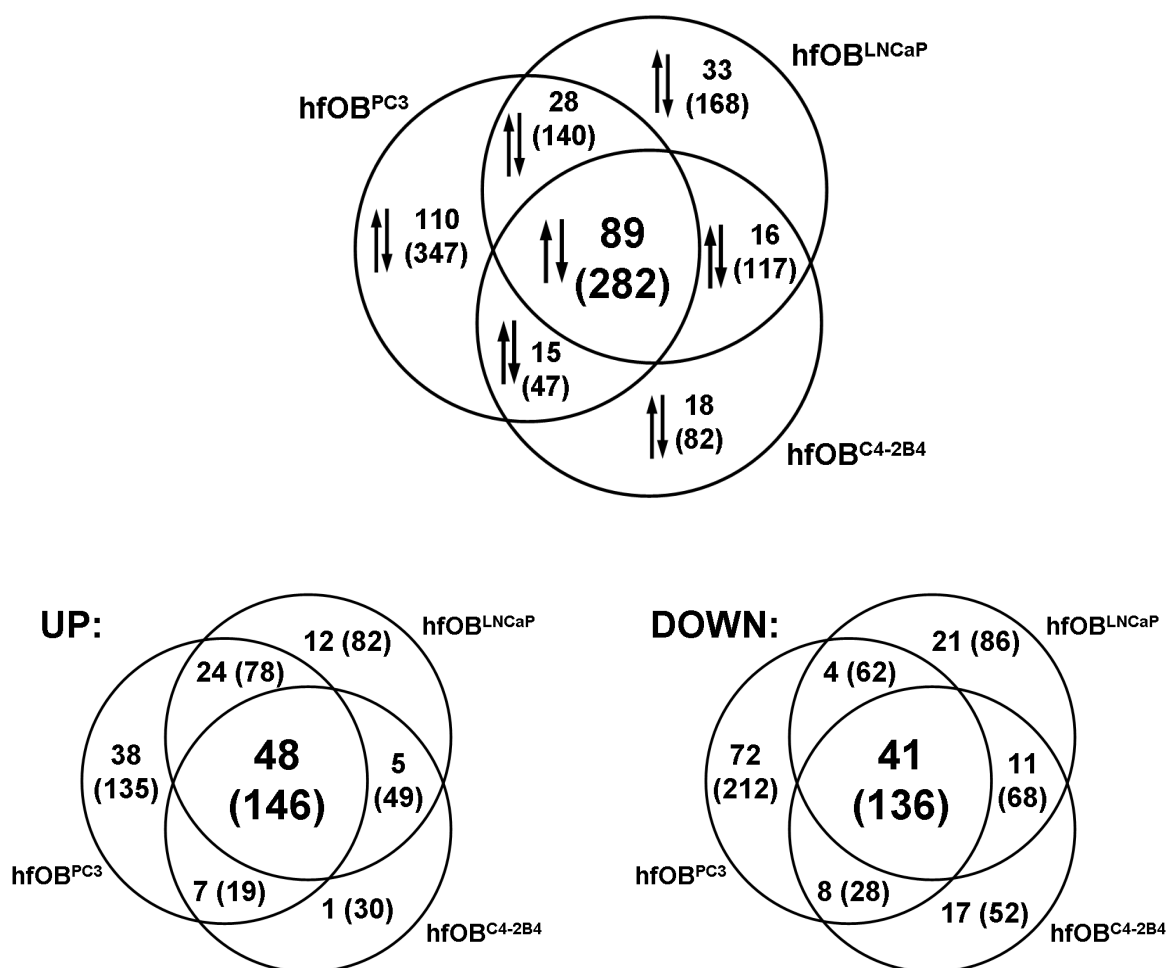


**Fig. 19 Gene expression alterations in osteoblasts due to their crosstalk with prostate cancer cells *via* released factors (Venn diagram).** Large-scale transcript profiling was performed using the Human Genome U133A GeneChip arrays (Affymetrix) comprising 14,500 gene equivalents. Transcript profiles of hfOB cocultured with each of three prostate cancer cell lines (PC3, LNCaP or C4-2B4) for 48 h in a bicompartiment system were compared to noncocultured hfOB. Numbers indicate genes with significant ( $\geq 2$ -fold) expression alterations; numbers in parentheses indicate the total sum of altered genes, comprising genes with significant and with tendentious ( $\geq 1.5$ -fold) alterations. *Note:* Genes altered significantly in 1 coculture combination and tendentiously in the 2 others were treated as tendentiously altered in 3 combinations, not as significantly altered only in 1. This approach was chosen to gain a more stringent selection of selectively altered genes.

### 3.2.2. Universal osteoblast responses - genes similarly affected in osteoblasts by both osteolytic and osteoblastic prostate cancer cells.

Osteolytic and osteoblastic processes are interactively involved in bone metastasis. Therefore, genes affected similarly in osteoblasts by the secretomes of osteolytic and osteoblastic cancer cells are of particular importance, because among these one would expect candidate genes playing general roles in bone metastasis. Their identification may offer clues as to the universal osteoblast response at a very early stage of prostate cancer metastasis, and thus

provide insights into potential mechanisms of the formation of osteoblastic lesions, as well as effects on prostate cancer stem cell niches.

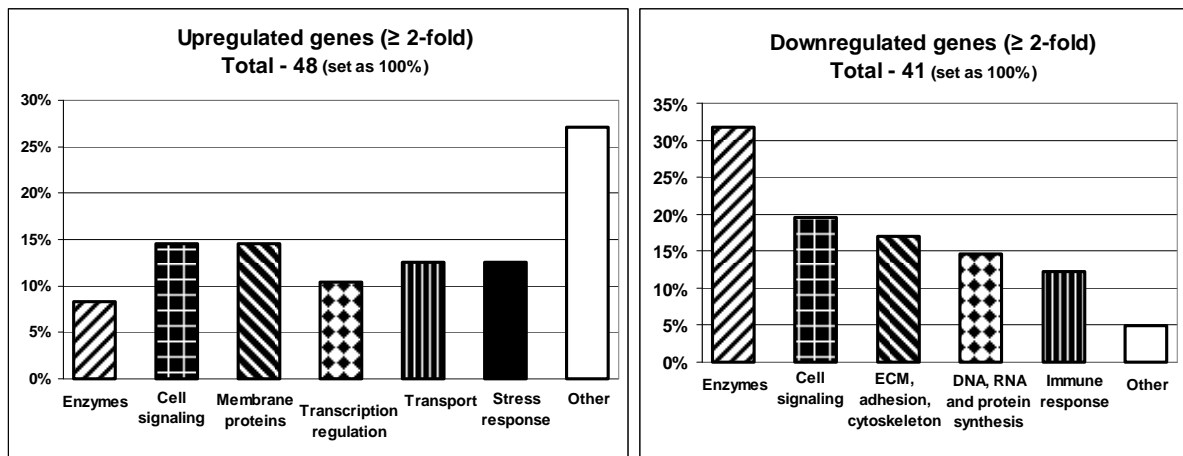


**Fig. 20** Functional classification of genes altered  $\geq 2$ -fold in osteoblasts by coculture for 48 h with each of three prostate cancer cell lines. For further details see Fig. 19.

Our analysis indicates that 89 genes became significantly affected by all three of the employed prostate cancer cell lines, i.e., by osteolytic and osteoblastic cancer cells. Functionally, this group comprises genes linked to various cellular processes. Among the 48 transcripts most strongly elevated in hfOB cocultured with all three prostate cancer cell lines, 6 were genes associated with stress response, 7 were associated with cell signaling and 5 with regulation of transcription, while 6 coded for solute carriers and proteins involved in vesicle trafficking, suggesting a switch of transcription programs and modulation of transport and secretory activities. Among the 41 transcripts most strongly repressed in all three coculture combinations, 13 coded for various enzymes, 7 represented extracellular matrix components, adhesion molecules and cytoskeletal proteins, 6 were associated with DNA replication, transcription or translation, and 5 with immune response and inflammation (Fig. 20). Interestingly, while the majority of functional groups encoding enzymes, signaling elements, etc. included, as one would expect, both upregulated and repressed transcripts, transcripts encoding stress-associated molecules were present only among the 41 upregulated genes, whereas transcripts associated with immune response and inflammation were found only in the downregulated group. (For full list see Supplementary Data).

In order to disclose details of the gene-to-function relationships, we have utilized information provided by available databases (Entrez Gene and PubMed; see Materials and

methods 2.3.4). Genes affected by the cell crosstalk have been arranged, according to major cellular tasks of gene products, into groups relating to modulation of pro- and antiapoptotic mechanisms, DNA and RNA synthesis, signaling, immune response, etc. Tab. 9 presents a broad selection of transcripts which were altered in osteoblasts - either significantly or tendentially - by all three prostate cancer cell lines, and which represent the relevant functional groups.

The overall pattern of transcriptional alterations was suggestive of stress-related growth arrest, with upregulation of stress-responsive transcripts encoding cell cycle repressors - *DUSP1*, coding for a specific antiproliferative phosphatase, and *TTK*, which encodes a kinase that halts mitosis in response to spindle damage. Also upregulated were other stress-induced transcripts, such as *PPP1R15A*, *RORA* and *TAF9B*, encoding a phosphatase, an orphan receptor, and a TATA box binding protein-associated factor, respectively. A concomitant elevation of genes encoding the apoptosis effector *CASP3*, the potentially proapoptotic *CLCA2* and *LRDD*, the pro-survival kinase *PIK3C2A* and of the antiapoptotic regulator *BCL2A1* could be observed, while proapoptotic molecules such as *BECN1*, *GLIPR1*, *FADD* and *IFI27* were downregulated, suggesting an overall pro-survival effect.

Simultaneously, there was evidence for strongly repressed proliferation, with concomitant repression of DNA, RNA and protein synthesis. Upregulation of genes encoding cell cycle repressors, such as *BTG1* and *COPS2*, was observed together with downregulation of transcripts such as *CIRBP*, *DDX5*, *MCM4* and *NASP*, associated with DNA replication and cell cycle progression. Similarly, the translation repressor gene *EIF4EBP1* was upregulated, while transcripts coding for tRNA synthetases (*MARS*, *NARS*) and components of translational machinery (*EIF5*, *PAIP1*, *SRP19*) were downregulated. An overall decrease of metabolic activity was also apparent, especially of lipid biosynthesis, as evidenced by upregulation of the negative regulator *INSIG1* and downregulation of enzymes participating in biosynthesis of fatty acids and cholesterol (*ACACA*, *ACLY*, *DHCR24*, *FASN*). Genes associated with proteasome function (*DSCR2*, *PSMA3*, *PSMA4*, *PSMD6*) were downregulated as well, suggesting a decrease in ubiquitin-dependent protein degradation.

Further important changes could be seen in regulons associated with cell adhesion, cytoskeletal organization and extracellular matrix formation, as well as genes linked to osteoblast differentiation and bone remodeling. The observed changes in signaling pathways suggested a repression of TGF $\beta$  signaling, with upregulation of genes of negative regulators *PPM1A* and *SNF1LK*, downregulation of the type II receptor *TGFBR2*, and the accessory molecule *DAB2*. Moreover, there was a corresponding downregulation of TGF $\beta$  target genes, including adhesion molecules (*CDH11*, *THBS1*), extracellular matrix components (*COL1A1*,

*COL1A2*, *COL3A1*, *TNC*) and cytokines (*CTGF*, *FST*, *FGF2*). Multiple genes associated with immune response and inflammation were strongly downregulated as well. Among them were *NEDD9*, encoding a cell cycle regulator and target of inflammatory cytokines; *STAT1*, encoding a central mediator of inflammatory signaling; genes for the chemokines *CCL2*, *CXCL6* and *CXCL12*; the proinflammatory cytokine *IL6*; *PTX3*, a marker of inflammation; and three molecules involved in inflammation-induced bone remodeling - *ADAMTS1*, *HMGB1* and *PAPPA*.

The changes seen in the osteoblast differentiation regulon included upregulation of genes encoding bone-stimulatory cytokines (*ADM*, *STC1*), signaling pathway components (*FGFR1*, *IRS2*) and transcription factors (*HES1*, *SP3*) associated with increased differentiation. By contrast, *DKK1* and *FST*, genes encoding inhibitors of osteoblast differentiation and bone formation, became downregulated.

To verify the array data, the expression of a number of up- and downregulated genes, with a varied intensity of the effect, was also analyzed by qRT-PCR performed on four to six individual biological replicate samples. In all the investigated cases, including tendentious alterations, gene expression changes observed on the array could be confirmed by qRT-PCR, showing that the array analysis was robust (Fig. 21 A-B).

Many of the gene expression changes which occurred universally in osteoblasts cocultured with all three prostate cancer cell lines were also caused by coculture with the non-osteotropic cancer cell line HeLa or the non-cancerous lung fibroblast line IMR-90. To exclude the possibility that the presence of a plastic transwell insert could interfere with experimental results, hfOB grown in wells with an empty insert were also assayed by qRT-PCR. It was found that the presence of an insert in itself either did not alter transcript levels at all or changes were very slight, causing no significant differences in the outcome of calculated relative expression values of the investigated genes (Fig. 21 A-B).

It is also unlikely that the expression alterations were due to increased medium exhaustion in coculture, since significant changes could already be observed after 24 h, e.g., upregulation of *NPPB* and repression of *CDH2*, *CDH11*, *IL6* and *TGFBR2* (Fig. 22). On the other hand, the transcript level of *STC1* remained unaltered during the first 24 h but became upregulated after 48 h (Fig. 22).

The possibility that a switch between culturing cells in wells and in inserts might affect gene expression has previously been excluded by Knerr *et al.*, 2004.

**Tab. 9 Universal transcription alterations in osteoblasts cocultured with prostate cancer cells.**

Genes were divided into functional groups on the basis of information from the Entrez Gene and PubMed databases ([www.ncbi.nlm.nih.gov](http://www.ncbi.nlm.nih.gov)). The table shows genes with known function, belonging to the described groups and upregulated, either significantly or tendentially, in all three coculture combinations. For further details see the legend to Fig. 19.

hfOB<sup>X</sup>, X-cocultured hfOB; ▲▲, ≥ 2-fold elevation; ▲, ≥ 1,5-fold elevation; ▽▽, ≥ 2-fold repression; ▽, ≥ 1,5-fold repression; nc, no change; \*, verified by qRT-PCR; #, transcript upregulated by TGFβ; I, immune response; \*\*, change seen only in qRT-PCR

Entrez GeneID	Gene Symbol	Gene Product	Description	hfOB <sup>PC3</sup> 48 h	hfOB <sup>LNCaP</sup> 48 h	hfOB <sup>C4-2B4</sup> 48 h
<b>Stress response; modulation of pro-and antiapoptotic mechanisms</b>						
597	<i>BCL2A1</i>	BCL2-related protein A1	Antiapoptotic regulator.	▲▲	▲▲	▲▲
836	<i>CASP3</i>	caspase 3, apoptosis-related cysteine peptidase	Central role in the execution-phase of cell apoptosis.	▲	▲▲	▲
9635	<i>CLCA2*</i>	chloride channel, calcium activated, family member 2	Ion channel; possible role in the early stages of the apoptotic cascade.	▲▲	▲▲	▲▲
1843	<i>DUSP1</i>	dual specificity phosphatase 1	Response to environmental stress, negative growth regulation.	▲	▲▲	▲▲
1647	<i>GADD45A</i>	growth arrest and DNA-damage-inducible, alpha	Transcript levels increase in stressful growth arrest conditions.	▲	▲	▲
55367	<i>LRDD</i>	leucine-rich repeats and death domain containing	May function as adaptor protein in cell death-related signaling.	▲	▲	▲▲
5286	<i>PIK3C2A</i>	phosphoinositide-3-kinase, class 2, alpha polypeptide	Crucial in pro-survival signaling; downregulation induces apoptosis.	▲	▲▲	▲
5494	<i>PPM1A</i>	protein phosphatase 1A (formerly 2C), magnesium-dependent, alpha isoform	Negative regulator of cell stress response pathways (p38, JNK kinase cascades); role in cell cycle control.	▲▲	▲▲	▲▲
23645	<i>PPP1R15A</i>	protein phosphatase 1, regulatory (inhibitor) subunit 15A	Transcript levels increase in stressful growth arrest conditions.	▲▲	▲▲	▲▲
3516	<i>RBPJ</i>	recombination signal binding protein for immunoglobulin kappa J region	Transcriptional repressor; antiapoptotic action in response to Notch signaling.	▲▲	▲	▲
6095	<i>RORA</i>	RAR-related orphan receptor A	Involved in cellular stress response.	▲▲	▲▲	▲▲
51616	<i>TAF9B</i>	TAF9B RNA polymerase II, TATA box binding protein (TBP)-associated factor, 31kDa	Regulates initiation of transcription by RNA Pol II; essential for cell viability, upregulated by apoptotic stimuli.	▲▲	▲▲	▲▲
7272	<i>TTK</i>	TTK protein kinase	Component of spindle assembly checkpoint - halts mitosis in response to spindle damage.	▲▲	▲▲	▲▲
<b>Proapoptotic proteins</b>						
8678	<i>BECN1</i>	beclin 1 (coiled-coil, myosin-like BCL2 interacting protein)	Proapoptotic protein.	▽	▽▽	▽
11010	<i>GLIPR1</i>	GLI pathogenesis-related 1 (glioma)	Proapoptotic protein.	▽▽	▽▽	▽
8772	<i>FADD</i>	Fas (TNFRSF6)-associated via death domain	Mediates cell apoptotic signals.	▽	▽▽	▽▽
3429	<i>IFI27<sup>I</sup></i>	interferon, alpha-inducible protein 27	Proapoptotic protein; impacts normal mitochondrial function.	▽	▽▽	▽▽
4599	<i>MXI<sup>I</sup></i>	myxovirus (influenza virus) resistance 1, interferon-inducible protein p78 (mouse)	Proapoptotic protein (putative).	▽▽	▽▽	▽▽
4739	<i>NEDD9<sup>I</sup></i>	neural precursor cell expressed, developmentally down-regulated 9	Cell cycle regulator (low levels cause mitotic arrest); involved in cell signaling and actin dynamics; target of inflammatory cytokines.	▽▽	▽▽	▽▽
7157	<i>TP53</i>	tumor protein p53 (Li-Fraumeni syndrome)	Stress response, cell cycle arrest, apoptosis.	▽▽	▽▽	▽

**Tab. 9 (continued)**

Entrez GeneID	Gene Symbol	Gene Product	Description	hfOB <sup>PC3</sup> 48 h	hfOB <sup>LNCaP</sup> 48 h	hfOB <sup>C4-2B4</sup> 48 h
<b>Decreased DNA and RNA synthesis, suppressed proliferation</b>						
694	<i>BTG1</i>	B-cell translocation gene 1, anti-proliferative	Member of an anti-proliferative gene family that regulates cell growth and differentiation.	▲▲	▲▲	▲
9318	<i>COPS2</i>	COP9 constitutive photomorphogenic homolog subunit 2 (Arabidopsis)	Transcriptional corepressor. Inhibits expression of the cell cycle regulator E2F1 and cell proliferation.	▲▲	▲	▲
8883	<i>APPBP1</i>	amyloid beta precursor protein binding protein 1	Required for cell cycle progression through the S/M checkpoint.	▽	▽▽	▽
1153	<i>CIRBP</i>	cold inducible RNA binding protein	Enhances cell proliferation.	▽▽	▽▽	▽▽
1655	<i>DDX5</i>	DEAD (Asp-Glu-Ala-Asp) box polypeptide 5	RNA-dependent ATPase, proliferation-associated nuclear antigen.	▽▽	▽▽	▽▽
3015	<i>H2AFZ</i>	H2A histone family, member Z	Structural component of chromatin.	▽	▽▽	▽▽
4173	<i>MCM4</i>	minichromosome maintenance complex component 4	Essential for initiation of DNA replication.	▽▽	▽▽	▽▽
4678	<i>NASP</i>	nuclear autoantigenic sperm protein (histone-binding)	Involved in transporting histones into the nucleus of dividing cells.	▽	▽▽	▽
6421	<i>SFPQ</i>	splicing factor proline/glutamine-rich (polypyrimidine tract binding protein associated)	Multiple functions in many nuclear processes.	▽▽	▽▽	▽▽
6432	<i>SFRS7</i>	splicing factor, arginine/serine-rich 7, 35kDa	Role in mRNA splicing.	▽▽	▽▽	▽
3925	<i>STMN1*</i>	stathmin 1/oncoprotein 18	Prevents assembly and promotes disassembly of microtubules; inhibiting expression of this protein reduces cell proliferation.	▽	▽**	▽**
<b>Decreased protein synthesis</b>						
1978	<i>EIF4EBP1</i>	eukaryotic translation initiation factor 4E binding protein 1	Translation repressor.	▲▲	▲▲	▲
708	<i>CIQBP</i>	complement component 1, q subcomponent binding protein	Subunit of pre-mRNA splicing factor.	▽	▽▽	▽▽
1983	<i>EIF5</i>	eukaryotic translation initiation factor 5	Translation initiation factor.	▽▽	▽▽	▽
4141	<i>MARS</i>	methionyl-tRNA synthetase	tRNA synthesis.	▽▽	▽▽	▽
4677	<i>NARS</i>	asparaginyl-tRNA synthetase	tRNA synthesis.	▽	▽▽	▽▽
10605	<i>PAIP1</i>	poly(A) binding protein interacting protein 1	Involved in translational initiation and protein biosynthesis.	▽▽	▽▽	▽▽
6728	<i>SRP19</i>	signal recognition particle 19kDa	Ribonucleoprotein, component of translational machinery.	▽▽	▽▽	▽
<b>Decreased proteasomal degradation of proteins</b>						
8624	<i>DSCR2</i>	Down syndrome critical region gene 2	Involved in the maturation of mammalian 20S proteasomes.	▽▽	▽	▽
5684	<i>PSMA3</i>	proteasome (prosome, macropain) subunit, alpha type, 3	Protein degradation.	▽▽	▽▽	▽
5685	<i>PSMA4</i>	proteasome (prosome, macropain) subunit, alpha type, 4	Protein degradation.	▽▽	▽▽	▽
9861	<i>PSMD6</i>	proteasome (prosome, macropain) 26S subunit, non-ATPase, 6	Protein degradation.	▽	▽▽	▽

**Tab. 9 (continued)**

Entrez GeneID	Gene Symbol	Gene Product	Description	hfOB <sup>PC3</sup> 48 h	hfOB <sup>LNCaP</sup> 48 h	hfOB <sup>C4-2B4</sup> 48 h
<b>Decreased lipid metabolism and cholesterol biosynthesis</b>						
3638	<i>INSIG1</i>	insulin induced gene 1	Regulator of lipid metabolism. Inhibits lipid synthesis.	▲▲	▲▲	▲▲
31	<i>ACACA</i>	acetyl-Coenzyme A carboxylase alpha	Fatty acid synthesis.	▽▽	▽▽	▽▽
47	<i>ACLY</i>	ATP citrate lyase	Synthesis of acetyl-CoA; lipogenesis, cholesterologenesis.	▽	▽▽	▽
8560	<i>DEGS1</i>	degenerative spermatocyte homolog 1, lipid desaturase (Drosophila)	Membrane fatty acid desaturase.	▽▽	▽▽	▽▽
1718	<i>DHCR24</i>	24-dehydrocholesterol reductase	Cholesterol biosynthesis.	▽▽	▽▽	▽▽
3295	<i>HSD17B4</i>	hydroxysteroid (17-beta) dehydrogenase 4	Beta-oxidation of fatty acids.	▽▽	▽▽	▽▽
2194	<i>FASN</i>	fatty acid synthase	Synthesis of long-chain saturated fatty acids.	▽	▽▽	▽▽
<b>Cytoskeleton</b>						
60	<i>ACTB*</i>	actin, beta	Major constituent of the cell contractile apparatus.	▽	▽**	▽**
10092	<i>ARPC5</i>	actin related protein 2/3 complex, subunit 5, 16kDa	Implicated in the control of actin polymerization.	▽	▽	▽
4771	<i>NF2</i>	neurofibromin 2 (bilateral acoustic neuroma)	Interacts with proteins involved in cytoskeletal dynamics.	▽▽	▽▽	▽▽
<b>Cell adhesion</b>						
1009	<i>CDH11</i> #	cadherin 11, type 2, OB-cadherin (osteoblast)	Component of adherens junctions; osteoblast-specific, role in osteoblast differentiation.	▽▽	▽▽	▽▽
7057	<i>THBS1</i> #	thrombospondin 1	Adhesion molecule (cell-cell, cell-matrix). Activates latent TGFβ.	▽▽	▽▽	▽▽
<b>Extracellular matrix</b>						
1277	<i>COL1A1</i> *#	collagen, type I, alpha 1	Bone matrix component (collagen).	▽▽	▽▽	▽▽
1278	<i>COL1A2</i> *#	collagen, type I, alpha 2	Bone matrix component (collagen).	▽▽	▽▽	▽▽
1281	<i>COL3A1</i> #	collagen, type III, alpha 1 (Ehlers-Danlos syndrome type IV, autosomal dominant)	ECM component (collagen).	▽▽	▽	▽
1301	<i>COL11A1</i>	collagen, type XI, alpha 1	ECM component (collagen).	▽▽	▽	▽
2202	<i>EFEMP1</i>	EGF-containing fibulin-like extracellular matrix protein 1	ECM component (non-collagenous).	▽▽	▽	▽
3371	<i>TNC</i> #	tenascin C (hexabrachion)	ECM component (non-collagenous).	▽▽	▽▽	▽
<b>Bone remodeling</b>						
1437	<i>CSF2</i>	colony stimulating factor 2 (granulocyte-macrophage)	Promotes osteoclastogenesis. Enhances osteolytic breast cancer metastasis.	▲▲	▲▲	▲▲
5329	<i>PLAUR*</i>	plasminogen activator, urokinase receptor	Membrane receptor for urokinase plasminogen activator, upregulation facilitates ECM remodeling.	▲	▲	▲
9510	<i>ADAMTS1</i> <sup>1</sup>	ADAM metallopeptidase with thrombospondin type 1 motif, 1	Inflammation-associated ECM remodeling.	▽▽	▽▽	▽▽
1956	<i>EGFR*</i>	epidermal growth factor receptor (erythroblastic leukemia viral (v-erb-b) oncogene homolog, avian)	Cell surface growth factor receptor. EGFR signaling in osteoblasts stimulates osteoclastogenesis by suppressing OPG expression.	▽**	▽**	▽

**Tab. 9 (continued)**

Entrez GeneID	Gene Symbol	Gene Product	Description	hfOB <sup>PC3</sup> 48 h	hfOB <sup>LNCaP</sup> 48 h	hfOB <sup>C4-2B4</sup> 48 h
3146	<i>HMGB1</i> <sup>1</sup>	high-mobility group box 1	Proinflammatory cytokine; osteoclastogenic factor, mediator of inflammatory bone loss.	▽	▽▽	▽
5069	<i>PAPPA</i> # <sup>1</sup>	pregnancy-associated plasma protein A	Metalloproteinase, target of inflammatory cytokines; involved in bone remodeling and bone formation.	▽▽	▽▽	▽▽
<b>Osteoblast differentiation</b>						
133	<i>ADM</i>	adrenomedullin	Potent anabolic agent for bone tissue; enhances cancer cell invasion.	▲▲	▲▲	▲
2260	<i>FGFR1</i>	fibroblast growth factor receptor 1 (fms-related tyrosine kinase 2, Pfeiffer syndrome)	Membrane receptor for fibroblast growth factors (FGFs). FGF signaling stimulates osteoblast differentiation.	▲▲	▲▲	▲▲
3280	<i>HES1</i>	hairy and enhancer of split 1, (Drosophila)	Transcription factor, cooperates with core binding factor 1 (CBFA1), stimulates osteoblast differentiation.	▲▲	▲▲	▲▲
8660	<i>IRS2</i>	insulin receptor substrate 2	Cytoplasmic mediator of cytokine signaling. Necessary for osteoblast differentiation and matrix synthesis.	▲▲	▲▲	▲▲
6670	<i>SP3</i> *	Sp3 transcription factor	Transcription factor essential for late bone development.	▲	▲**	▲**
6781	<i>STC1</i> *	stanniocalcin 1	Antiapoptotic cytokine. Stimulates osteoblast differentiation; putative factor in osteoblastic bone metastasis.	▲▲	▲▲	▲
22943	<i>DKK1</i> *	dickkopf homolog 1 ( <i>Xenopus laevis</i> )	Wnt signaling antagonist; inhibits osteoblast differentiation and bone formation.	▽▽	▽▽	▽▽
2247	<i>FGF2</i> #	fibroblast growth factor 2 (basic)	Can stimulate osteoblast differentiation or apoptosis, depending on the differentiation stage.	▽▽	▽▽	▽▽
10468	<i>FST</i> #	follistatin	Antagonist of activin A signaling; inhibits osteoblast differentiation.	▽▽	▽▽	▽▽
6772	<i>STAT1</i> <sup>1</sup>	signal transducer and activator of transcription 1, 91kDa	Signaling mediator of JAK/STAT pathway; involved in inflammatory signaling. Attenuates osteoblast differentiation and bone formation.	▽▽	▽▽	▽▽
<b>Cell signaling - TGFβ pathway</b>						
5494	<i>PPM1A</i>	protein phosphatase 1A (formerly 2C), magnesium-dependent, alpha isoform	Terminates TGFβ signaling by dephosphorylating activated Smad 2/3.	▲▲	▲▲	▲▲
150094	<i>SNF1LK</i>	SNF1-like kinase	Negative regulation of TGFβ signaling.	▲▲	▲▲	▲
1490	<i>CTGF</i> #	connective tissue growth factor	Enhances TGFβ binding to its receptors.	▽▽	▽▽	▽
1601	<i>DAB2</i> #	disabled homolog 2, mitogen-responsive phosphoprotein	Links cell surface receptors to downstream signaling pathways. Participates in TGFβ signaling via Smads and JNK.	▽▽	▽	▽▽
7048	<i>TGFBR2</i> *	transforming growth factor, beta receptor II (70/80kDa)	Receptor for TGFβ.	▽▽	▽▽	▽▽
<b>Cell signaling - other</b>						
3556	<i>IL1RAP</i>	interleukin 1 receptor accessory protein	Regulates cell sensitivity to interleukin 1.	▲▲	▲▲	▲▲
6236	<i>RRAD</i>	Ras-related associated with diabetes	Ras-related small G protein.	▲▲	▲▲	▲▲
25907	<i>TMEM158</i>	transmembrane protein 158	Marker of activated Ras signaling.	▲▲	▲▲	▲▲



**Tab. 9 (continued)**

Entrez GeneID	Gene Symbol	Gene Product	Description	hfOB <sup>PC3</sup> 48 h	hfOB <sup>LNCaP</sup> 48 h	hfOB <sup>C4-2B4</sup> 48 h
6347	<i>CCL2</i> <sup>1</sup>	chemokine (C-C motif) ligand 2	Chemoattractant for monocytes.	▽▽	▽▽	▽▽
6387	<i>CXCL12</i> # <sup>1</sup>	chemokine (C-X-C motif) ligand 12 (stromal cell-derived factor 1)	Chemoattractant for hematopoietic cells and metastasizing cancer cells.	▽▽	▽▽	▽
3569	<i>IL6</i> # <sup>1</sup>	interleukin 6 (interferon, beta 2)	Proinflammatory, pleiotropic cytokine.	▽▽	▽▽**	▽▽**
5156	<i>PDGFRA</i>	platelet-derived growth factor receptor, alpha polypeptide	Mitogen for cells of mesenchymal origin.	▽▽	▽▽	▽
5567	<i>PRKACB</i>	protein kinase, cAMP-dependent, catalytic, beta	Central role in cell signaling.	▽	▽▽	▽▽
5806	<i>PTX3</i> <sup>1</sup>	pentraxin-related gene, rapidly induced by IL-1 beta	Involved in inflammatory processes; marker of inflammation.	▽▽	▽▽	▽▽
5999	<i>RGS4</i>	regulator of G-protein signaling 4	Inhibits G protein signaling.	▽▽	▽▽	▽▽
<b>Genes altered in osteoblasts by two but not three prostate cancer cell lines, confirmed by qRT-PCR</b>						
2309	<i>FOXO3</i> * <sup>1</sup>	forkhead box O3	Transcription factor; functions as a trigger for apoptosis in osteoblasts.	▲	nc	▲**
9518	<i>GDF15</i> * <sup>1</sup>	growth differentiation factor 15	Increases the osteolytic component of prostate cancer bone metastases - induces osteoclast differentiation and activation.	▲▲	▲**	nc
4879	<i>NPPB</i> * <sup>1</sup>	natriuretic peptide precursor B	Promotes endochondral ossification and stem cell proliferation.	▲▲	nc	▲

**Tab. 10 Comparison of transcription alterations selective for osteoblasts cocultured with PC3 (osteolytic) and C4-2B4 (osteoblastic) prostate cancer cells.**

Genes were divided into functional groups on the basis of information from the Entrez Gene and PubMed databases ([www.ncbi.nlm.nih.gov](http://www.ncbi.nlm.nih.gov)). For further details see the legend to Fig. 19. Transcription alterations observed in only one coculture combination on the array, but confirmed by qRT-PCR as present in two or three coculture combinations have been included in Table 1.

hfOB<sup>X</sup>, X-cocultured hfOB; ▲▲, ≥ 2-fold elevation; ▲, ≥ 1,5-fold elevation; ▽▽, ≥ 2-fold repression; ▽, ≥ 1,5-fold repression; nc, no change; \*, verified by qRT-PCR; #, transcript upregulated by TGFβ; I, immune response; \*\*, change seen only in qRT-PCR

Entrez GeneID	Gene Symbol	Gene Product	Description	hfOB <sup>PC3</sup> 48 h	hfOB <sup>C4-2B4</sup> 48 h
<b>Stress response; modulation of pro- and antiapoptotic mechanisms</b>					
3708	<i>ITPR1</i>	inositol 1,4,5-triphosphate receptor, type 1	Calcium channel required for apoptotic cell death.	▲▲	nc
9467	<i>SH3BP5</i>	SH3-domain binding protein 5 (BTK-associated)	Mitochondrial protein, phosphorylated by stress-activated protein kinase 3.	▲▲	nc
7133	<i>TNFRSF1B</i>	tumor necrosis factor receptor superfamily, member 1B	Suppressor of death receptor-mediated apoptosis.	▲▲	nc
10628	<i>TXNIP</i>	thioredoxin interacting protein	Glucocorticoid-regulated primary response gene involved in mediating glucocorticoid-induced apoptosis.	nc	▽▽
<b>Decreased DNA and RNA synthesis, suppressed proliferation</b>					
1028	<i>CDKN1C</i>	cyclin-dependent kinase inhibitor 1C (p57, Kip2)	Negative regulator of cell proliferation - strong inhibitor of G1 cyclin/Cdk complexes.	▲▲	nc
1020	<i>CDK5</i>	cyclin-dependent kinase 5	Cell cycle control.	▽▽	nc
11052	<i>CPSF6</i>	cleavage and polyadenylation specific factor 6, 68kDa	Subunit of a cleavage factor required for 3' RNA cleavage and polyadenylation processing.	▽▽	nc
1503	<i>CTPS</i>	CTP synthase	Nucleotide synthesis.	▽▽	nc
2071	<i>ERCC3</i>	excision repair cross-complementing rodent repair deficiency, complementation group 3 (xeroderma pigmentosum group B complementing)	ATP-dependent DNA helicase, functions in nucleotide excision repair. Also functions in class II transcription (as a subunit of TFIIH).	▽▽	nc
64785	<i>GINS3</i>	GINS complex subunit 3 (Psf3 homolog)	Essential for the initiation of DNA replication.	▽▽	nc
8520	<i>HAT1</i>	histone acetyltransferase 1	Acetylation of newly synthesized cytoplasmic histones, which plays an important role in replication-dependent chromatin assembly.	▽▽	nc
3182	<i>HNRPA</i>	heterogeneous nuclear ribonucleoprotein A/B	RNA binding protein, associates with pre-mRNA in the nucleus.	▽▽	nc
5654	<i>HTRA1</i>	HtrA serine peptidase 1	Regulates availability of insulin-like growth factors and possibly cell growth.	▽▽	nc
3609	<i>ILF3</i>	interleukin enhancer binding factor 3, 90kDa	Complexes with other proteins, dsRNAs, small noncoding RNAs, and mRNAs to regulate gene expression and stabilize mRNAs.	▽▽	nc
4331	<i>MNAT1</i>	menage a trois homolog 1, cyclin H assembly factor ( <i>Xenopus laevis</i> )	Involved in the assembly of the kinase complex that activates cyclin-dependent kinases, which participate in cell cycle control.	▽▽	nc
51728	<i>POLR3K</i>	polymerase (RNA) III (DNA directed) polypeptide K, 12.3 kDa	Small essential subunit of RNA polymerase III, the polymerase responsible for synthesizing transfer and small ribosomal RNAs in eukaryotes.	▽▽	nc
80324	<i>PUS1</i>	pseudouridylylase 1	Converts uridine into pseudouridine after the nucleotide has been incorporated into RNA.	▽▽	nc
3431	<i>SP110</i>	SP110 nuclear body protein	Component of the nuclear body, a multiprotein complex that may participate in the regulation of transcription. May play a role in transcription activation and in ribosome biogenesis.	▽▽	nc

**Tab. 10 (continued)**

Entrez GeneID	Gene Symbol	Gene Product	Description	hfOB <sup>PC3</sup> 48 h	hfOB <sup>C4-2B4</sup> 48 h
54962	<i>TIPIN</i>	TIMELESS interacting protein	Nuclear protein. Depletion of endogenous tipin results in reduced growth rate, which may be due in part to inefficient progression of S phase and DNA synthesis.	▽▽	nc
8295	<i>TRRAP</i>	transformation/transcription domain-associated protein	Recruitment of histone acetyltransferase complexes to chromatin during transcription, replication and DNA repair.	▽▽	nc
79084	<i>WDR77</i>	WD repeat domain 77	Component of methyltransferase complex that modifies spliceosomal proteins.	▽▽	nc
8317	<i>CDC7</i>	cell division cycle 7 homolog ( <i>S. cerevisiae</i> )	Cell division cycle protein with kinase activity that is critical for the G1/S transition.	nc	▽▽
2965	<i>GTF2HI</i>	general transcription factor IIH, polypeptide 1, 62kDa	Transcription initiation.	nc	▽▽
10614	<i>HEXIM1</i>	hexamethylene bis-acetamide inducible 1	Suppresses transcription elongation. Directly associates with glucocorticoid receptor to suppress glucocorticoid-inducible gene activation.	nc	▽▽
<b>Gene-specific regulation of transcription</b>					
23253	<i>ANKRD12</i>	Ankyrin repeat domain 12	Transcriptional coregulator.	▲▲	nc
1195	<i>CLK1</i>	CDC-like kinase 1	Kinase indirectly involved in pre-mRNA processing, may influence splice site selection.	▲▲	nc
4601	<i>MXI1</i>	MAX interactor 1	Transcriptional repressor.	▲▲	nc
864	<i>RUNX3</i>	runt-related transcription factor 3	Transcription factor.	▲▲	nc
8091	<i>HMGA2</i>	high mobility group AT-hook 2	Transcriptional regulator.	▽▽	nc
4150	<i>MAZ</i>	MYC-associated zinc finger protein (purine-binding transcription factor)	Transcription factor, inflammation-responsive.	▽▽	nc
9111	<i>NMI<sup>I</sup></i>	N-myc (and STAT) interactor	Interacts with transcription factors, augments STAT-mediated transcription in response to interferon.	▽▽	nc
1997	<i>ELF1</i>	E74-like factor 1 (ets domain transcription factor)	Transcription factor.	nc	▽▽
<b>Protein synthesis, modification and degradation</b>					
1917	<i>EEF1A2</i>	eukaryotic translation elongation factor 1 alpha 2	Component of translational machinery.	▲▲	nc
29071	<i>C1GALT1C1</i>	C1GALT1-specific chaperone 1	Molecular chaperone.	▽▽	nc
54431	<i>DNAJC10</i>	DnaJ (Hsp40) homolog, subfamily C, member 10	Putative co-chaperone in the endoplasmic reticulum.	▽▽	nc
60681	<i>FKBP10</i>	FK506 binding protein 10, 65 kDa	Molecular chaperone localized in the ER.	▽▽	nc
23463	<i>ICMT</i>	isoprenylcysteine carboxyl methyltransferase	Posttranslational protein modification in the ER.	▽▽	nc
5696	<i>PSMB8<sup>I</sup></i>	proteasome (prosome, macropain) subunit, beta type, 8 (large multifunctional peptidase 7)	Protein degradation (proteasome subunit). Interferon-induced.	▽▽	nc
871	<i>SERPINH1</i>	serpin peptidase inhibitor, clade H (heat shock protein 47), member 1, (collagen binding protein 1)	Putative molecular chaperone involved in the maturation of collagen molecules. Localizes to the ER.	▽▽	nc
54982	<i>CLN6</i>	ceroid-lipofuscinosis, neuronal 6, late infantile, variant	Possibly involved in the degradation of posttranslationally modified proteins in lysosomes.	nc	▽▽

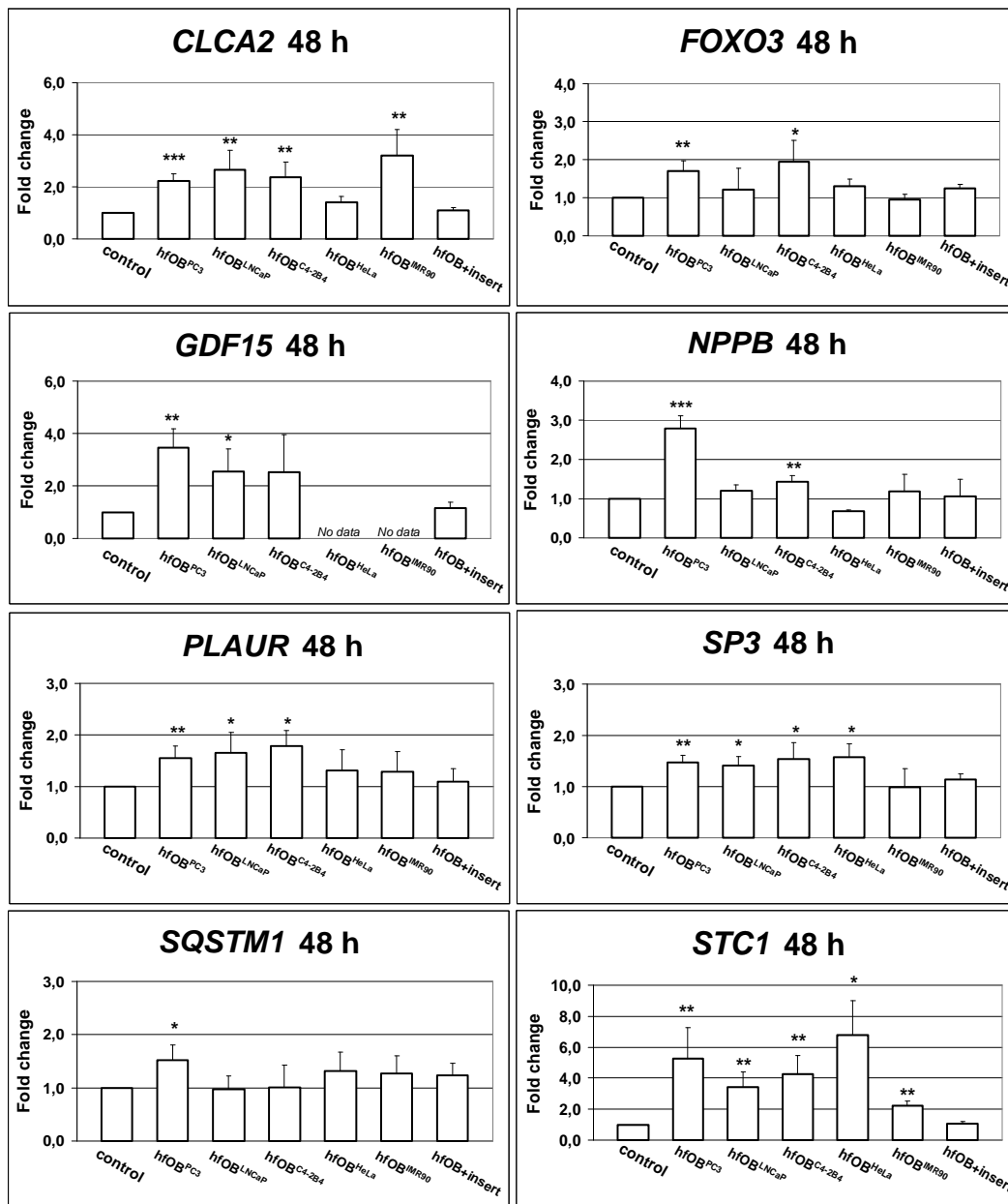
**Tab. 10 (continued)**

Entrez GeneID	Gene Symbol	Gene Product	Description	hfOB <sup>PC3</sup> 48 h	hfOB <sup>C4-2B4</sup> 48 h
<b>Transport</b>					
4864	<i>NPC1</i>	Niemann-Pick disease, type C1	Membrane protein, intracellular cholesterol transport.	▲▲	nc
5172	<i>SLC26A4</i>	solute carrier family 26, member 4	Transport across membranes.	▲▲	nc
51312	<i>SLC25A37</i>	solute carrier family 25, member 37	Transport across membranes.	▲▲	nc
1174	<i>AP1S1</i>	adaptor-related protein complex 1, sigma 1 subunit	Part of the clathrin coat assembly complex which links clathrin to receptors in coated vesicles. These vesicles are involved in endocytosis and Golgi processing.	▽▽	nc
3839	<i>KPNA3</i>	karyopherin alpha 3 (importin alpha 4)	Involved in nuclear protein import.	▽▽	nc
9688	<i>NUP93</i>	nucleoporin 93kDa	Component of nuclear pore complex.	▽▽	nc
6522	<i>SLC4A2</i>	solute carrier family 4, anion exchanger, member 2 (erythrocyte membrane protein band 3-like 1)	Membrane-bound protein, mediates anion exchange.	▽▽	nc
6747	<i>SSR3</i>	signal sequence receptor, gamma (translocon-associated protein gamma)	Glycosylated ER membrane receptor associated with protein translocation across the ER membrane.	▽▽	nc
23404	<i>EXOSC2</i>	exosome component 2	Exosome component (cellular transport).	nc	▽▽
8675	<i>STX16</i>	syntaxin 16	Found on cell membranes, permits specific synaptic vesicle docking and fusion.	nc	▽▽
<b>Cytokines, cell surface receptors and cell signaling</b>					
394	<i>ARHGAP5</i>	Rho GTPase activating protein 5	Negatively regulates Rho GTPases.	▲▲	nc
960	<i>CD44</i>	CD44 molecule (Indian blood group)	Cell-surface glycoprotein involved in cell-cell interactions, cell adhesion and migration.	▲▲	nc
7852	<i>CXCR4</i>	chemokine (C-X-C motif) receptor 4	Cell surface chemokine receptor.	▲▲	nc
9289	<i>GPR56</i>	G protein-coupled receptor 56	Cell signaling.	▲▲	nc
2872	<i>MKNK2</i>	MAP kinase interacting serine/threonine kinase 2	Cell signaling.	▲▲	nc
5801	<i>PTPRR</i>	protein tyrosine phosphatase, receptor type, R	Regulator of cell signaling cascades.	▲▲	nc
5979	<i>RET</i>	ret proto-oncogene	Cell surface receptor tyrosine kinase.	▲▲	nc
58528	<i>RRAGD</i>	Ras-related GTP binding D	G protein. Cell signaling.	▲▲	nc
57124	<i>CD248</i>	CD248 molecule, endosialin	Cell surface adhesion molecule.	▽▽	nc
8760	<i>CDS2</i>	CDP-diacylglycerol synthase (phosphatidate cytidyltransferase) 2	Cell signaling - regulates the amount of phosphatidylinositol available for signaling.	▽▽	nc
91851	<i>CHRD1</i>	chordin-like 1	Antagonist of bone morphogenetic protein-4.	▽▽	nc
2919	<i>CXCL1<sup>I</sup></i>	chemokine (C-X-C motif) ligand 1 (melanoma growth stimulating activity, alpha)	Proinflammatory chemokine.	▽▽	nc
1825	<i>DSC3</i>	desmocollin 3	Calcium-dependent adhesive glycoprotein, component of the desmosome cell-cell junction.	▽▽	nc
1906	<i>EDN1#</i>	endothelin 1	Osteoblast mitogen, pro-osteoblastic factor in osteoblastic prostate cancer metastasis. TGFβ target.	▽▽	nc
2150	<i>F2RL1</i>	coagulation factor II (thrombin) receptor-like 1	Cell signaling - transmembrane receptor, couples to G proteins.	▽▽	nc
166647	<i>GPR125</i>	G protein-coupled receptor 125	Initiates signaling <i>via</i> G proteins.	▽▽	nc
3434	<i>IFIT1<sup>I</sup></i>	interferon-induced protein with tetratricopeptide repeats 1	Interferon-induced negative-feedback regulator of virus-triggered signaling.	▽▽	nc
9562	<i>MINPP1</i>	multiple inositol polyphosphate histidine phosphatase, 1	Cell signaling - hydrolyzes inositol phosphate metabolites.	▽▽	nc

**Tab. 10 (continued)**

Entrez GeneID	Gene Symbol	Gene Product	Description	hfOB <sup>PC3</sup> 48 h	hfOB <sup>C4-2B4</sup> 48 h
56106	<i>PCDHGA10</i> /// <i>PCDHGA11</i> /// <i>PCDHGA12</i> /// <i>PCDHGA3</i> /// <i>PCDHGA5</i> /// <i>PCDHGA6</i>	protocadherin gamma subfamily A, 12/// protocadherin gamma subfamily A, 11/// protocadherin gamma subfamily A, 10 /// protocadherin gamma subfamily A, 6 /// protocadherin gamma subfamily A, 5 /// protocadherin gamma subfamily A, 3	Cell-cell adhesion protein.	▽▽	nc
8434	<i>RECK</i>	reversion-inducing-cysteine-rich protein with kazal motifs	Membrane glycoprotein.	▽▽	nc
7424	<i>VEGFC</i>	vascular endothelial growth factor C	Cytokine, mediator of angiogenesis.	▽▽	nc
<b>NF-κB pathway components and target genes</b>					
4792	<i>NFKBIA</i>	nuclear factor of kappa light polypeptide gene enhancer in B-cells inhibitor, alpha	Upregulated by NF-κB (negative feedback), marker of activated NF-κB pathway.	▲	nc
54101	<i>RIPK4</i>	receptor-interacting serine-threonine kinase 4	Ser/Thr protein kinase, can activate NF-κB.	▲▲	nc
8878	<i>SQSTM1</i> *	sequestosome 1	Mediates NF-κB activation.	▲	nc
6648	<i>SOD2</i>	superoxide dismutase 2, mitochondrial	Upregulated by NF-κB.	▲▲	nc
<b>Metabolism</b>					
10840	<i>ALDH1L1</i>	aldehyde dehydrogenase 1 family, member L1	Metabolic enzyme.	▲▲	nc
3099	<i>HK2</i>	hexokinase 2	Metabolic enzyme.	▲▲	nc
5209	<i>PFKFB3</i>	6-phosphofructo-2-kinase/fructose-2,6-biphosphatase 3	Metabolic enzyme.	▲▲	nc
1743	<i>DLST</i>	dihydrolipoamide S-succinyltransferase (E2 component of 2-oxo-glutarate complex)	Metabolic enzyme.	▽▽	nc
55568	<i>GALNT10</i>	UDP-N-acetyl-alpha-D-galactosamine:polypeptide N-acetylgalactosaminyltransferase 10 (GalNAc-T10)	Synthesis of mucin-type oligosaccharides.	▽▽	nc
3052	<i>HCCS</i>	holocytochrome c synthase (cytochrome c heme-lyase)	Metabolic enzyme.	▽▽	nc
262	<i>AMD1</i>	adenosylmethionine decarboxylase 1	Intermediate enzyme in polyamine biosynthesis.	nc	▽▽
9517	<i>SPTLC2</i>	serine palmitoyltransferase, long chain base subunit 2	Key enzyme in sphingolipid biosynthesis.	nc	▽▽
<b>Structural proteins</b>					
2201	<i>FBN2</i>	fibrillin 2 (congenital contractual arachnodactyly)	Component of connective tissue microfibrils.	▲▲	nc
3017	<i>HIST1H2BD</i>	histone cluster 1, H2bd	Chromatin component (histone).	▲▲	nc
72	<i>ACTG2</i>	actin, gamma 2, smooth muscle, enteric	Cytoskeleton component.	▽▽	nc
10097	<i>ACTR2</i>	ARP2 actin-related protein 2 homolog (yeast)	Involved in cytoskeletal dynamics.	▽▽	nc
1634	<i>DCN</i>	decorin	Binds to collagen fibrils, plays a role in matrix assembly.	▽▽	nc
4281	<i>MID1</i>	midline 1 (Opitz/BBB syndrome)	Associates with microtubules in the cytoplasm, likely involved in the formation of multiprotein structures acting as anchor points to microtubules.	▽▽	nc
3916	<i>LAMP1</i>	lysosomal-associated membrane protein 1	Membrane glycoprotein.	▽▽	nc
81493	<i>SYNC1</i>	syncoilin, intermediate filament 1	Member of the intermediate filament family.	nc	▽▽
7094	<i>TLN1</i>	talín 1	Cytoskeletal protein, concentrated in areas of cell-substratum and cell-cell contacts.	nc	▽▽

A.



B.

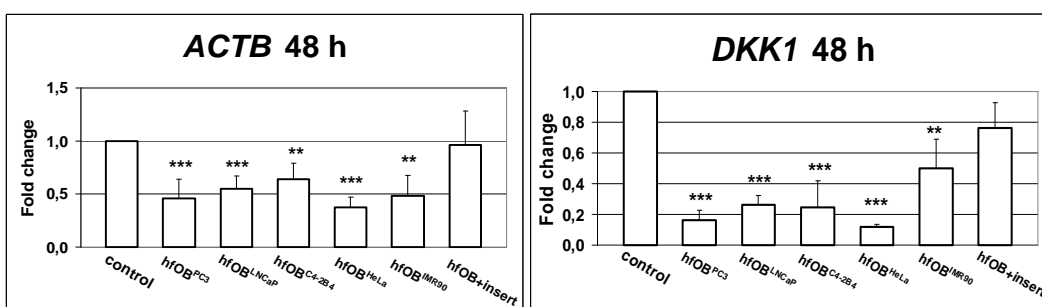
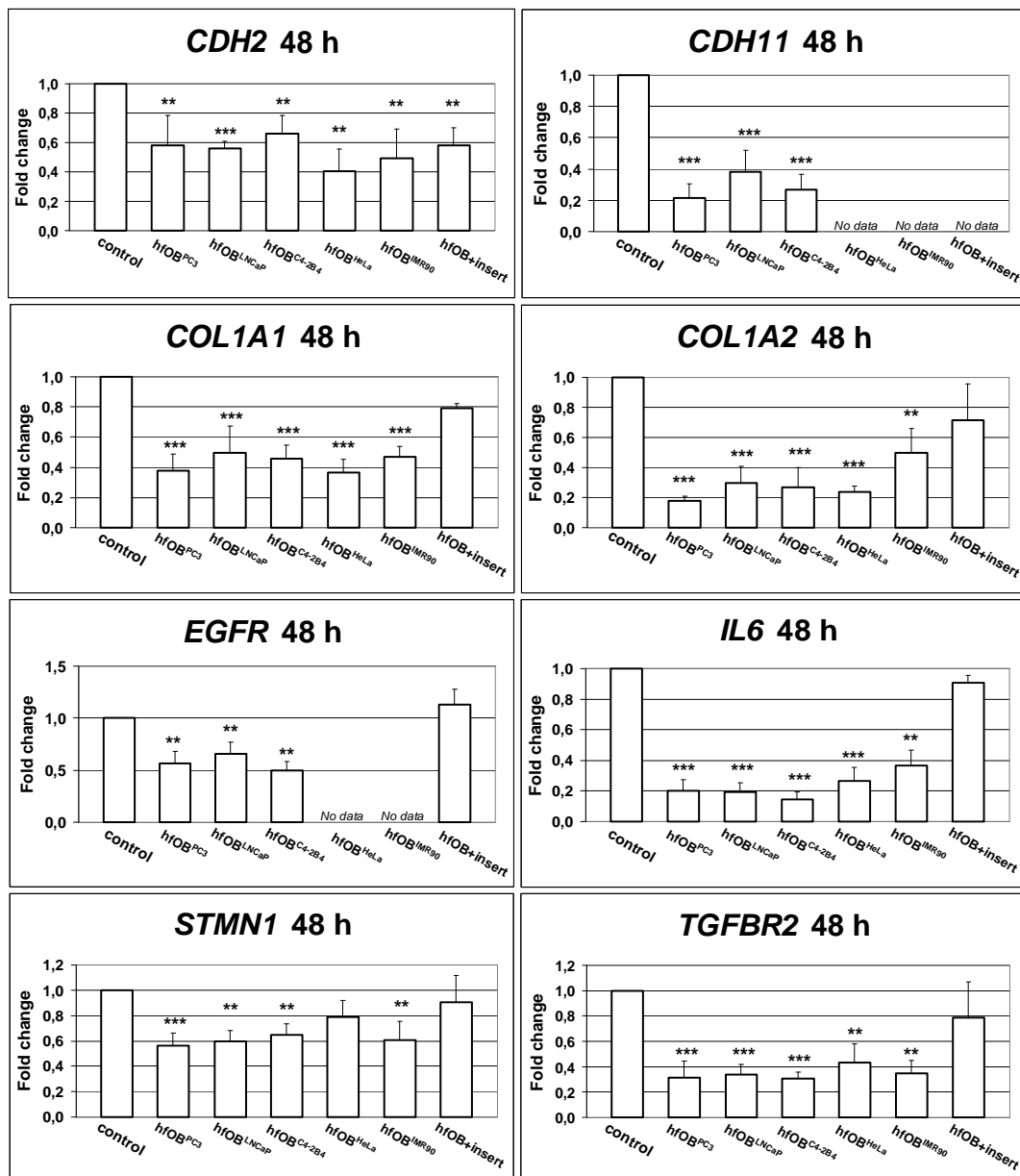
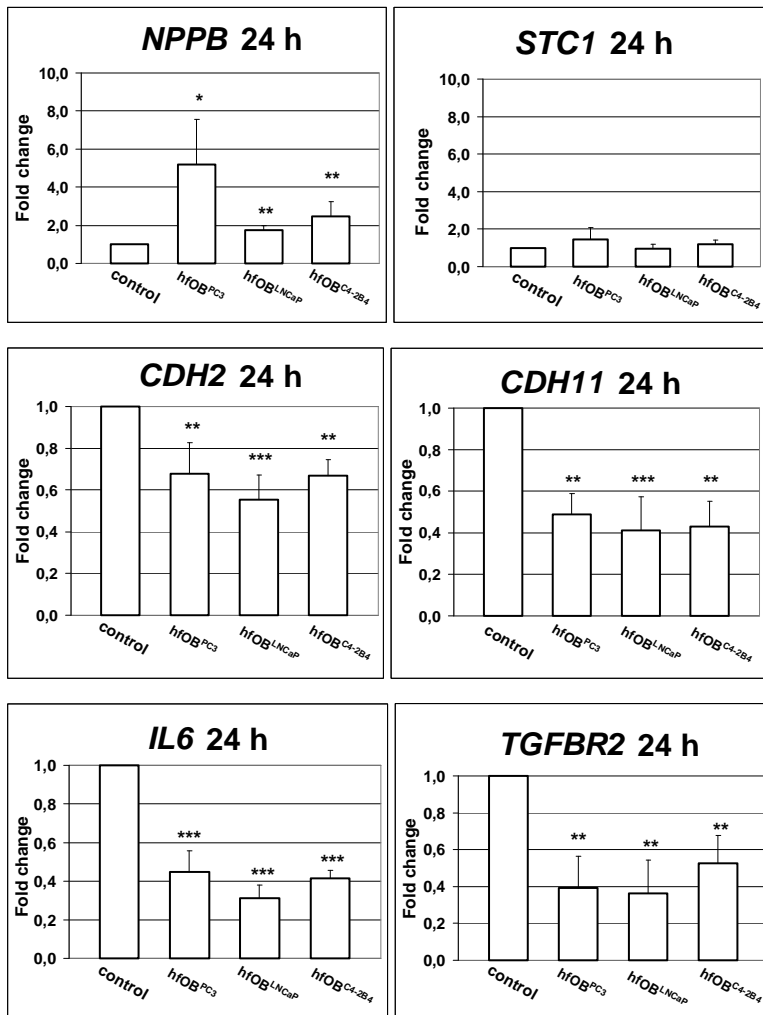


Figure continued on next page.



**Fig. 21 Verification and extension of array data. (A) Upregulated genes. (B) Downregulated genes.** qRT-PCR was performed on cDNA from hfOB cocultured with the described cell lines or cultured with an empty transwell insert. Shown are the means of expression alterations in comparison to noncultured hfOB (control bar). hfOB<sup>X</sup>, X-cocultured hfOB. Error bars represent the mean  $\pm$  SD of at least three independent determinations. \*  $p < 0,05$ ; \*\*  $p < 0,01$ ; \*\*\*  $p < 0,0001$

*Note:* In array data *FOXO3*, *GDF15*, *NPPB*, *SP3*, *SQSTM1*, *ACTB*, *IL6* and *STMN1* were altered only in hfOB<sup>PC3</sup>, whereas *EGFR* was downregulated only in hfOB<sup>C4-2B4</sup>.



**Fig. 22 Transcription alterations in osteoblasts cocultured with prostate cancer cells for 24 h.** hfOB<sup>X</sup>, X-cocultured hfOB. Error bars represent the mean  $\pm$  SD of at least three independent determinations. \*  $p < 0,05$ ; \*\*  $p < 0,01$ ; \*\*\*  $p < 0,0001$

For a number of markers of the bone regulon, the array yielded no useful data. The signals were either insufficient due to the limited sensitivity of microarrays or the respective genes were not represented on the array. These genes were subjected to additional analysis by qRT-PCR (Table 11). The transcripts of the osteoinductive molecule BMP2 and the osteoblast-specific transcription factor CBFA1 became upregulated in osteoblasts due to coculture with both osteolytic and osteoblastic prostate cancer cell lines, whereas *OPN* and *OPG*, two transcriptional targets of TGF $\beta$ , showed strong downregulation. This is perfectly in accordance with the patterns of increased osteoblast differentiation and repressed TGF $\beta$  signaling suggested by the array data. The expression of *AP* and *OC*, two further markers of osteoblast differentiation, and of *RANKL* remained unchanged in osteoblasts cocultured with all three prostate cancer cell lines. *NOG*, which encodes a BMP signaling antagonist, and *IL6R*, which encodes the IL6 receptor,



were strongly upregulated, perhaps as an autocrine response to the rising levels of BMP2 and decreasing levels of IL6, respectively (Tab. 11).

*RANKL* and *OPG* expression was analyzed after 24 h of coculture as well. It was found that *OPG* was already significantly downregulated after 24 h, while *RANKL* expression remained unchanged at both time points (Fig. 23)

**Tab. 11 Transcription alterations in osteoblasts cocultured with prostate cancer cells. Osteoblast differentiation and bone remodeling.** To investigate the expression of transcripts from the bone regulon for which the array yielded no useful data (genes not represented on the array, or insufficient signal), qRT-PCR was performed on cDNA from hfOB cocultured with each of three prostate cancer cell lines or cultured with an empty transwell insert. Shown are the means of expression alterations in comparison to noncocultured hfOB, from at least three independent determinations.

▲▲, fold change  $\geq 2$ ; ▲, fold change  $\geq 1,45$ ; ▽, fold change  $\leq 0,69$  (-1,45); ▽▽, fold change  $\leq 0,5$  (-2); **nc**, no change; **nd**, no data. U - transcript levels undetectable. hfOB<sup>X</sup>, X-cocultured hfOB; # , transcript upregulated by TGFβ.  $p < 0,05$

Entrez GeneID	Gene Symbol	Gene Product	hfOB <sup>PC3</sup> 48 h	hfOB <sup>LNCaP</sup> 48 h	hfOB <sup>C4-2B4</sup> 48 h	hfOB <sup>HeLa</sup> 48 h	hfOB <sup>IMR90</sup> 48 h	hfOB +insert 48 h
650	<i>BMP2</i>	bone morphogenetic protein 2	▲	▲	▲	▲	nc	nc
860	<i>CBFA1</i>	core binding factor 1	▲	▲	▲	nc	nc	nc
3570	<i>IL6R</i>	interleukin 6 receptor	▲▲	▲▲	▲▲	▲▲	U	▲
9241	<i>NOG</i>	noggin	▲▲	▲▲	▲▲	▲	▲	nc
4982	<i>OPG</i> #	osteoprotegerin	▽▽	▽▽	▽▽	▽▽	▽▽	nc
6696	<i>OPN</i> #	osteopontin	▽▽	▽▽	▽▽	▽▽	▽▽	▽
249	<i>AP</i>	alkaline phosphatase	nc	nc	nc	nc	nc	nd
632	<i>OC</i>	osteocalcin	nc	nc	nc	nc	nc	nd
8600	<i>RANKL</i>	receptor activator of nuclear factor kappa B ligand	nc	nc	nc	nc	nc	nd

To further address the possibility that medium exhaustion could be affecting the expression changes seen in osteoblasts after coculture, the levels of selected transcripts from the bone regulon and the TGFβ signaling pathway were also compared between hfOB after 24 and 48 h of monoculture. The observed changes did not tally with the changes caused by coculture with prostate cancer cells. Only 4 transcripts out of 16 were significantly affected; the short period of culture at 37°C appeared to increase the expression of *AP*, *COL1A1* and *IL6* in hfOB and downregulate *OPG* (Fig. 24).

Significantly, the levels of three transcripts became elevated in osteoblasts after coculture with all three prostate cancer cell lines, but not with HeLa or IMR-90. These transcripts, potentially having a special importance for prostate cancer metastasis, were *CBFA1*, *NPPB* and *PLAUR*.

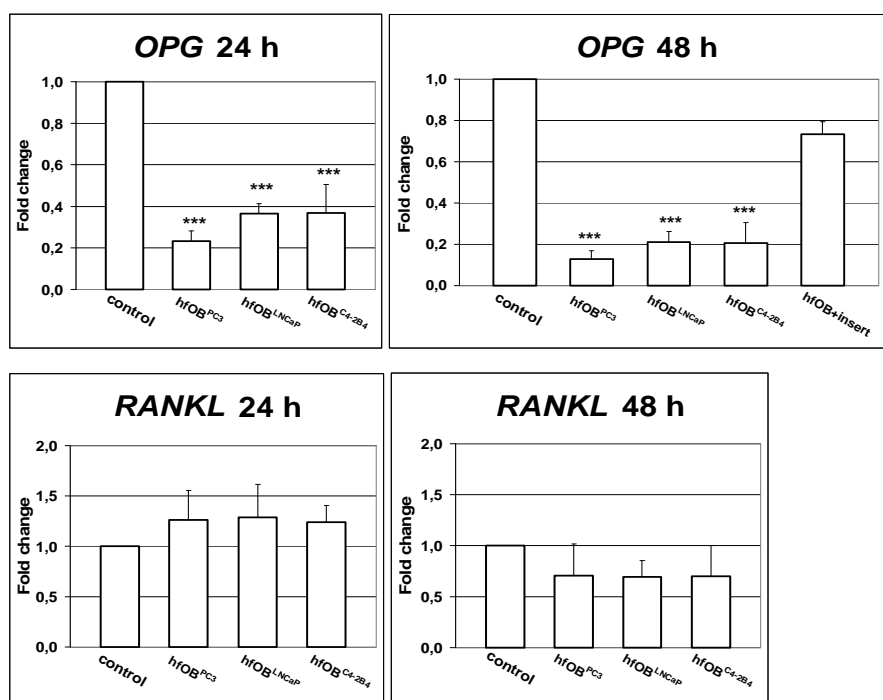


**Fig. 23** Transcription alterations of *OPG* and *RANKL* in osteoblasts cocultured with prostate cancer cells. Error bars represent the mean  $\pm$  SD of at least three independent determinations. \*\*\*  $p < 0,0001$

**A.**

Gene Symbol	Expression change - 48h vs. 24h
<i>AP</i>	▲▲ (+5,44)***
<i>COL1A1</i>	▲▲ (+2,19)**
<i>OPG</i>	▽▽ (-3,45)***
<i>IL6</i>	▲▲ (+3,16)***

\*\*  $p < 0,01$ ; \*\*\*  $p < 0,001$

**B.**

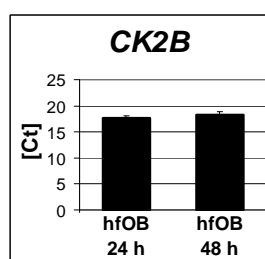
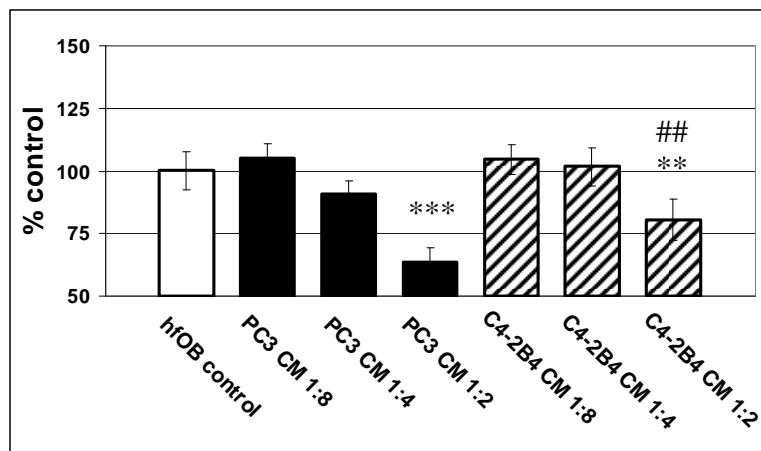


**Fig. 24** Differences in gene expression between osteoblasts after 24 h and 48 h of growth in monoculture. (A) Osteoblast-specific genes and signaling pathway components. qRT-PCR data, expressed as the ratio to *CK2B* mRNA, were compared for the following 16 genes: *BMP2*, *CBFA1*, *AP*, *COL1A1*, *OPN*, *OPG*, *RANKL*, *DKK1*, *NOG* (bone regulon); *TGFBI*, *TGFBR1*, *TGFBR2*, *SMAD3*, *SMAD7* ( $TGF\beta$  signaling); *IL6*, *IL6R*. Genes not included in the table remained unaltered. ▲▲, fold change  $\geq 2$ ; ▽▽, fold change  $\leq 0,5$  (-2); (B) *CK2B* mRNA levels in osteoblasts after 24 h and 48 h.

### 3.2.3. Universal osteoblast responses – both osteolytic and osteoblastic prostate cancer cells suppress proliferation, but to different extents.

To explore the question whether prostate cancer cells exert negative effects on osteoblast proliferation as the expression data seem to suggest, and whether osteolytic PC3 and osteoblastic C4-2B4 cells differ in their effect, hfOB cells were treated for 72 h with CM from these cell lines in varying concentrations, containing 5% FCS. The MTT assay was used to quantify viable, metabolically active cells. It was found that factors released by both cell lines and active in CM inhibited hfOB proliferation - to ca. 60% of the control in the case of PC3 and ca. 80% of the control in the case of C4-2B4. Thus, the upregulation of negative cell cycle regulators and repression of proliferation factors seen in array data appears to have the expected functional consequences. Both prostate cancer cell lines negatively influenced hfOB proliferation, but the effect of PC3 was stronger and this difference was statistically significant (Fig. 25A).

**A.**



\*\* p < 0,01 \*\*\* p < 0,0001 (vs. control)  
## p < 0,01 (vs. PC3 CM 1:2)

**B.**

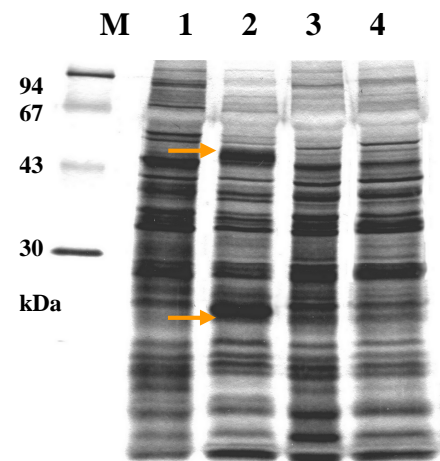


**Fig. 25 Secretomes of different cancer cell lines differ in the extent of their effect on osteoblast proliferation. (A) Effect of medium conditioned by prostate cancer cells on osteoblast proliferation after 72 h.** Cell viability was determined using the MTT test. Error bars represent the mean  $\pm$  SD of at least three independent determinations. **(B) SDS-PAGE gel of secreted proteins from osteoblasts and prostate cancer cell lines.** Cells: 1, hfOB; 2, PC3; 3, LNCaP; 4, C4-2B4. Orange arrows indicate protein bands of ca. 54 and 24 kDa present in PC3 CM, but not LNCaP CM or C4-2B4 CM.

Importantly, the secretome of PC3 cells differs significantly from the secretomes of LNCaP and C4-2B4. Already a simple 1D SDS-PAGE gel shows differences in the band pattern (Fig. 25B). In a project aimed at identifying the factors responsible for the osteolytic properties of PC3, the proteins with an apparent molecular weight of ca. 54 and 24 kDa which are secreted in high amounts by PC3, but not by LNCaP or C4-2B4, could be interesting candidates to consider.

#### **3.2.4. Cell type-specific osteoblast responses - osteolytic and osteoblastic prostate cancer cell lines may have differing effects on the osteoblast transcriptome.**

As Fig. 19 shows, some gene expression changes were selectively caused in osteoblasts by only one prostate cancer cell line, but not by the others. Since the prostate cancer lines used produce different types of bone lesions in immunocompromised mice, we hypothesized that these selectively induced transcriptional alterations may give an insight as to the early molecular events that ultimately give rise to differing metastasis phenotypes - impaired osteoblast differentiation in the case of osteolytic lesions, enhanced osteoblast differentiation in the case of osteoblastic ones. Since LNCaP causes mixed-type metastatic bone lesions in the nude mouse model, a comparison of expression alterations between osteoblasts cocultured with the osteolytic PC3 and the osteoblastic C4-2B4 appeared to be particularly appropriate to get hints as to expression patterns possibly specific for an osteolytic and an osteoblastic metastasis phenotype.

The osteolytic PC3 line caused relatively dramatic gene expression changes in osteoblasts as opposed to rather moderate changes caused by the osteoblastic C4-2B4; 110 and 18 genes became selectively affected by PC3 and C4-2B4, respectively (see Fig. 19). Table 10 provides a compilation of genes altered  $\geq 2$ -fold only by PC3 or by C4-2B4, ordered into functional groups on the basis of information from the databases Entrez Gene and PubMed (see Materials and methods 2.3.4).

The genes affected in osteoblasts exclusively by PC3 cells appeared to strengthen stress response and further suppress proliferation, as indicated by the upregulation of genes encoding stress response molecules *ITPR1*, *SH3BP5* and *TNFRSF1B* and the inhibitor of cell proliferation *CDKN1C*, as well as the downregulation of numerous genes associated with DNA replication, transcription and cell division, such as *CDK5* and *MNAT1*, linked to cell cycle control, *GINS3*, encoding a molecule necessary for DNA replication, and *GTF2A*, *ILF3* and *POL3RK*, linked to RNA synthesis. Several genes involved in protein synthesis and modification were also

downregulated, fitting in with this picture. Further effects caused in osteoblasts by PC3, but not C4-2B4, included the up- or downregulation of genes encoding a number of transcription factors, cell surface receptors, cytokines, signaling mediators and molecules involved in transport, as well as metabolic enzymes and structural proteins. Interestingly, among the signaling pathway components selectively upregulated by PC3 cells were genes encoding two activators of NF- $\kappa$ B signaling (*RIPK4*, *SQSTM1*) and two NF- $\kappa$ B target genes (*NFKBIA*, *SOD2*).

In contrast to the quite dramatic alterations induced by PC3, C4-2B4 cells only downregulated a handful of genes (Tab. 10). Among these were *TXNIP*, *ELF1*, *EXOSC2* and *STX16*, encoding an apoptosis mediator, a transcription factor and two molecules participating in vesicle transport respectively, as well as *AMD1* and *SPTLC2*, which encode two anabolic enzymes - one participating in the biosynthesis of polyamines, the other of sphingolipids. None of these molecules have previously been described as playing a role in osteoinductive processes.

**Tab. 12 Transcription alterations in osteoblasts cocultured with prostate cancer cells. TGF $\beta$  signaling pathway.** qRT-PCR data (no expression changes seen in array, or undetectable signal). Shown are the means of expression alterations in comparison to noncocultured hfOB, from at least three independent determinations.  $\blacktriangle\blacktriangle$ , fold change  $\geq 2$ ;  $\blacktriangle$ , fold change  $\geq 1,45$ ;  $\nabla$ , fold change  $\leq 0,69$  (-1,45);  $\nabla\nabla$ , fold change  $\leq 0,5$  (-2); **nc**, no change; **nd**, no data. hfOB<sup>X</sup>, X-cocultured hfOB; #, transcript upregulated by TGF $\beta$ . p < 0,05

Entrez GeneID	Gene Symbol	Gene Product	hfOB <sup>PC3</sup> 48 h	hfOB <sup>LNCaP</sup> 48 h	hfOB <sup>C4-2B4</sup> 48 h	hfOB <sup>HeLa</sup> 48 h	hfOB <sup>LMR90</sup> 48 h
7040	<i>TGFBI</i>	transforming factor beta 1	nc	nc	nc	nc	$\nabla$
7046	<i>TGFBRI</i>	transforming factor beta receptor I	nc	nc	nc	nc	nc
4087	<i>SMAD2</i>	SMAD family member 2	nc	nc	nc	nd	nd
4088	<i>SMAD3</i>	SMAD family member 3	$\blacktriangle\blacktriangle$	nc	nc	nc	nc
4092	<i>SMAD7</i>	SMAD family member 7	$\blacktriangle\blacktriangle$	nc	nc	nc	nc

Together, these results suggest that at a very early stage of metastasis formation, osteolytic cancer cells perturb osteoblast function much more strongly than osteoblastic ones, although the data for individual genes must be interpreted with caution due to limited sensitivity of the array. Data verification and extension by qRT-PCR showed that, although on the array the levels of some transcripts appeared to change in osteoblasts cocultured only with one prostate cancer cell line, these genes in fact became altered in all three coculture combinations (*ACTB*, *EGFR*, *IL6*, *SP3*, *STMN1*). Nonetheless, it could be shown using qRT-PCR that various gene expression changes were indeed selectively induced by one or two prostate cancer cell lines (Fig. 21, Tab.

12). *FOXO3* and *NPPB* became upregulated after 48 h in osteoblasts due to coculture with PC3 and C4-2B4, but not LNCaP, whereas *SQSTM1*, *SMAD3* and *SMAD7* were upregulated after 48 h only by PC3 cells. Also the extent of expression alterations might indicate selective effects, e.g., a slight upregulation of *NPPB* occurred after 24 h due to LNCaP, whereas C4-2B4 and, especially, PC3 cells caused a pronounced effect (Fig. 22). Thus, the possibility of determining an early transcriptional footprint (for *in vivo* footprints see Eisenberger *et al.*, 2008) of osteolytic vs. osteoblastic metastasis in osteoblasts reacting to factors secreted by cancer cells presents an interesting ground for further study. A full list of the genes altered significantly in only one coculture combination on the array can be found as Supplementary Data.

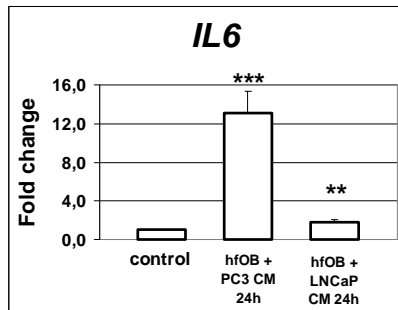
#### **3.2.5. The effect of prostate cancer cells on IL6 production by osteoblasts can depend on the experimental model.**

*IL6* transcript levels dropped to ca. 15-20% of the control in hfOB after 48 h of coculture with PC3, LNCaP or C4-2B4 (Fig. 21B). Yet a study published in 2002 by Garcia-Moreno *et al.* has described increased production of IL6 by osteoblasts treated with medium conditioned by PC3 cells [Garcia-Moreno *et al.* 2002]. The discrepancy in results may be due to the fact that these investigators conducted their experiments in a FCS-free setting, while the coculture model described here involves growing cells with medium containing 10% FCS. Treating FCS-starved cells with conditioned medium is a popular experimental model [Blaszczyk *et al.* 2004, Lu *et al.* 2004 and others], but the presence or absence of FCS is often discussed as the reason for varying results reported by different laboratories.

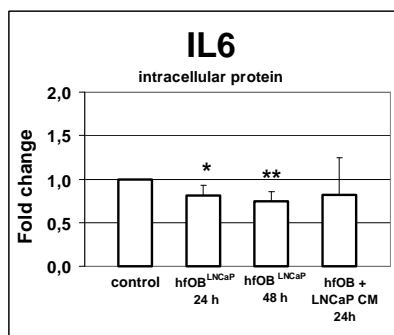
It was confirmed that IL6, which became strongly downregulated both on mRNA (Fig. 21B) and on protein level (Fig. 26A) in osteoblasts cocultured with prostate cancer cells with 10% FCS, indeed did become upregulated on the mRNA level in osteoblasts treated with FCS-free medium conditioned by PC3 or LNCaP cells (Fig. 26A). Garcia-Moreno *et al.* reported very low IL6 secretion by PC3, but the PC3 cells used here secreted high amounts of this cytokine (Fig. 12A), so in assays involving the protein level, hfOB were treated with conditioned medium from the LNCaP line, which secretes almost no IL6. While IL6 intracellular levels remained unchanged in hfOB treated with LNCaP-CM (Fig. 26B), a significant increase in secreted IL6 protein could be seen (Fig. 26C), mirroring the results obtained by Garcia-Moreno *et al.* in osteoblasts treated with PC3-CM. However, data from the coculture model are probably more

representative of the *in vivo* situation, since FCS deprivation creates additional strong stress for osteoblasts.

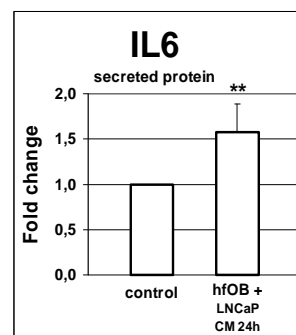
A.



B.



C.



Representative experiments:

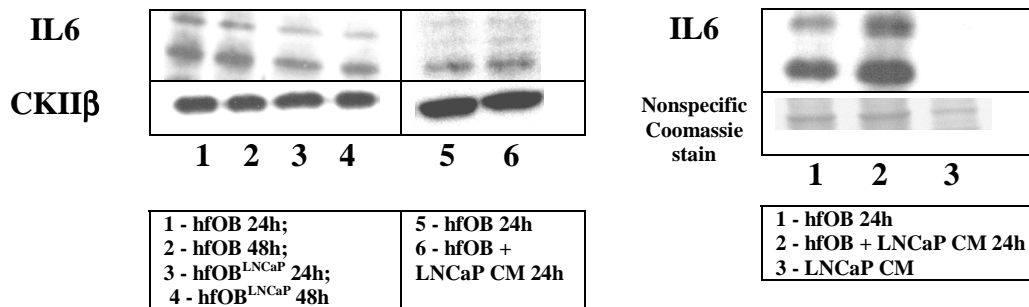


**Fig. 26** The effect of prostate cancer cells on IL6 production by osteoblasts can depend on the experimental model. (A) *IL6* mRNA levels in osteoblasts after treatment with CM from prostate cancer cells. (B) *IL6* intracellular protein levels (normalized to *CKIIβ*) in osteoblasts in the insert coculture system and after treatment with CM from prostate cancer cells. (C) *IL6* secretion by osteoblasts after treatment with CM from prostate cancer cells. Error bars represent the mean  $\pm$  SD of at least three independent determinations.

\*  $p < 0,05$ ; \*\*  $p < 0,01$ ; \*\*\*  $p < 0,001$

### 3.2.6. BNP may be potentially relevant in prostate cancer bone metastasis.

The *NPPB* gene encodes the precursor of the brain natriuretic peptide (BNP), a member of a family of three natriuretic peptides, which play a crucial role in cardiovascular and renal homeostasis [Woodard & Rosado 2007]. BNP overexpression in mice causes increased endochondral ossification and skeletal overgrowth [Chusho *et al.* 2000]. *NPPB* is one of the transcripts that became upregulated in hfOB after coculture with PC3, LNCaP or C4-2B4, but not with the non-prostate cell lines HeLa or IMR-90 (Fig. 21A).

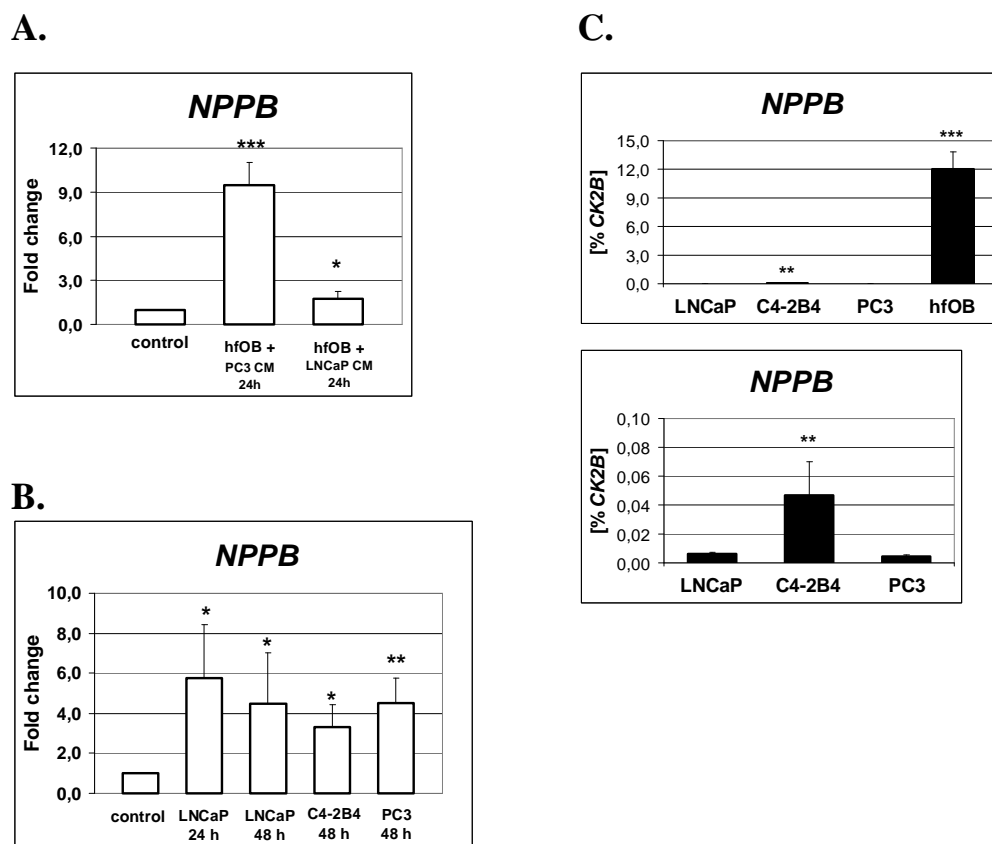


**Fig. 27** *NPPB* expression by prostate cancer cells and osteoblasts. (A) *NPPB* mRNA levels in osteoblasts after treatment with CM from prostate cancer cells. (B) Changes in *NPPB* mRNA expression in prostate cancer cells after coculture with osteoblasts. (C) Steady-state levels of *NPPB* mRNA in osteoblasts and prostate cancer cells. Error bars represent the mean  $\pm$  SD of at least three independent determinations. \*  $p < 0,05$ ; \*\*  $p < 0,01$ ; \*\*\*  $p < 0,001$

*NPPB* became significantly elevated in osteoblasts after only 24 h of coculture with all three prostate cancer cell lines, but especially with PC3 (Fig. 23) and the effect was still evident after 48 h in hfOB<sup>PC3</sup> and hfOB<sup>C4-2B4</sup> (Fig. 21A). Treatment with prostate cancer cell-conditioned medium in a FCS-free setting similarly enhanced the expression of this transcript (Fig. 27A).



Even more interestingly, *NPPB* became strongly upregulated in all three prostate cancer cell lines after coculture with hfOB (Fig. 27B) and the osteotropic C4-2B4 cells showed a much higher steady-state expression of *NPPB* mRNA than the parental line LNCaP (Fig. 27C). These early results suggest a potential importance of BNP in the skeletal metastases of prostate cancer.

There are 3 receptors for natriuretic peptides: NPR (natriuretic peptide receptor)-A, NPR-B and NPR-C, also known respectively as GC (guanylyl cyclase)-A, GC-B and GC-C. GC-A and GC-B have guanylyl cyclase activity and mediate most biological effects of the ligands, while GC-C is implicated in biological clearance of the ligands (negative feedback mechanism). BNP binds to GC-A with high affinity, but also with lower affinity to GC-B [Waschek 2004]. The Affymetrix array showed that hfOB express the mRNA for GC-A, GC-B and GC-C, and the levels of those transcripts did not become altered after crosstalk with prostate cancer cells (data not shown). Thus, hfOB are potentially responsive to BNP both in the absence and in the presence of prostate cancer cells.

The *NPPB* promoter has been cloned and characterized [Weidemann *et al.* 2008]. *In silico* analysis (TESS) of the *NPPB* promoter (Fig. 28) showed potential binding sites for the transcription factor HES1, which according to the array data becomes strongly upregulated in hfOB after coculture with prostate cancer cells (Tab. 9), as well as 3 putative binding sites for IRF1/2 and 1 putative binding site for C-EBP $\beta$ , two known downstream targets of IL6 signaling. Interestingly, *NPPB* is induced most strongly in osteoblasts cocultured with PC3 cells, which secrete very high levels of IL6. The *NPPB* promoter also contains hypoxia-responsive, HIF1 $\alpha$ -binding elements, characterized by Weidemann *et al.* [Weidemann *et al.* 2008] as well as putative binding sites for transcription factors inducible by the WNT- $\beta$ -catenin pathway.

**Fig. 28** *In silico* analysis of the *NPPB* promoter sequence - GenBank accession number AB084517. Potential transcription factor binding sites are listed along with the upstream signaling pathways known to activate those transcription factors.

**Blue** - Putative hypoxia response elements (HREs): RCGTG (R = purine) [Weidemann *et al.* 2008]

**Green** - Putative transcription factor binding sites (TESS analysis)

**TIS** - Transcription initiation site [Weidemann *et al.* 2008]

**HES1**

1 aagcttgctt ttttagaaa caccttgtga tcacctggc agtgattatg agcttcaggt ctggaatcag actgctggct

**AP-1**

81 agactaatca gactggtag aatccaggat ttatcatgtg tcaattgtgt gacttttga aagtagatta attcatgaac

**IRF1/2**<sup>IL6</sup> **TBP**

161 accattcct cctctgaagt gaggaataat aaccgtgctt ttccacctc aggggcagat gctatttttt aggcaagatc

241 tgcttagagg tcccagttc ttattgctgc ctttctctgc tgaactctt ctcccctcat agacagctcc actcctccag

**AP-1** **TBP**

321 cctgctgctt gttgacacca attctctgga aggggagtga catcagtc atagcttta ggggggtatt taagctgcta

**AP-1, Sp1**<sup>TGFβ</sup>, **IRF1/2**<sup>IL6</sup>

401 tgacttctc caggggcatt tctctccaaa gtctcacttc taatcaccag gccacctgct aatgataatt agatcatggg

481 tggtcagatg aaggaggcac tgggagaggg gaaatccca tatctctggt atcccagca atagataacc atcattccag

**TCF-4E**<sup>Wnt/β-catenin</sup>

561 ccatcctttt gtttttttc ttctttctt tctttcttc ctctttctt tctttcttt tctctctct gcaaccagg ctggagtga

**HRE** **IRF1/2**<sup>IL6</sup>

651 gtggcgtgat ctcagctcac tgcaacctcc acctctggg ttcaagtgat tctcttctc cagcctccc agtagctggg

731 actacaggcg cctgccacca tgcccagcta attttggtg attttagtag agacgggggt tcacctgggt ctcgatctcc

**HES1** **TCF3**<sup>Wnt/β-catenin</sup> **TCF-4E**<sup>Wnt/β-catenin</sup>

811 tgacctcgtg atccgaccgc ctggcctctcaaagtgctg ggattacagg cgtgaaccac catgcccage ctatcctttt

**HRE**

891 gtttccatc ctgtgtggc ttggtggggg agaggaggtg ttgacacgtg gaggacacac atataaggca ttcttgggtg

971 actcgtcat cactggacc tatctctcaa aatccagcg aatctgctc ttcctttaa ggagtgaag aagggtcagc

AP2

1051 attccagaag ttctggtca taccaggct ttaatgaat tgccactggg gaatcagcat cccgttctg taaggactat

HRE

1131 aagatggcgg attgtgagag catagggaaa ggtctggag gtctctgtc cttgctccac gcaggtcttt ctggcctgaa

1211 aatcccgttg aagagagcag ctctgagag tttgctcaa gttccctcgg ggtgatcagc accacggaca

HIF ancillary sequence -492 Main hypoxia-responsive HRE -466

1281 cgccccgag gaccgcagg caggcagggt gcacagcggc gagcaggtgc tgcgtacgt gcgggccagg

Sp1<sup>TGFβ</sup>

AP-1

1351 gaactcgcgc ggggagggga gaggcgccgc ggtggcggg gtcttgccg gggtgtttt cgtgtgagt

HRE

C/EBPβ<sup>IL6</sup>

1421 caccccgtgc tccccgct cacg/cgtc ctggaaagc cgggtctc cctgctttt ccagcaacgg

1491 tggggtgggg aggcaggaag aaagcggcct ctaggacac ctggacattt gcaggaaagg aagaagcggg

TBP

1561 agacggggac ttgtctgtg ctccagcgcg ttctgccc cggcccgac cggcccatt tctatacaag

HRE

Sp1<sup>TGFβ</sup>

1631 gtcggctctg cccggtctcc acctcccacg/cgcaggegc ggaggggetc attcccgggc cctgatctca

1701 gagggccgga atgtggctga taaatcagag ataaccctgc atggcagggc agggccgaca ctcagctcca

+1

1771 ggataaaagg ccacggtgtc ccgaggagcc aggaggagca cccgcaggc tgagggcagg tggaagcaa

^TIS

1841 **accggacgc atcgacgag ctgcagcagc agcagaagca gcagcagcag cctccgagt cctccagag**

## **4. Discussion**

### **4.1. Bone metastasis - the significance of “seed-soil” interactions and validity of the *in vitro* model.**

The formation of skeletal metastases is a site-specific multistep series of events, dependent on peculiar properties of tumor cells and on supportive factors present in the microenvironment of the metastatic site. It has long been known that the skeleton presents a particularly hospitable terrain for the spread of tumors such as prostate cancer. Elucidation of the molecular mechanisms that stand behind prostate cancer metastasis to bone is essential for the development of new therapeutic approaches.

To explain non-random patterns of metastasis, in 1889 Stephen Paget proposed the hypothesis, still valid today, that metastases form when the tumor cells (“seeds”) and the target organ (“soil”) are compatible [Fidler 2003]. Metastatic cancer cells require properties that allow them not only to adapt to a foreign microenvironment but to subvert it in a way that is conducive to their continued proliferation and survival [Bacac & Stamenkovic 2008]. Many studies have underscored the importance of the bone microenvironment, and especially of osteoblast-derived factors, in the establishment of prostate cancer metastases [Logothetis & Lin 2005]. Factors produced by osteoblasts stimulate prostate cancer cell growth, chemotaxis and expression of matrix proteases, regulate migration, modulate adhesion properties, enhance survival and may reduce sensitivity to apoptosis induced by cytostatics [Lang *et al.* 1995, Festuccia *et al.* 1999, Jacob *et al.* 1999, Shulby *et al.* 2000, Tenta *et al.* 2005].

The experiments presented here focus on the role of paracrine interactions between metastasizing prostate cancer cells and bone cells. The human cell lines used are widely utilized by researchers and well described. The human fetal osteoblast line hfOB 1.19 [Harris *et al.* 1995] expresses osteoblast-characteristic genes, as confirmed by qRT-PCR. Knerr *et al.* (2004) have shown that the transcriptional alterations induced in prostate cancer cells by crosstalk with hfOB cells closely resemble those induced by crosstalk with primary osteoblasts isolated from mouse calvariae. The prostate cancer cell lines LNCaP, C4-2B4 and PC3 can be considered representative of different stages of human prostate cancer. Clinically, the lethal phenotypes of this malignancy are characterized by their progression to androgen independence and propensity to form skeletal metastases [Thalmann *et al.* 2000]. The bone metastases observed in prostate cancer patients are predominantly of a mixed osteoblastic-osteolytic type, where overall bone remodeling is increased, but bone formation exceeds bone resorption [Keller & Brown 2004].

The LNCaP line, derived from a lymph node metastasis, is androgen-responsive [Horoszewicz *et al.* 1983]. PC3, derived from a bone metastasis, is androgen-independent [Kaighn *et al.* 1979] and C4-2B4, a subline of LNCaP isolated from a bone metastasis after rounds of serial selection in immunocompromised mice, is androgen-independent as well [Thalmann *et al.* 2000]. When injected into immunocompromised mice, LNCaP cells form tumors at the injection site, but have a low propensity for growth in bone. After intraosseal injection of LNCaP into immunocompromised mice, researchers have reported either generation of tumors that later spontaneously regressed [Soos *et al.* 1997] or a complete lack of growth in bone [Fisher *et al.* 2002]. LNCaP cells are, however, able to colonize fragments of human bone implanted into severe combined immunodeficient (SCID) mice, in the so-called SCID-hu model [Nemeth *et al.* 1999], forming mixed osteoinductive-osteolytic lesions. In contrast, both C4-2B4 [Thalmann *et al.* 2000] and PC3 cells [Soos *et al.* 1997, Nemeth *et al.* 1999, Fisher *et al.* 2002] have an enhanced propensity for bone homing and colonization, as shown *in vivo* in mouse models. C4-2B4 form osteoblastic lesions [Thalmann *et al.* 2000], whereas PC3 form osteolytic lesions and have a high invasive capability, infiltrating the bone marrow, bone and surrounding soft tissues [Soos *et al.* 1997, Fisher *et al.* 2002]. It has not been determined whether these cell lines are derived from subpopulations of cancer cells with osteotropic qualities resulting from mutations within the primary tumor, or whether their aggressive phenotype evolves as a result of interactions with the bone microenvironment. Possibly both mechanisms play a part.

The *in vitro* model used here only investigates soluble factor-mediated crosstalk between two cell types. It takes into account neither the mechanistics of metastasis nor the complexity of interactions at the metastatic site in the organism, where multiple cell types influence each other *via* soluble molecules and adhesive contact. However, it has been utilized by researchers before and proven to reflect, to a degree, processes that take place *in vivo* [Yang *et al.* 2001, Knerr *et al.* 2004]. The altered patterns of gene expression described here also conform to data from published *in vivo* studies, as discussed below.

### **4.2. Modulation of the prostate cancer cell phenotype by the osteoblast secretome - an early step on the path to skeletal metastases.**

#### **4.2.1. Osteomimicry is induced in prostate cancer cells by crosstalk with osteoblasts and may facilitate cancer cell survival in bone.**

It has been proposed that interaction with osteoblasts enables metastasizing prostate cancer cells to assume an osteomimetic, or bone-like phenotype, which aids their survival and growth in bone [Koeneman *et al.* 1999]. It has also been demonstrated that crosstalk solely through soluble factors is sufficient to induce gene expression changes in both prostate cancer cells and osteoblasts [Yang *et al.* 2001, Pinski *et al.* 2001, Zayzafoon *et al.* 2004]. A study by Knerr *et al.* (2004) has shown that osteoblast-released factors alter the adhesive properties of prostate cancer cells, suppress their proliferation and induce osteomimicry.

The data presented here indicate that the expression of multiple bone-associated genes by prostate cancer cell lines is either constitutively high or becomes induced after coculture with osteoblasts or exposure to osteoblast-conditioned medium. In the LNCaP line, which represents an early stage of prostate cancer, osteoblast-released factors elevated the expression of genes such as *COL1A1*, *OPG*, *RANKL* and *NOG*, which are constitutively highly expressed in the osteotropic, bone metastasis-derived cell lines C4-2B4 and PC3. It appears that the osteomimetic phenotype induced by exposure to the osteoblast secretome is permanently enforced in cancer cells derived from bone metastases. This is in line with findings from a microarray study showing that osteoblast-derived factors induce a gene expression pattern in non-metastatic cancer cells similar to that found in prostate cancer cells derived from bone metastases [Fu *et al.* 2002]. C4-2B4 cells showed a significantly higher baseline expression of *AP*, *COL1A1*, *OPG*, *RANKL* and *NOG* than their parental line LNCaP, matching a report by Lin *et al.* (2001) that characterized C4-2B as possessing osteoblast-like traits. Moreover, expression of genes characteristic of osteomimicry is not restricted to the osteoinductive phenotype in prostate cancer cell lines, as the osteolytic PC3 line expressed high levels of *BMP2*, *CBFA1*, *COL1A1* and *OPG*. However, PC3 also showed a high baseline expression of *DKK1* and *NOG*, which inhibit bone formation, whereas baseline expression of *DKK1* and *NOG* in the osteoblastic LNCaP and C4-2B4 was very low. These data match recent reports that *DKK1* and *NOG* are highly expressed by osteolytic cancer cell lines, but not osteoinductive ones, and may be an important determinant of the type of metastatic lesions induced in bone [Hall *et al.* 2005, Schwaninger *et al.* 2007, Dai *et al.* 2008].

The expression of bone-specific proteins by malignant cells could aid bone colonization in many ways. Results presented here show that osteoblast-released factors induced prostate cancer cells to express elevated levels of mRNAs such as *BMP2*, *AP*, *COL1A1*, *OPN*, *RANKL* and *OPG*. The molecules coded by these mRNAs may facilitate bone metastasis by various mechanisms. *BMP2* has been shown to stimulate prostate cancer cell migration and invasion, and to promote the formation of osteoblastic lesions in mouse tibia [Feeley *et al.* 2005]. Elevated levels of *COL1A1* and *OPN* mRNA have been found in tumors induced by intratibial inoculation of PC3 cells in immunocompromised mice [Fisher *et al.* 2002]. Adhesion to type I collagen increases the proliferative capacity of the PC3 line, and may facilitate the colonization and growth of prostate cancer cells in the bone microenvironment [Kiefer *et al.* 2001]. *OPN*, an acidic adhesive glycoprotein, promotes cell motility, invasion and survival. Its role in tumor progression and metastasis is well documented [Rangaswami *et al.* 2006]. *OPN* may act as a paracrine and autocrine mediator of prostate cancer progression, enhancing the proliferative and invasive capacity of the cancer cells, as shown by studies using neutralizing antibodies [Thalmann *et al.* 1999] and protein overexpression [Khodavirdi *et al.* 2006].

*RANKL* and *OPG*, too, are strongly implicated in the pathogenesis of bone metastases [Wittrant *et al.* 2004, Blair *et al.* 2005]. Analysis of surgical biopsy specimens showed that expression of both these molecules correlates with more aggressive, advanced, metastatic prostate cancer. Furthermore, bone metastases were consistently immunoreactive for *OPG* and *RANKL* compared with nonosseous metastases or primary tumors [Brown *et al.* 2001, Chen *et al.* 2006]. *RANKL* stimulates bone resorption, which has been postulated as a prerequisite for the successful seeding of tumor cells into bone and their development into secondary lesions [Keller & Brown 2004]. On the other hand, *OPG* levels are elevated in the serum of patients with advanced prostate cancer [Brown *et al.* 2001] and *OPG* can inhibit bone resorption associated with prostate cancer bone metastasis, leading to an increase in bone mass [Corey *et al.* 2005]. These findings underscore a possible role for *OPG* in the development of osteoblastic lesions.

Moreover, although *OPG* is a well-known antagonist of *RANKL*, it not only inhibits osteoclastogenesis, but can also promote the survival of cancer cells by binding the tumor necrosis factor-related apoptosis inducing ligand (*TRAIL*) secreted by invading monocytes and blocking *TRAIL*-mediated tumor cell apoptosis [Holen & Shipman 2006]. Such an effect has been demonstrated *in vitro* in prostate cancer [Holen *et al.* 2002], breast cancer [Holen *et al.* 2005] and multiple myeloma [Shipman & Croucher 2003] cells. It has been suggested that increased cancer cell survival through the inhibition of *TRAIL*-induced apoptosis may be a mechanism involved in very early metastasis development, when there is only a low number of

cancer cells present [Holen & Shipman 2006]. Significantly higher levels of OPG are secreted by androgen-independent prostate cancer cells [Holen *et al.* 2002] and the serum OPG level appears to be a strong independent risk factor predictive of prostate cancer-related death [Jung *et al.* 2004].

Importantly, it is the RANKL/OPG ratio that decides whether osteoclast-mediated bone resorption becomes stimulated or inhibited [Hofbauer & Heufelder 2001, Hofbauer *et al.* 2001]. In the experimental model described here, expression of *RANKL* mRNA was low as compared to *OPG* both in prostate cancer cells and in osteoblasts, whereas hfOB expressed much higher levels of *OPG* than any prostate cancer cell line, suggesting that *OPG* expression by osteoblasts might be the factor that has the greatest influence on the overall RANKL/OPG ratio. *OPG* expression in osteoblasts significantly dropped after only 24 h of crosstalk with prostate cancer cells, and remained repressed after 48 h; thus, the net result could be an increase in bone resorption, regardless of OPG secretion by the cancer cells. The fact that the PC3 line expresses *OPG* at a high level also suggests that the osteoprotective effect of cancer cell-secreted OPG can be negated by other concurrently secreted factors.

Since the concentrations of secreted RANKL and OPG were not measured, it is not possible to say, at this stage, how their overall ratio changed as a result of prostate cancer cell crosstalk with osteoblasts. However, it can be hypothesized that OPG levels become locally elevated in the vicinity of OPG-secreting cancer cells in the bone marrow, protecting them from apoptosis induced by immune system cells [Holen *et al.* 2002, Shipman & Croucher 2003, Holen *et al.* 2005]; thus, OPG upregulation in cancer cells might contribute to disease progression regardless of the net RANKL/OPG ratio in the bone microenvironment and its effect on osteoclasts.

In sum, osteomimicry caused by exposure to osteoblast-released factors appears to be an example of adaptive changes induced in cancer cells by their microenvironment, leading to increased cancer cell survival and growth.



4.2.2. The first response of prostate cancer cells to the osteoblast secretome involves intensified IL6 and TGF $\beta$  signaling, which may participate in the induction of osteomimicry.

When prostate cancer cells metastasize to bone, they encounter an environment rich in IL6 and TGF $\beta$ 1. Both IL6 and TGF $\beta$  signaling have been linked to prostate cancer progression.

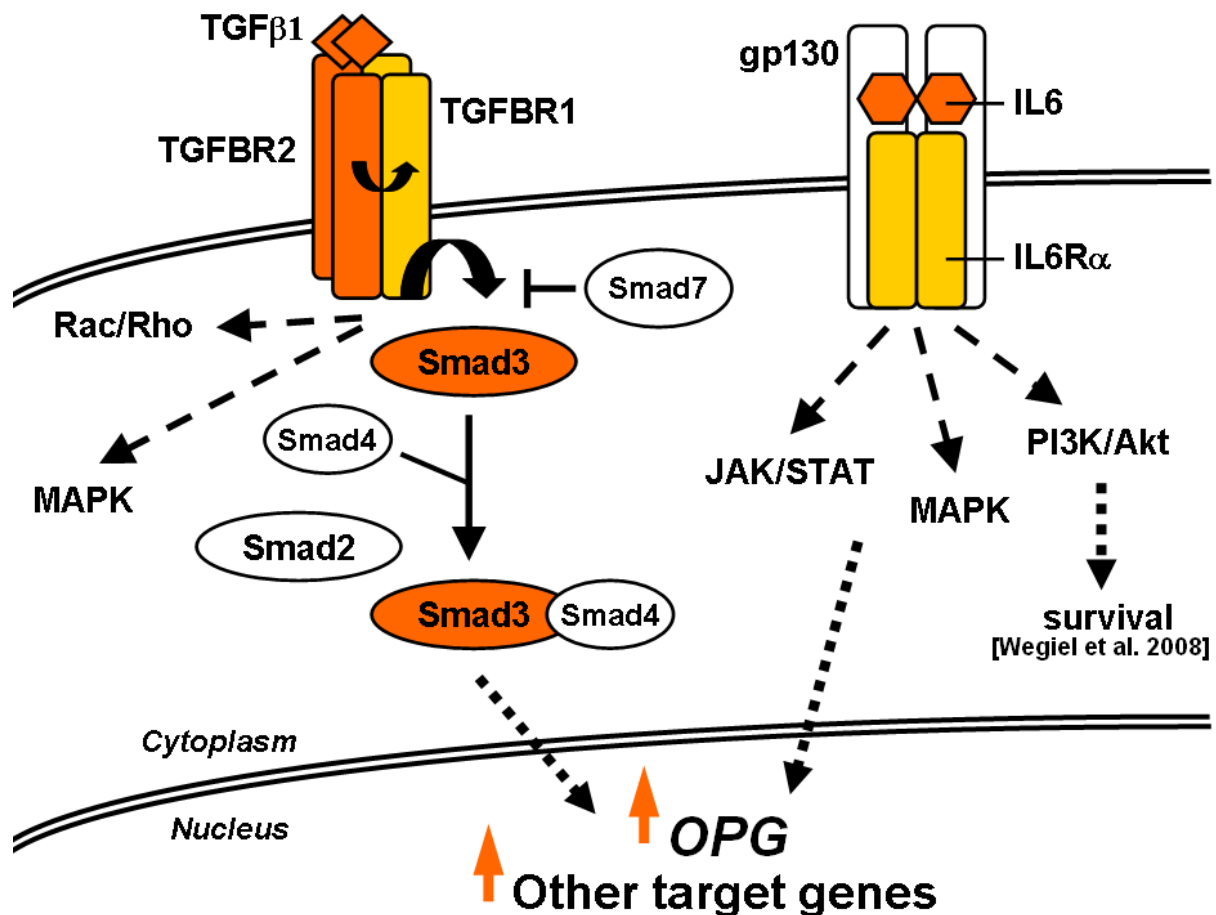


**Fig. 29** Alterations in TGF $\beta$  and IL6 signaling in prostate cancer cells exposed to osteoblast-released factors. Model based on qRT-PCR data. Red - molecules elevated in LNCaP exposed to osteoblast-released factors AND in osteotropic cell lines C4-2B4 and/or PC3 as compared to LNCaP. Orange - molecules elevated in LNCaP exposed to osteoblast-released factors.

The osteomimetic molecule OPG has been described as a TGF $\beta$ -inducible gene, and the TGF $\beta$ -responsive sites in its promoter have been mapped [Thirunavukkarasu *et al.* 2001]. IL6

has also been shown to increase OPG expression in osteoblasts [Palmqvist *et al.* 2002]. The data presented here demonstrate that IL6 and TGF $\beta$ 1 are abundantly expressed and secreted both by osteoblasts and by the PC3 prostate cancer cell line, which has a high constitutive expression of *OPG*. In LNCaP cells, which represent an early stage of prostate cancer, osteoblast-released IL6 and TGF $\beta$ 1 upregulate *OPG* mRNA, and furthermore, crosstalk with osteoblasts increases the expression of these factors and of their receptors (Fig. 29). The net result could be an increased propensity for survival in bone.

IL6 is a pleiotropic cytokine involved in immune responses. It regulates the proliferation, apoptosis, angiogenesis and differentiation of various cell types. IL6 binds to its specific receptor, IL6 receptor alpha (IL6R $\alpha$ ), an 80 kDa glycosylated transmembrane protein belonging to the cytokine receptor superfamily. The activated IL6R $\alpha$  interacts with gp130, a transmembrane cytokine receptor capable of signal transduction through the Janus kinase/signal transduction and activator of transcription (JAK/STAT), mitogen-activated protein kinase (MAPK) and phosphatidylinositol-3 kinase/Akt (PI3K/Akt) pathways [Kamimura *et al.* 2003, Heinrich *et al.* 2003].

IL6 is an established marker of morbidity in metastatic prostate cancer and a candidate for targeted therapy [Drachenberg *et al.* 1999, Shariat *et al.* 2001]. This cytokine can act on prostate cancer cells both through its own receptor and through the androgen receptor (AR), contributing to androgen independence [Culig *et al.* 2002, Culig *et al.* 2005]. The concentrations of IL6 and IL6R are dramatically elevated in prostate cancer tissues [Giri *et al.* 2001]. IL6 is a positive growth factor for many prostate cancer cell lines, with the exception of IL6-negative LNCaP, in which treatment with exogenous IL6 causes growth arrest [Culig *et al.* 2005]; however, ectopically expressed IL6 stimulates cell growth in LNCaP [Lou *et al.* 2000] and chronic treatment of IL6-negative LNCaP cells with exogenous IL6 triggers a positive feedback, turning it from a paracrine growth inhibitor to an autocrine growth stimulator [Hobisch *et al.* 2001, Lee *et al.* 2007]. It has been suggested that IL6 undergoes such a functional transition during progression of prostate cancer to the androgen-independent phenotype [Chung *et al.* 1999, Lee *et al.* 2007]. IL6, both endogenous and exogenous, also protects prostate cancer cells from apoptosis [Cavarretta *et al.* 2006, Wegiel *et al.* 2008]. IL6 is abundantly produced by osteoblasts, and osteoblast-conditioned medium containing this cytokine can promote prostate cancer cell proliferation and progression to androgen independence [Blaszczyk *et al.* 2004, Lu *et al.* 2004].

IL6 and other IL6-type cytokines stimulate osteoblast differentiation in murine and human osteoblastic cell lines [Bellido *et al.* 1997]. IL6 in collaboration with the soluble form of its receptor stimulates the differentiation of committed osteoprogenitors in the bone marrow [Erices *et al.* 2002]. IL6 receptor expression increases during *in vitro* osteoblast differentiation and IL6 enhances the expression of osteoblast-specific differentiation markers in proper sequential order [Li *et al.* 2008b].

TGF $\beta$  signaling controls a diverse set of cellular processes, including cell proliferation, migration, differentiation and apoptosis. TGF $\beta$ , the founding member of the TGF $\beta$  superfamily, mediates its effects through two serine/threonine kinase receptors, termed the TGF $\beta$  type I (TGFBR1) and type II (TGFBR2) receptors. Ligand binding to TGFBR2 triggers recruitment of TGFBR1 and the formation of an active, heterotetrameric receptor complex [Shi & Massague 2003, ten Dijke & Hill 2004]. Further propagation of TGF $\beta$  signaling can occur through SMAD-dependent (canonical) or SMAD-independent (noncanonical) pathways [Derynck & Zhang 2003]. Signaling through the SMAD family of proteins is triggered by phosphorylation of the receptor-activated (R-) SMADs, SMAD2 and SMAD3, by TGFBR1. After phosphorylation, R-SMADs form complexes with the required common mediator SMAD, SMAD4, translocate to the nucleus and activate or repress transcription of target genes, functionally interacting with many other DNA-binding transcription factors. An inhibitory SMAD, SMAD7, plays an essential role in the negative-feedback regulation of TGF $\beta$  signaling by inhibiting signal transduction at the receptor level. It can interfere with R-SMAD binding to receptors, as well as facilitate ubiquitin-mediated degradation of activated TGFBR1 [Moustakas *et al.* 2001, Shi & Massague 2003, ten Dijke & Hill 2004].

Three closely related mammalian isoforms of TGF $\beta$  exist, known as TGF $\beta$ 1, - $\beta$ 2, and - $\beta$ 3. Of these three, TGF $\beta$ 1 is the most abundant one, and it is present in high amounts in bone [Janssens *et al.* 2005]. TGF $\beta$ 1 is highly expressed in prostate tumors and can enhance cancer growth and metastasis, once the malignant cells acquire resistance to its antiproliferative and proapoptotic effects [Wikstrom *et al.* 2001]. TGF $\beta$ 1 overproduction is strongly associated with poor clinical outcome in prostate cancer [Wikstrom *et al.* 1998], and inhibition of TGF $\beta$  signaling suppresses progression of androgen-independent human prostate cancer in immunocompromised mice [Zhang *et al.* 2005b]. In an *in vivo* model of bone metastasis, TGF $\beta$ 1 was shown to stimulate the proliferation of rat prostate cancer cells, osteoclast activation and osteolysis [Sato *et al.* 2008]. Osteoblast-derived TGF $\beta$ 1 enhances prostate cancer cell

chemotaxis, adhesion and their ability to invade bone matrix [Festuccia *et al.* 1999, Festuccia *et al.* 2000].

TGF $\beta$ 1 is the most abundant growth factor in human bone, and affects osteoblast differentiation, matrix formation and mineralization. It is stored in the bone matrix in a latent form and becomes released and activated upon bone resorption. TGF $\beta$ 1 inhibits the late differentiation of osteoblasts, but stimulates the proliferation and differentiation of osteoblast progenitors [Janssens *et al.* 2005, Kanaan & Kanaan 2006]. It has been shown to activate the transcription of genes characteristic for the osteoblast phenotype, such as *OPN* [Noda *et al.* 1988, Wrana *et al.* 1991] and *OPG* [Thirunavukkarasu *et al.* 2001].

Although IL6 and TGF $\beta$ 1 are a potent example of the common growth factor tropisms existing between osteoblasts and prostate cancer cells, an association between these molecules and osteomimicry has not been reported in literature.

The fact that osteoblast-released factors elevate levels of *IL6* mRNA in LNCaP is particularly interesting in the face of recent reports that directly link the acquisition of autocrine IL6 signaling by this cell line with cancer progression [Hobisch *et al.* 2001, Cavarretta *et al.* 2006, Lee *et al.* 2007]. Osteoblast-released TGF $\beta$ 1 also appears to increase *TGFBI* expression in LNCaP, supporting the argument that growth factor tropisms in osteoblasts and prostate cancer cells are closely synchronised and a switch from paracrine to autocrine stimulation can easily occur.

The ability of LNCaP cells to respond to TGF $\beta$ 1 has been controversial, with some researchers reporting a lack of sensitivity due to a silenced *TGFBR1* [Kim *et al.* 1996a], while others observed sensitivity after growth factor stimulation [Schuurmans *et al.* 1991]. It has also been suggested that LNCaP sensitivity to TGF $\beta$ 1 could be modulated by androgens such as dihydrotestosterone, which affects *TGFBR2* expression by this cell line [Kim *et al.* 1996b]. The seemingly contradictory results might be explained by varying promoter methylation status of *TGFBR1* and *TGFBR2* in LNCaP under different experimental conditions, since LNCaP gain sensitivity to TGF $\beta$  after treatment with demethylating agents [Zhang *et al.* 2005b]. The data presented here show that LNCaP cells express *TGFBR1* and low, but detectable amounts of *TGFBR2* mRNA, and thus are potentially responsive to TGF $\beta$  signaling. Both *TGFBR1* and *TGFBR2* become upregulated in LNCaP after exposure to osteoblast-released factors, suggesting that factors present in the bone microenvironment may increase the sensitivity of this cell line to TGF $\beta$ . Enhanced TGF $\beta$  signaling has been associated with prostate cancer progression, angiogenesis, metastasis and a poor clinical outcome [Wikstrom *et al.* 1998, Zhang *et al.* 2005a].

However, in the non-malignant prostate, TGF $\beta$ 1 inhibits epithelial cell proliferation and induces apoptosis, and it has been postulated that prostate cancer cells acquire resistance to its antiproliferative and proapoptotic effects by losing their TGF $\beta$  receptors [Guo & Kyprianou 1999, Wikstrom *et al.* 2001]. Since crosstalk with osteoblasts appears to enhance TGF $\beta$  receptor expression in prostate cancer cells, presumably other factors present in the bone microenvironment render them insensitive to the proapoptotic action of TGF $\beta$ 1. Such a factor might be IL6, capable of exerting an antiapoptotic effect on prostate cancer cells [Cavarretta *et al.* 2006, Wegiel *et al.* 2008].

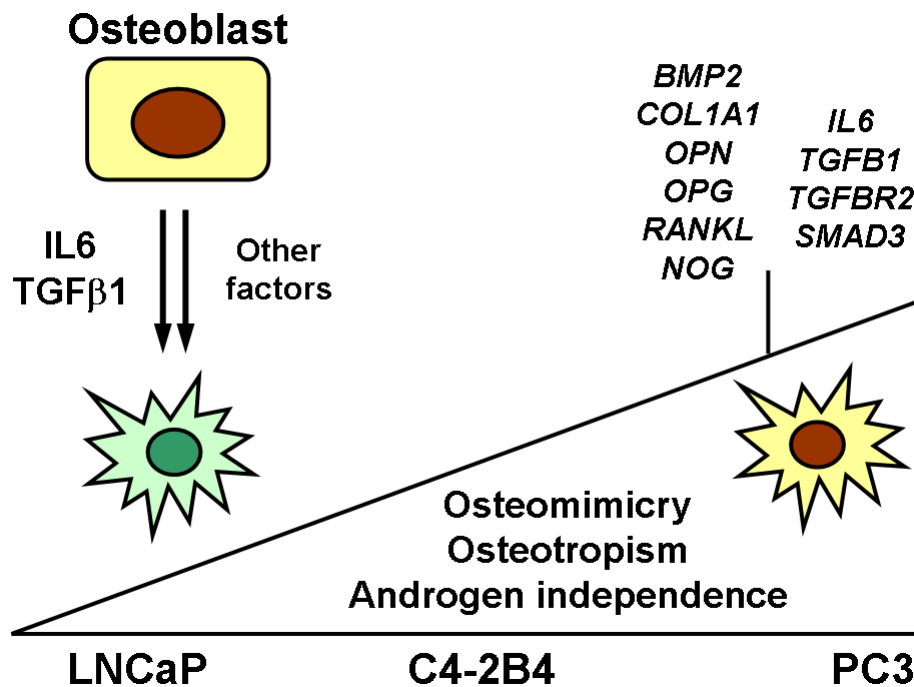


**Fig. 30** Development of an osteomimetic phenotype in prostate cancer cells residing in bone. Model based on qRT-PCR data.

Baseline expression of *TGFB1*, *TGFBR2* and *SMAD3*, but not *SMAD2*, was positively correlated with the osteomimetic and osteotropic characteristics of prostate cancer cell lines. *SMAD3*, but not *SMAD2*, became upregulated in LNCaP after crosstalk with osteoblasts or exposure to osteoblast-conditioned medium. Although TGF $\beta$  activates both SMAD2 and SMAD3 in most cells, there is evidence that these two proteins mediate differing transcriptional responses and play distinct roles in the pathophysiological effects of TGF $\beta$ . E.g. SMAD3 and not

SMAD2 is the key mediator of pathogenic effects in fibrosis [Roberts *et al.* 2003, Brown *et al.* 2007]. A hierarchical model of gene regulation by TGF $\beta$  has been proposed, where SMAD3 was demonstrated to be the critical mediator for expression of immediate-early target genes [Yang *et al.* 2003]. It has been suggested that TGF $\beta$  receptors directly activate SMAD3 and that SMAD2 merely transmodulates the signals [Brown *et al.* 2007]. Furthermore, SMAD3 appears to play a role in bone formation by osteoblasts, as SMAD3 overexpression mimicked the stimulatory effects of TGF $\beta$  on the expression of bone matrix proteins in a mouse osteoblastic cell line [Sowa *et al.* 2002]. It is tempting to speculate that osteomimicry might be mediated in part by TGF $\beta$  signaling *via* SMAD3.

A model of the molecular events associated with prostate cancer progression in bone, based on the experimental data presented here, is shown in Fig. 30.

Transcript profiling of cells in an *in vitro* metastasis model makes it possible to study the earliest stages of the processes which culminate in the formation of lethal metastatic lesions in bone. It appears that osteoblast-released soluble factors trigger osteomimicry in prostate cancer cells and this phenotype becomes permanent in cell lines derived from bone lesions. *OPG*, an osteomimetic gene and tumor survival factor, becomes upregulated in prostate cancer cells by osteoblast-secreted IL6 and TGF $\beta$ 1. Furthermore, crosstalk with osteoblasts leads to enhancement of autocrine IL6 and TGF $\beta$  signaling in prostate cancer cells. These data provide a new insight into the role of the bone microenvironment in the progression of metastatic prostate cancer.

### **4.3. The osteoblast response to prostate cancer cells - potential consequences for the microenvironment and for the whole organism.**

#### **4.3.1. Alterations of the osteoblast phenotype induced by crosstalk with prostate cancer cells.**

##### ***4.3.1.1. Gene expression pattern suggestive of preosteocytic differentiation.***

A distinctive feature of skeletal lesions in prostate cancer is dysregulated osteoblast proliferation and differentiation, leading to increased formation of woven bone. Prostate cancer cells secrete multiple factors that perturb osteoblast biology [Keller *et al.* 2001, Chirgwin *et al.* 2004, Keller & Brown 2004, Logothetis & Lin 2005, Virk & Lieberman 2007 and others]. Thus, we hypothesized that the transcriptional response of osteoblasts to the secretome of prostate

cancer cells might yield an insight into the molecular events that take place at the earliest stage of bone metastasis.

The immortalized human fetal osteoblast line hfOB 1.19 expresses osteoblast-specific markers, and provides a suitable model for the study of osteoblast differentiation [Harris 1995]. Large-scale transcript profiling of hfOB after coculture with prostate cancer cells has shown transcription alterations suggestive of suppressed proliferation together with decreased metabolic activity, matrix synthesis and adhesion. Changes in the expression of signaling molecules were also observed; there has been evidence for a general repression of TGF $\beta$  signaling, as well as downregulation of transcripts associated with immune response and inflammation. On the other hand, several factors associated with increased osteoblast differentiation became upregulated.

Human osteoblast differentiation can be divided into four stages: preosteoblast, osteoblast, preosteocyte and osteocyte. Each stage is characterized by expression of distinct protein markers as well as by individual morphological features [Billiard *et al.* 2003, Franz-Odenaal *et al.* 2006]. In a study by Billiard *et al.* (2003), conditionally immortalized adult human osteoblast cell lines representing various stages of differentiation were subjected to transcript profiling and provided expression patterns suggesting decreased proliferation and increased apoptosis in preosteocytic cells. The levels of transcripts representing the cytoskeleton, extracellular matrix, and adhesion regulons also changed. Moreover, dramatic downregulation of several immune response factors was observed. These results bear a striking similarity to the transcriptional alterations which we find to occur in hfOB cocultured with prostate cancer cells. Among the gene expression changes observed by Billiard *et al.* between the preosteoblastic and preosteocytic stage of differentiation was downregulation of *COL1A1*, *COL3A1*, *CDH11*, *OPG*, *CTGF*, *FST*, *CXCL12* and *PTX3*; all these alterations were also found to occur in hfOB after 48 h of coculture with prostate cancer cells. Thus, it appears that factors released by prostate cancer cells may induce osteoblasts to exhibit signs of differentiation towards preosteocytes. Significantly, the transformation from osteoblast to osteocyte can take as little as 2-5 days in rabbit and rat models [Franz-Odenaal *et al.* 2006], so the time window of 48 h could be long enough to observe a gene expression pattern characteristic for preosteocytes. Furthermore, the suppression of the TGF $\beta$  pathway in hfOB after coculture fits well into that picture, since recent investigation by Borton *et al.* (2001) has suggested that attenuating TGF $\beta$ -related signaling mechanisms can increase the propensity of an osteoblast to mature

into an osteocyte. Further implications of inhibited TGF $\beta$  signaling will be discussed in section 4.3.4.

Interestingly, *CBFA1*, the transcription factor that plays a central role in osteogenic gene expression and bone formation [Ducy *et al.* 2000] became upregulated in osteoblasts cocultured with prostate cancer cells. This effect occurred simultaneously with the upregulation of transcription factors *HES1*, known to stimulate osteoblast differentiation by augmenting the protein level and activity of CBFA1 [Suh *et al.* 2008] and *SP3*, which acts downstream of CBFA1 to induce skeletal ossification in mice [Goellner *et al.* 2001], as well as the downregulation of *STAT1*, which can function as a cytoplasmic attenuator of CBFA1 [Takayanagi *et al.* 2005]. These alterations appear to underscore the potential significance of elevated *CBFA1* expression. Transcriptional upregulation of *CBFA1* can also be considered an indication of inhibited canonical TGF $\beta$  signaling, since it has been reported that TGF $\beta$  stimulation causes repression of the *CBFA1* promoter in osteoblasts, with SMAD3 mediating the repressive effect [Alliston *et al.* 2001].

It has been reported that soluble factors released by bone-derived prostate cancer cell lines can promote the differentiation of osteoblast precursors through a CBFA1-dependent pathway [Yang *et al.* 2001]. However, in the study by Yang *et al.*, CBFA1 upregulation on the mRNA and protein level was observed together with elevated alkaline phosphatase activity and increased expression of osteoblast markers, whereas the data presented here indicate that in hfOB cocultured with prostate cancer cells, the expression of the main osteoblastic markers other than *CBFA1* was either unchanged (*AP*, *OC*) or downregulated (*COL1A1*, *OPN*). Furthermore, it has been reported that CBFA1 negatively controls osteoblast terminal differentiation to osteocytes, helping maintain cells of the osteoblastic lineage in an immature state [Liu *et al.* 2001]. Thus, CBFA1 upregulation in hfOB after coculture with prostate cancer cells does not fully fit into a preosteocytic gene expression pattern and would need further study to elucidate its implications.

It has also been reported that prostate cancer cells can promote early osteoblast differentiation by activating the sonic hedgehog pathway in preosteoblasts [Zunich *et al.* 2009]. It must be noted that the effect of prostate cancer cells on osteoblast differentiation may depend on factors such as the initial differentiation stage of the osteoblasts, the osteoblast and prostate cancer cell lines used, and other experimental conditions. Significantly, another study showed that OPG expression became reduced in primary mouse osteoblasts cultured in the presence of prostate cancer cells [Fizazi *et al.* 2001], and we could observe an analogous effect in hfOB, becoming established after only 24 h of coculture.



Reduced OPG production by osteoblasts promotes bone resorption by osteoclasts - a crucial step in the establishment and progression of skeletal metastatic lesions [Keller & Brown 2004, Roato *et al.* 2008, Zheng *et al.* 2008]; it is also observed in the course of osteoblast differentiation to preosteocytes [Billiard *et al.* 2003].

The levels of some transcripts which became altered in hfOB after coculture with prostate cancer cells (*CDH2*, *OPN*, *IL6R*) also became slightly altered in hfOB cultured with an empty insert. A likely explanation could be that the diffusion of bioactive molecules through the well becomes impaired by the presence of a membrane, so the hfOB growing under an insert receive a stronger cue to differentiate through autocrine stimulation by the factors they themselves are secreting into the medium. The fact that *CDH2* became significantly downregulated under these conditions after only 24 h suggests that medium exhaustion under the insert is not the cause. However, out of 23 surveyed transcripts affected in hfOB by the prostate cancer cell secretome, 20 were not significantly altered in the presence of an empty insert, so this interfering factor apparently has minimal influence on results.

It was found that many of the transcriptional alterations induced in hfOB by crosstalk with prostate cancer cells can also be induced by coculture with the cervical cancer line HeLa or with normal lung fibroblasts. Here it must be noted as an important point that, while the factors secreted by prostate cancer cells facilitate the development of bone metastases, they do not determine bone tropism. The special propensity of prostate cancer cells to arrest, survive and grow in bone is thought to stem from mechanisms such as the expression of adhesion molecules that facilitate interaction with blood vessel endothelium, extravasation and subsequent attachment to the bone matrix, as well as sensitivity to chemotactic cues. In particular, chemokine signaling can affect organ-specific metastasis development, depending on the profile of chemokine receptors expressed by the cancer cells [Chambers *et al.* 2002, Cooper *et al.* 2003, Buijs & van der Pluijm 2009]. Once the prostate cancer cells become lodged in bone, the local concentration of released bioactive molecules will be much higher than their levels in systemic circulation, and the impact on the bone microenvironment correspondingly drastic. Thus, although other cell types may secrete factors capable of producing the same transcriptional changes in osteoblasts as the factors secreted by prostate cancer cells, these changes could still be important in the context of prostate cancer bone metastases.

### ***4.3.1.2. Potential osteoinductive mechanisms with significance for metastasis.***

Osteoblasts cocultured with all three prostate cancer cell lines expressed increased levels of transcripts coding for secreted molecules capable of promoting osteoblast proliferation and differentiation, such as *ADM*, *STC1* and *BMP2*. *ADM* codes for adrenomedullin (ADM), a peptide which acts as a strong mitogen for osteoblasts and increases indices of bone formation [Cornish *et al.* 2003]. *STC1* codes for stanniocalcin 1 (STC1), a glycoprotein hormone highly expressed in osteoblasts during embryonic mouse osteogenesis [Yoshiko *et al.* 2002], and capable of accelerating osteogenic development in osteoblast colonies [Yoshiko *et al.* 2003]. *BMP2* codes for bone morphogenetic protein-2 (BMP2), member of a family of signaling molecules that play a pivotal role in skeletal morphogenesis [Wan & Cao 2005] and are essential for expression of the osteoblast phenotype [Phimphilai *et al.* 2006]. BMPs enhance osteoblast differentiation and function [Canalis *et al.* 2003] and appear to contribute significantly to dysregulated bone formation in osteoblastic metastases [Feeley *et al.* 2005, Schwaninger *et al.* 2007]; it has been suggested that ADM and STC1 might facilitate this process as well [Chirgwin *et al.* 2004]. Apart from an autocrine effect on osteoblasts, these factors could also promote the development of metastatic lesions in other ways as well, e.g. by stimulating the proliferative and invasive capacities of the malignant cells and by inducing osteomimicry. It has been shown that osteoblast-derived BMP2 enhances prostate cancer cell motility, promoting their migration [Lai *et al.* 2008], while ADM can stimulate the proliferation and invasion of pancreatic cancer cells [Ramachandran *et al.* 2007].

A concomitant coculture-induced effect noted in hfOB is the downregulation of genes coding for two soluble inhibitors of osteoblast differentiation, *FST* and *DKK1*. *FST* codes for follistatin, a TGF $\beta$  target molecule [Zhang *et al.* 1997] that inhibits activin A signaling in osteoblasts [Hashimoto *et al.* 1992] and delays activin-induced endochondral ossification [Funaba *et al.* 1996]. The role of DKK1 in bone and implications of its downregulation are discussed in more detail below. In sum, the proposed model would be that in response to factors released by prostate cancer cells, differentiated osteoblasts expressing high levels of collagen type I shift into the preosteocytic stage, decreasing matrix production. However, they also release molecules that stimulate the commitment of mesenchymal stem cells to osteoprogenitors, osteoprogenitor proliferation and differentiation into osteoblasts, simultaneously downregulating the expression of molecules that inhibit these processes. In effect, osteoblastic differentiation becomes increased in the manner typical for prostate cancer metastatic lesions.

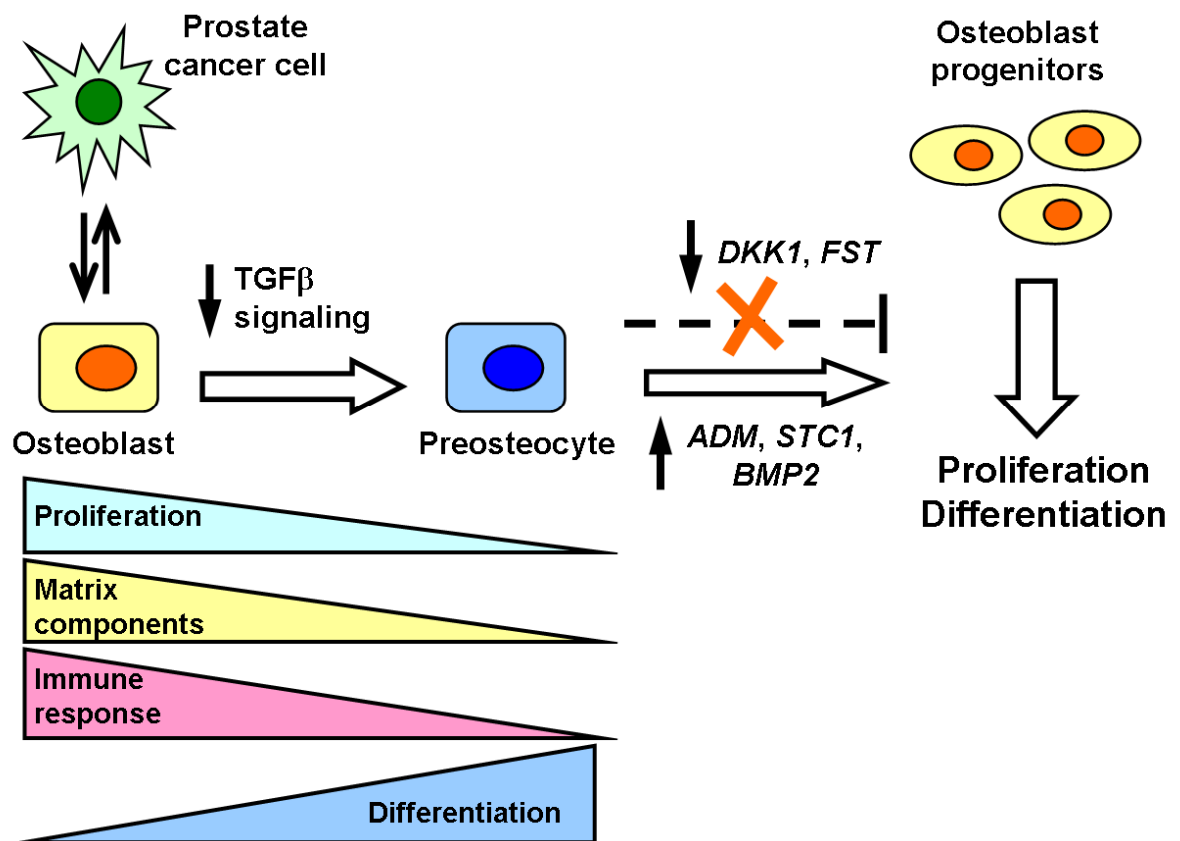


Fig. 31 Effect of prostate cancer cells on cells of the osteoblast lineage. Model based on array data.

A further transcript, *PLAUR*, became upregulated in hfOB cocultured with prostate cancer cells, but not with HeLa or with normal lung fibroblasts. *PLAUR* encodes uPAR, the membrane receptor of urokinase-type plasminogen activator (uPA), a serine protease. Upon binding to its receptor, uPA catalyzes the formation of plasmin from plasminogen, initiating a proteolytic cascade that contributes to ECM breakdown. The uPA/uPAR system has been implicated in multiple biological processes, including angiogenesis, monocyte migration, trophoblast implantation and wound healing, as well as in cancer invasion and metastasis [Wang 2001]. It has been shown that uPA expression by prostate cancer cells contributes to bone matrix degradation and intrasosseous tumor growth [Dong *et al.* 2008] and that uPA stimulates osteoblast proliferation [Rabbani *et al.* 1990]; an increase in uPAR expression by osteoblasts would facilitate these processes as well.

### 4.3.1.3. *DKK1 in prostate cancer bone metastasis.*

The WNT proteins are a large family of soluble glycoproteins that are essential for normal bone development, enhancing osteoblast differentiation, function and lifespan, and thus increasing bone mass [Emami & Corey 2007, Krishnan *et al.* 2006, Yavropoulou & Yovos 2007, Milat & Ng 2009 and others]. DKK1, a soluble inhibitor of WNT signaling, blocks osteoblastic differentiation and bone formation [Qiang *et al.* 2008] and may also promote osteoclastogenesis by inhibiting OPG transcriptional induction by WNTs [Fujita & Janz 2007]. There is strong evidence that DKK1 is one of the key factors mediating the formation of osteolytic lesions of multiple myeloma [Tian *et al.* 2003, Qiang *et al.* 2008] and metastatic breast cancer [Bu *et al.* 2008]. Accordingly, downregulation of DKK1 in osteoblasts, for example by tumor-secreted ET1 [Clines *et al.* 2007], has been proposed as one of the mechanisms that contribute to increased bone formation in prostate cancer. Furthermore, evidence exists that DKK1 expression by prostate cancer cells can act as a switch that transitions the phenotype of prostate cancer metastases from osteolytic to osteoblastic. Prostate cancer cells express WNT ligands and when concomitant DKK1 expression is low, the osteoinductive activity of WNTs becomes unmasked, leading to increased bone formation at the metastatic site [Hall *et al.* 2005, Hall *et al.* 2006, Hall *et al.* 2006b].

The fact that *DKK1* became strongly repressed in hfOB after coculture with prostate cancer cells reinforces the possibility that reduced DKK1 expression is a significant factor in the development of osteoblastic metastases (Fig. 32). It is worth noting that the osteolytic PC3 cells reduced *DKK1* expression in hfOB in the same degree as LNCaP and C4-2B4; however, in contrast to these osteoinductive cell lines, PC3 itself expresses *DKK1* at a high level, matching the model put forward by Hall *et al.* (2006). Conditioned medium from PC3 cells has been found to inhibit osteoblast differentiation and bone nodule formation [Kido *et al.* 1997]. Interestingly, Hall *et al.* have proposed that DKK1 is upregulated in primary prostate tumors, but as the cancer progresses, DKK1 expression declines, particularly in advanced bone metastases, which is corroborated by *in vivo* data from tissue microarrays [Hall *et al.* 2008]. Hence, the fact that *DKK1* expression by PC3 cells decreases after coculture with osteoblasts would fit this model.

DKK1 downregulation in the osteoblastic niche may also have direct implications for the cancer cells. The WNT signaling pathway leads to tumor formation when aberrantly activated, and WNT signaling is active in many cancers [Giles *et al.* 2003]. In prostate cancer cells, autocrine WNT effects can include enhanced proliferation and protection against apoptosis [Hall

*et al.* 2006]. DKK1 secreted by mesenchymal stem cells has been shown to inhibit cancer cell proliferation by blocking WNT signaling [Qiao *et al.* 2008, Zhu *et al.* 2009]. Thus, reduced DKK1 production by osteoblasts may contribute to making the bone microenvironment more conducive to cancer cell growth. However, prostate cancer cells can also gain resistance to DKK1 by acquiring constitutive activation of the WNT pathway through mutations in its regulatory components leading to increased transcription activation by  $\beta$ -catenin, as is commonly the case in colon cancer [Giles *et al.* 2003]; thus, high autocrine DKK1 expression by cancer cells, as exemplified by the PC3 line, does not have to translate into suppressed proliferation and survival.

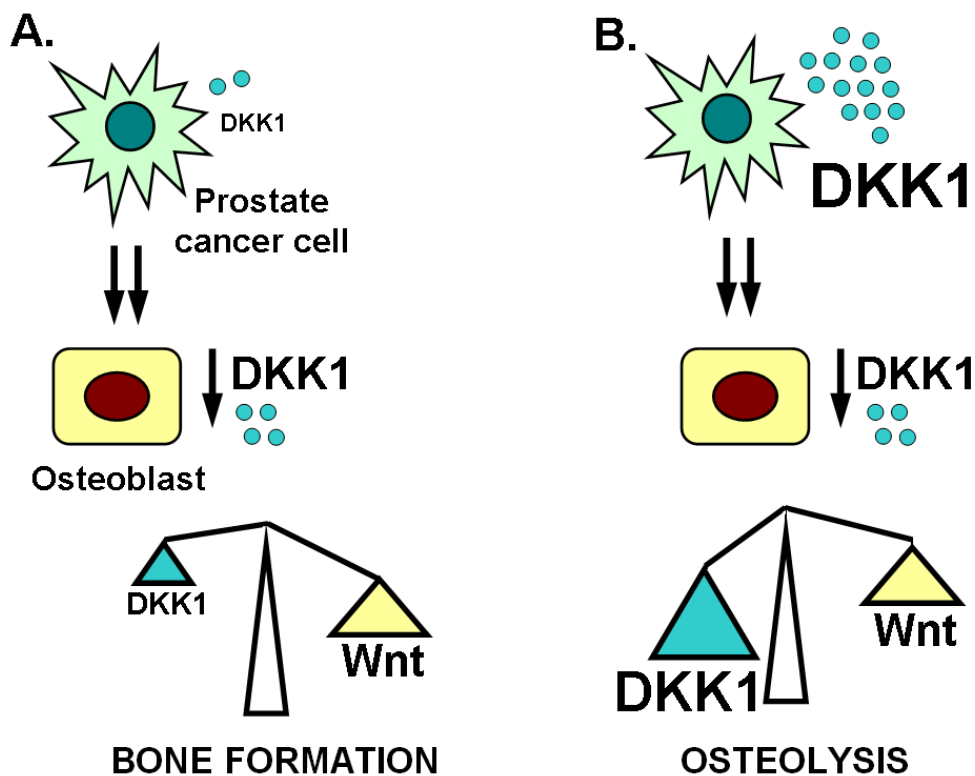


**Fig. 32 A model of the role of DKK1 in determining the phenotype of metastatic lesions in bone.** Model based on qPCR data and on literature [Hall *et al.* 2006, Hall *et al.* 2006b]. A - Osteoblastic/mixed metastasis (LNCaP, C4-2B4). B - Osteolytic metastasis (PC3).

### ***4.3.1.4. The potential significance of BNP in prostate cancer bone metastasis.***

Changes in *NPPB* expression by osteoblasts have not previously been discussed in the context of bone metastasis. This gene codes for the precursor of the brain natriuretic peptide (BNP). BNP belongs to a family of three structurally related signaling molecules, involved in cardiovascular homeostasis and in organ development. There are three guanylyl cyclase receptors for these ligands, known as GC-A, GC-B and GC-C. Natriuretic peptides exert their effects primarily by modulating intracellular cGMP levels [Waschek 2004, Woodard & Rosado 2007]. One of the members of this family, type C natriuretic peptide (CNP), is a known regulator of osteoblast function; it decreases DNA synthesis in osteoblasts [Suda *et al.* 1996] and stimulates osteoblastic differentiation, acting *via* GC-B [Inoue *et al.* 1996]. BNP also activates the GC-B receptor, although with a lesser affinity than CNP. When BNP is overexpressed in mice, they exhibit elevated plasma cGMP levels, increased endochondral ossification and skeletal overgrowth, and effects of BNP on bone are likely to be mediated at least partly by GC-B, since a cross between BNP-overproducing mice and mice lacking GC-A yields mice with no skeletal defects [Chusho *et al.* 2000]. BNP has also been shown to exert functional opposition to TGF $\beta$  in primary fibroblasts, abrogating TGF $\beta$ -induced effects on gene expression [Kapoun *et al.* 2004].

The transcript for the BNP precursor became elevated after just 24 h in hfOB cocultured with prostate cancer cells or treated with prostate cancer cell-conditioned medium. Elevated expression of *NPPB* was maintained in hfOB after 48 h of coculture with prostate cancer cells, but no upregulation was noted in hfOB cocultured for 48 h with non-osteotropic HeLa cells or with normal fibroblasts. Interestingly, this transcript also became strongly upregulated in LNCaP, C4-2B4 and PC3 after coculture with hfOB, and was elevated in the osteotropic, osteoinductive prostate cancer cell line C4-2B4 in comparison to its parental line LNCaP. Higher expression of *NPPB* by C4-2B4 as compared to LNCaP has also been noted in a transcript profiling study by Fu *et al.* (2002). Thus, a link between this transcript and the pathogenesis of prostate cancer bone metastases appears highly probable. The Affymetrix array showed that hfOB expressed the mRNA for BNP receptors both before and after coculture, and thus are potentially responsive to this molecule. Increased BNP levels might, largely by autocrine stimulation, contribute to increased differentiation of osteoblasts and also decrease their sensitivity to TGF $\beta$ , thus mediating some of the effects on gene expression seen on the array.

### 4.3.3. Prostate cancer cells may suppress the host's immune response.

Although the immune system can recognize and destroy developing tumors, it is well known that tumor cells employ many mechanisms to evade, thwart or subvert immune responses, ultimately resulting in tumor growth in immunocompetent hosts. These mechanisms include tumor-induced impairment of antigen presentation, activation of negative costimulatory signals, and upregulation of immunosuppressive factors [Crocì *et al.* 2007, Rabinovich *et al.* 2007].

The skeletal and immune systems appear to function in tight interplay and possess overlapping regulatory mechanisms [Lorenzo *et al.* 2008]. Remarkably, the genes encoding a number of immune response factors became downregulated in hfOB after coculture with all three prostate cancer cell lines. Among them were chemokines, proapoptotic proteins, markers of inflammation such as *STAT1* and *IL6*, a central mediator of inflammatory signaling and a proinflammatory cytokine respectively, and three molecules associated with inflammation-induced bone remodeling - *ADAMTS1*, *HMGB1* and *PAPPA*.

Inflammation, the body's reaction to trauma or infection, is characterized by an influx of soluble mediators and cells that eliminate pathogens and initiate tissue repair. Current opinion holds that inflammation can stimulate, but also inhibit the progression of malignant disease, depending on the context [Le Bitoux & Stamenkovic 2008]. Importantly, in inflammatory states, local production of proinflammatory cytokines by inflamed tissues leads to stimulation of osteoclastogenesis and bone destruction [Lorenzo *et al.* 2008]. The observed changes in the osteoblast transcriptome could, thus, have a mixed impact on metastasizing cancer cells. Reduced bone remodeling would slow down the release of growth factors that fuel cancer cell proliferation, but at the same time, decreased production of cytokines and chemokines by the bone microenvironment could impair the response of immune system cells to cancer cell antigens, contributing to creation of a niche that enables the survival of prostate cancer stem cells in bone.

Downregulation of proteasomal components, as well as proteins participating in proteasome assembly and protein ubiquitination, also occurred in hfOB after coculture with all three prostate cancer cell lines and can be interpreted as a further indication of impaired immune response mechanisms. Misfolded, foreign and other abnormal proteins are degraded through the ubiquitin- and proteasome-dependent pathway; this proteolytic system generates peptides from intracellular antigens, which are then presented to T cells. In this way, the proteasome plays a central role in cellular immunity [Konstantinova *et al.* 2008].

Kinder *et al.* (2007) have reported that osteoblasts undergo an inflammatory stress response after treatment with medium conditioned by breast cancer cells, exhibiting impaired matrix production, increased apoptosis, and increased secretion of osteoclastogenic cytokines such as IL6. The experimental model employed by these researchers involved culturing osteoblasts with conditioned medium in the presence of 10% FCS, the same serum concentration as the one used in the coculture model described here. Thus, the difference in results cannot be due to the presence or absence of serum, but rather to other reasons, e.g. possibly, osteoblast responses to breast and prostate cancer cells may differ.

### **4.3.4. Modulation of TGF $\beta$ signaling in osteoblasts as one of the switches differentiating between osteolytic and osteoblastic metastasis?**

The strength and duration of TGF $\beta$  signaling is largely dependent on negative feedback initiated during signal progression. The array data indicate that canonical TGF $\beta$  signaling was strongly inhibited in osteoblasts after coculture with all three prostate cancer cell lines, as evidenced by upregulation of the negative regulators *PPM1A* and *SNF1LK*, and concomitant downregulation of the TGF $\beta$  receptor *TGFBR2*, the accessory protein *DAB2* and of numerous target genes (Fig. 33, Tab. 16).

In canonical TGF $\beta$  signaling, receptor-activated SMAD proteins translocate into the nucleus, where they regulate transcription [Shi & Massague 2003]. TGF $\beta$  receptors can also activate other signaling molecules which modulate SMAD activity, as well as allow SMAD-independent, or noncanonical TGF $\beta$  responses. TGF $\beta$  can activate the ERK, JNK and p38 MAPK kinase pathways, as well as Rho-like GTPases which mediate changes in cytoskeletal organization and epithelial-to-mesenchymal transition [Derynck & Zhang 2003]. The type II TGF $\beta$  receptor kinase, *TGFBR2*, functions as a ligand-binding molecule and phosphorylates the type I receptor, initiating both canonical and noncanonical signaling [Shi & Massague 2003]. Signal transduction downstream is facilitated by the adaptor molecules SARA (SMAD anchor for receptor activation) [Tsukazaki *et al.* 1998] and disabled 2 (*DAB2*). *DAB2* expression is induced by TGF $\beta$  and this protein is required for TGF $\beta$ -induced epithelial-mesenchymal transition, while its absence induces apoptosis [Prunier & Howe 2005]. *DAB2* forms a critical link in the TGF $\beta$  pathway, aiding in signal transmission from the receptor complex to SMADs [Hocevar *et al.* 2001], but also stimulating activation of the JNK pathway *via* the TGF $\beta$ -activated kinase 1 (*TAK1*) [Hocevar *et al.* 2005].



Tab. 16 Target genes of TGF $\beta$  signaling downregulated in osteoblasts cocultured with prostate cancer cells.

Gene	Gene product	TGF $\beta$ isoform	TGF $\beta$ signaling pathway	Cell type	References
<i>ACTN1</i>	actinin, alpha 1	TGF $\beta$ 1	Canonical (via SMAD2/3), noncanonical (p38)	Normal mammary epithelium, various cancer cell lines (e.g. breast, cervix)	Bakin <i>et al.</i> 2004
<i>CDH2</i>	cadherin 2, type 1, N-cadherin (neuronal)	TGF $\beta$ 1	Noncanonical (JNK)	Stromal myofibroblasts	De Wever <i>et al.</i> 2004
<i>CDH11</i>	cadherin 11, type 2, OB-cadherin (osteoblast)	TGF $\beta$ 1	Not determined	Cytotrophoblasts	Getsios <i>et al.</i> 1998
<i>COL1A1</i>	collagen, type I, alpha 1	TGF $\beta$ 1	Canonical (via SMAD3)	Normal fibroblasts	Verrecchia <i>et al.</i> 2001
<i>COL1A2</i>	collagen, type I, alpha 2	TGF $\beta$ 1	Canonical (via SMAD3)	Normal fibroblasts	Verrecchia <i>et al.</i> 2001
<i>COL3A1</i>	collagen, type III, alpha 1 (Ehlers-Danlos syndrome type IV, autosomal dominant)	TGF $\beta$ 1	Canonical (via SMAD3)	Normal fibroblasts	Verrecchia <i>et al.</i> 2001
<i>CTGF</i>	connective tissue growth factor	TGF $\beta$ 1	Canonical (via SMAD3) and JNK activation both necessary	Normal fibroblasts	Holmes <i>et al.</i> 2001, Utsugi <i>et al.</i> 2003
<i>CXCL12</i>	chemokine (C-X-C motif) ligand 12 (stromal cell-derived factor 1)	TGF $\beta$ 1	Not determined	Peritoneal mesothelial cells	Kajiyama <i>et al.</i> 2007
<i>DAB2</i>	disabled homolog 2, mitogen-responsive phosphoprotein	TGF $\beta$ 2	Not determined	Non-transformed epithelial cells	Prunier <i>et al.</i> 2005
<i>FGF2</i>	fibroblast growth factor 2 (basic)	TGF $\beta$ 1	Canonical (via SMAD3)	Prostate stromal fibroblasts	Yang <i>et al.</i> 2008
<i>FST</i>	folliculin	Not specified	Not determined	Normal hepatocytes	Zhang <i>et al.</i> 1997
<i>IL6</i>	interleukin 6	TGF $\beta$ 1	Not determined	Primary osteoblasts	Franchimont <i>et al.</i> 2000
<i>PAPPA</i>	pregnancy-associated plasma protein A	TGF $\beta$ 1	Not determined	Primary osteoblasts	Ortiz <i>et al.</i> 2003
<i>OPG</i>	osteoprotegerin	TGF $\beta$ 1, -2, -3	Canonical (via SMAD2/3)	Bone stromal cells, osteosarcoma	Thirunavukkarasu <i>et al.</i> 2001
<i>OPN</i>	osteopontin	TGF $\beta$ 1	Not determined	Osteosarcoma, primary osteoblasts	Noda <i>et al.</i> 1988, Wrana <i>et al.</i> 1991
<i>THBS1</i>	thrombospondin 1	TGF $\beta$ 1	Noncanonical (p38)	Osteosarcoma	Okamoto <i>et al.</i> 2002
<i>TNC</i>	tenascin C (hexabrachion)	TGF $\beta$ 1	Canonical (via SMAD3)	Dermal fibroblasts	Jinnin <i>et al.</i> 2004
<i>TPM1</i>	tropomyosin 1 (alpha)	TGF $\beta$ 1	Canonical (via SMAD2/3), noncanonical (p38)	Normal mammary epithelium, various cancer cell lines (e.g. breast, cervix)	Bakin <i>et al.</i> 2004
<i>UGDH</i>	UDP-glucose dehydrogenase	Not specified	Not determined	Various, e.g. normal fibroblasts, breast cancer cells, hepatoma	Bontemps <i>et al.</i> 2003

The *SNF1LK* and *PPM1A* genes encode proteins that inhibit SMAD-dependent signaling. The sucrose nonfermented 1-like kinase (SNF1LK) is a serine/threonine kinase which cooperates with SMAD7 to downregulate the activated type I receptor, participating in negative feedback regulation [Kowanetz *et al.* 2008]. The protein phosphatase 1A (PPM1A) is responsible for SMAD2 and SMAD3 dephosphorylation, which results in their dissociation from SMAD4 and nuclear export [Lin *et al.* 2006]. Thus, SMAD-dependent signaling in osteoblasts after coculture with prostate cancer cells appears repressed. Analysis of the literature data available for

downregulated target genes (Tab. 16) supports this premise. *COL1A1*, *COL1A2*, *COL3A1* [Verrecchia *et al.* 2001], *FGF2* [Yang *et al.* 2008], *OPG* [Thirunavukkarasu *et al.* 2001] and *TNC* [Jinnin *et al.* 2004] are all established targets of canonical signaling via SMADs, while the transcriptional induction of *CTGF* [Holmes *et al.* 2001, Utsugi *et al.* 2003] by TGF $\beta$  requires both canonical and noncanonical signaling. *CDH2* upregulation by TGF $\beta$  in stromal myofibroblasts is mediated by signaling via JNK [De Wever *et al.* 2004] and *THBS1* upregulation by TGF $\beta$  in osteosarcoma cells occurs *via* p38 [Okamoto *et al.* 2002], but the possibility of SMAD participation in these effects has not been excluded, and it is known that MAPK kinase pathways may cooperate with SMAD signaling, for example by phosphorylating and activating SMADs [Derynck & Zhang 2003].

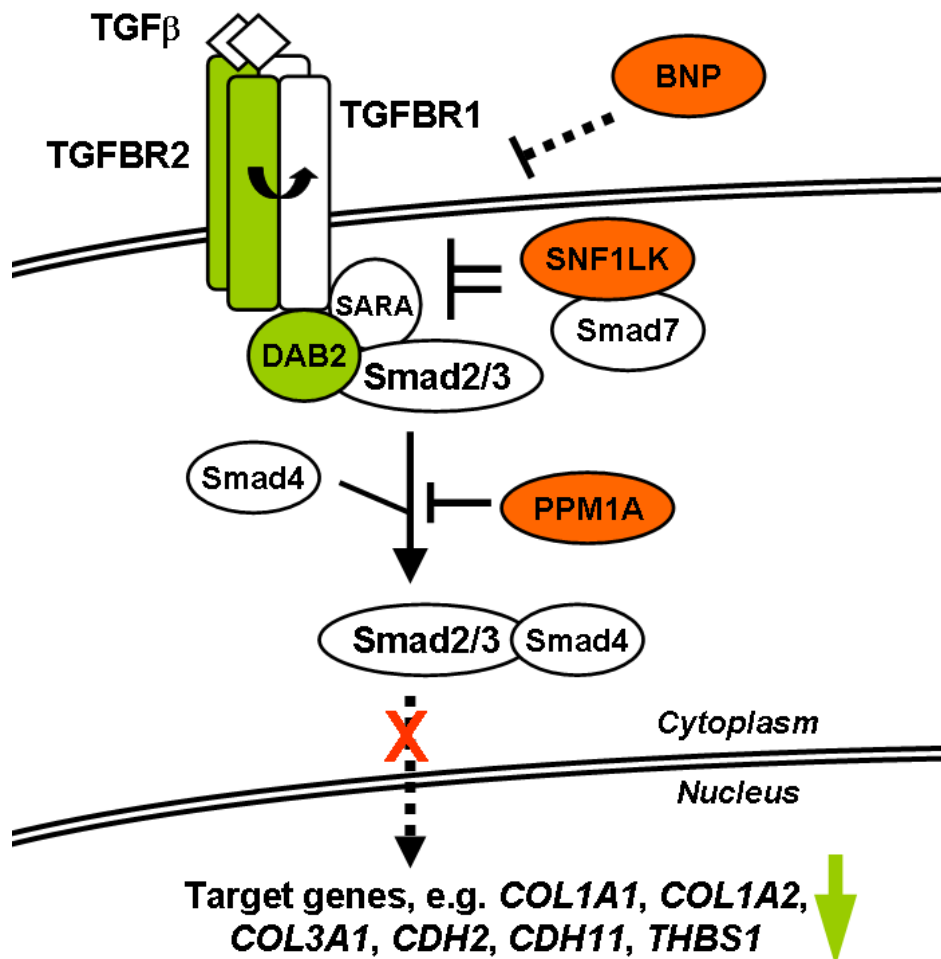


Fig. 33 Inhibition of canonical TGF $\beta$  signaling in osteoblasts cocultured with prostate cancer cells. Model based on array data. Red - upregulated molecules; green - downregulated molecules.

The effects of TGF $\beta$  on osteoblast differentiation depend on the extracellular milieu and the differentiation stage of the cells. TGF $\beta$  promotes osteoblast proliferation, as well as the early stages of differentiation and the expression of matrix proteins, but inhibits osteoblast maturation and matrix mineralization [Janssens *et al.* 2005]. TGF $\beta$ -induced repression of *CBFA1* by SMAD3 decreases CBFA1 and OC expression and blocks terminal osteoblast differentiation [Alliston *et al.* 2001], while expression of a dominant negative TGF $\beta$  receptor type II in osteoblasts leads to decreased bone remodeling and increased trabecular bone formation in mice [Filvaroff *et al.* 1999]. TGF $\beta$  secreted by an osteolytic breast cancer cell line has been reported to seriously impair osteoblast function, inhibiting their differentiation and capability to mineralize a matrix, as well as reducing adhesion and causing disassembly of actin fibers [Mercer *et al.* 2004], possibly leading to decreased bone formation and mechanical strength. Thus, inhibition of TGF $\beta$  signaling in osteoblasts could be proposed as a mechanism leading to increased osteoblast maturation and contributing to the formation of osteoblastic metastases in prostate cancer. BNP, upregulated in osteoblasts by crosstalk with prostate cancer cells, could further contribute to the blockade of TGF $\beta$  effects on transcription, as described by Kapoun *et al.* (2004), and increase osteoblastic differentiation, as suggested by Chusho *et al.* (2000).

In a model consisting of human bone fragments implanted in SCID mice, PC3 cells induced osteolytic metastases after inoculation, whereas the tumors induced by LNCaP represented a mixed osteolytic-osteoblastic type [Nemeth *et al.* 1999]. C4-2B4, a bone metastasis-derived, androgen-independent subline of LNCaP, forms osteoinductive skeletal lesions when injected into immunocompromised mice [Thalmann *et al.* 2000]. The osteolytic PC3 line secretes a different profile of bioactive factors than the osteoblastic C4-2B4, e.g., producing high levels of the osteoblast-inhibitory molecules DKK1 and NOG [Hall *et al.* 2005, Schwaninger *et al.* 2007]. For this reason, we hypothesized that osteoblasts might react differently to coculture with PC3 than with osteoblastic CaP cell lines, providing additional clues as to early mechanisms of osteolytic and osteoblastic metastasis. Interestingly, coculture with PC3 appeared to uniquely affect the expression of many more genes than coculture with C4-2B4, with evidence for a more pronounced stress response, stronger repression of the cell cycle, DNA, RNA and protein synthesis. A cell proliferation assay confirmed that factors released by PC3 inhibited hfOB proliferation more strongly than factors released by C4-2B4. PC3 cells also selectively modulated the expression of a number of transcription factors, signaling pathway components, cytokines and adhesion molecules,

suggesting that osteolytic and osteoinductive prostate cancer cells may create and occupy differing osteoblastic niches.

We could confirm by qRT-PCR that two downstream targets of TGF $\beta$  signaling - *SMAD3* and *SMAD7* - became upregulated in hfOB cocultured with PC3 cells, suggesting that some activity of the TGF $\beta$  pathway was selectively retained, since *SMAD3* is a TGF $\beta$  signaling mediator [Shi & Massague 2003] and *SMAD7* represents a TGF $\beta$  target gene upregulated as a negative feedback mechanism [Afrakhte *et al.* 1998]. Also upregulated in this coculture combination was the transcript encoding sequestosome 1 (SQSTM1). SQSTM1 is a scaffolding protein that functions as a coactivator of NF- $\kappa$ B signaling [Wooten *et al.* 2005]. Evidence exists that NF- $\kappa$ B and TGF $\beta$  pathways influence each other. For example, it has been shown by Eliseev *et al.* that in osteosarcoma cells, NF- $\kappa$ B represses BMP/SMAD signaling and BMP2-induced differentiation through *SMAD7* [Eliseev *et al.* 2006]. Tentatively, a mechanism could be proposed where increased NF- $\kappa$ B activation leads to upregulation of *SMAD7* in osteoblasts cocultured with osteolytic prostate cancer cells, with further consequences for osteoblast function. Interestingly, it has been shown that autocrine stimulation with TGF $\beta$ 2 maintains constitutive NF- $\kappa$ B signaling in PC3 cells, protecting them against apoptosis [Lu *et al.* 2004]; thus, TGF $\beta$ 2 secreted by PC3 might activate NF- $\kappa$ B signaling in osteoblasts as well.

As a further point, differential activation of the TGF $\beta$  pathway has been proposed to occur in osteocytes in response to different types of bone disease. Osteoporosis, bone metastases and multiple myeloma appear to induce distinct transcriptional footprints in osteocytes, involving the SMAD and MAPK branches of TGF $\beta$  signaling [Eisenberger *et al.* 2007]. It is possible that similar mechanisms of differing stress responses involving TGF $\beta$  pathway components might function in all cells of the osteoblast/osteocyte lineage.

#### **4.4. Crosstalk between prostate cancer cells and osteoblasts in light of the cancer stem cell hypothesis: does the bone furnish a niche for cancer stem cells?**

The cancer stem cell (CSC) model states that tumors contain a reservoir of self-renewing cells, which are resistant to conventional therapies and can survive to repopulate the tumor. Normal stem cells have the ability to perpetuate themselves through self-renewal and to generate

mature cells of a particular tissue through differentiation [Reya *et al.* 2001] and CSCs probably arise from mutated stem or progenitor cells which acquire the ability to proliferate uncontrollably [Li & Neaves 2006, Kasper 2008]. Evidence is accumulating that prostate cancers contain such a therapy-resistant stem cell fraction that mediates the progression of this malignancy after androgen deprivation [Kasper 2008, Kelly & Yin 2008, Lang *et al.* 2009].

It is thought that CSCs and normal stem cells utilize similar molecular mechanisms to drive self-renewal, and similar signaling pathways may induce them to differentiate. To maintain their pluripotency, stem cells require a niche where they can undergo self-renewal in response to balanced signals provided by specialized niche cells [Reya *et al.* 2001, Li & Neaves 2006]. Recent publications suggest that osteoblasts are a crucial component of the hematopoietic stem cell (HSC) niche, responsible for maintaining HSC quiescence and shielding them from harmful influences. The functions of the HSC niche depend on the expression of a broad array of adhesion molecules and cytokines [Suda *et al.* 2005]. The transcriptional changes observed by us in osteoblasts may be important in the light of their potential niche function. On the one hand, the functional alterations induced by crosstalk with prostate cancer cells might impair their ability to act properly as a niche component. Even more intriguingly, osteoblasts may also furnish a niche for prostate CSCs and their crosstalk with prostate cancer cells may contribute to this ability. The presence of disseminated cancer cells in the bone marrow of prostate cancer patients is an early event; it has been suggested that the bone marrow enables these cells to stay quiescent and survive for long periods [Pantel & Brakenhoff 2004, Buijs & van der Pluijm 2009].

It has been demonstrated that TGF $\beta$ /SMAD signaling is required to keep human embryonic stem cells in their pluripotent, undifferentiated state [James *et al.* 2005]. TGF $\beta$  plays a key role in regulating self-renewal and differentiation within normal and malignant breast tissue. Putative breast CSCs have a mesenchymal phenotype and active TGF $\beta$  signaling [Tan *et al.* 2009]. Global gene expression profiling has shown a prominent role of TGF $\beta$ /SMAD signaling in the maintenance of adult murine prostate stem cells. The results also suggested that the prostate progenitor lineage may be more similar to embryonic than to hematopoietic stem cells [Blum *et al.* 2009]. Other researchers have reported that TGF $\beta$  is responsible for maintaining the dormancy of prostatic stem cells in the normal mouse prostate [Salm *et al.* 2005]. In the light of the above reports, it is interesting that *TGFB1*, *TGFBR1*, *TGFBR2* and *SMAD3* become upregulated in prostate cancer cells after crosstalk with osteoblasts, a cell type known to provide stem cell niche signals [Wilson & Trumpp 2006, Zhu & Emerson 2004, Neiva *et al.* 2005, Suda

*et al.* 2005] and an abundant source of TGF $\beta$ 1. Furthermore, high endogenous levels of *TGFB1*, *TGFBR2* and *SMAD3* mRNA can be observed in the PC3 line, which is poorly differentiated [Kaighn *et al.* 1979], highly invasive [Soos *et al.* 1997, Fisher *et al.* 2002] and has been shown to possess a stem cell-like subpopulation, capable of self-renewal and initiating serially transplantable tumors [Li *et al.* 2008].

Another osteoblast-released factor which can potentially enhance the survival of prostate CSCs is FGF2, abundantly secreted by hfOB. The FGF2 pathway is one of the most significant regulators of human embryonic stem cells, sustaining their self-renewal and pluripotency. It is also strongly implicated in tumorigenesis [Dvorak *et al.* 2006] FGF2 is known to play a role in prostate cancer development and progression [Kwabi-Addo *et al.* 2004], although its role in the maintenance of prostate CSCs remains unclear.

Interestingly, a role for BNP in embryonic stem cell maintenance has recently been reported. Abdelalim and Tooyama (2009) discovered that endogenous BNP signaling is essential for the proliferation of murine embryonic stem cells, whereas BNP knockdown increased apoptosis rates. An intriguing question to investigate would be whether BNP promotes the proliferation and survival of the stem cell subpopulation in prostate cancer cell lines.

Finally, type 1 collagen, abundantly secreted by osteoblasts [Mackie 2003], has been implicated in the maintenance of CSCs. It is highly expressed along the invasive front of colorectal cancer and has been reported to promote the expression of a stem cell phenotype in human colorectal carcinoma cells [Kirkland *et al.* 2009]. Although *COL1A1* and *COL1A2* mRNA levels sank in hfOB after crosstalk with prostate cancer cells, type 1 collagen would remain a significant component of the osteoblast niche, since the initial levels of expression were very high. Furthermore, in the model presented in Fig. 31, decreased expression of collagens and other ECM proteins by osteoblasts differentiating to preosteocytes is accompanied by increased differentiation of osteoprogenitors, which would be a rich collagen source.

In sum, the presented *in vitro* data together with published reports suggest possible mechanisms through which osteoblasts might support the survival and growth of prostate CSCs in bone. These mechanisms include secretion of TGF $\beta$ 1 and stimulation of canonical TGF $\beta$  signaling in prostate cancer cells, secretion of FGF2, BNP and of type 1 collagen.

To conclude, the changes induced in osteoblasts by crosstalk with prostate cancer cells indicate possible mechanisms by which osteoblasts might enhance the invasive, osteomimetic and stem cell-like properties of tumor cells, as well as contribute to the abnormal bone formation

seen in metastatic lesions. Moreover, some of the crosstalk-induced changes in osteoblasts might be a reflection of the generalized impairment of immunity which is often a feature of advanced cancer. Although all the hypotheses presented in the above section on the basis of array data from an *in vitro* setting must be considered tentative, they match data published by other groups, outlining potentially interesting directions for further study.

## **5. Conclusions**

- Transcriptional alterations caused by cell crosstalk *via* soluble factors are a very early event in cancer metastasis to bone.
- Prostate cancer cells exposed to the osteoblast secretome show evidence of osteomimicry, concomitant with intensified IL6 and TGF $\beta$  signaling.
- Osteoblasts exposed to the secretome of prostate cancer cells exhibit gene expression alterations suggestive of repressed proliferation, decreased matrix synthesis and inhibited immune response, which together indicate enhanced preosteocytic differentiation.
- The changes induced in osteoblasts by crosstalk with prostate cancer cells suggest possible mechanisms by which osteoblasts might enhance the invasive, osteomimetic and stem cell-like properties of tumor cells, as well as contribute to the abnormal bone formation seen in metastatic lesions and to the generalized impairment of immunity which is often a feature of advanced cancer.
- At the early stages of prostate cancer bone metastasis, TGF $\beta$  signaling appears to become differently modulated in osteoblasts and in cancer cells as a result of their crosstalk, with accompanying changes in gene transcription.



## References

- Abdelalim EM, Tooyama I. (2009) *BNP signaling is crucial for embryonic stem cell proliferation*. PLoS ONE. 4: e5341.
- Afrakhte M, Moren A, Jossan S, Itoh S, Sampath K, Westermarck B, Heldin CH, Heldin NE, ten Dijke P. (1998) *Induction of inhibitory Smad6 and Smad7 mRNA by TGF-beta family members*. Biochem Biophys Res Commun. 249: 505-511.
- Alliston T, Choy L, Ducy P, Karsenty G, Derynck R. (2001) *TGF-beta-induced repression of CBFA1 by Smad3 decreases cbfa1 and osteocalcin expression and inhibits osteoblast differentiation*. EMBO J. 20: 2254-2272.
- Almeida M, Han L, Bellido T, Manolagas SC, Kousteni S. (2005) *Wnt proteins prevent apoptosis of both uncommitted osteoblast progenitors and differentiated osteoblasts by beta-catenin-dependent and -independent signaling cascades involving Src/ERK and phosphatidylinositol 3-Kinase/AKT*. J Biol Chem. 50: 41342-41351.
- Arya M, Bott SR, Shergill IS, Ahmed HU, Williamson M, Patel HR. (2006) *The metastatic cascade in prostate cancer*. Surg Oncol. 15: 117-128.
- Bacac M, Stamenkovic I. (2008) *Metastatic cancer cell*. Annu Rev Pathol Mech Dis. 3: 221-47.
- Bakin AV, Safina A, Rinehart C, Daroqui C, Darbary J, Helfman DM. (2004) *A critical role of tropomyosins in TGF-beta regulation of the actin cytoskeleton and cell motility in epithelial cells*. Mol Biol Cell. 15: 4682-4694.
- Bellido T, Borba VZ, Roberson P, Manolagas SC. (1997) *Activation of the Janus kinase/STAT (signal transducer and activator of transcription) signal transduction pathway by interleukin-6-type cytokines promotes osteoblast differentiation*. Endocrinology. 138: 3666-3676.
- Billiard J, Moran RA, Whitley MZ, Chatterjee-Kishore M, Gillis K, Brown EL, Komm BS, Bodine PVN. (2003) *Transcriptional profiling of human osteoblast differentiation*. J Cell Biochem. 89: 389-400.
- Blair JM, Zhou H, Seibel MJ, Dunstan CR (2006) *Mechanisms of disease: roles of OPG, RANKL and RANK in the pathophysiology of skeletal metastasis*. Nat Clin Pract Oncol. 3: 41-49.
- Blaszczak N, Masri BA, Mawji NR, Ueda T et al. (2004) *Osteoblast-derived factors induce androgen-dependent proliferation and expression of prostate-specific antigen in human prostate cancer cells*. Clin Cancer Res. 10: 1860-1869.
- Blum R, Gupta R, Burger PE, Ontiveros CS, Salm SN, Xiong X, Kamb A, Wesche H, Marshall L, Cutler G, Wang X, Zavadil J, Moscatelli D, Wilson EL. (2009) *Molecular signatures of prostate stem cells reveal novel signaling pathways and provide insights into prostate cancer*. PLoS One. 4: e5722.
- Bogdanos J, Karamanolakis D, Tenta R, Tsintavis A, Milathianakis C, Mitsiades C, Koutsilieris M. (2003) *Endocrine/paracrine/autocrine survival factor activity of bone microenvironment participates in the development of androgen ablation and chemotherapy refractoriness of prostate cancer metastasis in the skeleton*. Endocr Relat Cancer. 10: 279-289.
- Bontemps Y, Vuillermoz B, Antonicelli F, Perreau C, Danan JL, Maquart FX, Wegrowski Y. (2003) *Specific protein-1 is a universal regulator of UDP-glucose dehydrogenase expression: its positive involvement in transforming growth factor-beta signaling and inhibition in hypoxia*. J Biol Chem. 278: 21566-21575.
- Borton AJ, Frederick JP, Datto MB, Wang XF, Weinstein RS. (2001) *The loss of Smad3 results in a lower rate of bone formation and osteopenia through dysregulation of osteoblast differentiation and apoptosis*. J Bone Miner Res. 16: 1754-1764.
- Boyce BF, Xing L. (2007) *Biology of RANK, RANKL, and osteoprotegerin*. Arthritis Res Ther. 9 Suppl 1: S1.
- Brown JM, Corey E, Lee ZD, True LD, Yun TJ, Tondravi M, Vessella RL (2001) *Osteoprotegerin and RANK ligand expression in prostate cancer*. Urology 57: 611-616.
- Brown KA, Pietenpol JA, Moses HL. (2007) *A tale of two proteins: differential roles and regulation of Smad2 and Smad3 in TGF-beta signaling*. J Cell Biochem. 101: 9-33.
- Bu G, Lu W, Liu CC, Selander K, Yoneda T, Hall C, Keller ET, Li Y. (2008) *Breast cancer-derived Dickkopf1 inhibits osteoblast differentiation and osteoprotegerin expression: implication for breast cancer osteolytic bone metastases*. Int J Cancer. 123(5): 1034-1042.
- Buijs JT, van der Pluijm G. (2009) *Osteotropic cancers: from primary tumor to bone*. Cancer Lett. 273: 177-193.
- Byers BA, Garcia AJ. (2004) *Exogenous Runx2 expression enhances in vitro osteoblastic differentiation and mineralization in primary bone marrow stromal cells*. Tissue Eng. 10(11-12):1623-1632.
- Canalis E, Economides AN, Gazzerro E. (2003) *Bone morphogenetic proteins, their antagonists, and the skeleton*. Endocr Rev. 24: 218-235.
- Cavarretta IT, Neuwirt H, Untergasser G, Moser PL, Zaki MH, Steiner H, Rumpold H, Fuchs D, Hobisch A, Nemeth JA, Culig Z. (2006) *The antiapoptotic effect of IL-6 autocrine loop in a cellular model of advanced prostate cancer is mediated by Mcl-1*. Oncogene: 1-11.
- Chambers AF, Groom AC, MacDonald IC. (2002) *Dissemination and growth of cancer cells in metastatic sites*. Nat Rev Cancer. 2: 563-572.
- Chen G, Sircar K, Aprikian A, Potti A, Goltzman D, Rabbani SA (2006) *Expression of RANKL/RANK/OPG in primary and metastatic human prostate cancer as markers of disease stage and functional regulation*. Cancer. 107: 289-298.
- Chirgwin JM, Mohammad KS, Guise TA. (2004) *Tumor-bone cellular interactions in skeletal metastases*. J Musculoskelet Neuronal Interact. 4: 308-318.
- Chomczynski P, Sacchi N. (1987) *Single-step method of RNA isolation by acid guanidium thiocyanate-phenol-chloroform extraction*. Anal Biochem. 162: 156-159.
- Choueiri MB, Tu SM, Yu-Lee LY, Lin SH (2006) *The central role of osteoblasts in the metastasis of prostate cancer*. Cancer Metastasis Rev. 25: 601-609.
- Chung TD, Yu JJ, Spiotto MT, Bartkowski M, Simons JW (1999) *Characterization of the role of IL-6 in the progression of prostate cancer*. Prostate. 38(3): 199-207.
- Chusho H, Ogawa Y, Tamura N, Suda M, Yasoda A, Miyazawa T, Kishimoto I, Komatsu Y, Itoh H, Tanaka K, Saito Y, Garbers DL, Nakao K. (2000) *Genetic models reveal that brain natriuretic peptide can signal through different tissue-specific receptor-mediated pathways*. Endocrinology. 141: 3807-3813.

- Clarke MF, Dick JE, Dirks PB, Eaves CJ, Jamieson CH, Jones DL, Visvader J, Weissman IL, Wahl GM. (2006) *Cancer stem cells - perspectives on current status and future directions: AACR workshop on cancer stem cells*. *Cancer Res.* 66: 9339-9344.
- Clines GA, Mohammad KS, Bao Y, Stephens OW, Suva LJ, Shaughnessy JD Jr, Foz JW, Chirgwin JM, Guise TA. (2007) *Dickkopf homolog 1 mediates endothelin-1-stimulated new bone formation*. *Mol Endocrinol.* 21: 486-498.
- Cocciadiferro L, Miceli V, Kang KS, Polito LM, Trosko JE, Carruba G. (2009) *Profiling cancer stem cells in androgen-responsive and refractory human prostate tumor cell lines*. *Ann N Y Acad Sci.* 1155: 257-262.
- Collins AT, Berry PA, Hyde C, Stower MJ, Maitland NJ. (2005) *Prospective identification of tumorigenic prostate cancer stem cells*. *Cancer Res.* 65: 10946-10951.
- Cooper CR, Chay CH, Gendernalik JD, Lee HL, Bhatia J, Taichman RS, McCauley LK, Keller ET, Pienta KJ. (2003) *Stromal factors involved in prostate carcinoma metastasis to bone*. *Cancer.* 97: 739-747.
- Corey E, Brown LG, Kiefer JA, Quinn JE, Pitts TE, Blair JM, Vessella RL. (2005) *Osteoprotegerin in prostate cancer bone metastasis*. *Cancer Res.* 65: 1710-1718.
- Cornish J, Naot D, Reid IR. (2003) *Adrenomedullin - a regulator of bone formation*. *Regul Pept.* 112: 79-86.
- Croci DO, Zacarias Fluck MF, Rico MJ, Matar P, Rabinovich GA, Scharovsky OG. *Dynamic cross-talk between tumor and immune cells in orchestrating the immunosuppressive network at the tumor microenvironment*. *Cancer Immunol Immunother.* 56: 1687-1700.
- Culig Z, Bartsch G, Hobisch A. (2002) *Interleukin-6 regulates androgen receptor activity and prostate cancer cell growth*. *Mol Cell Endocrinol.* 197: 231-238.
- Culig Z, Steiner H, Bartsch G, Hobisch A. (2005) *Interleukin-6 regulation of prostate cancer cell growth*. *J Cell Biochem.* 95(3): 497-505.
- Dai J, Hall CL, Escara-Wilke J, Mizokami A, Keller JM, Keller ET. (2008) *Prostate cancer induces bone metastasis through Wnt-induced bone morphogenetic protein-dependent and independent mechanisms*. *Cancer Res.* 68: 5785-5794.
- Datta HK, Ng WF, Walker JA, Tuck SP, Varanasi SS. (2008) *The cell biology of bone metabolism*. *J Clin Pathol.* 61: 577-587.
- De Wever O, Westbroek W, Verloes A, Bloemen N, Bracke M, Gespach C, Bruyneel E, Mareel M. (2004) *Critical role of N-cadherin in myfibroblast invasion and migration in vitro stimulated by colon cancer cell-derived TGF-beta or wounding*. *J Cell Sci.* 117: 4691-4703.
- Derynck R, Zhang YE. (2003) *Smad-dependent and Smad-independent pathways in TGF-beta family signalling*. *Nature.* 425: 577-584.
- Devlin HL, Mudryj M. (2009) *Progression of prostate cancer: Multiple pathways to androgen independence*. *Cancer Lett.* 274: 177-186.
- Dong Z, Saliganan AD, Meng H, Nabha SM, Sabbota AL, Sheng S, Bonfil RD, Cher ML. (2008) *Prostate cancer cell-derived urokinase-type plasminogen activator contributes to intraosseous tumor growth and bone turnover*. *Neoplasia.* 10: 439-449.
- Dorai T, Dutcher JP, Dempster DW, Wiernik PH. (2004) *Therapeutic potential of curcumin in prostate cancer--V: Interference with the osteomimetic properties of hormone refractory C4-2B prostate cancer cells*. *Prostate.* 60: 1-17.
- Drachenberg DE, Elgamal AA, Rowbotham R, Peterson M, Murphy GP (1999) *Circulating levels of interleukin-6 in patients with hormone refractory prostate cancer*. *Prostate.* 41: 127-133.
- Ducy P (2000) *Cbfa1: A molecular switch in osteoblast biology*. *Dev Dynamics.* 219: 461-471.
- Ducy P, Zhang R, Geoffroy V, Ridall AL, Karsenty G. (1997) *Osf2/Cbfa1: a transcriptional activator of osteoblast differentiation*. *Cell.* 89: 747-754.
- Dvorak P, Dvorakova D, Hampl A. (2006) *Fibroblast growth factor signaling in embryonic and cancer stem cells*. *FEBS Letters.* 580: 2869-2874.
- Edlund M, Sung SY, Chung LW. (2004) *Modulation of prostate cancer growth in bone microenvironments*. *J Cell Biochem.* 91: 686-705.
- Eisenberger S, Ackermann K, Voggenreiter G, Sueltmann H, Kasperk C, Pyerin W. (2008) *Metastases and multiple myeloma generate distinct transcriptional footprints in osteocytes in vivo*. *J Pathol.* 214: 617-626.
- Eliseev RA, Schwarz EM, Zuscik MJ, O'Keefe RJ, Drissi H, Rosier RN. (2006) *Smad7 mediates inhibition of Saos2 osteosarcoma cell differentiation by NF-kappaB*. *Exp Cell Res.* 312: 40-50.
- Emami KH, Corey E. (2007) *When prostate cancer meets bone: control by Wnts*. *Cancer Lett.* 253: 170-179.
- Erices A, Conget P, Rojas C, Minguell JJ. (2002) *gp130 activation by soluble interleukin-6 receptor/interleukin-6 enhances osteoblastic differentiation of human bone marrow-derived mesenchymal stem cells*. *Exp Cell Res.* 280: 24-32.
- Fakhry A, Ratisoontorn C, Vedchalam C, Salhab I, Koyama E, Leboy P, Pacifici M, Kirschner RE, Nah HD. (2005) *Effects of FGF-2/9 in calvarial bone cell cultures: differentiation stage-dependent mitogenic effect, inverse regulation of BMP-2 and noggin, and enhancement of osteogenic potential*. *Bone.* 36: 254-266.
- Farhadi J, Jaquiere C, Barbero A, Jakob M, Schaeren S, Pierer G, Heberer M, Martin I. (2005) *Differentiation-dependent upregulation of BMP-2, TGF-beta1, and VEGF expression by FGF2 in human bone marrow stromal cells*. *Plast Reconstr Surg.* 116: 1379-1386.
- Feeley BT, Gamradt SC, Hsu WK, Liu N, Krenk L, Robbins P, Huard J, Lieberman JR (2005) *Influence of BMPs on the formation of osteoblastic lesions in metastatic prostate cancer*. *J Bone Miner Res.* 20: 2189-2199.
- Festuccia C, Angelucci A, Gravina GL, Villanova I, Teti A, Albini A, Bologna M. (2000) *Osteoblast-derived TGF-beta1 modulates matrix degrading protease expression and activity in prostate cancer cells*. *Int J Cancer.* 85(3): 407-415.
- Festuccia C, Bologna M, Gravina GL, Guerra F, Angelucci A, Villanova I, Millimaggi D, Teti A. (1999) *Osteoblast conditioned media contain TGF-beta1 and modulate the migration of prostate tumor cells and their interactions with extracellular matrix components*. *Int J Cancer.* 81(3): 395-403.
- Fidler I. (2003) *The pathogenesis of cancer metastasis: the 'seed and soil' hypothesis revisited*. *Nat Rev Cancer.* 3: 1-6.

- Filvaroff E, Erlenbacher A, Ye J, Gitelman SE, Lotz J, Heillman M, Derynck R. (1999) *Inhibition of TGF-beta receptor signaling in osteoblasts leads to decreased bone remodeling and increased trabecular bone mass*. Development. 126: 4267-4279.
- Fisher JL, Schmitt JF, Howard ML, Mackie PS, Choong PF, Risbridger GP. (2002) *An in vivo model of prostate carcinoma growth and invasion in bone*. Cell Tissue Res. 307: 337-345.
- Fizazi K, Yang J, Peleg S, Sikes CR, Kreimann EL, Daliani D, Olive M, Raymond KA, Janus TJ, Logothetis CJ, Karsenty G, Navone NM. (2003) *Prostate cancer cells-osteoblast interaction shifts expression of growth/survival-related genes in prostate cancer and reduces expression of osteoprotegerin in osteoblasts*. Clin Cancer Res. 9(7): 2587-2597.
- Franceschi RT, Xiao G. (2003) *Regulation of the osteoblast-specific transcription factor, Runx2: responsiveness to multiple signal transduction pathways*. J Cell Biochem. 88(3): 446-454.
- Franchimont N, Rydziel S, Canalis E. (2000) *Transforming growth factor-beta increases interleukin-6 transcripts in osteoblasts*. Bone. 26: 249-253.
- Franz-Ondendaal TA, Hall BK, Witten PE. (2006) *Buried alive: How osteoblasts become osteocytes*. Dev Dyn. 235: 176-190.
- Fu Z, Dozmorov IM, Keller ET. (2002) *Osteoblasts produce soluble factors that induce a gene expression pattern in non-metastatic prostate cancer cells, similar to that found in bone metastatic prostate cancer cells*. Prostate. 51: 10-20.
- Fujita K, Janz S. (2007) *Attenuation of WNT signaling by DKK-1 and -2 regulates BMP2-induced osteoblast differentiation and expression of OPG, RANKL and M-CSF*. Mol Cancer. 6:71.
- Funaba M, Ogawa K, Murata T, Fujimura H, Murata E, Abe M, Takahashi M, Torii K. (1996) *Follistatin and activin in bone: expression and localization during endochondral bone development*. Endocrinology. 137: 4250-4259.
- Garcia-Moreno C, Mendez-Davila C, de la Piedra C, Castro-Errecaborde NA, Traba ML. (2002) *Human prostatic carcinoma cells produce an increase in the synthesis of interleukin-6 by human osteoblasts*. Prostate. 50: 241-246.
- Gaur T, Lengner CJ, Hovhannisyanyan H, Bhat RA, Bodine PVN, Komm BS, Javed A, van Wijnen AJ, Stein JL, Stein GS, Lian JB. (2005) *Canonical WNT signaling promotes osteogenesis by directly stimulating Runx2 gene expression*. J Biol Chem. 280: 33132-33140.
- Getsios S, Chen GT, Huang DT, MacCalman CD. (1998) *Regulated expression of cadherin-11 in human extravillous cytotrophoblasts undergoing aggregation and fusion in response to transforming growth factor beta-1*. J Reprod Fertil. 114: 357-363.
- Gey GO, Coffman WD, Kubicek MT. (1952) *Tissue culture studies of the proliferative capacity of cervical carcinoma and normal epithelium*. Cancer Res. 12: 264-265.
- Giles RH, van Es JH, Clevers H. (2003) *Caught up in a Wnt storm: Wnt signaling in cancer*. Biochim Biophys Acta. 1653: 1-24.
- Giri D, Ozen M, Ittmann M. (2001) *Interleukin-6 is an autocrine growth factor in human prostate cancer*. Am J Pathol. 159: 2159-2165.
- Glass DA, Bialek P, Ahn JD, Patel MS, Clevers H, Taketo MM, Long F, McMahon AP, Lan RA, Karsenty G. (2005) *Canonical Wnt signaling in differentiated osteoblasts controls osteoclast differentiation*. Dev Cell. 8: 751-764.
- Goellner H, Dani C, Phillips B, Philipsen S, Suske G. (2001) *Impaired ossification in mice lacking the transcription factor Sp3*. Mech Dev. 106: 77-83.
- Guillen C, de Gortazar AR, Esbrit P. (2004) *The interleukin-6/soluble interleukin-6 receptor system induces parathyroid hormone-related protein in human osteoblastic cells*. Calcif Tissue Int. 75: 153-159.
- Guise TA. (2000) *Molecular mechanisms of osteolytic bone metastases*. Cancer. 88: 2892-2898.
- Guise TA, Mohammad KS, Clines G, Stebbins EG, Wong DH, Higgins LS, Vessella R, Corey E, Padalecki S, Suva L, Chirgwin JM. (2006) *Basic mechanisms responsible for osteolytic and osteoblastic bone metastases*. Clin Cancer Res. 12: 6213-6216.
- Guo Y, Kyprianou N (1999) *Restoration of transforming growth factor beta signaling pathway in human prostate cancer cells suppresses tumorigenicity via induction of caspase-1-mediated apoptosis*. Cancer Res. 59: 1366-1371.
- Hadjidakis DJ, Androulakis II. (2006) *Bone remodeling*. Ann NY Acad Sci. 1092: 385-396.
- Hall CL, Bafico A, Dai J, Aaronson SA, Keller ET. (2005) *Prostate cancer cells promote osteoblastic bone metastases through Wnts*. Cancer Res. 65: 7554-7560.
- Hall CL, Daignault SD, Shah RB, Pienta KJ, Keller ET. (2008) *Dickkopf-1 expression increases early in prostate cancer development and decreases during progression from primary tumor to metastasis*. Prostate. 68: 1396-1404.
- Hall CL, Kang S, MacDougald OA, Keller ET. (2006) *Role of Wnts in prostate cancer bone metastases*. J Cell Biochem. 97: 661-672.
- Hall CL, Keller ET. (2006) *The role of Wnts in bone metastases*. Cancer Metastasis Rev. 25: 551-558.
- Harris SA, Enger RJ, Riggs BL, Spelsberg TC. (1995) *Development and characterization of a conditionally immortalized human fetal osteoblastic cell line*. J Bone Miner Res. 10(2): 178-186.
- Hashimoto M, Shoda A, Inoue S, Yamada R, Kondo T, Sakurai T, Ueno N, Muramatsu M. (1992) *Functional regulation of osteoblastic cells by the interaction of activin-A with follistatin*. J Biol Chem. 267: 4999-5004.
- Heinrich PC, Behrmann I, Haan S, Hermanns HM, Uller-Newen GM, Schaper F. (2003) *Principles of interleukin (IL)-6-type cytokine signalling and its regulation*. Biochem J. 374: 1-20.
- Hobisch A, Ramoner R, Fuchs D, Godoy-Tundidor S, Bartsch G, Klocker H, Culig Z. (2001) *Prostate cancer cells (LNCaP) generated after long-term interleukin 6 (IL-6) treatment express IL-6 and acquire an IL-6 partially resistant phenotype*. Clin Cancer Res. 7: 2941-2948.
- Hocevar BA, Prunier C, Howe PH. (2005) *Disabled-2 (Dab2) mediates transforming growth factor beta (TGFbeta)-stimulated fibronectin synthesis through TGFbeta-activated kinase 1 and activation of the JNK pathway*. J Biol Chem. 280: 25920-25927.
- Hocevar BA, Smine A, Xu XX, Howe PH. (2001) *The adaptor molecule Disabled-2 links the transforming growth factor beta receptors to the Smad pathway*. EMBO J. 20: 2789-2801.

- Hofbauer LC, Dunstan CR, Spelsberg TC, Riggs BL, Khosla S. (1998) *Osteoprotegerin production by human osteoblast lineage cells is stimulated by vitamin D, bone morphogenetic protein-2, and cytokines*. *Biochem Biophys Res Commun*. 250: 776-781.
- Hofbauer LC, Heufelder AE. (2001) *Role of receptor activator of nuclear factor-kappaB ligand and osteoprotegerin in bone cell biology*. *J Mol Med*. 79: 243-253.
- Hofbauer LC, Neubauer A, Heufelder AE. (2001) *Receptor activator of nuclear factor-kappaB ligand and osteoprotegerin: potential implications for the pathogenesis and treatment of malignant bone diseases*. *Cancer*. 92: 460-470.
- Holen I, Cross SS, Neville-Webber HL, Cross NA, Balasubramanian SP, Croucher PI, Evans CA, Lippitt JM, Coleman RE, Eaton CL. (2005) *Osteoprotegerin (OPG) expression by breast cancer cells in vitro and breast tumours in vivo - a role in tumour cell survival?* *Breast Cancer Res Treat*. 92: 207-215.
- Holen I, Croucher PI, Hamdy FC, Eaton CL. (2002) *Osteoprotegerin (OPG) is a survival factor for human prostate cancer cells*. *Cancer Res*. 62(6):1619-1623.
- Holen I, Shipman CM. (2006) *Role of osteoprotegerin (OPG) in cancer*. *Clin Sci*. 110: 279-291.
- Holmes A, Abraham DJ, Sa S, Shiwen X, Black CM, Leask A. (2001) *CTGF and SMADs, maintenance of scleroderma phenotype is independent of SMAD signaling*. *J Biol Chem*. 276: 10594-10601.
- Horoszewicz JS, Leong SS, Kawinski E, Karr JP, Rosenthal H, Ming Chu T, Mirand EA, Murphy GP (1983) *LNCaP model of human prostatic carcinoma*. *Cancer Res*. 43: 1809-1818.
- Hosokawa K, Arai F, Yoshihara H, Nakamura Y, Gomei Y, Iwasaki H, Miyamoto K, Shima H, Ito K, Suda T. (2007) *Function of oxidative stress in the regulation of hematopoietic stem cell-niche interaction*. *Biochem Biophys Res Commun*. 363: 578-583.
- Huang WC, Wu D, Xie Z, Zhau HE, Nomura T, Zayzafoon M, Pohl J, Hsieh CL, Weitzmann MN, Farach-Carson MC, Chung LW (2006)  *$\beta$ 2-Microglobulin is a signaling and growth-promoting factor for human prostate cancer bone metastasis*. *Cancer Res*. 66: 9108-9116.
- Huang WC, Xie Z, Konaka H, Sodek J, Zhau HE, Chung LW. (2005) *Human osteocalcin and bone sialoprotein mediating osteomimicry of prostate cancer cells: role of cAMP-dependent protein kinase A signaling pathway*. *Cancer Res*. 65(6): 2303-2313.
- Inoue A, Hiruma Y, Hirose S, Yamaguchi A, Furuya M, Tanaka S, Hagiwara H. (1996) *Stimulation by C-type natriuretic peptide of the differentiation of clonal osteoblastic MC3T3-E1 cells*. *Biochem Biophys Res Commun*. 221: 703-707.
- Jacob K, Webber M, Benayahu D, Kleinman HK (1999) *Osteonectin promotes prostate cancer cell migration and invasion: a possible mechanism for metastasis to bone*. *Cancer Res*. 59: 4453-4457.
- James D, Levine AJ, Besser D, Hemmati-Brianlou A. (2005) *TGFbeta/activin/nodal signaling is necessary for the maintenance of pluripotency in human embryonic stem cells*. *Development*. 132: 1273-1282.
- Janssens K, ten Dijke P, Janssens S, Van Hul W (2005) *Transforming growth factor- $\beta$ 1 to the bone*. *Endocr Rev*. 26(6): 743-774.
- Jemal A, Siegel R, Ward E, Hao Y, Xu J, Murray T, Thun MJ. (2008) *Cancer statistics, 2008*. *CA Cancer J Clin*. 58: 71-96.
- Jinnin M, Ihn H, Asano Y, Yamane K, Trojanowska M, Tamaki K. (2004) *Tenascin-C upregulation by transforming growth factor-beta in human dermal fibroblasts involves Smad3, Sp1, and Ets1*. *Oncogene*. 23: 1656-1667.
- Juarez J, Bendall L. (2004) *SDF-1 and CXCR4 in normal and malignant hematopoiesis*. *Histol Histopathol*. 19: 299-309.
- Jung K, Lenn M, Stephan C, Von Hosslin K, Semjonow A, Sinha P, Loening SA. (2004) *Comparison of 10 serum bone turnover markers in prostate carcinoma patients with bone metastatic spread: diagnostic and prognostic implications*. *Int J Cancer*. 111: 783-791.
- Kaighn ME, Narayan KS, Ohnuki Y, Lechner JF, Jones LW. (1979) *Establishment and characterization of a human prostatic carcinoma cell line (PC-3)*. *Invest Urol*. 17(1): 16-23.
- Kajiyama H, Shibata K, Terauchi M, Ino K, Nawa A, Kikkawa F. (2008) *Involvement of SDF1 alpha/CXCR4 axis in the enhanced peritoneal metastasis of epithelial ovarian carcinoma*. *Int J Cancer*. 122: 91-99.
- Kamimura D, Ishihara K, Hirano T. (2003). *IL-6 signal transduction and its physiological roles: the signal orchestration model*. *Rev Physiol Biochem Pharmacol*. 149: 1-38.
- Kanaan RA, Kanaan LA (2006) *Transforming growth factor  $\beta$ 1, bone connection*. *Med Sci Monit*. 12(8): 164-169.
- Kapoun AM, Liang F, O'Young G, Damm DL, Quon D, White RT, Munson K, Lam A, Schreiner GF, Protter AA. (2004) *B-Type natriuretic peptide exerts broad functional opposition to transforming growth factor-beta in primary human cardiac fibroblasts: fibrosis, myofibroblast conversion, proliferation, and inflammation*. *Circ Res*. 94: 453-461.
- Karsenty G, Wagner EF. (2002) *Reaching a genetic and molecular understanding of skeletal development*. *Dev Cell*. 2: 389-406.
- Kasper S. (2008) *Stem cells: The root of prostate cancer?* *J Cell Physiol*. 216: 332-336.
- Keller ET, Brown J (2004) *Prostate cancer bone metastases promote both osteolytic and osteoblastic activity*. *J Cell Biochem*. 91: 718-729.
- Keller ET, Zhang J, Cooper CR, Smith PC, McCauley LK, Pienta KJ, Taichman RS. (2001) *Prostate carcinoma skeletal metastases: Cross-talk between tumor and bone*. *Cancer Metastasis Rev*. 20: 333-349.
- Kelly K, Yin JJ. (2008) *Prostate cancer and metastasis initiating stem cells*. *Cell Res*. 18: 528-537.
- Khodavirdi AC, Song Z, Yang S, Zhong C, Wang S, Wu H, Pritchard C, Nelson PS, Roy-Burman P. (2006) *Increased expression of osteopontin contributes to the progression of prostate cancer*. *Cancer Res*. 66: 883-888.
- Kido J, Yamauchi N, Ohishi K, Kataoka M, Nishikawa S, Nakamura T, Kadono H, Ikedo D, Ueno A, Nonomura N, Okuyama A, Nagata T. (2007) *Inhibition of osteoblastic cell differentiation by conditioned medium derived from the human prostatic cancer cell line PC-3 in vitro*. *J Cell Biochem*. 67: 248-256.
- Kiefer JA, Farach-Carson MC (2001) *Type I collagen-mediated proliferation of PC3 prostate carcinoma cell line: implications for enhanced growth in the bone microenvironment*. *Matrix Biol*. 20: 429-437.

- Kim IY, Ahn HJ, Zelner DJ, Shaw JW, Sensibar JA, Kim JH, Kato M, Lee C. (1996) *Genetic change in transforming growth factor beta (TGF-beta) receptor type I gene correlates with insensitivity to TGF-beta1 in human prostate cancer cells.* Cancer Res. 56: 44-48.
- Kim IY, Zelner DJ, Sensibar JA, Ahn HJ, Park L, Kim JH, Lee C. (1996) *Modulation of sensitivity to transforming growth factor-beta1 (TGF-beta1) and the level of type II TGF-beta receptor in LNCaP cells by dihydrotestosterone.* Exp Cell Res. 222: 103-110.
- Kinder M, Chislock E, Bussard KM, Shuman L, Mastro AM. (2007) *Metastatic breast cancer induces an osteoblast inflammatory response.* Exp Cell Res. 314: 173-183.
- Kingsley LA, Fournier PG, Chirgwin JM, Guise TA. (2007) *Molecular biology of bone metastasis.* Mol Cancer Ther. 6: 2609-2617.
- Kirkland SC. (2009) *Type I collagen inhibits differentiation and promotes a stem cell-like phenotype in human colorectal carcinoma cells.* Br J Cancer. Jun 30 [Epub ahead of print].
- Klarmann GJ, Hurt EM, Mathews LA, Zhang X, Duhagon MA, Mistree T, Thomas SB, Farrar WL. (2009) *Invasive prostate cancer cells are tumor initiating cells that have a stem cell-like genomic signature.* Clin Exp Metastasis. 26: 433-446.
- Knerr K, Ackermann K, Neidhart T, Pyerin W. (2004) *Bone metastasis: Osteoblasts affect growth and adhesion regulons in prostate tumor cells and provoke osteomimicry.* Int J Cancer. 111(1): 152-159.
- Kobayashi T, Kronenberg H. (2005) *Minireview: Transcriptional regulation in development of bone.* Endocrinology. 146: 1012-1017.
- Koeneman KS, Yeung F, Chung LW. (1999) *Osteomimetic properties of prostate cancer cells: a hypothesis supporting the predilection of prostate cancer metastasis and growth in the bone environment.* Prostate. 39(4): 246-261.
- Konstantinova IM, Tsimokha AS, Mittenberg AG. (2008) *Role of proteasomes in cellular regulation.* Int Rev Cell Mol Biol. 267: 59-124.
- Kowanetz M, Loenn P, Vanlandewijck M, Kowanetz K, Heldin Ch, Moustakas A. (2008) *TGFbeta induces SIK to negatively regulate type I receptor kinase signaling.* J Cell Biol. 182: 655-62.
- Kozawa O, Suzuki A, Uematsu T. (1997) *Basic fibroblast growth factor induces interleukin-6 synthesis in osteoblasts: autoregulation by protein kinase C.* Cell Signal. 9: 463-468.
- Kozlow W, Guise TA. (2005) *Breast cancer metastasis to bone: mechanisms of osteolysis and implications for therapy.* J Mammary Gland Biol Neoplasia. 10: 169-180.
- Krishnan V, Bryant HU, MacDougal OA. (2006) *Regulation of bone mass by Wnt signaling.* J Clin Invest. 116: 1202-1209.
- Kwabi-Addo B, Ozen M, Ittmann M. (2004) *The role of fibroblast growth factors and their receptors in prostate cancer.* Endocr Rel Cancer. 11: 709-724.
- Laemmli UK. (1970) *Cleavage of structural proteins during the assembly of the head of bacteriophage T4.* Nature. 227(5259): 680-685.
- Lai TH, Fong YC, Fu WM, Yang RS, Tang CH. (2008) *Osteoblast-derived BMP-2 enhances the motility of prostate cancer cells via activation of integrins.* Prostate. 68: 1341-1353.
- Lang SH, Frame FM, Collins AT. (2009) *Prostate cancer stem cells.* J Pathol. 217: 299-306.
- Lang SH, Miller WR, Habib FK. (1995) *Stimulation of human prostate cancer cell lines by factors present in human osteoblast-like cells but not in bone marrow.* Prostate. 7(5): 287-293.
- Le Bitoux MA, Stamenkovic I. (2008) *Tumor-host interactions: the role of inflammation.* Histochem Cell Biol. 130: 1079-1090.
- Lee SO, Chun JY, Nadiminty N, Lou W, Gao AC (2007) *Interleukin-6 undergoes transition from growth inhibitor associated with neuroendocrine differentiation to stimulator accompanied by androgen receptor activation during LNCaP prostate cancer cell progression.* Prostate. 67: 764-773.
- Li H, Chen X, Calhoun-Davis T, Claypool K, Tang DG. (2008) *PC3 human prostate carcinoma cell holoclones contain self-renewing tumor-initiating cells.* Cancer Res. 68: 1820-1825.
- Li L, Neaves WB. (2006) *Normal stem cells and cancer stem cells: the niche matters.* Cancer Res. 66: 4553-4557.
- Li Y, Backesjo CM, Haldosen LA, Lindgren U. (2008) *IL-6 receptor expression and IL-6 effects change during osteoblast differentiation.* Cytokine. 43: 165-173.
- Lian JB, Stein GS, Javed A, van Wijnen AJ, Stein JL, Montecino M, Hassan MQ, Gaur T, Lengner CJ, Yound DW. (2006) *Networks and hubs for the transcriptional control of osteoblastogenesis.* Rev Endocr Metab Disord. 7: 1-16.
- Lian JB, Stein GS. (1995) *Development of the osteoblast phenotype: molecular mechanisms mediating osteoblast growth and differentiation.* Iowa Orthop J. 15: 118-140.
- Lin DL, Tarnowski CP, Zhang J, Dai J, Rohn E, Patel AH, Morris MD, Keller ET. (2001) *Bone metastatic LNCaP-derivative C4-2B prostate cancer cell line mineralizes in vitro.* Prostate. 473: 212-221.
- Lin X, Duan X, Liang YY, Su Y, Wrighton KH, Long J, Hu M, Davis CM, Wang J, Brunnicardi FC, Shi Y, Chen YG, Meng A, Feng XH. (2006) *PPM1A functions as a Smad phosphatase to terminate TGFbeta signaling.* Cell. 125: 915-928.
- Lindemann RK, Ballschmieter P, Nordheim A, Dittmer J. (2001) *Transforming growth factor-beta regulates parathyroid hormone-related protein expression in MDA-MB-231 breast cancer cells through a novel Smad/Ets synergism.* J Biol Chem. 276: 46661-46670.
- Liu W, Toyosawa S, Furuichi T, Kanatani N, Yoshida C, Liu Y, Himeno M, Narai S, Yamaguchi T, Komori J. (2001) *Overexpression of Cbfa1 in osteoblasts inhibits osteoblast maturation and causes osteopenia with multiple fractures.* J Cell Biol. 155: 157-166.
- Lobo NA, Shimono Y, Qian D, Clarke MF. (2007) *The biology of cancer stem cells.* Annu Rev Cell Dev Biol. 23: 675-699.
- Logothetis CJ, Lin SH. (2005) *Osteoblasts in prostate cancer metastasis to bone.* Nat Rev Cancer. 5(1): 21-28.
- Lorenzo J, Horowitz M, Choi Y. (2008) *Osteoimmunology: interactions of the bone and immune system.* Endocr Rev. 29: 403-440.

- Lou W, Zuyao N, Dyer K, Tweardy DJ, Gao AC. (2000) *Interleukin-6 induces prostate cancer cell growth accompanied by activation of Stat3 signaling pathway*. Prostate. 42: 239-242.
- Lowry OH, Rosebrough NJ, Farr AL, Randall RJ. (1951) *Protein measurement with the Folin phenol reagent*. J Biol Chem. 193: 265-275.
- Lu T, Burdelya LG, Swiatkowski SM, Boiko AD, Howe PH, Stark GR, Gudkov AV. (2004) *Secreted transforming growth factor beta-2 activates NF-kappaB, blocks apoptosis, and is essential for the survival of some tumor cells*. PNAS 101: 7112-7117.
- Lu Y, Zhang J, Dai J, Dehne LA, Mizokami A, Yao Z, Keller ET. (2004) *Osteoblasts induce prostate cancer proliferation and PSA expression through interleukin-6-mediated activation of the androgen receptor*. Clin Exp Metastasis. 21(5): 399-408.
- Mackie EJ. (2003) *Osteoblasts: novel roles in orchestration of skeletal architecture*. Int J Biochem Cell Biol. 35: 1301-1305.
- Manolagas SC. (2000) *Birth and death of bone cells: basic regulatory mechanisms and implications for the pathogenesis and treatment of osteoporosis*. Endocr Rev. 21: 115-137.
- Marie PJ. (2003) *Fibroblast growth factor signaling controlling osteoblast differentiation*. Gene 316: 23-32.
- Marie PJ. (2008) *Transcription factors controlling osteoblastogenesis*. Arch Biochem Biophys. 473: 98-105.
- Massard C, Deutsch E, Soria JC. (2006) *Tumour stem cell-targeted treatment: elimination or differentiation*. Ann Oncol. 17: 1620-1624.
- Mastro AM, Gay CV, Welch DR, Donahue HJ, Jewell J, Mercer R, DiGirolamo D, Chislock EM, Guttridge K. (2004) *Breast cancer cells induce osteoblast apoptosis: a possible contributor to bone degradation*. J Cell Biochem. 91: 265-276.
- Mercer RR, Miyasaka C, Mastro AM. (2004) *Metastatic breast cancer cells suppress osteoblast adhesion and differentiation*. Clin Exp Metastasis. 21: 427-435.
- Milat F, Ng KW. (2009) *Is Wnt signalling the final common pathway leading to bone formation?* Mol Cell Endocrinol. doi:10.1016/j.mce.2009.06.002 (article in press).
- Mori S, Murakami-Mori K, Bonavida B. (1999) *Interleukin-6 induces G1 arrest through induction of p27(Kip1), a cyclin-dependent kinase inhibitor, and neuron-like morphology in LNCaP prostate tumor cells*. Biochem Biophys Res Commun. 257(2): 609-614.
- Morinaga T, Nakagawa N, Yasuda H, Tsuda E, Higashio K. (1998) *Cloning and characterization of the gene encoding human osteoprotegerin/osteoclastogenesis-inhibitory factor*. Eur. J. Biochem. 254: 685-691.
- Moustakas A, Souchelnytskyi S, Heldin CH. (2001) *Smad regulation in TGF-beta signal transduction*. J Cell Sci. 114: 4359-4369.
- Mundy GR (2002) *Metastasis to bone: causes, consequences and therapeutic opportunities*. Nat Rev Cancer. 2: 584-593.
- Neiva K, Sun YX, Taichman RS. (2005) *The role of osteoblasts in regulating hematopoietic stem cell activity and tumor metastasis*. Braz J Med Biol Res. 38: 1449-1454.
- Nemeth JA, Harb JF, Barroso U, He Z, Grignon DJ, ML (1999) *Severe combined immunodeficient-hu model of human prostate cancer metastasis to human bone*. Cancer Res. 59: 1987-1993.
- Nichols WW, Murphy DG, Cristofalo VJ, Toji LH, Greene AE, Dwight SA. (1977) *Characterization of a new human diploid cell strain, IMR-90*. Science. 196: 60-63.
- Nilsson SK, Johnston HM, Whitty GA, Williams M, Webb RJ, Denhardt DT, Bertonecello I, Bendall LJ, Simmons PJ, Haylock DN. (2005) *Osteopontin, a key component of the hematopoietic stem cell niche and regulator of primitive hematopoietic progenitor cells*. Blood. 106: 1232-1239.
- Noble BS. (2008) *The osteocyte lineage*. Arch Biochem Biophys. 473: 106-11.
- Noda M, Yoon K, Prince CW, Butler WT, Rodan GA. (1988) *Transcriptional regulation of osteopontin production in rat osteosarcoma cells by type beta transforming growth factor*. J Biol Chem. 263: 13916-13921.
- Okamoto M, Lee C, Oyasu R. (1997) *Interleukin-6 as a paracrine and autocrine growth factor in human prostatic carcinoma cells in vitro*. Cancer Res. 57: 141-146.
- Okamoto M, Ono M, Uchiumi T, Ueno H, Kohno K, Sugimachi K, Kuwano M. (2002) *Up-regulation of thrombospondin-1 gene by epidermal growth factor and transforming growth factor beta in human cancer cells - transcriptional activation and messenger RNA stabilization*. Biochim Biophys Acta. 1574: 24-34.
- Ortiz CO, Chen BK, Bale LK, Overgaard MT, Oxvig C, Conover Ca. (2003) *Transforming growth factor-beta regulation of the insulin-like growth factor binding protein-4 protease system in cultured human osteoblasts*. J Bone Miner Res. 18: 1066-1072.
- Palmqvist P, Persson E, Conaway HH, Lerner UH. (2002) *IL-6, leukemia inhibitory factor, and oncostatin M stimulate bone resorption and regulate the expression of receptor activator of NF-kappa B ligand, osteoprotegerin, and receptor activator of NF-kappa B in mouse calvariae*. J Immunol. 169(6): 3353-3362.
- Pantel K, Brakenhoff RH. (2004) *Dissecting the metastatic cascade*. Nat Rev Cancer. 4: 448-456.
- Phimphilai M, Zhao Z, Boules H, Roca H, Franceschi RT. (2006) *BMP signaling is required for RUNX2-dependent induction of the osteoblast phenotype*. J Bone Miner Res. 21: 637-646.
- Pinski J, Parikh A, Bova GS, Isaacs JT. (2001) *Therapeutic implications of enhanced G(0)/G(1) checkpoint control induced by coculture of prostate cancer cells with osteoblasts*. Cancer Res. 61(17): 6372-6376.
- Pinzone JJ, Hall BM, Thudi NK, Vonau M, Qiang YW, Rosol TJ, Shaughnessy JD. (2008) *The role of Dickkopf-1 in bone development, homeostasis and disease*. Blood. 113: 517-525.
- Prunier C, Howe PH. (2005) *Disabled-2 (Dab2) is required for transforming growth factor beta-induced epithelial to mesenchymal transition (EMT)*. J Biol Chem. 280: 17540-17548.
- Pyerin W, Ackermann K. (2003) *Genes encoding human protein kinase CK2 and their functional links*. Prog Nucl Acid Res Mol Biol. 74: 239-269.
- Qiang YW, Barlogie B, Rudikoff S, Shaughnessy JD. (2008) *Dkk1-induced inhibition of Wnt signaling in osteoblast differentiation is an underlying mechanism of bone loss in multiple myeloma*. Bone. 42: 669-680.

- Qiao L, Xu ZL, Zhao TJ, Ye LH, Zhang XD. (2008) *Dkk-1 secreted by mesenchymal stem cells inhibits growth of breast cancer cells via depression of Wnt signalling*. *Cancer Lett.* 269: 67-77.
- Rabbani SA, Desjardins J, Bell AW, Banville D, Mazar A, Henkin J, Goltzman D (1990) *An amino-terminal fragment of urokinase isolated from a prostate cancer cell line (PC-3) is mitogenic for osteoblast-like cells*. *Biochem Biophys Res Commun.* 173: 1058-1064.
- Rabinovich GA, Gabrilovich D, Sotomayor EM. (2007) *Immunosuppressive strategies that are mediated by tumor cells*. *Annu Rev Immunol.* 25: 267-296.
- Ramachandran V, Arumugam T, Hwang RF, Greenson JK, Simeone DM, Logsdon CD. (2007) *Adrenomedullin is expressed in pancreatic cancer and stimulates cell proliferation and invasion in an autocrine manner via the adrenomedullin receptor, ADMR*. *Cancer Res.* 67: 2666-2675.
- Rangaswami H, Bulbule A, Kundu GC (2006) *Osteopontin: role in cell signaling and cancer progression*. *Trends Cell Biol.* 16: 79-87.
- Rentsch CA, Cecchini MG, Thalmann GN. (2009) *Loss of inhibition over master pathways of bone mass regulation results in osteosclerotic bone metastases in prostate cancer*. *Swiss Med Wkly.* 139: 220-225.
- Reya T, Morrison SJ, Clarke MF, Weissman IL. (2001) *Stem cells, cancer, and cancer stem cells*. *Nature.* 414: 105-111.
- Ritchie CK, Andrews LR, Thomas K, Tindall DJ, Fitzpatrick L (1997) *The effects of growth factors associated with osteoblasts on prostate carcinoma proliferation and chemotaxis: implications for the development of metastatic disease*. *Endocrinology.* 138: 1145-1150.
- Roato I, D'Amelio P, Gorassini E, Grimaldi A, Bonello L, Fiori C, Delsedime L, Tizzani A, De Libero A, Isaia G, Ferracini R. (2008) *Osteoclasts are active in bone forming metastases of prostate cancer patients*. *PLoS ONE.* 3: e3627.
- Roberts AB, Russo A, Felici A, Flanders KC. (2003) *Smad3: a key player in pathogenetic mechanisms dependent on TGF-beta*. *Ann NY Acad Sci.* 995: 1-10.
- Salm SN, Burger PE, Coetzee S, Goto K, Moscatelli D, Wilson EL. (2005) *TGF-beta maintains dormancy of prostatic stem cells in the proximal region of ducts*. *J Cell Biol.* 170: 81-90.
- Sato S, Futakuchi M, Ogawa K, Asamoto, Kimihisa N, Asai K, Shirai T. (2008) *Transforming growth factor  $\beta$  derived from bone matrix promotes cell proliferation of prostate cancer and osteoclast activation-associated osteolysis in the bone microenvironment*. *Cancer Sci* 99: 316-323.
- Schroeder TM, Jensen ED, Westendorf JJ. (2005) *Runx2: a master organizer of gene transcription in developing and maturing osteoblasts*. *Birth Defects Res C Embryo Today.* 75: 213-225.
- Schuermans AL, Bolt J, Veldscholte J, Mulder E. (1991) *Regulation of growth of LNCaP human prostate tumor cells by growth factors and steroid hormones*. *J Steroid Biochem Mol Biol.* 40: 193-197.
- Schwaninger R, Rentsch CA, Wetterwald A, van der Horst G, van Bezooijen RL, van der Pluijm G, Loewik CW, Ackermann K, Pyerin W, Hamdy FC, Thalmann GN, Cecchini MG. (2007) *Lack of noggin expression by cancer cells is a determinant of the osteoblast response in bone metastases*. *Am J Pathol.* 170: 160-175.
- Shariat SF, Andrews B, Kattan MW, Kim J, Wheeler TM, Slawin KM. (2001) *Plasma levels of interleukin-6 and its soluble receptor are associated with prostate cancer progression and metastasis*. *Urology.* 58: 1008-1015.
- Shi Y, Massague J. (2003) *Mechanisms of TGF-beta signaling from cell membrane to the nucleus*. *Cell.* 113: 685-700.
- Shipman CM, Croucher PI. (2003) *Osteoprotegerin is a soluble decoy receptor for tumor necrosis factor-related apoptosis-inducing ligand/Apo2 ligand and can function as a paracrine survival factor for human myeloma cells*. *Cancer Res.* 63: 912-916.
- Shulby SA, Dolloff NG, Stearns ME, Meucci O, Fatatis A. (2004) *CX3CR1-fractalkine expression regulates cellular mechanisms involved in adhesion, migration, and survival of human prostate cancer cells*. *Cancer Res.* 64(14): 4693-4698.
- Siegal CB, Schwab G, Nordan RP, Fitzgerald DJ, Pastan I. (1990) *Expression of the interleukin 6 receptor and interleukin 6 in prostate carcinoma cells*. *Cancer Res.* 50: 7786-7788.
- Sims NA, Gooi JH. (2008) *Bone remodeling: Multiple cellular interactions required for coupling of bone formation and resorption*. *Sem Cell Dev Biol.* 19: 444-451.
- Soos G, Jones RF, Haas GP, Wang CY. (1997) *Comparative intraosseal growth of human prostate cancer cell lines LNCaP and PC3 in the nude mouse*. *Anticancer Res.* 17: 4253-4258.
- Sowa H, Kaji H, Yamaguchi T, Sugimoto T, Chihara K. (2002) *Smad3 promotes alkaline phosphatase activity and mineralization of osteoblastic MC3T3-E1 cells*. *J Bone Miner Res.* 17: 1190-1199.
- Stier S, Forkert R, Lutz C, Neuhaus T, Gruenewald E, Cheng T, Dombkowski D, Calvi LM, Rittling SR, Scadden DT. (2005) *Osteopontin is a hematopoietic stem cell niche component that negatively regulates stem cell pool size*. *J Exp Med.* 201: 1781-1791.
- Suda M, Tanaka K, Fukushima M, Natsui K, Yasoda A, Komatsu Y, Ogawa Y, Itoh H, Nakao K. (1996) *C-type natriuretic peptide as an autocrine/paracrine regulator of osteoblast. Evidence for possible presence of bone natriuretic peptide system*. *Biochem Biophys Res Commun.* 223: 1-6.
- Suda T, Arai F, Hirao A. (2005) *Hematopoietic stem cells and their niche*. *Trends Immunol.* 26: 426-433.
- Suh JH, Lee HW, Lee JW, Kim JB. (2008) *Hes1 stimulates transcriptional activity of Runx2 by increasing protein stabilization during osteoblast differentiation*. *Biochem Biophys Res Commun.* 367: 97-102.
- Sung SY, Hsieh CL, Law A, Zhou HE, Pathak S, Multani AS, Lim S, Coleman IM, Wu LC, Figg WD, Dahut WL, Nelson P, Lee JK, Amin M, Lyles P, Johnstone PA, Marshall FF, Chung LW. (2008) *Coevolution of prostate cancer and bone stroma in three-dimensional coculture: Implications for cancer growth and metastasis*. *Cancer Res.* 68: 9996-10003.
- Taguchi Y, Yamamoto M, Yamate T, Lin SC, Mochizuki H, DeTogni P, Nakayama N, Boyce BF, Abe E, Manolagas SC. (1998) *Interleukin-6-type cytokines stimulate mesenchymal progenitor differentiation toward the osteoblastic lineage*. *Proc Assoc Am Physicians.* 110(6): 559-574.
- Takayanagi H, Kim S, Koga T, Taniguchi T. (2005) *Stat1-mediated cytoplasmic attenuation in osteoimmunology*. *J Cell Biochem.* 94: 232-240.

- Tan AR, Alexe G, Reiss M. (2009) *Transforming growth factor-beta signaling: emerging stem cell target in metastatic breast cancer?* Breast Cancer Res Treat. 115: 453-495.
- ten Dijke P, Hill CS. (2004) *New insights into TGF- $\beta$ -Smad signalling.* Trends Biochem Sci. 29: 265-273.
- Tenta R, Sotiriou E, Pitulis N, Thyphronitis G, Koutsilieris M. (2005) *Prostate cancer cell survival pathways activated by bone metastasis microenvironment.* J Musculoskelet Neuronal Interact. 5: 135-144.
- Thalmann GN, Sikes RA, Devoll RE, Kiefer JA, Markwalder R, Klima I, Farach-Carson CM, Studer UE, Chung LWK (1999) *Osteopontin: possible role in prostate cancer progression.* Clin Cancer Res. 5: 2271-2277.
- Thalmann GN, Sikes RA, Wu TT, Degeorges A, Chang SM, Ozen M, Pathak S, Chung LW. (2000) *LNCaP progression model of human prostate cancer: Androgen-independence and osseous metastasis.* Prostate. 44: 91-103.
- Thirunavukkarasu K, Miles RR, Halladay DL, Yang X, Galvin RJ, Chandrasekhar S, Martin TJ, Onyia JE. (2001) *Stimulation of osteoprotegerin (OPG) gene expression by transforming growth factor-beta (TGF-beta). Mapping of the OPG promoter region that mediates TGF-beta effects.* J Biol Chem. 276(39): 36241-36250.
- Tian E, Zhan F, Walker R, Rasmussen E, Yupo M, Barlogie B, Shaughnessy J. (2003) *The role of the Wnt-signaling antagonist DKK1 in the development of osteolytic lesions in multiple myeloma.* N Engl J Med. 349: 2483-2494.
- Tsukazaki T, Chiang TA, Davison AF, Attisano L, Wrana JL. (1998) *SARA, a FYVE domain protein that recruits Smad2 to the TGFbeta receptor.* Cell. 95: 779-791.
- Utsugi M, Dobashi K, Ishizuka T, Masubuchi K, Shimizu Y, Nakazawa T, Mori M. (2003) *C-Jun-NH2-terminal kinase mediates expression of connective tissue growth factor induced by transforming growth factor-beta1 in human lung fibroblasts.* Am J Respir Cell Mol Biol. 28: 754-761.
- Van Obberghen-Schilling E, Roche NS, Flanders KC, Sporn MB, Roberts AB. (1988) *Transforming growth factor  $\beta$ 1 positively regulates its own expression in normal and transformed cells.* J Biol Chem. 263: 7741-7746.
- Verrecchia F, Chu ML, Mauviel A. (2001) *Identification of novel TGF-beta/Smad gene targets in dermal fibroblasts using a combined cDNA microarray/promoter transactivation approach.* J Biol Chem. 276: 17058-17062.
- Virk MS, Lieberman JR. (2007) *Tumor metastasis to bone.* Arthr Res Ther. 9 (Suppl 1): S5 (doi:10.1186/ar2169).
- Wain HM, Bruford EA, Lovering RC, Lush MJ, Wright MW, Povey S. (2002) *Guidelines for human gene nomenclature.* Genomics. 79: 464-470.
- Wan M, Cao X. (2005) *BMP signaling in skeletal development.* Biochem Biophys Res Commun. 328: 651-657.
- Wang Y. (2001) *The role and regulation of urokinase-type plasminogen activator receptor gene expression in cancer invasion and metastasis.* Med Res Rev. 21: 146-170.
- Waschek JA. (2004) *Developmental actions of natriuretic peptides in the brain and skeleton.* Cell Mol Life Sci. 61: 2332-2342.
- Watabe T, Miyazono K. (2009) *Roles of TGF-beta family signaling in stem cell renewal and differentiation.* Cell Res. 19: 103-115.
- Wegiel B, Bjartel A, Culig Z, Persson JL. (2008) *Interleukin-6 activates PI3K/Akt pathway and regulates cyclin A1 to promote prostate cancer cell survival.* Int J Cancer. 122: 1521-1529.
- Weidemann A, Klanke B, Wagner M, Volk T, Willam C, Wiesener MS, Eckardt KU, Warnecke C. (2008) *Hypoxia, via stabilization of the hypoxia-inducible factor HIF-1 $\alpha$ , is a direct and sufficient stimulus for brain-type natriuretic peptide induction.* Biochem J. 409: 233-242.
- Wikstrom P, Damber JE, Bergh A (2001) *Role of transforming growth factor- $\beta$ 1 in prostate cancer.* Microsc Res Tech. 52: 411-419.
- Wikstrom P, Stattin P, Franck-Lissbrant I, Damber JE, Bergh A (1998) *Transforming growth factor  $\beta$ 1 is associated with angiogenesis, metastasis, and poor clinical outcome in prostate cancer.* Prostate. 37: 19-29.
- Wilson A, Trumpp A. (2006) *Bone-marrow haematopoietic stem-cell niches.* Nat Rev Immunol. 6: 93-106.
- Wittrant Y, Theoleyre S, Chipoy C, Padrines M, Blanchard F, Heymann D, Redini F (2004) *RANKL/RANK/OPG: new therapeutic targets in bone tumours and associated osteolysis.* Biochim Biophys Acta. 1704: 49-57.
- Woodard GE, Rosado JA. (2007) *Recent advances in natriuretic peptide research.* J Cell Mol Med. 11: 1263-1271.
- Wooten MW, Geetha T, Seibenhener ML, Babu JR, Diaz-Meco MT, Moscat J. (2005) *The p62 scaffold regulates nerve growth factor-induced NF-kappaB activation by influencing TRAF6 polyubiquitination.* J Biol Chem. 280: 35625-35629.
- Wrana JL, Kubota T, Zhang Q, Overall CM, Aubin JM, Butler WT, Sodek J. (1991) *Regulation of transformation-sensitive secreted phosphoprotein (SPPI/osteopontin) expression by transforming growth factor-beta. Comparisons with expression of SPARC (secreted acidic cysteine-rich protein).* Biochem. J. 273: 523-531.
- Yamaguchi A, Komori T, Suda T. (2000) *Regulation of osteoblast differentiation mediated by bone morphogenetic proteins, hedgehogs, and Cbfa1.* Endocr Rev. 21: 393-411.
- Yang F, Strand DW, Rowley DR. (2008) *Fibroblast growth factor-2 mediates transforming growth factor-beta action in prostate cancer reactive stroma.* Oncogene. 27: 450-459.
- Yang J, Fizazi K, Peleg S, Sikes CR, Raymond AK, Jamal N, Hu M, Olive M, Martinez LA, Wood CG, Logothetic CJ, Karsenty G, Navone NM. (2001) *Prostate cancer cells induce osteoblast differentiation through a Cbfa1-dependent pathway.* Cancer Res. 61: 5652-5659.
- Yang YC, Piek E, Zavadil J, Liang D, Xie D, Heyer J, Pavlidis P, Kucherlapati R, Roberts AB, Boettinger EP (2003) *Hierarchical model of gene regulation by transforming growth factor  $\beta$ .* PNAS 100: 10269-10274.
- Yavropoulou MP, Yovos JG. (2007) *The role of the Wnt signaling pathway in osteoblast commitment and differentiation.* Hormones. 6: 279-294.
- Yeh LC, Zavala MC, Lee JC. (2002) *Osteogenic protein-1 and interleukin-6 with its soluble receptor synergistically stimulate rat osteoblastic cell differentiation.* J Cell Physiol. 190(3): 322-31.
- Yin JJ, Pollock CB, Kelly K. (2005) *Mechanisms of cancer metastasis to the bone.* Cell Res. 15: 57-62.
- Yin T, Li L. (2006) *The stem cell niches in bone.* J Clin Invest. 116: 1195-201.



- Yoshiko Y, Aubin JE, Maeda N. (2002) *Stanniocalcin 1 (STC1) protein and mRNA are developmentally regulated during embryonic mouse osteogenesis: the potential of STC1 as an autocrine/paracrine factor for osteoblast development and bone formation*. J Histochem Cytochem. 50: 483-491.
- Yoshiko Y, Maeda N, Aubin JE. (2003) *Stanniocalcin 1 stimulates osteoblast differentiation in rat calvaria cell cultures*. Endocrinology 144: 4134-4143.
- Zayzafoon M, Abdulkadir SA, McDonald JM. (2004) *Notch signaling and ERK activation are important for the osteomimetic properties of prostate cancer bone metastatic cell lines*. J Biol Chem. 279(5): 3662-3670.
- Zhang F, Lee J, Lu S, Pettaway CA, Dong Z. (2005) *Blockade of transforming growth factor-beta signaling suppresses progression of androgen-independent human prostate cancer in nude mice*. Clin Cancer Res. 11: 4512-4520.
- Zhang J, Dai J, Qi Y, Lin DL, Smith P, Strayhorn C, Mizokami A, Fu Z, Westman J, Keller ET. (2001) *Osteoprotegerin inhibits prostate cancer-induced osteoclastogenesis and prevents prostate tumor growth in the bone*. J Clin Invest. 107: 1235-1244.
- Zhang J, Niu C, Ye L, Huang H, He X, Tong WG, Ross H, Haug J, Johnson T, Feng JQ, Harris S, Wiedemann LM, Mishina Y, Li L. (2003) *Identification of the haematopoietic stem cell niche and control of the niche size*. Nature. 425: 836-841.
- Zhang Q, Rubenstein JN, Jang TL, Pins M, Javonovic B, Yang X, Kim SJ, Park I, Lee C. (2005) *Insensitivity to transforming growth factor-beta results from promoter methylation of cognate receptors in human prostate cancer cells (LNCaP)*. Mol Endocrinol. 19: 2390-2399.
- Zhang S, Fei T, Zhang L, Zhang R, Chen R, Chen F, Ning Y, Han Y, Feng XH, Meng A, Chen YG. (2007) *Smad7 antagonizes transforming growth factor-beta signaling in the nucleus by interfering with functional Smad-DNA complex formation*. Mol Cell Biol. 27: 4488-4499.
- Zhang YQ, Kanzaki M, Shibata H, Kojima I. (1997) *Regulation of the expression of follistatin in rat hepatocytes*. Biochim Biophys Acta. 1354: 204-210.
- Zheng Y, Zhou H, Fong-Yee C, Modzelewski JR, Seibel MJ, Dunstan CR. (2008) *Bone resorption increases tumour growth in a mouse model of osteosclerotic breast cancer metastasis*. Clin Exp Metastasis. 25: 559-567.
- Zhu HJ, Burgess AW. (2001) *Regulation of transforming growth factor-beta signaling*. Mol Cell Biol Res Commun. 4: 321-330.
- Zhu J, Emerson SG. (2004) *A new bone to pick: osteoblasts and the haematopoietic stem-cell niche*. BioEssays 26: 595-599.
- Zhu Y, Sun Z, Han Q, Liao L, Wang J, Bian C, Li J, Yan X, Liu Y, Shao C, Zhao RC. (2009) *Human mesenchymal stem cells inhibit cancer cell proliferation by secreting DKK-1*. Leukemia. 23: 925-33.
- Zunich SM, Douglas T, Valdovinos M, Chang T, Bushman W, Walterhouse D, Iannaccone P, Lamm ML. (2009) *Paracrine sonic hedgehog signalling by prostate cancer cells induces osteoblast differentiation*. Mol Cancer. 8: 12 (doi: 10.1186/1476-4598-8-12).

## Supplementary data

**Tab. 1 Genes significantly ( $\geq 2$ -fold) UPREGULATED in all three coculture combinations.**

Genes were divided into functional groups on the basis of information from the Entrez Gene and PubMed databases ([www.ncbi.nlm.nih.gov](http://www.ncbi.nlm.nih.gov)). For experimental details see Results, the legend to Fig. 19.

Entrez GeneID	Gene symbol	Gene product	Function
<b>Enzymes (metabolism)</b>			
272	<i>AMPD3</i>	adenosine monophosphate deaminase (isoform E)	enzyme; metabolism
55768	<i>NGLY1</i>	N-glycanase 1	enzyme; metabolism
80055	<i>PGAP1</i>	GPI deacylase	enzyme; metabolism
25976	<i>TIPARP</i>	TCDD-inducible poly(ADP-ribose) polymerase	enzyme; metabolism
<b>Cell signaling</b>			
1437	<i>CSF2</i>	colony stimulating factor 2 (granulocyte-macrophage)	cytokine
1848	<i>DUSP6</i>	dual specificity phosphatase 6	signal transduction
2260	<i>FGFR1</i>	fibroblast growth factor receptor 1 (fms-related tyrosine kinase 2, Pfeiffer syndrome)	signal transduction
3556	<i>IL1RAP</i>	interleukin 1 receptor accessory protein	signal transduction
8660	<i>IRS2</i>	insulin receptor substrate 2	signal transduction
64840	<i>PORCN</i>	porcupine homolog (Drosophila)	endoplasmic reticulum; protein processing; processing of Wnt signaling components
6236	<i>RRAD</i>	Ras-related associated with diabetes	signal transduction
<b>Membrane proteins</b>			
9635	<i>CLCA2</i>	chloride channel, calcium activated, family member 2	ion channel, adhesion molecule
9976	<i>CLEC2B</i>	C-type lectin domain family 2, member B	adhesion molecule
667	<i>DST</i>	dystonin	adhesion molecule
1837	<i>DTNA</i>	dystrobrevin, alpha	membrane protein
4311	<i>MME</i>	membrane metallo-endopeptidase	surface marker; peptidase; inactivates hormones
8496	<i>PPFIBP1</i>	PTPRF interacting protein, binding protein 1 (liprin beta 1)	plasma membrane, protein interactions
7037	<i>TFRC</i>	transferrin receptor (p90, CD71)	membrane receptor

<b>Transcription regulation</b>			
3638	<i>INSIG1</i>	insulin induced gene 1	lipid metabolism; regulatory protein; endoplasmic reticulum
80853	<i>JHDM1D</i>	jumonji C domain-containing histone demethylase 1 homolog D ( <i>S. cerevisiae</i> )	transcription regulation
9734	<i>HDAC9</i>	histone deacetylase 9	transcription regulation
3280	<i>HES1</i>	hairy and enhancer of split 1, ( <i>Drosophila</i> )	transcription factor; osteoblast differentiation
4783	<i>NFIL3</i>	nuclear factor, interleukin 3 regulated	transcription factor
<b>Transport</b>			
2017	<i>CTTN</i>	cortactin	cytoskeleton/vesicle transport
2803	<i>GOLGA4</i>	golgi autoantigen, golgin subfamily a, 4	Golgi apparatus (vesicle transport)
9818	<i>NUPL1</i>	nucleoporin like 1	nuclear pore complex (transport)
10802	<i>SEC24A</i>	SEC24 related gene family, member A ( <i>S. cerevisiae</i> )	vesicle transport
9871	<i>SEC24D</i>	SEC24 related gene family, member D ( <i>S. cerevisiae</i> )	vesicle transport
55186	<i>SLC25A36</i>	solute carrier family 25, member 36	solute carrier
<b>Stress response</b>			
597	<i>BCL2A1</i>	BCL2-related protein A1	stress response; antiapoptotic protein
5494	<i>PPM1A</i>	protein phosphatase 1A (formerly 2C), magnesium-dependent, alpha isoform	negative regulator of stress response; cell cycle control; terminates TGFβ signaling
23645	<i>PPP1R15A</i>	protein phosphatase 1, regulatory (inhibitor) subunit 15A	stress response
6095	<i>RORA</i>	RAR-related orphan receptor A	stress response
51616	<i>TAF9B</i>	TAF9B RNA polymerase II, TATA box binding protein (TBP)-associated factor, 31kDa	transcription initiation
7272	<i>TTK</i>	TTK protein kinase	required for progression of mitosis (cell proliferation)
<b>Other</b>			
27065	<i>D4S234E</i>	DNA segment on chromosome 4 (unique) 234 expressed sequence	other
10144	<i>FAM13A1</i>	family with sequence similarity 13, member A1	other
55785	<i>FGD6</i>	FYVE, RhoGEF and PH domain containing 6	other
54985	<i>HCFC1R1</i>	host cell factor C1 regulator 1 (XPO1 dependent)	other
652526 /// 727927 /// 9659	<i>LOC727927</i> /// <i>PDE4DIP</i>	phosphodiesterase 4D interacting protein (myomegalin) /// similar to phosphodiesterase 4D interacting protein isoform 2	other
654342	<i>LOC654342</i>	Similar to lymphocyte-specific protein 1	other
375449	<i>MAST4</i>	Microtubule associated serine/threonine kinase family member 4	other
4884	<i>NPTX1</i>	neuronal pentraxin I	other
8731	<i>RNMT</i>	RNA (guanine-7-) methyltransferase	other
51750	<i>RTELI</i> /// <i>TNFRSF6B</i>	tumor necrosis factor receptor superfamily, member 6b, decoy /// regulator of telomere elongation helicase 1	telomere maintenance

23429	<i>RYBP</i>	RING1 and YY1 binding protein	other
25907	<i>TMEM158</i>	transmembrane protein 158	other
7267	<i>TTC3</i>	tetratricopeptide repeat domain 3	other

**Tab. 2 Genes significantly ( $\geq 2$ -fold) DOWNREGULATED in all three coculture combinations.**

For details see the legend to Tab. 1.

Entrez GeneID	Gene symbol	Gene product	Function
<b>Enzymes</b>			
31	<i>ACACA</i>	acetyl-Coenzyme A carboxylase alpha	fatty acid synthesis (lipid metabolism)
18	<i>ABAT</i>	4-aminobutyrate aminotransferase	enzyme
875	<i>CBS</i>	cystathionine-beta-synthase	enzyme; metabolism
8560	<i>DEGS1</i>	degenerative spermatocyte homolog 1, lipid desaturase ( <i>Drosophila</i> )	lipid metabolism
1718	<i>DHCR24</i>	24-dehydrocholesterol reductase	cholesterol biosynthesis (lipid metabolism)
1719	<i>DHFR</i>	dihydrofolate reductase	enzyme; nucleotide synthesis
3295	<i>HSD17B4</i>	hydroxysteroid (17-beta) dehydrogenase 4	enzyme; fatty acid catabolism (lipid metabolism)
3417	<i>IDH1</i>	isocitrate dehydrogenase 1 (NADP+), soluble	enzyme; metabolism
51056	<i>LAP3</i>	leucine aminopeptidase 3	aminopeptidase
4247	<i>MGAT2</i>	mannosyl (alpha-1,6-)-glycoprotein beta-1,2-N-acetylglucosaminyltransferase	Golgi enzyme
11098	<i>PRSS23</i>	protease, serine, 23	serine protease
7296	<i>TXNRD1</i>	thioredoxin reductase 1	enzyme; protection against oxidative stress
10269	<i>ZMPSTE24</i>	zinc metalloproteinase (STE24 homolog, <i>S. cerevisiae</i> )	protease
<b>Cell signaling</b>			
2247	<i>FGF2</i>	fibroblast growth factor 2 (basic)	cytokine
22943	<i>DKK1</i>	dickkopf homolog 1 ( <i>Xenopus laevis</i> )	secreted protein
10468	<i>FST</i>	follicle-stimulating hormone receptor 1	cytokine
4739	<i>NEDD9</i>	neural precursor cell expressed, developmentally down-regulated 9	signal transduction
8829	<i>NRP1</i>	neuropilin 1	membrane coreceptor to tyrosine kinase receptor
60676	<i>PAPPA</i>	pregnancy-associated plasma protein A, pappalysin 1	metalloproteinase; regulates growth factor availability
5999	<i>RGS4</i>	regulator of G-protein signaling 4	G-protein signaling
7048	<i>TGFBR2</i>	transforming growth factor, beta receptor II (70/80kDa)	growth factor receptor

<b>ECM, adhesion, cytoskeleton</b>			
347902	<i>AMIGO2</i>	adhesion molecule with Ig-like domain 2	adhesion molecule
1009	<i>CDH11</i>	cadherin 11, type 2, OB-cadherin (osteoblast)	adhesion molecule
1277	<i>COL1A1</i>	collagen, type I, alpha 1	ECM component
1278	<i>COL1A2</i>	collagen, type I, alpha 2	ECM component
4771	<i>NF2</i>	neurofibromin 2 (bilateral acoustic neuroma)	cytoskeleton
7057	<i>THBS1</i>	thrombospondin 1	adhesion molecule
10330	<i>TMEM4</i>	transmembrane protein 4	interacts with cytoskeleton
<b>DNA, RNA and protein synthesis</b>			
11056	<i>DDX5</i>	DEAD (Asp-Glu-Ala-Asp) box polypeptide 5	proliferation-associated nuclear antigen; splicing, translation
1153	<i>CIRBP</i>	cold inducible RNA binding protein	cell proliferation
90993	<i>CREB3L1</i>	cAMP responsive element binding protein 3-like 1	transcription factor
4173	<i>MCM4</i>	minichromosome maintenance complex component 4	initiation of replication
10605	<i>PAIP1</i>	poly(A) binding protein interacting protein 1	translation initiation, protein biosynthesis
6421	<i>SFPQ</i>	splicing factor proline/glutamine-rich (polypyrimidine tract binding protein associated)	multifunctional nuclear protein
<b>Immune response</b>			
9510	<i>ADAMTS1</i>	ADAM metallopeptidase with thrombospondin type 1 motif, 1	inflammatory processes, matrix remodeling
6347	<i>CCL2</i>	chemokine (C-C motif) ligand 2	cytokine; inflammatory response
4599	<i>MX1</i>	myxovirus (influenza virus) resistance 1, interferon-inducible protein p78 (mouse)	immune response
5806	<i>PTX3</i>	pentraxin-related gene, rapidly induced by IL-1 beta	marker of inflammation
6772	<i>STAT1</i>	signal transducer and activator of transcription 1, 91kDa	transcription factor; immune response
<b>Other</b>			
4591	<i>TRIM37</i>	tripartite motif-containing 37	unknown
25972	<i>UNC50</i>	unc-50 homolog (C. elegans)	fibroblast differentiation

**Tab. 3 Significant transcription alterations selective for hfOB<sup>PC3</sup>, hfOB<sup>LNCaP</sup> or hfOB<sup>C4-2B4</sup>.**

Genes were divided into functional groups on the basis of information from the Entrez Gene and PubMed databases ([www.ncbi.nlm.nih.gov](http://www.ncbi.nlm.nih.gov)). For experimental details see Results, the legend to Fig. 19. Transcription alterations observed in only one coculture combination on the array, but confirmed by qRT-PCR as present in two or three coculture combinations have been included in Results, Tab. 9.

hfOB<sup>X</sup>, X-cocultured hfOB; ▲▲, ≥ 2-fold elevation; ▲, ≥ 1,5-fold elevation; ▽▽, ≥ 2-fold repression; ▽, ≥ 1,5-fold repression; nc, no change; \*, verified by qRT-PCR; #, transcript upregulated by TGFβ; I, immune response; \*\*, change seen only in qRT-PCR

Entrez GeneID	Gene Symbol	Gene Product	Description	hfOB <sup>PC3</sup> 48 h	hfOB <sup>LNCaP</sup> 48 h	hfOB <sup>C4-2B4</sup> 48 h
<b>Stress response; modulation of pro- and antiapoptotic mechanisms</b>						
3708	<i>ITPR1</i>	inositol 1,4,5-triphosphate receptor, type 1	Calcium channel required for apoptotic cell death.	▲▲	nc	nc
9467	<i>SH3BP5</i>	SH3-domain binding protein 5 (BTK-associated)	Mitochondrial protein, phosphorylated by stress-activated protein kinase 3.	▲▲	nc	nc
7133	<i>TNFRSF1B</i>	tumor necrosis factor receptor superfamily, member 1B	Suppressor of death receptor-mediated apoptosis.	▲▲	nc	nc
8793	<i>TNFRSF10D</i>	tumor necrosis factor receptor superfamily, member 10d, decoy with truncated death domain	Inhibitory role in TRAIL-induced cell apoptosis.	nc	▲▲	nc
23300	<i>ASCIZ</i>	ATM/ATR-Substrate Chk2-Interacting Zn2+-finger protein	DNA repair, depletion increases apoptosis after DNA damage.	nc	▽▽	nc
10628	<i>TXNIP</i>	thioredoxin interacting protein	Glucocorticoid-regulated primary response gene involved in mediating glucocorticoid-induced apoptosis.	nc	nc	▽▽
<b>Decreased DNA and RNA synthesis, suppressed proliferation</b>						
1028	<i>CDKN1C</i>	cyclin-dependent kinase inhibitor 1C (p57, Kip2)	Negative regulator of cell proliferation - strong inhibitor of G1 cyclin/Cdk complexes.	▲▲	nc	nc
5586	<i>PKN2</i>	protein kinase N2	Ser/Thr kinase and Rho/Rac effector protein, essential regulator of both entry into mitosis and exit from cytokinesis	nc	▲▲	nc
22936	<i>ELL2</i>	elongation factor, RNA polymerase II, 2	Component of transcriptional machinery.	nc	▲▲	nc
1020	<i>CDK5</i>	cyclin-dependent kinase 5	Cell cycle control.	▽▽	nc	nc
11052	<i>CPSF6</i>	cleavage and polyadenylation specific factor 6, 68kDa	Subunit of a cleavage factor required for 3' RNA cleavage and polyadenylation processing.	▽▽	nc	nc
1503	<i>CTPS</i>	CTP synthase	Nucleotide synthesis.	▽▽	nc	nc
2071	<i>ERCC3</i>	excision repair cross-complementing rodent repair deficiency, complementation group 3 (xeroderma pigmentosum group B complementing)	ATP-dependent DNA helicase, functions in nucleotide excision repair. Also functions in class II transcription (as a subunit of TFIIH).	▽▽	nc	nc
64785	<i>GINS3</i>	GINS complex subunit 3 (Psf3 homolog)	Essential for the initiation of DNA replication.	▽▽	nc	nc
2958	<i>GTF2A2</i>	general transcription factor IIA, 2, 12kDa	Regulates transcription initiation.	▽	nc	nc
8520	<i>HAT1</i>	histone acetyltransferase 1	Acetylation of newly synthesized cytoplasmic histones, which plays an important role in replication-dependent chromatin assembly.	▽▽	nc	nc
3182	<i>HNRPAB</i>	heterogeneous nuclear ribonucleoprotein A/B	RNA binding protein, associates with pre-mRNA in the nucleus.	▽▽	nc	nc
5654	<i>HTRA1</i>	HtrA serine peptidase 1	Regulates availability of insulin-like growth factors and possibly cell growth.	▽▽	nc	nc

Entrez GeneID	Gene Symbol	Gene Product	Description	hfOB <sup>PC3</sup> 48 h	hfOB <sup>LNCaP</sup> 48 h	hfOB <sup>C4-2B4</sup> 48 h
3609	<i>ILF3</i>	interleukin enhancer binding factor 3, 90kDa	Complexes with other proteins, dsRNAs, small noncoding RNAs, and mRNAs to regulate gene expression and stabilize mRNAs.	▽▽	nc	nc
4331	<i>MNAT1</i>	menage a trois homolog 1, cyclin H assembly factor ( <i>Xenopus laevis</i> )	Involved in the assembly of the kinase complex that activates cyclin-dependent kinases, which participate in cell cycle control.	▽▽	nc	nc
51728	<i>POLR3K</i>	polymerase (RNA) III (DNA directed) polypeptide K, 12.3 kDa	Small essential subunit of RNA polymerase III, the polymerase responsible for synthesizing transfer and small ribosomal RNAs in eukaryotes.	▽▽	nc	nc
80324	<i>PUS1</i>	pseudouridylate synthase 1	Converts uridine into pseudouridine after the nucleotide has been incorporated into RNA. Pseudouridine may have a functional role in tRNAs and may assist in the peptidyl transfer reaction of rRNAs.	▽▽	nc	nc
3431	<i>SP110</i>	SP110 nuclear body protein	Component of the nuclear body, a multiprotein complex that may participate in the regulation of transcription.. May play a role in transcription activation and in ribosome biogenesis.	▽▽	nc	nc
54962	<i>TIPIN</i>	TIMELESS interacting protein	Nuclear protein. Depletion of endogenous tipin results in reduced growth rate, which may be due in part to inefficient progression of S phase and DNA synthesis.	▽▽	nc	nc
8295	<i>TRRAP</i>	transformation/transcription domain-associated protein	Recruitment of histone acetyltransferase complexes to chromatin during transcription, replication and DNA repair.	▽▽	nc	nc
79084	<i>WDR77</i>	WD repeat domain 77	Component of methyltransferase complex that modifies spliceosomal proteins.	▽▽	nc	nc
4609	<i>MYC</i>	v-myc myelocytomatosis viral oncogene homolog (avian)	Multifunctional, nuclear phosphoprotein that plays a role in cell cycle progression, apoptosis and cellular transformation. Transcription factor.	nc	▽▽	nc
4999	<i>ORC2L</i>	origin recognition complex, subunit 2-like (yeast)	Essential for initiation of DNA replication.	nc	▽▽	nc
8317	<i>CDC7</i>	cell division cycle 7 homolog ( <i>S. cerevisiae</i> )	Cell division cycle protein with kinase activity that is critical for the G1/S transition.	nc	nc	▽▽
2965	<i>GTF2H1</i>	general transcription factor IIH, polypeptide 1, 62kDa	Transcription initiation.	nc	nc	▽▽
10614	<i>HEXIM1</i>	hexamethylene bis-acetamide inducible 1	Suppresses transcription elongation. Directly associates with glucocorticoid receptor to suppress glucocorticoid-inducible gene activation.	nc	nc	▽▽
<b>Gene-specific regulation of transcription</b>						
23253	<i>ANKRD12</i>	Ankyrin repeat domain 12	Transcriptional coregulator.	▲▲	nc	nc
1195	<i>CLK1</i>	CDC-like kinase 1	Kinase indirectly involved in pre-mRNA processing, may influence splice site selection.	▲▲	nc	nc
4601	<i>MXI1</i>	MAX interactor 1	Transcriptional repressor.	▲▲	nc	nc
864	<i>RUNX3</i>	runt-related transcription factor 3	Transcription factor.	▲▲	nc	nc
604	<i>BCL6</i>	B-cell CLL/lymphoma 6 (zinc finger protein 51)	Transcriptional repressor.	nc	▲▲	nc
81606	<i>LBH</i>	limb bud and heart development homolog (mouse)	Putative transcriptional activator.	nc	▲▲	nc
10308	<i>ZNF267</i>	zinc finger protein 267	Transcriptional repressor.	nc	▲▲	nc
8091	<i>HMGA2</i>	high mobility group AT-hook 2	Transcriptional regulator.	▽▽	nc	nc
4150	<i>MAZ</i>	MYC-associated zinc finger protein (purine-binding transcription factor)	Transcription factor, inflammation-responsive.	▽▽	nc	nc
9111	<i>NMI<sup>I</sup></i>	N-myc (and STAT) interactor	Interacts with transcription factors, augments STAT-mediated transcription in response to interferon.	▽▽	nc	nc

1997	<i>ELF1</i>	E74-like factor 1 (ets domain transcription factor)	Transcription factor.	nc	nc	▽▽
<b>Protein synthesis, modification and degradation</b>						
1917	<i>EEF1A2</i>	eukaryotic translation elongation factor 1 alpha 2	Component of translational machinery.	▲▲	nc	nc
9958	<i>USP15</i>	ubiquitin specific peptidase 15	Dissassembly of polyubiquitin chains on degraded proteins.	nc	▲▲	nc
29071	<i>C1GALT1C1</i>	C1GALT1-specific chaperone 1	Molecular chaperone.	▽▽	nc	nc
54431	<i>DNAJC10</i>	DnaJ (Hsp40) homolog, subfamily C, member 10	Putative co-chaperone in the endoplasmic reticulum.	▽▽	nc	nc
60681	<i>FKBP10</i>	FK506 binding protein 10, 65 kDa	Molecular chaperone localized in the ER.	▽▽	nc	nc
23463	<i>ICMT</i>	isoprenylcysteine carboxyl methyltransferase	Posttranslational protein modification in the ER.	▽▽	nc	nc
5696	<i>PSMB8<sup>1</sup></i>	proteasome (prosome, macropain) subunit, beta type, 8 (large multifunctional peptidase 7)	Protein degradation (proteasome subunit). Interferon-induced.	▽▽	nc	nc
871	<i>SERPINH1</i>	serpin peptidase inhibitor, clade H (heat shock protein 47), member 1, (collagen binding protein 1)	Putative molecular chaperone involved in the maturation of collagen molecules. Localizes to the ER.	▽▽	nc	nc
908	<i>CCT6A</i>	chaperonin containing TCP1, subunit 6A (zeta 1)	Molecular chaperone (protein folding).	nc	▽▽	nc
51809	<i>GALNT7</i>	UDP-N-acetyl-alpha-D-galactosamine:polypeptide N-acetylgalactosaminyltransferase 7 (GalNAc-T7)	Protein glycosylation.	nc	▽▽	nc
54982	<i>CLN6</i>	ceroid-lipofuscinosis, neuronal 6, late infantile, variant	Possibly involved in the degradation of posttranslationally modified proteins in lysosomes.	nc	nc	▽▽
9997	<i>SCO2</i>	SCO cytochrome oxidase deficient homolog 2 (yeast)	The yeast gene enables assembly of the cytochrome c oxidase complex, which catalyzes the transfer of reducing equivalents from cytochrome c to molecular oxygen and pumps protons across the inner mitochondrial membrane.	nc	nc	▽▽
<b>Cytokines, cell surface receptors and cell signaling</b>						
394	<i>ARHGAP5</i>	Rho GTPase activating protein 5	Negatively regulates Rho GTPases.	▲▲	nc	nc
960	<i>CD44</i>	CD44 molecule (Indian blood group)	Cell-surface glycoprotein involved in cell-cell interactions, cell adhesion and migration.	▲▲	nc	nc
7852	<i>CXCR4</i>	chemokine (C-X-C motif) receptor 4	Cell surface chemokine receptor.	▲▲	nc	nc
9289	<i>GPR56</i>	G protein-coupled receptor 56	Cell signaling.	▲▲	nc	nc
2872	<i>MKNK2</i>	MAP kinase interacting serine/threonine kinase 2	Cell signaling.	▲▲	nc	nc
5801	<i>PTPRR</i>	protein tyrosine phosphatase, receptor type, R	Regulator of cell signaling cascades.	▲▲	nc	nc
5979	<i>RET</i>	ret proto-oncogene	Cell surface receptor tyrosine kinase.	▲▲	nc	nc
58528	<i>RRAGD</i>	Ras-related GTP binding D	G protein. Cell signaling.	▲▲	nc	nc
7189	<i>TRAF6</i>	TNF receptor-associated factor 6	Signal transducer in the NF-kB pathway acting in response to proinflammatory cytokines.	nc	▲▲	nc
57124	<i>CD248</i>	CD248 molecule, endosalin	Cell surface adhesion molecule.	▽▽	nc	nc
8760	<i>CDS2</i>	CDP-diacylglycerol synthase (phosphatidate cytidyltransferase) 2	Cell signaling - regulates the amount of phosphatidylinositol available for signaling.	▽▽	nc	nc
91851	<i>CHRDL1</i>	chordin-like 1	Antagonist of bone morphogenetic protein-4.	▽▽	nc	nc
2919	<i>CXCL1<sup>1</sup></i>	chemokine (C-X-C motif) ligand 1 (melanoma growth stimulating activity, alpha)	Proinflammatory chemokine.	▽▽	nc	nc
1825	<i>DSC3</i>	desmocollin 3	Calcium-dependent adhesive glycoprotein, component of the desmosome cell-cell junction.	▽▽	nc	nc
1906	<i>EDN1#</i>	endothelin 1	Osteoblast mitogen, pro-osteoblastic factor in osteoblastic prostate cancer metastasis. TGFβ target.	▽▽	nc	nc
2150	<i>F2RL1</i>	coagulation factor II (thrombin) receptor-like 1	Cell signaling - transmembrane receptor., couples to G proteins.	▽▽	nc	nc



166647	<i>GPR125</i>	G protein-coupled receptor 125	Initiates signaling <i>via</i> G proteins.	▽▽	nc	nc
3434	<i>IFIT1</i>	interferon-induced protein with tetratricopeptide repeats 1	Interferon-induced negative-feedback regulator of virus-triggered signaling.	▽▽	nc	nc
9562	<i>MINPP1</i>	multiple inositol polyphosphate histidine phosphatase, 1	Cell signaling - hydrolyzes inositol phosphate metabolites.	▽▽	nc	nc
56106	<i>PCDHGA10</i> /// <i>PCDHGA11</i> /// <i>PCDHGA12</i> /// <i>PCDHGA3</i> /// <i>PCDHGA5</i> /// <i>PCDHGA6</i>	protocadherin gamma subfamily A, 12 /// protocadherin gamma subfamily A, 11 /// protocadherin gamma subfamily A, 10 /// protocadherin gamma subfamily A, 6 /// protocadherin gamma subfamily A, 5 /// protocadherin gamma subfamily A, 3	Cell-cell adhesion protein.	▽▽	nc	nc
8434	<i>RECK</i>	reversion-inducing-cysteine-rich protein with kazal motifs	Membrane glycoprotein.	▽▽	nc	nc
7424	<i>VEGFC</i>	vascular endothelial growth factor C	Cytokine, mediator of angiogenesis.	▽▽	nc	nc
3676	<i>ITGA4</i>	integrin, alpha 4 (antigen CD49D, alpha 4 subunit of VLA-4 receptor)	Cell adhesion (integrin family).	nc	▽▽	nc
<b>NF-kB pathway components and target genes</b>						
54101	<i>RIPK4</i>	receptor-interacting serine-threonine kinase 4	Ser/Thr protein kinase, can activate NF-kB.	▲▲	nc	nc
6648	<i>SOD2</i>	superoxide dismutase 2, mitochondrial	Upregulated by NF-kB.	▲▲	nc	nc
<b>Transport</b>						
4864	<i>NPC1</i>	Niemann-Pick disease, type C1	Membrane protein, intracellular cholesterol transport.	▲▲	nc	nc
5172	<i>SLC26A4</i>	solute carrier family 26, member 4	Transport across membranes.	▲▲	nc	nc
51312	<i>SLC25A37</i>	solute carrier family 25, member 37	Transport across membranes.	▲▲	nc	nc
28231	<i>SLCO4A1</i>	solute carrier organic anion transporter family, member 4A1	Transport across membranes.	nc	▲▲	nc
1174	<i>AP1S1</i>	adaptor-related protein complex 1, sigma 1 subunit	Part of the clathrin coat assembly complex which links clathrin to receptors in coated vesicles. These vesicles are involved in endocytosis and Golgi processing.	▽▽	nc	nc
3839	<i>KPNA3</i>	karyopherin alpha 3 (importin alpha 4)	Involved in nuclear protein import.	▽▽	nc	nc
9688	<i>NUP93</i>	nucleoporin 93kDa	Component of nuclear pore complex.	▽▽	nc	nc
6522	<i>SLC4A2</i>	solute carrier family 4, anion exchanger, member 2 (erythrocyte membrane protein band 3-like 1)	Membrane-bound protein, mediates anion exchange.	▽▽	nc	nc
6747	<i>SSR3</i>	signal sequence receptor, gamma (translocon-associated protein gamma)	Glycosylated ER membrane receptor associated with protein translocation across the ER membrane.	▽▽	nc	nc
9114	<i>ATP6V0D1</i>	ATPase, H+ transporting, lysosomal 38kDa, V0 subunit d1	Component of vacuolar ATPase, which mediates acidification of eukaryotic intracellular organelles, necessary e.g. for protein sorting and zymogen activation.	nc	▽▽	nc
5527	<i>CCDC91</i>	coiled-coil domain containing 91	Promotes movement of clathrin-coated vesicles and lysosomal enzyme sorting.	nc	▽▽	nc
3838	<i>KPNA2</i>	karyopherin alpha 2 (RAG cohort 1, importin alpha 1)	Nuclear transport of proteins.	nc	▽▽	nc

51393	<i>TRPV2</i>	transient receptor potential cation channel, subfamily V, member 2	Ion channel, may be involved in nociception.	nc	▽▽	nc
23404	<i>EXOSC2</i>	exosome component 2	Exosome component (cellular transport).	nc	nc	▽▽
8675	<i>STX16</i>	syntaxin 16	Found on cell membranes, permits specific synaptic vesicle docking and fusion.	nc	nc	▽▽
<b>Metabolism</b>						
10840	<i>ALDH1L1</i>	aldehyde dehydrogenase 1 family, member L1	Metabolic enzyme.	▲▲	nc	nc
3099	<i>HK2</i>	hexokinase 2	Metabolic enzyme.	▲▲	nc	nc
5209	<i>PFKFB3</i>	6-phosphofructo-2-kinase/fructose-2,6-biphosphatase 3	Metabolic enzyme.	▲▲	nc	nc
1743/ 1744	<i>DLST</i> /// <i>DLSTP</i>	dihydroipoamide S-succinyltransferase (E2 component of 2-oxo-glutarate complex) /// dihydroipoamide S-succinyltransferase pseudogene (E2 component of 2-oxo-glutarate complex)	Metabolic enzyme.	▽▽	nc	nc
55568	<i>GALNT10</i>	UDP-N-acetyl-alpha-D-galactosamine:polypeptide N-acetylgalactosaminyltransferase 10 (GalNAc-T10)	Synthesis of mucin-type oligosaccharides.	▽▽	nc	nc
3052	<i>HCCS</i>	holocytochrome c synthase (cytochrome c heme-lyase)	Metabolic enzyme.	▽▽	nc	nc
34	<i>ACADM</i>	acyl-Coenzyme A dehydrogenase, C-4 to C-12 straight chain	Metabolic enzyme (mitochondrial fatty acid beta-oxidation).	nc	▽▽	nc
5019	<i>OXCT1</i>	3-oxoacid CoA transferase 1	Metabolic enzyme (mitochondrial ketone body catabolism).	nc	▽▽	nc
641371	<i>ACOT1</i> /// <i>ACOT2</i>	acyl-CoA thioesterase 2 /// acyl-CoA thioesterase 1	Metabolic enzyme.	nc	▽▽	nc
2530	<i>FUT8</i>	fucosyltransferase 8 (alpha (1,6) fucosyltransferase)	Synthesis of complex glycopeptides.	nc	▽▽	nc
3954	<i>LETM1</i>	Leucine zipper-EF-hand containing transmembrane protein 1	Regulation of mitochondrial biogenesis and ATP production.	nc	▽▽	nc
262	<i>AMD1</i>	adenosylmethionine decarboxylase 1	Intermediate enzyme in polyamine biosynthesis.	nc	nc	▽▽
9517	<i>SPTLC2</i>	serine palmitoyltransferase, long chain base subunit 2	Key enzyme in sphingolipid biosynthesis.	nc	nc	▽▽
<b>Structural proteins</b>						
2201	<i>FBN2</i>	fibrillin 2 (congenital contractural arachnodyly)	Component of connective tissue microfibrils.	▲▲	nc	nc
3017	<i>HIST1H2BD</i>	histone cluster 1, H2bd	Chromatin component (histone).	▲▲	nc	nc
72	<i>ACTG2</i>	actin, gamma 2, smooth muscle, enteric	Cytoskeleton component.	▽▽	nc	nc
	<i>ACTR2</i>	ARP2 actin-related protein 2 homolog (yeast)	Involved in cytoskeletal dynamics.	▽▽	nc	nc
1634	<i>DCN</i>	decorin	Binds to collagen fibrils, plays a role in matrix assembly.	▽▽	nc	nc
4281	<i>MID1</i>	midline 1 (Opitz/BBB syndrome)	Associates with microtubules in the cytoplasm, likely involved in the formation of multiprotein structures acting as anchor points to microtubules.	▽▽	nc	nc
3916	<i>LAMP1</i>	lysosomal-associated membrane protein 1	Membrane glycoprotein.	▽▽	nc	nc
8365	<i>HIST1H4H</i>	histone cluster 1, H4h	Chromatin component (histone).	nc	▽▽	nc
81493	<i>SYNC1</i>	syncoilin, intermediate filament 1	Member of the intermediate filament family.	nc	nc	▽▽
7094	<i>TLN1</i>	talin 1	Cytoskeletal protein, concentrated in areas of cell-substratum and cell-cell contacts. Plays a role in the assembly of actin filaments, in cell attachment to the ECM and cell migration.	nc	nc	▽▽

<b>Other</b>						
55917	<i>CTTNBP2NL</i>	CTTNBP2 N-terminal like	Function unknown.	▲▲	nc	nc
54629	<i>FAM63B</i>	family with sequence similarity 63, member B	Function unknown.	▲▲	nc	nc
9788	<i>MTSS1</i>	metastasis suppressor 1	Function unknown.	▲▲	nc	nc
22990	<i>PCNX</i>	pecanex homolog (Drosophila)	Function unknown.	▲▲	nc	nc
5187	<i>PER1</i>	period homolog 1 (Drosophila)	Involved in regulation of circadian rhythms in the brain.	▲▲	nc	nc
83937	<i>RASSF4</i>	Ras association (RalGDS/AF-6) domain family 4	Function unknown.	▲▲	nc	nc
728695	<i>SPANXB1</i> /// <i>SPANXB2</i>	SPANX family, member B2 /// SPANX family, member B1	Functions in spermatogenesis.	▲▲	nc	nc
7163	<i>TPD52</i>	tumor protein D52	Function unknown.	▲▲	nc	nc
9960	<i>USP3</i>	ubiquitin specific peptidase 3	Deubiquitinates histones. Role in preventing chromatin damage.	▲▲	nc	nc
81553	<i>FAM49A</i>	family with sequence similarity 49, member A	Function unknown.	nc	▲▲	nc
221037	<i>JMJD1C</i>	jumonji domain containing 1C	Function unknown.	nc	▲▲	nc
54469	<i>ZFAND6</i>	Zinc finger, AN1-type domain 6	Function unknown.	nc	▲▲	nc
399491	<i>LOC399491</i>	LOC399491 protein	Function unknown.	nc	nc	▲▲
29	<i>ABR</i>	active BCR-related gene	Function unknown.	▽▽	nc	nc
208	<i>AKT2</i>	v-akt murine thymoma viral oncogene homolog 2	Ser/Thr kinase.	▽▽	nc	nc
9532	<i>BAG2</i>	BCL2-associated athanogene 2	Inhibits chaperone activity of Hsc70.	▽▽	nc	nc
51200	<i>CPA4</i>	carboxypeptidase A4	Zinc-containing endopeptidase.	▽▽	nc	nc
2633	<i>GBP1</i> <sup>1</sup>	guanylate binding protein 1, interferon-inducible, 67kDa	Binds guanine nucleotides. Induced by interferon.	▽▽	nc	nc
10964	<i>IFI44L</i> <sup>1</sup>	interferon-induced protein 44-like	Function unknown.	▽▽	nc	nc
3430	<i>IFI35</i> <sup>1</sup>	interferon-induced protein 35	Interferon-induced., relocalizes in apoptotic cells.	▽▽	nc	nc
4323	<i>MMP14</i>	matrix metalloproteinase 14 (membrane-inserted)	ECM remodeling.	▽▽	nc	nc
4600	<i>MX2</i> <sup>1</sup>	myxovirus (influenza virus) resistance 2 (mouse)	Nuclear and cytoplasmic localization. Upregulated by interferon-alpha.	▽▽	nc	nc
4938	<i>OAS1</i> <sup>1</sup>	2',5'-oligoadenylate synthetase 1, 40/46kDa	Interferon-induced protein, involved in the innate immune response to viral infection.	▽▽	nc	nc
55714	<i>ODZ3</i>	odz, odd Oz/ten-m homolog 3 (Drosophila)	Function unknown.	▽▽	nc	nc
10745	<i>PHTF1</i>	putative homeodomain transcription factor 1	Function unknown.	▽▽	nc	nc
23753	<i>SDF2L1</i>	stromal cell-derived factor 2-like 1	Function unknown.	▽▽	nc	nc
60559	<i>SPCS3</i>	signal peptidase complex subunit 3 homolog (S. cerevisiae)	Function unknown.	▽▽	nc	nc
23424	<i>TDRD7</i>	tudor domain containing 7	Function unknown.	▽▽	nc	nc
57215	<i>THAP11</i>	THAP domain containing 11	Contains a DNA-binding domain.	▽▽	nc	nc
23670	<i>TMEM2</i>	transmembrane protein 2	Function unknown.	▽▽	nc	nc
85453	<i>TSPYL5</i>	TSPYL-like 5	Function unknown.	▽▽	nc	nc
10190	<i>TXNDC9</i>	thioredoxin domain containing 9	Function unknown.	▽▽	nc	nc
81839	<i>VANGL1</i>	vang-like 1 (van gogh, Drosophila)	Function unknown.	▽▽	nc	nc
90233	<i>ZNF551</i>	zinc finger protein 551	Function unknown.	▽▽	nc	nc

221154	<i>EFHA1</i>	EF-hand domain family, member A1	Function unknown.	<b>nc</b>	▽▽	<b>nc</b>
24147	<i>FJX1</i>	four jointed box 1 (Drosophila)	Function unknown.	<b>nc</b>	▽▽	<b>nc</b>
81887	<i>LASIL</i>	LAS1-like (S. cerevisiae)	Function unknown.	<b>nc</b>	▽▽	<b>nc</b>
83752	<i>LONP2</i>	Lon peptidase 2, peroxisomal	Proteolysis of mitochondrial substrates.	<b>nc</b>	▽▽	<b>nc</b>
84939	<i>MUM1</i>	melanoma associated antigen (mutated) 1	Function unknown.	<b>nc</b>	▽▽	<b>nc</b>
1809	<i>DPYSL3</i>	dihydropyrimidinase-like 3	Function unknown.	<b>nc</b>	<b>nc</b>	▽▽
54737	<i>HSMPP8</i>	M-phase phosphoprotein, mpp8	Function unknown.	<b>nc</b>	<b>nc</b>	▽▽
6428	<i>SFRS3</i>	splicing factor, arginine/serine-rich 3	Target gene of beta-catenin/TCF4 signaling.	<b>nc</b>	<b>nc</b>	▽▽

## Curriculum vitae

### Personal information

Name:	<b>Agnieszka Anna Halas</b>
Address:	Tulipanowa 68 20-827 Lublin Poland
Phone number:	(48 81) 746 67 84
Date of birth:	31.12.1980 in Lublin
Nationality:	Polish
Family:	single, no children

### Education

1987-1995	Elementary School No. 9, Lublin
1995 - 1999	Stanisław Staszic High School No.1, Lublin
1999	Maturity exams
1999 - 2002	Vocational undergraduate studies at the Maria Curie-Skłodowska University in Lublin, Department of Biology and Earth Sciences, major in biotechnology
01.07.2002	Bachelor's thesis defence <i>(Advances in the research on bioartificial liver devices)</i>
2002 - 2004	Graduate studies at the Maria Curie-Skłodowska University in Lublin, Faculty of Biology and Earth Sciences, major in biotechnology
01.09 - 30.09.2003	Internship at the Institute of Immunology and Experimental Therapy, Polish Academy of Arts and Sciences, Wrocław, Poland
31.05.2004	Master's thesis defence <i>(An evaluation of the antineoplastic properties of quinaldic acid in cell cultures)</i>
05.06 - 30.09.2004	Internship at the University of Idaho (Moscow, Idaho, USA) - Department of Microbiology, Molecular Biology and Biochemistry
24.05 - 22.07.2005	Internship at the German Cancer Research Center, Heidelberg, Germany - Department of Biochemical Cell Physiology (A135/PROMET)
2006-2009	Doctoral studies at the German Cancer Research Center, Heidelberg - Department of Biochemical Cell Physiology
12.2009	Doctoral thesis defence - Technical University in Kaiserslautern, Germany <i>(Crosstalk of cells in bone metastasis: Molecular and cellular analysis of the mutual effects of prostate cancer cells and osteoblasts)</i>

Heidelberg, 09.11.2009

## Erklärung

Hiermit versichere ich ausdrücklich, dass ich die vorliegende Arbeit selbständig und ohne fremde Hilfe verfasst habe. Andere als die von mir angegebenen Quellen und Hilfsmittel wurden nicht benutzt und die aus den verwendeten Werken wörtlich oder inhaltlich entnommenen Stellen sind einzeln, nach Autor, Jahr der Erscheinens, Titel, Journal, Band und Seite kenntlich gemacht. Die Dissertation wurde keinem Fachvertreter einer anderen Hochschule zur Überprüfung vorgelegt und ich habe mich nicht anderweitig um Zulassung zur Promotion beworben.

Heidelberg, im November 2009

Agnieszka Halas

### *Translation:*

I hereby declare that I have written this dissertation independently and with no assistance from other persons. No other sources than those listed by me were used. All content that has been derived from outside sources (either as literal quotation or as paraphrasis) has been clearly indicated by bibliographical entries, listing the author(s), year of publication, title, journal, volume and page(s).

The dissertation has not been submitted for review to a representative of another university, nor have I applied for a doctoral promotion elsewhere.